NTNU
Norges teknisk-naturvitenskapelige universitet

The Norwegian University of Science and Technology

Report no:
NTNU-dr.ing. 2001:21
ITEV-report 2001:01
Classification
Open

POSTADRESSE
NTNU
INSTITUTT FOR TERMISK ENERGI
OG VANNKRAFT
Kolbjørn Hejes vei 1A
N-7491 Trondheim - NTNU

TELEFONER
Sentralbord NTNU: 73 59 40 00
Instituttkontor: 73 59 27 00
Vannkraftlaboratoriet: 73 59 38 57

TELEFAX
Instituttkontor: 73 59 83 90
Vannkraftlaboratoriet: 73 59 38 54

Title of report	**Date**
Variation in Aircraft Engine Exhaust Emissions in Relation to Flight Altitude and Degraded Engine Performance	Spring 2001
	No. of pages/appendixes 156 / 128
Author Paul Arentzen	**Project manager** Jan M. Øverli
Division Faculty of Mechanical Engineering, Department of Thermal Energy and Hydropower	**Project no.**
ISBN no. 82-7984-183-0	**Price group**

Abstract
This work is a study to quantify the exhaust emissions from a short-haul commercial jet flight and the way engine fouling and aging influence these quantities. Focus was set on the distribution of the released gases along the altitude scale.
A 500 km Boeing 737-400 domestic flight in Norway was chosen as the representative case flight, and the range from sea level to cruise altitude at 11278 m was studied. Engine cold end fouling was simulated by shifting the characteristics of the compressor sections, realistic increments were chosen in accordance with the literature recommendations. Carbon dioxide, water vapor, nitric oxides, carbon monoxide and unburned hydrocarbon emissions are subjects of the study.
Two independent computer-modeling systems were used to simulate the flight and calculate the emission quantities. A simple model is based on a parametric study of the engines and a rough representation of the airplane. Turbomatch was used in this work to generate engine data for all operational and engine conditions, and a somewhat more detailed and comprehensive representation of the aircraft was set up. Emission indices were established to suit the CFM56-3C1 engine, and used similarly in the two models.
The predictions came quite close for the carbon dioxide, water vapor and nitric oxide emissions. Carbon monoxide and unburned hydrocarbons emissions are only studied in the larger model.
The distribution of the exhaust emissions over the altitude range of operation for a one hour jet transport flight is found. It is evident that in the extreme low and the cruise altitude levels of the atmosphere, emissions per altitude increment are 30 – 50 % higher than in the intermediate levels. The unburned hydrocarbons are the exception as most of these emissions end up close to cruise altitude.
Simulations demonstrate how the emissions of carbon dioxide, water vapor and nitric oxide increase almost linearly with an engine degradation parameter, the nitric oxides three to four times faster than the other two. Carbon monoxide and unburned hydrocarbon emissions are predicted to drop considerably with engine performance degradation.
A literature review is offered to document the current status and practice regarding gas turbine compressor fouling and cleaning for aircraft engines and other applications.

	Indexing Terms: English	**Indexing Terms: Norwegian**
Group 1	Exhaust Emissions	Eksosutslipp
Group 2	Fuel Consumption	Brennstofforbruk
Selected by author	Aircraft Engines	Flymotorer
	Altitude Distribution	Høydefordeling
	Engine Fouling	Tilgroing

Variation in Aircraft Engine Exhaust Emissions in Relation to Flight Altitude and Degraded Engine Performance

by

Paul Arentzen

A thesis submitted to
The Norwegian University of Science and Technology
for the degree of
Doktor Ingeniør
(Doctor of Engineering)

March 2001
The Norwegian University of Science and Technology
The Department of Thermal Energy and Hydropower
N-7034 Trondheim, Norway

ABSTRACT

This work is a study to quantify the exhaust emissions from a short-haul commercial jet flight and the way engine fouling and aging influence these quantities. Focus was set on the distribution of the released gases along the altitude scale, and the particular relevance to sub-Arctic regions is pointed out. An introductory study shows the continuously increasing trend of commercial air traffic with the steepest rate of growth occurring in what are traditionally considered low technology regions.

A 500 km Boeing 737-400 domestic flight in Norway was chosen as the representative case flight, and the range from sea level to cruise altitude at 11 278 m was studied. Engine cold end fouling was simulated by shifting the characteristics of the compressor sections, realistic increments were chosen in accordance with the literature recommendations. Carbon dioxide, water vapor, nitric oxides, carbon monoxide and unburned hydrocarbon emissions are subjects of the study.

Two independent computer-modeling systems were used to simulate the flight and calculate the emission quantities. A simple model is based on a parametric study of the engines and a rough representation of the airplane. This model is much smaller and far less laborious then the second code, the Turbomatch, which is developed at Cranfield University in England for gas turbine analyses. Turbomatch was used in this work to generate engine data for all operational and engine conditions, and a somewhat more detailed and comprehensive representation of the aircraft was set up. Emission indices were established to suit the CFM56-3C1 engine, and used similarly in the two models.

The predictions came quite close for the carbon dioxide, water vapor and nitric oxide emissions. Carbon monoxide and unburned hydrocarbons emissions are only studied in the larger model.

The distribution of the exhaust emissions over the altitude range of operation for a one hour jet transport flight is found. It is evident that in the extreme low and the cruise altitude levels of the atmosphere, emissions per altitude increment are 30 – 50 % higher than in the intermediate levels. The unburned hydrocarbons are the exception as most of these emissions end up close to cruise altitude.

An engine degradation parameter that is primarily related to cold end fouling, was defined, and simulations demonstrate how the emissions of carbon dioxide, water vapor and nitric oxide increase almost linearly with this parameter, the nitric oxides three to four times faster than the other two. The relative increase with engine degradation for these emission species is slightly steeper for the higher flight altitudes. Carbon monoxide and unburned hydrocarbon emissions are predicted to drop considerably with engine performance degradation.
A literature review is offered to document the current status and practice regarding gas turbine compressor fouling and cleaning for aircraft engines and other applications. Smaller engines, such as helicopter engines and turboprops, are plagued by fouling and efficient procedures for cleaning are available. For larger turbofan engines, fouling is not so much in focus possibly because it is a less dominant reason for engine performance degradation.

PREFACE AND ACKNOWLEDGEMENTS

Airplanes and aero-engines have been the main points of focus in my professional career in the past decade. As propulsion of aircraft was the essence of my teaching during this period, it became a meaningful choice of subject for doctoral research. Part-time study and research along with the fulfillment of teaching obligations is a perfect situation for profit in both areas; inspiration from young students' opinions of the research and the benefit of newly acquired knowledge in the classroom. Young people have every reason to be environmentally conscious, so has every parent and engineer. The aviation industry and sector has had its share of the attention and criticism over the years regarding pollution of the air and the consequences. These aspects are important incentives for the present study.
This thesis is a dissertation for the dr. ing. degree (Doctor of Engineering). I am grateful to The Department of Thermal Energy and Hydropower at The Norwegian University of Science and Technology for their interest in the project. The guidance, support and encouragement from my research supervisor Professor Jan M. Øverli has been of great importance all along.

Thanks to the following people and institutions:

- Professor R. Singh at Cranfield University, UK, for sharing my interest and making possible an eight-week stay at Cranfield University and the use of the Turbomatch Scheme.

- The Research Council of Norway for funding the stay at Cranfield University,

- Director Technical Operations T. Helgaland at Braathens airline for providing useful information on the Boeing 737-400 aircraft and operation,

- Dr. Kajal Gupta at NASA Dryden and Dr. David R. Downing at the Department of Aerospace Engineering at the University of Kansas for reading the manuscript and giving valuable criticism and for their advice regarding the English language,

- Stewart Clark at the Norwegian University of Science and Technology for doing the final English editing,

- Colleagues at Agder University College for their support and for giving me the opportunity to pursue this task.

Their contributions are highly appreciated.

Finally thanks to my wife Kari, and to my family for their patience and sacrifices during this long period when I have neglected my family responsibilities as this endeavor has taken nearly seven years.

Grimstad, March 2001

Paul Arentzen

TABLE OF CONTENTS

NOMENCLATURE

Symbols

A	flow area; constant
a	speed of sound; constant
a	acceleration; constant
b	airfoil cord; constant
b	constant
c	constant
c	constant
C	constant
c_p	specific enthalpy, air
C_D	drag coefficient
C_L	lift coefficient
d	constant
d	constant
D	drag
D_c	tip diameter

e	polytropic efficiency; exponential (= 2.7183); constant
e	constant
E	coefficient of entrainment
E_c	cascade coefficient of entrainment
f	fuel-air ratio; constant
f	constant
$\bar{f}$	fraction of total air participating in combustion
F	thrust
g	acceleration of gravity; constant
g	constant
G	gravity force
h	altitude; distance from center plane
h_{PR}	low heating value of fuel
L	lift; radius
k_f	factor of fouling, Equation (6.14)
Δk_{Hf}	"work done" factor including fouling, Equation (6.13)
K	constant
K_f	efficiency scaling factor
K_p	equilibrium constant
K1	constant
K2	constant
m	mass; constant
$\dot{m}$	mass flow rate
$\bar{\dot{m}}_a$	air flow participating in combustion
M	Mach number; constant

n	constant
N	rotational speed
N1	rotational speed, low pressure spool
N2	rotational speed, high pressure spool
p	pressure; partial pressure
P	maximum pressure in combustor; power
P_v	fuel efficiency loss, Equation (6.8)
ΔP	pressure drop across the combustor
ΔP_L	pressure drop across the combustor liner
r	constant
$\bar{r}_h$	hub/tip ratio of first compressor stage
R	gas constant, air; ground friction
s	constant
S	surface area
S_{ref}	aircraft reference area
St_k	Stokes number
t	time; pitch of airfoil cascade; constant
t_{res}	combustor residence time
T	temperature, absolute
T_{ad}	adiabatic flame temperature
T_{st}	stoichiometric flame temperature
$\Delta T_{t,stg}$	average total temperature rise per compressor stage
V	speed
V_B	combustor volume
V_E	the part of V_B in which fuel evaporation takes place

W	total weight of aircraft
x	constant
X	constant
y	constant
z	constant
α	bypass ratio
β	aircraft angle of incidence
β_I	airfoil angle of incidence
ε	expansion number in Equation (6.7)
δ	corrected pressure
∂	partial derivative
Δ	change
$\Delta\beta$	flow directional change over cascade
$\Delta\beta_{If}$	change in rotor inlet angle due to fouling
Φ	engine degradation parameter
ϕ	flow coefficient
γ	ratio of specific heats, air
γ_v	fouling intensity, Equations (6.6) and (6.7)
λ	factor of excess air in combustion
η	efficiency
η_{ref}	design point efficiency
μ	friction coefficient
π	pressure ratio
Π	product

θ	corrected temperature
ρ	density, air
τ	temperature ratio
τ_λ	$= \frac{c_{pT} \cdot T_{t4}}{c_{pC} \cdot T_0}$

Subscripts

a	air
AG	aerodynamic while on the ground
B	combustion chamber
D	diffuser
EI	emission index
c	corrected
C	compressor; engine cold end; core
CL	low pressure compressor
CH	high pressure compressor
f	fuel; flaps
f	fouled condition
F	fan; bypass
g	landing gear
in	combustion chamber inlet
mH	mechanical, high pressure spool
mL	mechanical, low pressure spool
N	nozzle (core flow); number of stages
N'	bypass nozzle

n	number compressor stages
oa	overall
p	parallel
pz	primary zone
r	ram
R	reference
T	turbine; engine hot end
t	total
TL	low pressure turbine
TH	high pressure turbine

Engine Station Numbers

0	ambient condition; undisturbed captured stream tube
1	inlet
2	compressor and fan face
2.5	low pressure compressor exit
3	compressor exit
4	turbine inlet
4.5	high pressure turbine exit
5	turbine exit
8	core nozzle throat
9	nozzle exit, core flow
13	fan exit
19	nozzle exit, bypass flow

Abbreviations / Acronyms

ACI	Airports Council International
A/C	aircraft
AIAA	American Institute of Aeronautics and Astronautics
CAEP	Committee on Aviation Environmental Protection
CFMI	CFM International
CH	high pressure compressor
CL	low pressure compressor
C0	identifies clean, new engine
D1, D2, D3	identify degraded engine conditions
EGT	exhaust gas temperature
EQHHPP	The Euro-Quebec Hydro-hydrogen Pilot Project
HP	high pressure
HS	Helicopter Service
HSCT	high speed civil transport
ICAO	International Civil Aviation Organization
ISA	international standard atmosphere
ISF	index of compressor sensitivity to fouling
LP	low pressure
LTO	landing and take-off
MFP	mass flow parameter
NASA	National Aeronautics and Space Administration
NILU	Norwegian Institute for Air Research
O/A	over all
RPM	revolutions per minute

RQL	rich, quench, lean (combustor)
SAS	Scandinavian Airlines System
SFC	specific fuel consumption
SST	supersonic transport
TBO	time between overhaul
TET	turbine entry temperature
TGT	turbine gas temperature
TH	high pressure turbine
TL	low pressure turbine
T/O	take-off
TSFC	trust specific fuel consumption
UHC	unburned hydrocarbons
VBV	variable bleed valves
VSV	variable stator vanes

1 INTRODUCTION

Aviation activity has increased continuously since the Wright brothers first flew in 1903, and this development has gained momentum after 1950. There is a general concern that pollution from aircraft may cause damage to both the global and the local environments, and thus adversely affect the living conditions of people as well as all other living creatures and vegetation on earth.
Airborne traffic is in a steadily growing trend, and all prognoses expect this growth to be stable at least for the first decade of the 21st century. There is a reason for grave concern, by the public and scientists.
Aeronautical engineers, like aircraft and jet engine manufacturers are making progress in designing and building more efficient and less polluting aircraft. Still more effort is necessary to keep up with the development in the volume of air traffic worldwide.
Problems related to aging aircraft are considered a major issue, particularly with respect to structures and possible failure due to corrosion and cracks. A similar focus should be put on the aircraft engines as old technology and insufficient maintenance are reasons for poor fuel economy and unfavorable emission characteristics.

1.1 Current Status of Aviation

Since World War II, flying has developed into a safe and quick means of transportation for many purposes. Air transportation is common in all parts of the world and accessible to many groups in society. In the industrialized countries flying is an affordable and easy way to travel for almost everyone. In 1995, the total number of passengers was close to 1.3 billion, and 21 million tonnes of freight was transported in all the 184 ICAO states (International Civil Aviation Organization, list of states in Appendix A).
Airplanes and aviation have been important in military actions since the First World War. Today extremely advanced aircraft operate in air force fleets worldwide. This demonstrates the development that has taken place in aviation on the military side as well.

In the mid forties the turbojet engine introduced a new era in civil and military aviation. Jet driven airplanes are capable of flying higher and faster than propeller airplanes and this potential is utilized today. Modern civil jet aircraft typically cruise at approximately 85 % of the speed of sound, or 910 km/h, and the optimum cruise altitude for medium- and long-haul flights is in the range of 10 000 – 12 000 m.
The operational performance of military aircraft is usually not published. In general however, the faster ones are normally capable of flying somewhere between twice and three times the speed of sound, and aircraft have been built for stable level flight at 85 000 feet, close to 25 000 m altitude ("The International Encyclopedia of Aircraft", Oriole Publishing Ltd., 1991).

1.2 Aircraft Categories and Operations

We usually divide global air activities into civil and military sectors, as already indicated. In many respects the aircraft and engines in the two categories have common features. Many of the major manufacturers supply equipment to both sectors and thus knowledge and experience from one can be easily transferred to the other.
Military training and wartime actions are in many respects quite different from most civil flying when it comes to the way the airplanes are handled and kept. Military operations in general can be quite irregular and thus different from the scheduled civil operations.
Civil aviation consists of commercial and non-commercial traffic (Nüβer, H.-G., Schmitt A., 1989). Commercial flying is divided into scheduled and charter traffic, and its purpose is the transport of passengers and freight. The commercial aviation fleet mostly consists of large aircraft powered by jet engines, the turbofans. Gas turbine-powered propellers are quite common on the smaller and slower airplanes, and such engines are known as turboprops.
In some instances it is convenient to categorize commercial traffic in three different groups depending on the distance of operations (Stinton, D., 1998):

a. short-haul flight; less than 2 500 km distance is typical,
b. medium-haul or continental flights; between countries on the same continent, from 2 500 - 4 500 km in length,
c. long-haul, intercontinental or overseas flights; usually more than 4 500 km.

The non-commercial air traffic is known as general aviation, which comprises all private airplane operation and the business transport of people and goods in company-owned aircraft. In this category we will find many different types of aircraft, including a large number of small propeller-driven airplanes using reciprocating engines, and flying at low altitude over non-scheduled routes.
A considerable number of helicopters is also found in the commercial fleet. Helicopters represent a totally different concept of flying. Larger helicopters are powered by gas turbines, while smaller helicopters often use reciprocating engines.

1.3 Emissions from Aviation, Engine Deterioration

All activities created by man generate waste. Aviation is no exception. Along with solid and fluid wastes that are left on the ground, the combustion engines emit exhaust gases into the atmosphere. The quantity of these gas emissions due to scheduled commercial airlines is approximately 1 billion tonnes per year (1997). That is 3 % of the annual total exhaust gases emitted on earth. Emissions from the aviation are therefore not a major share of the total air pollution on a global basis. It may nevertheless, have unique and detrimental effects on the environment because a large portion, unlike all other man-made emissions, is released at high altitudes.

The earth's atmosphere is the recipient for all these gases, phenomena such as acid rain, global warming, depletion of the ozone layer are the environmental consequences.

Given a fixed traffic pattern, the production of wastes from transport activities is basically a continuous process. The recipients have certain capacities to modify and recycle wastes into components that originally belong in the environment and thus keep the quantities of polluting material at a constant level. If these capacities are exceeded, the waste will have to accumulate somewhere.

Some of the waste materials are substances that are present in the atmosphere by nature, emissions however cause higher than normal concentrations locally and the balance in the environment shifts in unfavorable directions. The highly concentrated species will eventually be distributed into the atmosphere, the ocean and the earth's surface and thus represent less of a threat to the environment. Again we are facing a capacity problem of how fast these waste components will spread and disappear.

Engines degrade over time, efficiency goes down, fuel consumption increases, and the quantities of emissions will change. For most of the emission gases there are direct relations between quantity and the amount of fuel being consumed. Overhaul and maintenance help bring engines back to reasonably good shape. Frequency of overhaul actions and total length of the engine's operating life play a key role in keeping engines up to their normal high efficiency and emission characteristics.

At the present time there seems to be general consensus that the capacity of the atmosphere to cope with all exhaust gases has been exceeded. The people involved in the aviation business express their concern to keep the time specific generation of wastes at the lowest possible level.

1.4 Scope of the Present Work

Despite the fact that a number of studies of aircraft emissions have been published in recent years, very little research on emission distribution over the altitude range of operation is documented. This issue is of particular interest when emissions from short flights are considered and where the cruise sequence is not the dominant part. The most common flight range for short-haul flights is around 500 km (Torenbeek, E., 1982).

Aircraft engine degradation from erosion, wear and tear, and fouling has been studied as a major cause of performance reduction and increased fuel consumption. Attempts to quantify the impact of engine deterioration on emission level, and the relation between the two, are not documented in the literature.

Apparently these aspects of aircraft emissions are not discussed extensively in the scientific community, they are not reflected in international regulations, and are not subject to political or public debate. It is therefore of great importance to study these issues on a scientific level, and to bring them to the attention of the aviation community, the authorities and the public. The issues are the focus of the present work.
This thesis will generate and present valuable guidance to how emission levels from the civil air traffic can be reduced by modifying the flight patterns. The results are also useful incentives to keep emissions at the lowest possible levels, by intensifying engine maintenance and cleaning.
Secondly the regulation authorities will find quantitative information as useful background to consider and establish emission requirements for the entire operating life of aircraft engines.
The demonstrations of how accurately the operation and maintenance of an aircraft can be modeled and manipulated and the emission quantities estimated, by simple computer simulation, should encourage the aircraft industry and airline companies to utilize such software to strengthen their own strategy and insight into emission abatement.
The objective of this work is to analyze, by computer simulation, a complete flight cycle and thereby investigate:

1. exhaust emission quantities at all relevant altitudes for representative domestic commercial air traffic,
2. how the technical condition of the engines will influence these emission quantities, and
3. the capacity of a small and quite simple computer model to calculate reliable estimates of aircraft emissions,

and to demonstrate how:

4. certain fractions of the total emissions from a short-haul flight end up at particular altitude levels,
5. relative changes in emission quantities depend on variations in the engine cold end condition.

This is accomplished by focusing on three main goals.

The distribution of major exhaust components over the entire flight altitude range of a short-haul flight, typically of less than one hour, is to be calculated. The genuine source of exhaust emissions is the combustion process inside the engines. The fuel consumption is a parameter that is very closely related to the forming of exhaust emissions and is important in the predictions of the emission quantities. Fuel consumption will therefore be calculated as well. Emphasis will be on commercial traffic, fixed-wing aircraft and turbofan engines only.

Secondly, the influence on emissions from gradually degrading engine performance will be studied; i.e. the overall change of emission quantities, and possible variations with altitude. Engine parameters and the flow situation inside the engine are altered with clogging of air passages, component wear and other aging phenomena. The chemical and physical conditions in the gases change; hence the rate of formation of exhaust

components will be affected. Fouling of the fan and compressor sections of the engine, known as engine cold end fouling, is chosen as the main cause of engine performance degradation in the study.

Thirdly it is to be demonstrated how aircraft emissions can be predicted with reasonable accuracy by a quite simple computer model, compared to a comprehensive modeling tool. A computer code for parametric gas turbine engine analysis has been developed, and tested against a larger and well-documented commercial program. A reasonably good correlation between the predictions of the two systems will indicate the reliability of the results and, accordingly support the simple model in forming a basis for a low user threshold tool in flight emission analyses.

The work is an over all study including flight route, the airplane, the aircraft engines and the combustion process. The aim has been to perform analyses of the total system and consequences of its operation.

1.5 Organization of the Thesis

The presentation of the thesis is organized in four sections. Chapters 2 and 3 constitute the introductory studies of aviation history and statistics that justify a closer focus on environmental consequences of increasing air traffic. Gaseous emissions and atmospheric mechanisms are studied in general. Mathematical representation methods for gas turbine engines are discussed as a preparative task to writing a computer code.
Chapters 4 and 5 present the computer models and modeling procedures. The case aircraft, engine and mission profile are introduced, and the emission indexes and the degradation process are discussed.
A comprehensive literature review on compressor fouling in general, and fouling of aircraft gas turbine engine compressors in particular is found in Chapter 6. The fouling mechanism and cleaning measures are studied. Fouling is said to be the main reason for engine degradation. It primarily effects the forward part, i.e. fan and compressor sections of the engine. This corresponds directly to the pattern of component performance deterioration used in the subject case of Chapters 4 and 5. Fairly simple washing procedures are applied in many cases to remove the fouling material and thereby restore the engine performance almost to its original level.
All results from the model calculations are presented and discussed in Chapter 7. The two different models are compared with respect to their capacity for predicting fuel consumption and emissions for the case flight. This is followed by the conclusions.

2 COMMERCIAL AVIATION AND EMISSIONS

2.1 History

Statistics from ICAO, the International Civil Aviation Organization (Cornish, J.L. et al., 1996, ICAO Journal, Vol. 51 - No.6, 1995), show a steady growth in commercial aviation around the world. In the post-war years, that is between 1950 and 1995 the number of passengers handled annually worldwide has increased from approximately 30 million to 1288 million, an annual growth rate of 8.7 %. The total load in tonnage, people and goods combined, show similar increase over the same period of time.
For a more recent and a shorter time span, 1978 - 1988, the number of airline passenger has shown 5 % annual growth. All commercial airlines in the world flew 940 billion passenger kilometers on scheduled flights in 1978, when the same figure for 1988 is 1700 billion, i.e. a 6.1 % increase annually. Each passenger flew longer flights in 1988 than ten years earlier. Also, there is a stronger increase in international rather than the domestic traffic over those particular ten years. An additional aspect is that the scheduled traffic has taken a larger share of the total performance over the years (Nüβer, H.-G., Schmitt A., 1989). Unscheduled flights carried 22 % of all passenger kilometers in 1978 while in 1988 the share is down to 18 %.
A most important pattern in this picture of growth is the strong increase in parts of the world where aviation until recently has been rather modest. In the ten year period 1978 - 1988, when we saw a world wide increase in air traffic of about 6 %, Asia and the Pacific region had a 9.5 % annual growth (Nüβer, H.-G., Schmitt A., 1989). Stastistics from the Airports Council International (ACI) regarding changes from 1993 to 1994 (Cornish, J.L. et al., 1996) show a similar trend. The commercial part of aviation has grown and expanded over the whole world.
The total number of flights, civil aircraft movements in the world, increased from 1993 to 1994 by 3 % (Australia not included). It should appear from Figure 2.1 that the growth rate is different from one continent to the other, and that the old western countries show a more moderate increase than the rest of the world.

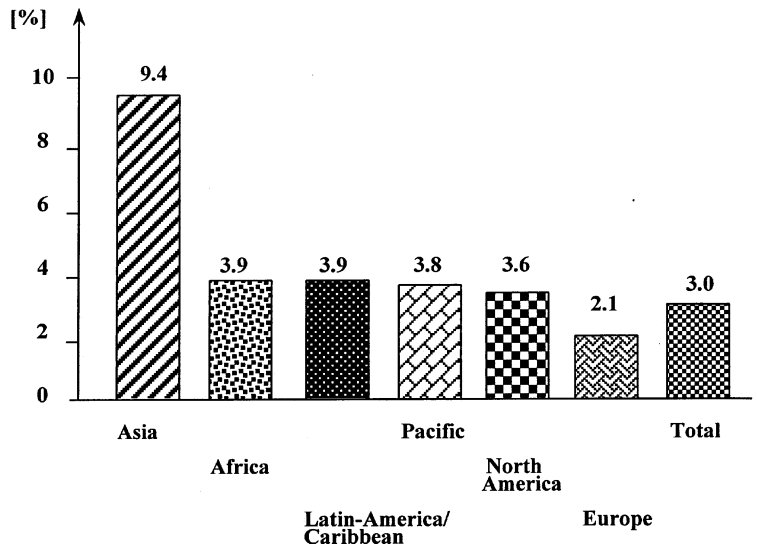

Figure 2.1 Diagram showing the increasing numbers of flights from 1993 to 1994. Data from (Cornish, J.L. et al., 1996)

As the present work is focusing on airplanes as environmental subjects, it is essential to study how the fleet of commercial airplanes has changed technically over the years. The numbers that appear in Figure 2.2 (Nüβer, H.-G., Schmitt A., 1989) show the development for the 10 years from 1978 to 1988, and three different trends are obvious:

1. the number of aircraft with reciprocating engines has been reduced by more than 50 %,
2. there are fewer engines on each airplane,
3. the so-called turboprop, gas turbine-powered propeller airplanes, has increased in numbers.

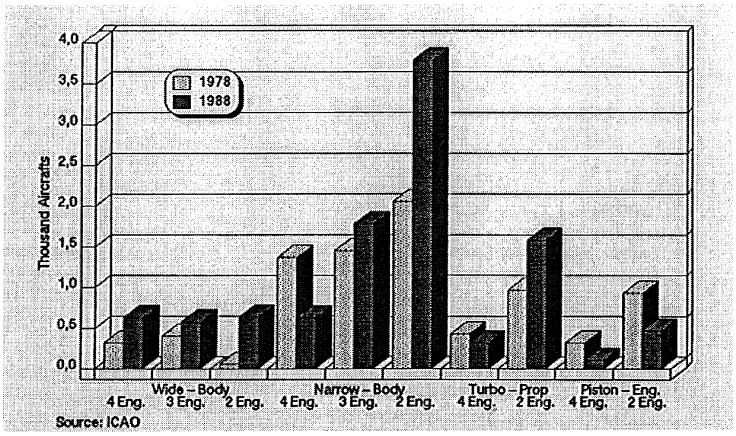

Figure 2.2 Total Commercial Transport Fleet Distinguished by type of Propulsion (Nüβer, H.-G., Schmitt A., 1989)

A more distinct interpretation shows that in 1988 the large majority, 95 % of the commercial fleet worldwide, had gas turbine engines, with approximately 20 % of them being propeller airplanes. The twin engine configuration is also about to take over from the three and four engine airplanes.

2.2 Distribution of Global Aviation

The fact that there is a great diversity in the density of commercial aviation around the world has some significance to the present work. The reason why the distribution is the way it appears in Table 2.1 (Cornish, J.L. et al., 1996), and key factors in the development for the near future may be found in a list presented by the French Institute of Air Transport. The factors that are influential to the global increase in airborne activity, are listed in order of importance, as follows (Cornish, J.L. et al., 1996):

1. the world economy (gross domestic product, international trade)
2. worldwide geo-politics
3. oil prices
4. environmental concern (ecology, noise, air quality, etc.)
5. regional development policies
6. impact of new communication technologies
7. mobility, management of time and organization of production
8. technical aerospace development
9. air transport organization and policy (deregulation, industry structure)

10. airspace congestion
11. competition from high-speed trains (in Europe)
12. marketing innovations (e.g., computer reservation systems, elimination of tickets and other uses of computer technology)

One may assume, though there is no such indication in the reference, that these factors apply to regional as well as the global growth, and thus the level of economic, technological and industrial development are the major driving factors for airborne activity in an area. This assumption is supported by the numbers in Table 2.1, which show that Europe and North America combined have close to 80 % of all air passenger traffic and 70 % of all airborne freight of goods in the world. Three out of four of all the airports in the world are located in either Europe or North America.
The majority of all commercial air traffic takes place on the western part of the Northern Hemisphere (ICAO Journal, Vol. 51 – No. 10).

Regions	Total Passengers	Total Cargo (tonnes)	Total Aircraft Movements	Number of Airports
Africa	13 680 624	164 205	302 359	18
Asia	47 567 164	1 092 262	508 588	12
Europe	632 328 691	9 239 677	10 928 560	187
Latin America/ Caribbean	106 746 534	2 547 212	2 295 045	38
North America	998 271 394	20 539 534	26 163 960	119
Pacific	267 932 115	8 394 541	3 325 073	27
Totals	**2 066 526 522**	**41 977 431**	**43 523 585**	**401**

***Note** – This Airport Traffic Report Summary has been prepared by Airports Council International and is a comparison of only those airports with complete data for the calendar year-to-date.*
***Passengers** – total passengers enplaned and deplaned, passengers in transit counted once.*
***Cargo** – loaded and unloaded freight and mail.*
***Aircraft Movements** – landing and take-off of an aircraft.*

Table 2.1 World Airport Traffic Report summary for 1993/1994 for ACI Member Airports (ACI, 1995) (Cornish, J.L. et al., 1996)

2.3 Prognoses and Forecasts

Predictions for expected growth in the coming years regarding expansion in commercial air traffic are presented in (Nüßer, H.-G., Schmitt A., 1989) from 1989. Numbers from international organizations and the major aircraft manufacturers are shown in Table 2.2.

Source (issued)	**Range of Forecast**	**Passenger** (*passenger·km*)		**Freight** (*tonne·km*)	
		GR (%)	GF	GR (%)	GF
ICAO (1989)	1988 - 2000	6.0	2.0	7.0	2.3
IATA (Sept. 1989)[1)]	1988 – 1993	7.05	1.4	7.0	1.4
Airbus (Nov. 1987)	1986 - 1996	5.7	1.74	6.7	1.9
	1996 - 2006	5.3	1.68		
	1986 - 2006	5.5	2.92		
Boeing (Febr. 1989)	1987 - 2000	5.9	2.1	6.0	2.1
	2000 - 2005	4.2	1.23		
	1987 - 2005	5.4	2.6		
MDD(Febr. 1989)	1987 - 2002	5.7	2.3	6.0	2.4
MBB (June 1989)	1988 - 2008	5.1[2)]	2.7		

Remarks: 1) Passengers and Freight in Border-Crossing Traffic
2) Scheduled and Charter Services
GR = Average Annual Growth Rate; GF = Growth Factor
MBB = Messerschmitt-Bölkow-Blohm Gmbh
MDD = McDonnell Douglas

Table 2.2 Comparison of Forecasts of Global Air Transport Demand - Scheduled Services

The prognoses show surprising unanimity. For the passenger traffic, an annual growth of close to 6 % is anticipated and the similar number for transport of goods is in excess of 6 % per year up to the year 2000. Aircraft manufacturers expect a minor reduction in the annual growth rate for the passenger traffic in the first 5 - 8 years of the new millenium.
The prognoses from the late eighties, viewed in retrospective, appear to be quite good and are supported by the ICAO statistics. Figures for tonne-kilometers transport, passengers and goods together are the most relevant for a comparison with the referenced prognoses.

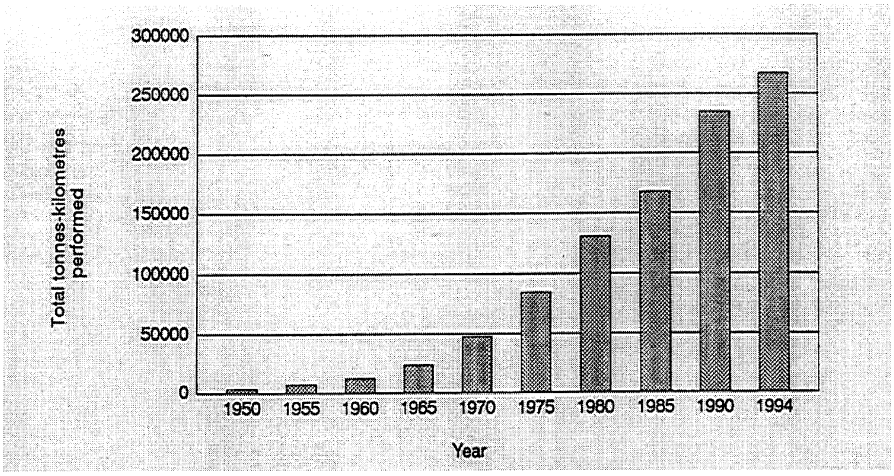

Figure 2.3 International and domestic total tonne-kilometers moved (passengers, baggage, freight and mail) of airlines of ICAO contracting states for 1950-1994 (ICAO, 1995) (Cornish, J.L. et al., 1996)
The left axis should be interpreted as million tonne-kilometers performed (PA)

The annual increase in tonne-kilometers freight was 6.9 % between 1985 and 1990, 3.3 % from 1990 to 1994, average over the 9 years was 5.3 %. Without being any more specific, it is obvious that there is close agreement between the prognoses and the real development for the same 9 years, and that should support our confidence in the prognoses for the first decade of the next century.
If that growth rate stays unchanged in the future, we will see the volume of worldwide commercial air traffic multiplying ten times from now until the year 2050.
According to ICAO the heaviest increase will occur in countries where today's traffic density is low; i.e. Asia and the Pacific region, Africa and Latin-America. The ICAO prognoses do not go beyond the year 2003 (Cornish, J.L. et al., 1996).
Looking back on the list of factors from the French Institute of Air Transport the five factors that influence this development the most are the world economy, worldwide geo-politics, oil prices, environmental concern and the regional development policies. Those are all frequently changing quantities, and nobody is really capable of predicting their total impact and the development. It seems clear after all, that one should assume a considerable increase in commercial flying over the coming five to ten years.

"Technical aerospace development" is also on the list from the French Institute of Air Transport. The Concord airplane, the first and only supersonic transport of the western world to this day, represented a giant leap in this development when it first flew, and supersonic civil transport airplanes are back on the drawing board. Great effort and financial funding have been put in to develop such aircraft. The High Speed Civil Transport (HSCT) is the name of the American project. An HSCT will of course go faster and also fly higher than

conventional subsonic transport airplanes, and the engine technology will most likely be quite different from existing turbofan engines. This development will raise environmental issues in the years ahead.

2.4 Commercial Air Traffic in Norway

2.4.1 Similarities and differences to the rest of the world

Since the end of the Second World War, Norwegian and Scandinavian aviation history is, roughly speaking, not very different from that of the rest of the western world. Norway does not have an aircraft manufacturer of its own, therefore American and European aircraft have been operated in this country, in both the civil and military sectors.
The growth in Norwegian civil aviation has not quite kept up with European trends. The latest figure in the ICAO statistics (ICAO Journal, Vol. 51 - No.6, 1995), which in this case covers Scandinavia as one unit, reports an increase from 1994 to 1995 for all traffic (in passenger-km) of 1 %, and international traffic 2 %. Corresponding figures for some countries in Europe and North America are as follows:

	All traffic [% passenger · km]	International traffic [% passenger · km]	
Finland	27	30	
Canada	11	13	
United Kingdom	9	9	
Germany	9	9	
Netherlands	9	9	
Spain	5	7	
USA	3	4	
France	0	0	
Greece	-6	-7	
Scandinavia	*1*	*2*	*(ICAO statistics)*
Norway	*4*	*3*	*(number of passengers, Norwegian Civil Aviation Administration)*
Total ICAO-states	6	9	

Table 2.3 Percentage growth in civil aviation, 1994 – 1995, for some ICAO states
(Information in *italics* is added by the author)

Numbers from the Norwegian Civil Aviation Administration (Luftfartsverket, "Civil Aviation Administration Annual Statistics", 1994, 1995, 1996) are different from the ICAO ones. This is obvious even though we do not find variables that completely correspond in the two publications. According to the Civil Aviation Administration, the number of passenger-kilometers flown domestically by Norwegian carriers increased by 5 % from 1994 to 1995. The number of passengers in and out of Norwegian airports in the same time span grew approximately 4 %, passengers on international flights in excess of 3 % (calculations based

on numbers from Luftfartsverket, "Civil Aviation Administration Annual Statistics", 1994, 1995, 1996). The reason for the deviation may be that ICAO only considers the SAS figures, and these may not be representative for the traffic at Norwegian airports.
Compared to average numbers for the ICAO, Norway appears to be slightly on the weak side, and its figures are quite similar to those for the USA.
Number of passenger-kilometers flown in Norway (domestic only) in 1995 was 3.57 billion. Freight and mail combined for the same year was 21 million tonne-kilometers (Luftfartsverket, "Civil Aviation Administration Annual Statistics", 1994, 1995, 1996). The average Norwegian flew around 800 km in 1995.
ICAO statistics for some countries in 1995, see Table 2.4 (the Traffic/inhabitant column is added by the author).

	Total traffic [10^9 ·pass.·km]	International [10^9 ·pass.·km]	Domestic [10^9 ·pass.·km]	Traffic/inhab. [km/person]
Finland	9	8	1	196
Canada	48	31	17	584
United Kingdom	152	146	6	105
Germany	64	58	6	77
Netherlands	46	46	0.06	4
Spain	28	19	9	230
USA	849	238	611	2444
France	68	45	23	400
Greece	8	7	1	94

Table 2.4 Passenger traffic in some ICAO states in 1995 (ICAO)

Apparently traveling by air is more common in Norway than in many other European countries.

The increase in number of airline passengers to and from Norwegian airports shows a further and steeper growth the following year. From 1995 to 1996 it was 10.7 % and for the international part alone 12.5 % (Luftfartsverket, "Civil Aviation Administration Annual Statistics", 1996).
In this work it is of interest to mention the international flights across Norwegian territory en route from one airport outside Norway to another. More than 14 000 flights and 9 million flown kilometers were logged in this category, and a 4.5 % increase in the kilometer figure was observed from 1995 to 1996. The 9 million kilometers add 15 % to the total distance (61.7 million kilometers) of domestic commercial flights in Norway.

2.4.2 The commercial fleet

The major airlines in the Norwegian civil air transport system (helicopter companies not included) are the Scandinavian Airlines System (SAS), Braathens and Widerøe's Flyveselskap A/S. Together they employ 93 % of all people in this business, SAS 50 %, Braathens 36.5 % and Widerøe's Flyveselskap A/S 7 % (in 1995) (Luftfartsverket, "Civil Aviation Administration Annual Statistics", 1994, 1995, 1996). These three companies operate twin engine aircraft exclusively for domestic flights; e.g. MD80s and MD 90s, DC-9s, Boeing 737s, and Dash 8s, all are jet aircraft except for the turboprop Dash 8.
Out of all fixed wing aircraft registered in Norway by companies (December 1995) there are 65 jet twins, 4 four engine turboprops and 67 turboprop twin engine airplanes. All the Braathens, Widerøe and Norwegian SAS airplanes are included in the lot.
The aircraft fleets of the three companies are quite modern. Braathens claim they have one of the newest fleets in Europe, less then 5 year-old airplanes on average. SAS is currently (1999 / 2000) buying new Boeing 737-600 airplanes and has 8 MD-90s. The company still has around 100 MD-80s and DC-9s. The Widerøe fleet consists of Dash 8 aircraft only, of which a constantly growing fraction is modern Dash 8-300 airplanes. This information is all according to the companies' Internet pages in March 2000.

2.4.3 Scheduled flights

In 1995, the commercial Norwegian airlines flew 213 937 domestic flights covering 61.7 million kilometers and a total flight time of 142 387 hours. The average flight distance and flight time are 288 km and 40 minutes, respectively.
Except for the connections between Oslo and the northern Norwegian cities and the Tromsø-Svalbard route, domestic flights in Norway are short. Typically Stavanger - Bergen, Bergen – Ålesund, and Oslo – Kristiansand are flights of 20 minutes or less. Braathens, one of the major operators in the domestic market, as an example, fly Boeing 737s that are capable of regular cruise flight around 40 000 feet altitude. In the very short flights of less than a half hour of duration they never reach that altitude. A standard flight leg will be the take-off and climb-out to 25 000 feet, then a few minutes cruise, and then descent.
The statistics from Luftfartsverket 1996 (Luftfartsverket, "Civil Aviation Administration Annual Statistics", 1996) reveal that 33 % of all scheduled domestic passenger traffic in Norway go to/from Oslo airports, 11 % to Stavanger, 15 % to Bergen, 6.6 % to the Moere airports and 12 % to Trondheim airport. 78 % of all departures/arrivals are at these airports. Domestic passenger movements between destinations from Trondheim and south are 68 percent of all passenger travel in Norway.
The Oslo airport Fornebu was the main hub for international flights until October 1998. 80 % of all airline passengers going to and coming from destinations abroad came through that airport. Stavanger and Bergen have 8 - 10 % each and the far northern airports Tromsoe and Bodoe have 0.2 % and zero respectively (Luftfartsverket, "Civil Aviation Administration Annual Statistics", 1994, 1995, 1996).

2.4.4 Reasons for the status of air transport in Norway

The rocky and mountainous country and the weather-beaten coastline offer harsh conditions for those who need to move around our country. Building roads and railways has become very expensive, going by sea is really unpleasant many times, and driving a car across the country may be quite uncomfortable, during the fall and winter seasons in particular. This probably explains why going by air is a convenient and necessary means for transportation to many people in Norway.
The population is sparse, particularly north of Trondheim, with the average for all of Norway being 14 people per square kilometer. Out of the 4.4 million people (1997) 87 % of all Norwegians live in the southern part of the country, that is from Trondheim and south, which again is 58 % of the total area.
On the west coast, the three centers: the Moere region, Bergen and Stavanger, in the south-east Oslo and the Oslo Fjord region (Oslo, Akershus, Østfold and Vestfold counties) and to the north, Trondheim have more than half the total population in Norway. 62 % of all industry (employees and gross value of production) are located in those five areas.
With the geographical distribution and social structure of our society, the Norwegian domestic air traffic typically has some clear characteristics:

1. many short flights, in some cases extremely short, between the centers of southern Norway,
2. longer flights to the northern destinations, in fact the per capita rate of flying is higher in the northern areas then for the rest of the country,
3. the feeder traffic from domestic airports to the international flights that for the most part go out of the Oslo airports.

Since North Sea oil was discovered, Norway has become one of the richest countries in the world. The standard of living and welfare benefits are high in Norway, many people travel for pleasure, and going by air is affordable. Quoting the Civil Aviation Administration Annual Statistics: "The Norwegian air traffic had a considerable growth in 1996. This was due to the continued cyclical upswing in the Norwegian economy, as well as increasing competition between the two largest airlines. These airlines celebrated the 50th anniversary by selling special fare tickets, which further increased the traffic growth."

2.5 Emissions from Aircraft

2.5.1 Categories

Among all categories of waste from commercial aviation activities the gaseous emissions from the engines are probably causing the most concern among the public. Total fuel consumption by aircraft in scheduled traffic in 1997 was approximately 250 million tonnes. According to (Nüβer, H.-G., Schmitt A., 1989) and assuming a more or less constant traffic growth, one billion tonnes of exhaust gases were released into the atmosphere from scheduled commercial air traffic alone that year. In fact that is not a large portion of the total emissions of pollutant gases to the atmosphere, in the range of 3 %. The reasons for particular concern

are the aircraft exhaust that is concentrated close to airports and the fraction that is released at high altitude.
Airborne traffic also contributes indirectly to air pollution by all the activity located close to airports such as cars and buses, and one may see considerable consequences locally from those emissions.
Fluid waste caused by air-related activities enters the environment close to airports (Cornish, J.L. et al.,1996 p33). Deicing chemicals for aircraft and runways, detergents, fuel leaks and leak from toilet containers, spill of oil and chemicals from maintenance shops are all examples of polluting fluids that may find their way to the sewage system, the surface water drains or directly into the ground water.
Examples of solid waste from the airport activity also exist. Trash, all the way from food leftovers to used writing paper and workshop material is generated here as in all parts of the society.
Aircraft noise was a big issue some ten years ago. Strict regulations have been set to lower the noise emissions from airplanes and limit night operations. The noise from air traffic is still of concern to people living in the vicinity of airports, and the low noise emission level is still emphasized as a quality of an airplane.
Fluid waste, solid waste and noise emissions at airports are all beyond the scope of the present work and will not be discussed any further.

2.5.2 Gaseous emissions

Two main categories of fuel are used in aircraft gas turbine engines, kerosene-based fuel Jet A is one example, and the other is gasoline fuels like Jet B and JP 4. All these fuels have certain features and properties in common. They are all light oil distillates with densities between 750 and 790 kg/m^3, and the specific energy of combustion ranges between 42 and 45 MJ/kg. Aromatic content is 22 - 25 percent (volume) and sulfur must not exceed 0.30 % (mass). According to recent references (Walsh, P.P., Fletcher, P., 1998), kerosene is used almost exclusively in aircraft engines today.
The physical properties are tailored to suit the special conditions that occur during flight, such as large pressure and temperature variations, and strict regulations to reduce fire hazard.
The main components in the aircraft engine exhaust, as with all combustion of hydrocarbons, are water vapor and carbon dioxide. If the conditions are not ideal for complete combustion, minor proportions of unburned hydrocarbons, generally identified as C_XH_Y or UHC, and carbon monoxide will be present in the exhaust. A quite small quantity of soot, which is pure solid carbon (C), is sometimes formed, and the really low sulfur content ends up as a minor portion of sulfur oxides SO_X.
With normal operation, the temperature in the combustion chamber is quite high with turbine inlet temperatures typically being at about 1500 K. The flow of fresh air into the hottest areas is high as well. Combined with certain flow parameters in the combustion zone this may give favorable conditions for the nitrogen in the air to combine with oxygen to form nitric oxides. This group is usually denoted N_XO_Y or just as NO_X.

The formation of water vapor and carbon dioxide is an unavoidable consequence of burning hydrocarbons. Quantities of these products are therefore directly linked and related to the chemical composition and the consumption of the fuel.
Sulfur oxides form directly on the sulfur that is present in the fuel.
Unburned hydrocarbons, carbon monoxide, soot and nitric oxides are produced depending on the conditions inside and downstream of the combustion zone. The amounts of these components in the exhaust therefore depend on the engine design, current mode of operation and the technical condition of the engine.
Estimates done by Lufthansa for the complete Lufthansa fleet in 1989 (Nüßer, H.-G., Schmitt A., 1989) show typical and probably representative figures for the relative content of air pollutants in aircraft exhaust, see Table 2.5. Parameters that typically influence the production of each particular component are listed as well.

	[g/kg]		Mainly depending on
H_2O	1239		fuel consumption
CO_2	3154		fuel consumption
CO	0.7 – 2.5	⎫	engine type
N_XO_Y	6.0 – 16.4	⎪	power setting
C_XH_Y	0.05 – 0.7	⎬	flight altitude
(C)	0.007 – 0.03	⎭	airspeed
SO_2	1		fuel quality

Table 2.5 Specific emissions of air pollutants (g/kg Kerosene) under cruise conditions for the Lufthansa fleet (Nüβer, H.-G., Schmitt A., 1989).

In engine operation other than cruise, the relative quantity of the exhaust components will change. At lower altitude the ambient temperature, pressure and air density are high. During take-off and climb the power settings are high, and in the descent phase the power setting is low compared to the cruise setting. Therefore the conditions inside and close to the combustion zone will change during the flight and affect the formation of exhaust gases.

2.5.3 Basic chemistry of combustion

The main chemical reaction inside the combustion chamber of a gas turbine running on a hydrocarbon fuel C_nH_m is generally described by the following equation:

$$C_nH_m + \lambda \cdot a\,(O_2 + 3.76\,N_2) \rightarrow b\,CO_2 + c\,H_2O + d\,CO + e\,H_2 + f\,O_2 + g\,N_2 \qquad (2.1)$$

The λ denotes the quantity of air taking part, as a fraction of what is necessary for complete oxidation of the fuel; $\lambda = 1$ giving a stoichiometric combustion. The coefficients *a* to *g* are evaluated when the equation is balanced for a particular fuel and air supply. For a stoichiometric reaction, coefficients *d*, *e* and *f* are close to zero. In the reaction products from a lean fuel/air mixture, $\lambda > 1$, no CO and H_2 will be present, all reacted into CO_2 and H_2O respectively and *d* and *e* are both zero. From a richer than stoichiometric reaction, $\lambda < 1$, all components except O_2 are present, meaning *f* is zero.

Equation (2.1) includes only reaction products that appear in relatively significant quantities. For the purpose of the present work the minor product species, unburned hydrocarbons, nitric oxides and sulfur oxides, also have to be considered. These reactions have been studied empirically and analytically during the last decades e.g. (Correa, S.M., 1992). Descriptions and methods as presented by Lefebvre in Lefebvre, A.H., 1983 is used extensively in the present work because its empirical approach allows for adjustments to the real case of this study.

It is a trivial fact that hydrocarbon burning is being used because the overall combustion is an exothermic reaction. The temperature of the products inside and immediately downstream of the reaction zone, given a specific fuel, among other factors, depends on the fuel-to-air ratio and admixing of cooling air. The highest adiabatic flame temperature is achieved with a close to stoichiometric mixture. The forming of certain exhaust components is highly dependent on the temperature and the mass flow rate in the flame and the combustion chamber. These are parameters that vary with engine loading, and the general trend of how emission quantities depend on loading is shown in Figure 2.4 (Lefebvre, A.H., 1983): in gas turbine engines at idle speed, i.e. low combustion temperatures and slow airflow into the engine, CO and UHC (HC) are emitted at a higher rates than otherwise, while NO_X emission is at its lowest. Smoke, which in this case is soot, has its minimum production rate at a slightly higher power setting. With increasing power and subsequent higher temperatures in the engine, both NO_X and smoke increase while CO and UHC fall.

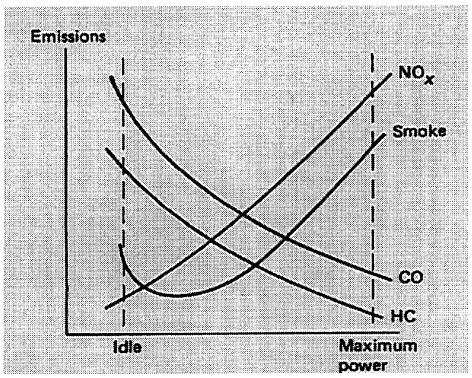

Figure 2.4 Emission characteristics of gas turbine engines (Lefebvre, A.H., 1983)

The relation between CO and NO_X emissions and the temperature in the flame, the primary-zone, is demonstrated by Lefebvre in Figure 2.5. The temperature range at which both components are kept at acceptable levels (according to automotive standards of 1977 (Lefebvre, A.H., 1983)) is 1600 K < T_{pz} < 1730 K.
The speed at which the chemical reactions occur is limiting to the quantities of certain emissions. In other words, the time at which the gases reside in the hottest zone, the residence time, is critical. This applies in particular to the CO and NO_X.
The carbon dioxide and water vapor are large fractions of the exhaust and therefore in practice independent of the varying quantities of the other species. For the purpose of the present study the quantities of the major combustion products, carbon dioxide and water vapor, are considered independent of the conditions inside and around the combustion zone in normal operation.
The formation of CO, UHC and NO_X, which depend on such parameters, will be discussed separately.

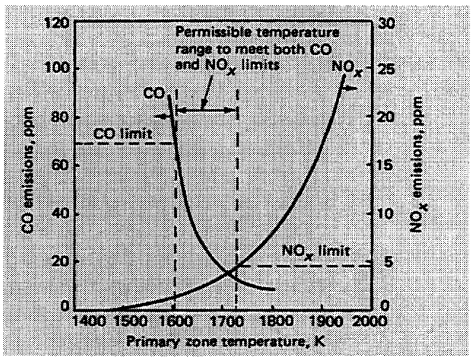

Figure 2.5 Influence of primary-zone temperature on CO and NO_X emissions (Lefebvre, A.H., 1983)

Carbon monoxide appears in the exhaust if either the primary zone has not been sufficiently hot for the oxidation of CO to CO_2, or the CO has been quenched too soon by cooling air or at colder combustor walls. With a slower admixing of the cooler air, additional oxygen is added to encourage further oxidation without cooling too drastically to freeze the CO.
The important reactions to remove CO are, according to Lefebvre (Lefebvre, A.H., 1983), at higher temperatures

$$CO + OH \leftrightarrow CO_2 + H \tag{2.2}$$

and at lower temperatures

$$CO + H_2O \leftrightarrow CO_2 + H_2 \tag{2.3}$$

Unburned hydrocarbons are droplets of pure fuel and lighter hydrocarbon molecules (Lefebvre, A.H., 1983). The reasons why these fuel remains are not burned are comparable to the lack of CO oxidation; too low temperature and quick cooling and quenching of the combustion process. In addition, the physical processes of the atomization of the fuel flow and the mixing of fuel and air are essential. When it is poor, the droplets get too large for complete evaporation, stopping fresh air from coming into contact with all the fuel during the hot zone passage.

The classical description of NO_X formation is presented in a large number of texts and articles. NO is produced by four different mechanisms in the combustion chamber:

1) The prompt NO is produced at the flame front especially where the local conditions are fuel-rich, and the reaction is fast. According to Lefebvre, A.H., 1983, prompt NO is produced at low temperatures, and the level of prompt NO_X cannot be predicted accurately. More recent texts like Røkke, N.A., 1994 explains that the reaction is not very sensitive to temperature, and confirm that the mechanism still is not very well understood.

2) Thermal NO forms in the post-flame gases by the oxidation of atmospheric nitrogen during a fairly slow set of reactions, the so-called Zeldovich chain mechanism:

$$O_2 \leftrightarrow 2O$$
$$O + N_2 \leftrightarrow NO + N$$
$$N + O_2 \leftrightarrow NO + O$$

This mechanism is dependent on the temperature and the highest rate of formation occurs at a moderately fuel-lean condition when the temperature is high and a sufficient amount of free oxygen is available.
The combustor residence time is an important parameter, and Equation (2.4) quoted in Lefebvre, A.H., 1983 gives a good indication on how the NO emission index, mass of NO per unit fuel, depends on adiabatic flame temperature T_{ad} [Kelvin] and combustor residence time t_{res} [milliseconds].

$$\ln \frac{NO_{EI}}{t_{res}} = -72.28 + 2.80\sqrt{T_{ad}} - \frac{T_{ad}}{38} \qquad (2.4)$$

3) The nitrous mechanism is formation of NO via N_2O. N_2O occurs mainly in fuel lean conditions (Røkke, N.A., 1994), and if the further reactions to NO and N_2 is quenched, N_2O will occur in the exhaust gas.

4) The fuel NO is the oxidation of fuel-bound nitrogen. In light distillate fuels the content of nitrogen is very low, and therefore this reaction is of little significance for aircraft engines.

Oxidation of NO into NO_2, which is more stable at lower temperatures, mainly happens when the temperature is in favor of this reaction, around 700 K. For a practical aircraft engine in flight, such conditions will normally occur in the exhaust stream outside the engine.
Sulfur oxides and soot, as already indicated, are only present in very small quantities in emissions from modern commercial aircraft. Descriptions of the formation mechanisms of these components are therefore omitted here, and emissions of sulfur oxides and soot are not discussed any further in this work.

2.5.4 Aircraft operation and emissions

Gaseous emissions form inside and close to the combustion zone. The main conditions that change with the variation in performance requirement, state of technology, and the engine status are:

- flow pattern in the combustion chamber,
- local and global fuel-to-air ratios inside and in the vicinity of the combustion zone,
- temperature, pressure and density of the air entering the combustion chamber.

In addition, when engine performance deteriorates, the fuel consumption will have to be increased to maintain output power.
It is obvious that when operation is optimized for the lowest possible fuel consumption, water vapor and carbon dioxide emissions are minimized as well. Other exhaust components are also related to the fuel consumption to some degree, this is discussed extensively later in this work. To keep their costs down, airlines will optimize flights with respect to fuel consumption; fly direct routes, avoid loitering around airports, and chose the most favorable speed/altitude pattern. No study has been reported on whether the fuel optimized operation is also a minimum CO, N_XO_Y and C_XH_Y emissions operation. Choice of altitude is not invariant to the detrimental effects from the exhaust gases on the atmosphere. The established flight routes may not be the most advantageous ones in this respect.
With varying flight altitude, i.e. changes in ambient temperature, pressure and air density, and different power settings, higher at take-off and climb, lower at cruise and even lower in the descent phase, changes in the conditions inside and close to the combustion zone are observed. In many flight conditions, engine components operate at reduced efficiency compared to their design values.
Performance reduction due to component and engine deterioration over time contributes to a general increase in fuel requirements and change in engine operation parameters. Engine maintenance is therefore of major importance to the level of emissions.
Aircraft and engine technologies have changed over the years and two driving factors in this development are improvements in fuel efficiency and emission characteristics. Airlines emphasize their environmental concern, the quality of their aircraft and the company strategy in that respect, even in the airlines' approach to the public. Maintaining engine efficiency so that it is close to the level of a new engine at all the times should be a major element in meeting such ambitions.

2.5.5 Aircraft emission regulations

Regulatory requirements issued and enforced by the ICAO focus only on the landing and take-off cycle, LTO, (below 3 000 feet above ground level). Also only new aircraft/engines are considered. The level of allowable emissions for a standard LTO cycle and a high bypass turbofan engine, in grams of emission per kilo-Newtons of thrust is (Intergovernmental Panel of Climate Change, 1999)

Unburned hydrocarbons (UHC):	19.6	g/kN
Carbon monoxide (CO):	118	g/kN
Nitric oxides (NO_X):	80.2	g/kN

Recently ICAO and CAEP (Committee on Aviation Environmental Protection) (Intergovernmental Panel of Climate Change, 1999) have considered emissions variability over the entire flight cycle.
It is acknowledged that engine deterioration is a reason for a change in specific fuel consumption (SFC) and engine temperatures. According to (Intergovernmental Panel of Climate Change, 1999): — "Economic considerations recently led to allowable SFC limits of between 2 and 4 % because of engine deterioration; exceedances lead to engine overhaul."

2.6 Environmental Issues Related to Gaseous Emissions from Air Traffic

2.6.1 Regional consequences, the LTO cycle

There seems to be general opinion that emissions from air traffic should be considered air pollution. Some of the exhaust components have a negative effect on living conditions and may cause discomfort and health problems, directly or indirectly to the local population as well as animals and plants. In the vicinity of major airports this is first of all a local problem, numbers of airplanes dump large quantities of exhaust during take-off, landing and taxiing every day. It all happens within a limited area and at low altitude.
The landing and take-off cycle (LTO) includes the descent from 915 m (3000 ft) above the airport, all motion on the ground and the first 915 m of climb (Knudsen, S., Strømsøe, S., 1990). Emissions from aircraft in the LTO envelope are usually defined as the local, or "the local and regional emissions" in the area. All emissions at altitudes higher than 915 m above ground level will be counted as global pollution.
Local emissions from aircraft will of course add to other air pollution in the area. Activities at an airport and close to it, such as the ground traffic, generate emissions. Smoke from the heating of nearby buildings and emissions from local industry may all be present. The quantity of aircraft exhaust is not necessarily a considerable contribution. However, when looking at the exhaust components we find some of them are significant for the conditions in the local environment.

NO_X in lower altitudes can contribute to the formation of acid rain, and it will take part in chemical processes that produce ozone, so called photochemical smog, urban smog (Archer L.J., 1993).
The impact of CO from aircraft on the local environment is not very severe. Studies find that aircraft generated CO represents just a few percent of total pollution in the region. Nevertheless, there are negative effects. These are mainly that 1) CO contributes along with NO_X in the formation of ozone, and 2) in locations where the CO concentrations are quite high, such as behind an aircraft during start up and taxiing, it may cause a reduction in mental and physical abilities of people.
According to (Archer L.J., 1993) hydrocarbons (UHC) from airports represent less then 0.5 % of all UHC in the ground air. Effects of low level hydrocarbons are the formation of smog, and they are prone to cause cancer.
The exhaust components that are large in volume, carbon dioxide CO_2 and water H_2O are not regarded as a threat to the local environment. At high altitude the situation is totally different and that will be discussed later. Low altitude SO_2 and soot (C) are also of minor importance. Airports are insignificant as compared to other local sources of SO_2 and soot. The quantity from jet engines is too small to have any impact to the ground air quality (Archer L.J., 1993).
Aviation authorities have requirements regarding the air quality around airports, and many of the larger airports have monitoring systems to check that the local levels of CO_2, NO_2 and HC are within acceptable limits. (Gardener, R.M., 1995)
The different components remain in the atmosphere for some time. NO_X in lower altitudes will be washed out by rainfall, normally within a few days, while the atmospheric life time for CO is 2 - 3 months and for CO_2 rather long, 50 - 200 years (Price, T., Probert, D., 1995).

2.6.2 Global Consequences

Stordal and Pedersen in the NILU report "Regional and Global Air Pollution from Aircraft" (Stordal, F., Pedersen, U., 1992) describe the physics of the global atmosphere in relation to high altitude emissions. A basic understanding of these principles are essential to see how pollution in these air masses is of any concern.
With the standard (average) atmosphere condition, the air temperature decreases linearly with altitude for approximately 11 000 meters. This lower part of the earth's atmosphere, called the troposphere, is characterized by a strong vertical mixing of air masses.
Above the troposphere there is a thin layer called the tropopause, and the following 30 – 40 km is the stratosphere. Climbing into the stratosphere, the temperature is constant at first, and then starts to rise again from an altitude of about 20 000 meters (Stordal, F., Pedersen, U., 1992). Ultra-violet light that is absorbed by ozone at these heights is the reason for such temperature gradient, and the gradient itself suppresses vertical air motion. With the lack of vertical motion, there is little exchange of emission gases in these areas, they will remain at steady altitude until they are broken down chemically or spread by diffusion.
The majority of atmospheric ozone O_3 is in the stratosphere, as shown in Figure 2.6 (Stordal, F., Pedersen, U., 1992). This high altitude ozone, with a peak concentration around 25 000 m altitude, has been subject to scientific and public attention in the last decade. The ozone concentration has decreased especially in arctic regions. There is reason for concern as the

stratospheric ozone is the shield that is protecting the earth surface from high ultra-violet radiation.

The tropopause altitude varies with latitude. It may be seen from the graph in Figure 2.7 (Stordal, F., Pedersen, U., 1992) that in the tropics, the stratosphere starts around 16 km while in the northern sub-arctic regions, like Scandinavia, the tropopause is down to around 5 000 meters.

The upper troposphere and stratosphere effects from aircraft emissions extend beyond regional borders. Except for increased cloud cover from aircraft contrails (stratospheric) which appears to be a local consequence, the two main effects are the ozone layer destruction and the greenhouse effect, both of which are issues of global importance.

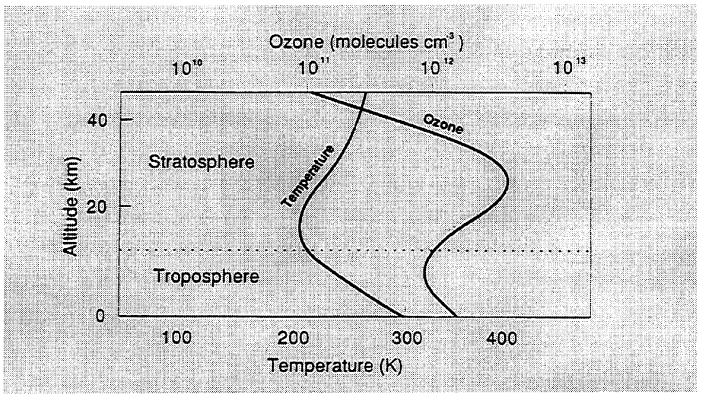

Figure 2.6 Temperature profile and distribution of ozone in the troposphere and the stratosphere (Stordal, F., Pedersen, U., 1992)

The protective ozone in the stratosphere is called the ozone layer. The nitric oxide NO_X reacts with oxygen atoms and ozone molecules such that ozone concentration is reduced. In a different mechanism NO_X and unburned hydrocarbons (methane) contribute to the formation of ozone. These two contradictory mechanisms both depend on ultra-violet radiation. The formation and destruction rates vary with altitude as shown in Figure 2.8 (Stordal, F., Pedersen, U., 1992). Figure 2.8 also shows that the net change in ozone due to nitric oxides and unburned hydrocarbon is positive below approximately 12 000 meters and negative above that level (Cornish, J.L. et al., 1996). Stratospheric emissions from aircraft thus contribute to the destruction of the ozone layer.

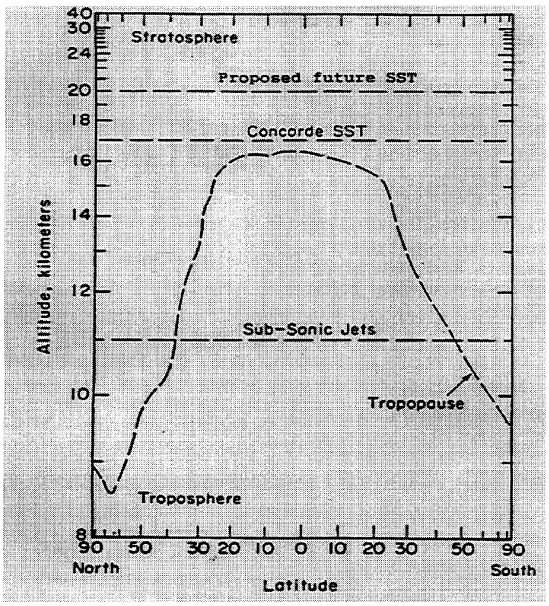

Figure 2.7 Tropopause altitudes at various latitudes (Stordal, F., Pedersen, U., 1992)

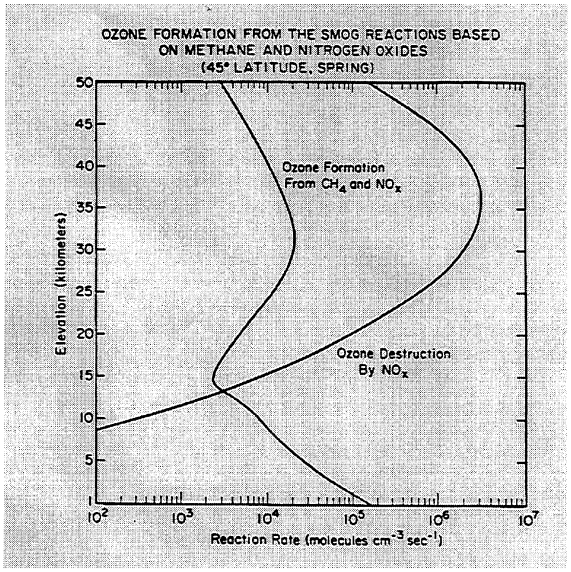

Figure 2.8 Rates of ozone formation and ozone destruction due to photochemical reactions involving NO_X species in the troposphere and the stratosphere (Stordal, F., Pedersen, U., 1992)

High energy radiation from space penetrates the atmosphere while infrared radiation from the earth's surface is absorbed by certain molecules present in the air, and the absorbed energy causes temperature increases. When anthropogenic emissions contribute to intensify this process, it is called the greenhouse effect. The accumulated heat is suspected to cause a global warming. Among the most important gases in this picture, the so-called greenhouse gases, are the main components in aircraft exhaust, i.e. H_2O, CO_2, CH_4 and NO_X.
The contrails, or line shaped clouds that form after airplanes flying at high altitudes are condensed water vapor from the exhaust and the immediate surrounding atmosphere. This is a most visible phenomenon, and a somewhat unpleasant nuisance to people enjoying the sunshine. A more serious effect is that contrails disturb and enhance the natural cloud cover and contribute to warming of the earth's surface. Contrails cover (1992) on annual average 0.1 % of the earth's surface and is projected to grow to 0.5 % during the next half century (Intergovernmental Panel of Climate Change, 1999).
One last aspect is that the earth's environment is far more sensitive to stratospheric than to surface emissions, the main reason being that at high altitude the gases have a very long residence time. Because of that, gases will accumulate and cause continuously increasing concentrations, and we do not know the long time consequences of this development (Price, T., Probert, D., 1995).

2.7 Current Status in Aircraft Exhaust Emission Abatement

2.7.1 Achievements and state of understanding

The exhaust emissions from jet engines have a potential to destroy the earth's environment, and fuel prices are uncomfortably high at times. For these reasons the efforts to directly and indirectly reduce the pollution, have followed two main tracks:

1) modification of the conditions inside and around the combustion process to avoid the formation of undesired gases, and

2) making the combustion process, the engine, and the entire airplane more efficient and thereby reduce both the fuel consumption and the amount of exhaust gases. Improving combustion efficiency will usually contribute along the first track as well.

Understanding the close relationship between the conditions in the combustion zone and the formation of the NO_X, CO and UHC components has led to certain modifications. The aim has been to control the fuel/air ratio, temperature and primary zone residence time, such that they may be kept closer to optimal levels in a wide range of operation.

> Fuel nozzle concepts that perform well in the atomization of the fuel and mixing with the air at all power settings are examples. The premixing and/or prevaporization is one principle that has been studied, i.e. the fuel/air is prepared for burning as it reaches the hot zone. The fuel is either fully vaporized or in small particles evenly distributed in the air. When the fuel mixture reaches the flame zone it will burn much faster than a fuel sprayed directly into the combustion zone. There will be no extremely hot spots in the flame zone and time that is required for the fuel to vaporize, mix with air and burn is reduced.

Also introducing rotating motion, swirl, in the combustion chamber will contribute to a better mixing upstream and downstream of the combustion zone.

Another technique called staged combustion has become a practical solution and is offered optionally with some engines, for example the recent models of the CFM56 engines from CFM International. In staged combustion, one combustion chamber set is optimized for lower power settings and will be in operation at those settings. At higher power requirement a second set of burners is activated, and operates while performance is at this level or higher. In this way combustion efficiency is kept closer to optimum at the most important power settings, and a cleaner combustion is achieved.
A different principle, not yet seen in practical aircraft engines, is based on the fact that NO_X production increases with the temperature. The rich, quench, lean combustor (RQL) has a rich fuel/air mixture primary zone followed by a quench zone where cold dilution air is mixed in to cool the gases and stop the high temperature reactions, and finally a lean burn zone where the combustion is completed at a relatively low temperature. This burner has shown good NO_X characteristics. An NO_X reduction of 50 % compared to conventional combustors is indicated (Zaralis et al., 1992) (Menon, S. et al., 1992).

Driven by increasing fuel prices in the early seventies a new concept was developed. Instead of the ducted fan on conventional turbofan engines, a fan-like propeller was fitted on large turbine engines. Prototypes were built and tested both by General Electric, the so-called "Unducted Fan", and Pratt & Whitney/Allison named theirs "The 578-DX Propfan". Calculations and tests documented fuel savings from 6 - 7 % and up to 40 - 50 % compared to conventional engines. These concepts were never taken into practical use in the western world (Fuller, N.H., 1994) (Jones, M.C., 1981) (French, T., 1988) (ICAO Journal, Vol. 46 - No. 2, 1990).

Recent work at NASA Dryden (Myers, L.P., Connors T.R., 1992) (Stewart, J.F., 1992) shows that by a more careful control of the flight, the fuel consumption can be lowered considerably. Integrated controllers for flight and engine operation will assist the pilot, and tests prove that a reduction in thrust-specific fuel consumption of approximately 15 % is achievable.
If such controller devices are implemented for aircraft in flight, it will of course make a great contribution to the effort on exhaust emission abatement.

There seems to be general awareness about the environmental issues related to air transport, in industry as well as the public domain. Manufacturers of engines and aircraft market their products as environmental friendly, the airlines inform their passenger how environmental consciousness is reflected in their company policy. Apparently the effort in making better equipment and more efficient routines has considerable momentum, and a series of improvements should be expected.

2.7.2 Possible solutions for the future

We may find in the future that the solution for low emission air traffic lies beyond the concept of burning fossil fuels. Serious studies and research in using hydrogen as the energy carrier for aircraft propulsion has been performed. The Tupolev Design Bureau in Russia

pioneered experiments of this kind (Pohl, H.W. et al., 1995) during the energy crises in the seventies. Gas turbine engines built for kerosene, with modifications, are able to run on hydrogen, and a TU-155 was flown on both liquid H_2 and natural gas.
The project later on proceeded as a collaboration between Tupolev and Deutche Aerospace Airbus. The project demonstrated the viability of hydrogen powered airplanes for passenger transport. Within the framework of the Euro-Quebec Hydro-hydrogen Pilot Project (EQHHPP) the effort has continued (Drolet, B. et al., 1996). Improvements and modifications of the engine and the combustion process were parts of the EQHHPP, which started in 1992.
The great advantages in using hydrogen fuel are that:

- H_2 may be produced without any pollution whatsoever, by using solar power and electrolysis,

- no carbon dioxide, unburned hydrocarbons, soot, or sulfur oxides are formed in the combustion process.

Still, water vapor is the major combustion product, and NO_X from the air nitrogen will be formed. As already discussed, both gases pose a threat to the global environment.
Interesting new concepts, among which hydrogen fuel is a good example, may be launched in the years to come. Solutions that are technically acceptable and environmentally favorable will be found. Whether or not the solutions will come into practical application is the next question. The industry and airline companies need to make profit, the level of safety, in the air and on the ground, is not to be traded with, and public acceptance is essential. There is usually a general reluctance towards new technology. National and global legislation will play a role in forcing the changes to be made. Future climate changes may urge society and also the aviation industry and airline passengers to change their opinions and choose less damaging solutions. Aviation may or may not be one of the battlefields in which the fight for a better environment will take place.
Even mass media are major players in this game. In his book "Selling Science. How the Press Covers Science and Technology" (Nelkin, D., 1994), D. Nelkin raises this issue. In his discussion of the role of media in the adoption of new technology he says, "Many factors enter the reader's social context, including the cumulative influence of past media images and various alternative sources of information and imaginary, such as fictional television stories, documentaries, comic strips, and other vehicles of popular culture." Also from The New York Times: "a breakthrough technology is a breakthrough only if people adopt it, using it to change the way they work and live." In other words, any new or improved concept or device invented and offered by the scientific and technological community is not necessarily taken into common use for the pure reason of being a good or a wise solution to some problem.
Aviation has in recent history changed everybody's opinion about travelling and transport more dramatically than any average man or woman would even dream of only a century ago. Quite possibly once again new answers to global concerns, about the environment, greenhouse effect and ozone layer destruction, will come through this field of technology.

3 TURBOFAN ENGINE PERFORMANCE — PRELIMINARY STUDIES

3.1 Introduction

The principle of a turbofan engine is sketched in Figure 3.1. The air flow into the engine is split in a core flow and bypass flow downstream of the large fan. The core flow is taking part in the combustion process, under high pressure. It then expands through turbines and the core nozzle. The bypass flow provides thrust by being compressed through the fan and then accelerated in the bypass nozzle. Most turbofans are two spool engines, which means that the fan and low pressure compressor rotate on a common shaft, the low pressure spool, and the high pressure compressor and the high pressure turbine are connected on the high pressure spool.

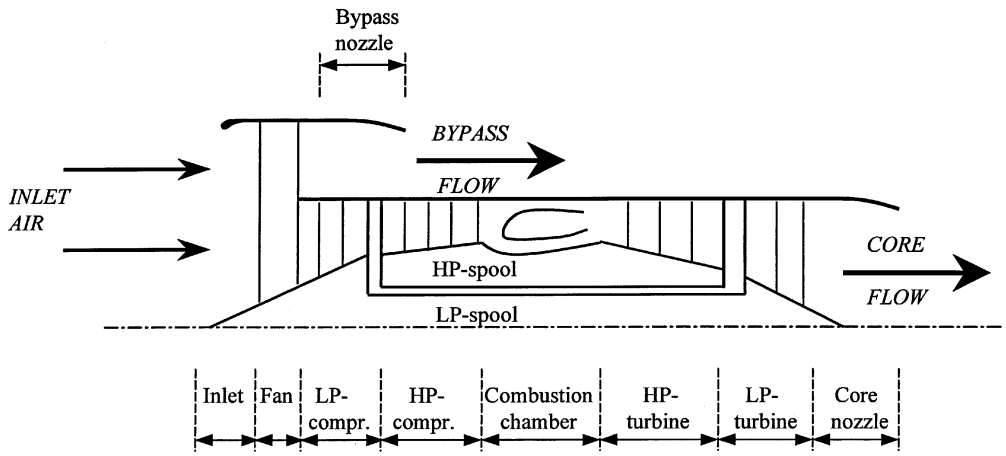

Figure 3.1 Schematic drawing showing a two spool turbofan engine, separate exhaust

Parametric studies can be used as a quite simple tool to analyse and thus help understand the behaviour of thermal energy engines. Both the design condition of the engines and other conditions for standard operation can be analyzed. One method for parametric studies was used as presented in this chapter, for two purposes:

1. to demonstrate how engine deterioration relates to changes in some key parameters that are influential for exhaust emissions, and

2. to form the basis of a simple computer model that is able to simulate engine operation and the variations in several engine parameters throughout a complete flight cycle.

3.2 Aircraft Engine Deterioration and its Influence on Certain Engine Parameters

The performance of any mechanical device deteriorates during operation, and aircraft gas turbine engines are no exception. The efficiency of the engines falls continuously with age and with time since overhaul. In a study by Lambert (Lambert, H.H., 1991) at NASA a reduction in the efficiency of aircraft engine components in the range of 1.0 – 2.5 %, due to normal wear, is said to be typical. Two consequences of reduced component efficiency are considered in this introductory study:

1. higher fuel consumption, and
2. increased turbine inlet temperature T_{t4}.

These two phenomena are of great importance with respect to exhaust emissions, firstly because CO_2 and H_2O quantities are proportional to fuel consumption. Secondly, the formation of NO_X and CO depends largely on the temperature in the combustion zone.

3.2.1 Simplified tools for gas turbine engine analyses

Jack D. Mattingly's book "Elements of Gas Turbine Propulsion" (Mattingly, J.D., 1996) and Louis A. Urban's paper "Gas Turbine Engine Parameter Interrelationships" (Urban L.A., 1969) both present methods for off-design calculations of aircraft gas turbine engines.
The Louis A. Urban paper is a thorough and comprehensive study of the gas turbine engine parameters' mutual sensitivity. His concept is that when a certain change in one parameter causes incremental changes in many other parameters in the engine, the sizes of these increments may be evaluated. Urban has developed an algebraic expression for a large number of such relations. For an individual engine, or a specific type of engine in a certain mode of operation, the relations turn out to be proportionalities, and sensitivity factors are defined. Typically the "0.5" in the following equation expresses what happens to turbine inlet temperature T_{t4} with a certain change in compressor exit pressure p_{t3}:

$$\frac{\partial p_{t3}}{p_{t3}} = \mathbf{0.5} \cdot \frac{\partial T_{t4}}{T_{t4}} \tag{3.1}$$

Such a linear relation may look like an over-simplification that is valid only for really small increments. Urban, however, extensively demonstrates how powerful the tool is to predict engine performance in stationary and transient operations.
Wallentinsen evaluated the method in his master's thesis at The Norwegian Institute of Technology (Wallentinsen, Å.R., 1980). The Urban procedure was programmed by Wallentinsen into a computer code and several real-life gas turbine engine cases were tested with the code. The results show reasonably good correlations to measured data.
The reason for giving this brief presentation of Urban's work is that the theoretical basis for his method is exactly the same as the one used by Mattingly, i.e. the thermodynamic equations for air flow through the components of gas turbine engines. Certain limitations and idealizations apply in both cases, major ones are that the ideal gas equation is valid throughout the flow and that component efficiencies are assumed constant.
A simple computer code for preliminary analyses of aircraft engines is published by Jack D. Mattingly in his book (Mattingly, J.D., 1996). This code has been used in the present work in a very first attempt to roughly quantify the deterioration impact on some engine parameters on aircraft engines. The theory and algorithm used by Mattingly is described extensively later in this chapter.
The Mattingly code consists of two major modules called "on-design" and "off-design" parts of the program. Flight conditions, engine configuration and parameters, fuel specification and air constants are input to the on-design part. One may choose a straightthrough calculation of the specified engine cycle, all parameters given. The code also has the capability to optimize certain conditions with respect to fuel consumption.
The analysis is all parametric in such a way that mainly non-dimensional and flow specific quantities are calculated. The thrust and a few other dimensional parameters are finally presented based on a default air mass flow of 90.7 kg/s.
The output data from the on-design analysis are used by the off-design part of the code to study engine performance in different flight conditions.

3.2.2 An introductory demonstration, the case engine and flight

The aircraft and engine used in this demonstration are not similar to the Boeing 737 / CFM56 configuration that is used later in this work. A large turbofan engine (similar in size and design to the Pratt & Whitney JT9) was chosen, assumed to power a commercial airliner, typically a Boeing 747 type aircraft (4 engines), in an overseas flight covering an 8 hour level cruise as part of the leg. The only reason for using such an engine in this early study is a certain similarity to the engine used by Mattingly in one of his textbook cases. The flight is considered to be performed with 4 new engines and then compared to 4 less efficient engines, in the following called "used engines". The duration of the flight and number of engines is only used to indicate very roughly the total fuel consumption. Flight altitude and speed and passengers and cargo weights are equivalent in all cases. Fuel load is allowed to vary.

3.2.3 Efficiency reductions and calculation procedures

Flight Mach number and altitude are chosen at 0.85 and 10 668m (35 000 ft) respectively. Important engine characteristics are approximately those of the JT9D engine. These include a bypass ratio at 5.0, overall pressure ratio at 25 and fan pressure ratio at 1.6. Cruise thrust for one new engine is 48.9 kN. Variation in thrust during the 8 hour cruise is not accounted for here.
Three different cases of reduced engine performance are studied. First, the compressor and turbine efficiencies are reduced by approximately 1 %. In the second case, efficiency reductions and increased pressure losses effect all the main components in the engines. Finally the low pressure compressor efficiency and high pressure turbine efficiency are varied separately and the influences on turbine inlet temperature and fuel requirement are studied.
The on-design calculation of the new engine was carried out in two steps:

1. First the turbine inlet temperature T_{t4} was optimized with respect to thrust specific fuel consumption (TSFC).

2. Then all non-dimensional and flow specific quantities were calculated for the optimum TSFC.

All temperatures, pressures and flow velocities in the engine are fixed from this point on. Sizing of the engine to comply with the appropriate thrust requirement can be done easily as both thrust and mass flow scales linearly with the cross section area (laws of continuity and momentum). TSFC is constant.
The used engine has to be treated differently. There is no procedure for the input of the modified efficiencies into the off-design module of the code. It has to be done during the on-design calculations. With lower efficiencies the engine still has to give the required thrust, and the physical size of the engine has to stay fixed. Keeping the old engine specific thrust (thrust/air mass flow rate) at the same magnitude as that for the new engine therefore makes sense.
Further the idea is that the used engine is somewhat outside of its design point in this situation, and it will not be correct to optimize the T_{t4}. As flight conditions and thrust requirement in the off-design situation diverge very little from on-design, the optimum T_{t4} will not be far off from the correct temperature.
The following two different methods are conducted and compared in the first set of off-design calculations:

Method A:

– the correct T_{t4} is determined through a manual trial and error procedure (using the computer code), this applies for the same thrust at an equivalent mass flow of air as for the new engine (it allows for the diameter of the captured air tube to stay fixed and thus the physical dimensions of the engine.),

Method B:

– the T_{t4} in the less efficient engine is optimized and the engine then scaled to the appropriate size (thrust). (This way the physical dimensions of the engine are not kept

perfectly unchanged, and optimum fuel consumption is probably too favorable for the degraded engine.)

From Table 3.4 it appears that the two methods indicate basically the same fuel requirement while by the method B a reduced air mass flow is calculated, and this does not seem reasonable. Complete output from the tests is found in Appendix E of this thesis. For further analyses method A was applied.
The used engines' higher fuel consumption requires more fuel to be carried on board the aircraft. Additional lift is necessary to carry the fuel and these engines therefore have to run at a slightly higher thrust than the new ones. This is accounted for by running the used engine through the off-design program at the suitable thrust level. A lift/drag ratio of 20 is used.
The fact that the total load of the aircraft continuously decreases during the flight applies to both the new and the used engines and is not taken into consideration at this early stage.

Compressor and turbine efficiency reduction:

Primarily only variations in the efficiencies of the compressor and turbine stages have been analyzed. All other losses and efficiencies are kept constant.
The performance and status of the compressor and turbine are given as the polytropic efficiencies. Differences in these efficiencies for new and used engines are set to 0.01 (approximately 1.0 %). The input quantities are listed in Table 3.1 and the component efficiencies are calculated by the on-design code as presented in Table 3.2. These are all state-of-the-art efficiencies for this type of engine.
The enthalpy of combustion of the fuel is 43.26 MJ/kg.

	new engine	**used engine**	**Δe**
e_{CL} and e_F	0.890	0.880	–0.010
e_{CH}	0.900	0.890	–0.010
e_{TH}	0.890	0.880	–0.010
e_{TL}	0.910	0.900	–0.010

Table 3.1 The original ("new") and the reduced ("used") polytropic efficiencies.

	new engine	**used engine**	$\Delta\eta$
η_{CL} and η_F	0.883	0.872	–0.011
η_{CH}	0.857	0.842	–0.014
η_{TH}	0.907	0.898*	–0.009
η_{TL}	0.921	0.912	–0.009

Table 3.2 Component efficiencies developed by the computer code, based on the polytropic efficiencies in Table 3.1.
*) Not evaluated by the Mattingly code, calculated manually from the HP turbine pressure ratios.

General deterioration:

In the second study a more general deterioration of the used engine is considered. Polytropic efficiencies for compressor and turbine components are reduced by only 0.005 (≈ 0.5 %) from the new engine figures. Stagnation pressure recovery for the diffuser, burner and nozzles are reduced 0.001 (0.1 %), and combustion efficiency and mechanical efficiency for the high and low pressure spools are reduced by 0.002 (≈0.2 %).
The figures in Table 3.3 apply.

	new engine	**used engine**	**difference**
e_{CL} and e_F	0.890	0.885	-0.005
e_{CH}	0.900	0.895	-0.005
e_{TH}	0.890	0.885	-0.005
e_{TL}	0.910	0.905	-0.005
π_D	0.995	0.994	-0.001
π_B	0.950	0.949	-0.001
π_N	0.995	0.994	-0.001
$\pi_{N'}$	0.995	0.994	-0.001
η_B	0.990	0.988	-0.002
η_{mH}	0.980	0.978	-0.002
η_{mL}	0.990	0.988	-0.002

Table 3.3 Efficiencies and losses for the new and the used engines, a general deterioration.

Ranges of compressor and turbine reductions

A series of calculations are performed to evaluate how the fuel consumption and turbine inlet temperature vary with compressor and turbine efficiencies. Based on the design point values, the efficiencies of the low pressure compressor and the high pressure turbine are varied over the ranges 0.8825 – 0.8558 and 0.9067 – 0.8853 respectively. Tables 3.6 and 3.7 show the input and the results from the analyses.

3.2.4 Calculated performance reduction due to lower efficiencies

Fuel consumption and turbine inlet temperature for the new and used engines, and the total amount of fuel required for the 8 hour flight are shown in the tables below.
From the three series of analyses of the engine and the flight conditions described, the following conclusions may be drawn:

1. A particular reduction in the four polytropic efficiencies e_{CL}, e_{CH}, e_{TL} and e_{TH}, all by 1.0 % will demand an increased fuel flow in cruise of 3.0 % and in the turbine inlet temperature by 2.0 %, see Table 3.4.

2. Less reduction in the component polytropic efficiencies, e_{CL}, e_{CH}, e_{TL} and e_{TH} all lowered by 0.5 %, at the same time pressure ratios π_N, $\pi_{N'}$, π_D and π_B reduced 0.1 % each, and the component efficiencies η_B, η_{mH} and η_{mL} all reduced 0.2 % cause a 2.5 % higher fuel flow and 1.4 % increase in the turbine inlet temperature. The numbers are presented in Table 3.5.

3. The fuel flow and the turbine inlet temperature are both considerably more sensitive to a reduced high pressure turbine performance than a change in performance of the low pressure compressor/fan. The following sensitivity factors are evaluated from the numbers in Tables 3.6 and 3.7 (the variations in the tables also imply minor changes in engine thrust of less than 0.5 %):

$$\frac{\partial \dot{m}_f}{\partial \eta_{CL}} \approx -60\ [\%] \tag{3.2}$$

$$\frac{\partial \dot{m}_f}{\partial \eta_{TH}} \approx -88\ [\%] \tag{3.3}$$

$$\frac{\partial T_{t4}}{\partial \eta_{CL}} \approx -500\ [K] \tag{3.4}$$

$$\frac{\partial T_{t4}}{\partial \eta_{TH}} \approx -600\ [K] \tag{3.5}$$

It is evident that a fall in high pressure turbine efficiency has an impact on fuel flow $\dot{m}_f$ that is 50 % stronger then a similar drop in low pressure compressor efficiency. The corresponding figure for T_{t4} is 20 %. The high pressure turbine operates over a larger pressure interval than the low pressure compressor, and that is a possible reason for these differences.
The relations are illustrated in the Figures 3.2 and 3.3.

	new engine	**used engine** *method A*	**used engine** *method B*	**difference** *new/used(A)*	**difference** *new/used(B)*
thrust F [N]	48 928	49 293	49 288	0.75 %	0.74 %
T_{t4} [K]	1 317	1 342	1 358	1.98 %	3.16 %
TSFC $[10^{-6} \cdot kg \cdot N^{-1} \cdot s^{-1}]$	22.49	22.97	22.97	2.21 %	2.21 %
air flow [kg/s]	328	329	322	0.27 %	–1.80 %
fuel flow [kg/s]	1.100	1.133	1.132	3.00 %	2.93 %
total fuel [kg] (4 eng., 8 hrs.)	126 711	130 476	130 430	3 765 [kg]	3 719 [kg]

Table 3.4 Fuel consumption and turbine inlet temperature for a new engine and a used engine, reduced efficiencies and performance only in the compressor and turbine sections. Alternative methods for used engine calculation are shown.

	new engine	**used engine** *(method A)*	**difference**
thrust [N]	48 928	49 235	0.63 %
T_{t4} [K]	1 317	1 335	1.39 %
TSFC $[10^{-6} \cdot kg \cdot N^{-1} \cdot s^{-1}]$	22.49	22.89	1.76 %
air flow [kg/s]	328	328	0.14 %
fuel flow [kg/s]	1.100	1.127	2.49 %
total fuel [kg] (4 eng., 8 hrs.)	126 711	129 868	3 157 [kg]

Table 3.5 Fuel consumption and turbine inlet temperature for a new engine and a used engine, reduced efficiencies and performance in all components of the used engine.

η_{CL}	T_{t4} [K]	F [N]	TSFC [$10^{-6} \cdot kg \cdot N^{-1} \cdot s^{-1}$]	Fuel con. [kg]	$\Delta \dot{m}_f$ [%]	$\Delta\eta_{CL}$
0.8825	1 317	48 928	22.48	126 710	(new eng.)	(new engine)
0.8771	1 319	48 968	22.53	127 085	0.30	–0.0054
0.8718	1 322	49 013	22.58	127 504	0.63	–0.0107
0.8664	1 324	49 053	22.64	127 913	0.95	–0.0161
0.8611	1 327	49 093	22.69	128 321	1.27	–0.0214
0.8558	1 330	49 119	22.75	128 728	1.59	–0.0267

Table 3.6 Variation in fuel consumption (all 4 engines, 8 hour flight) with low pressure compressor efficiency.

η_{TH}	T_{t4} [K]	F [N]	TSFC [$10^{-6} \cdot kg \cdot N^{-1} \cdot s^{-1}$]	Fuel con. [kg]	$\Delta \dot{m}_f$ [%]	$\Delta\eta_{TH}$
0.9067	1 317	48 928	22.48	126 710	(new eng.)	(new engine)
0.9024	1 319	48 977	22.54	127 156	0.35	–0.0043
0.8981	1 322	49 026	22.60	127 635	0.73	–0.0086
0.8939	1 324	49 070	22.66	128 119	1.11	–0.0128
0.8896	1 327	49 119	22.73	128 616	1.50	–0.0171
0.8853	1 329	49 164	22.79	129 101	1.89	–0.0214

Table 3.7 Variation in fuel consumption (all 4 engines, 8 hour flight) with high pressure turbine efficiency.

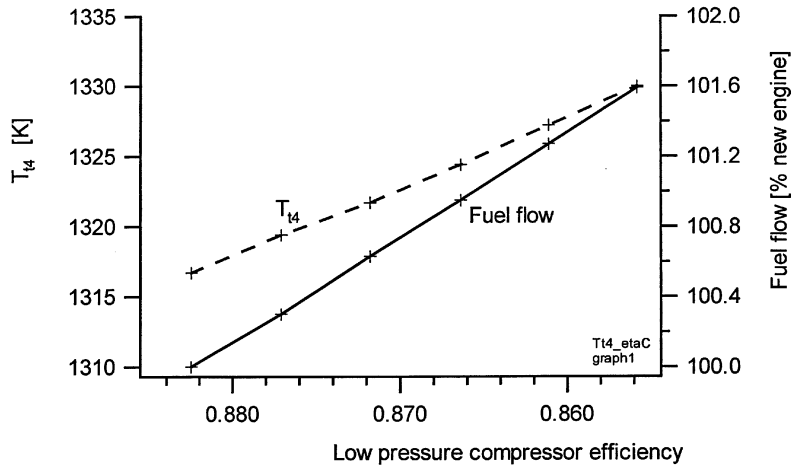

Figure 3.2 Variations in fuel consumption and turbine inlet temperature with low pressure compressor efficiency.

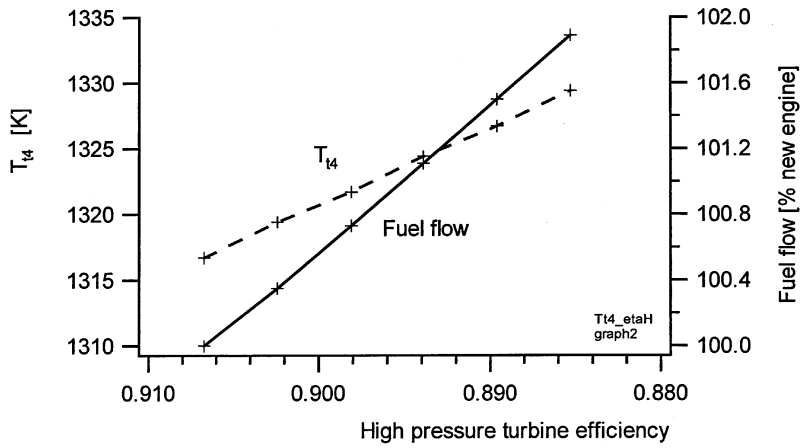

Figure 3.3 Variations in fuel consumption and turbine inlet temperature with high pressure turbine efficiency.

3.3 Development of a Simple Engine and Aircraft Computer Model based on Parametric Engine Analyses

Based on the conclusions from the preliminary studies a further investigation was done of aircraft emissions and the influence of engine deterioration. At first a quite simple computer model was written. For the engine analyses the method in (Mattingly, J.D., 1996) was used, and the aircraft kinetics and kinematics were calculated by an impulse-momentum equation.

3.3.1 The Mattingly algorithm and computer code

The method from Mattingly's book (Mattingly, J.D., 1996) was chosen because it is easily available and well documented. It has already been introduced quite briefly and a more thorough presentation is offered here. The procedure starts out with a well-described mode of operation for one particular aircraft engine, the so-called reference condition or on-design condition. It is imperative that this is a well analyzed engine or a real one. Figures and numbers that do not match properly will cause meaningless results. For a separate exhaust, two spool turbofan engine with the fan and the low pressure compressor both attached to the low pressure spool, the following four independent variables are defined: M_0, T_0, p_0 and T_{t4}.

There is also a set of given constants:

$\pi_{D\,max}$, π_B, π_{TH}, π_N, $\pi_{N'}$	(pressure)
τ_{TH}	(temperature)
η_F, η_{CH}, η_B, η_{mH}, η_{mL}	(efficiencies)
γ_C, γ_T, c_{pC}, c_{pT}	(air)
h_{PR}	(fuel)

From the thermodynamic equations expressions for all remaining variables, called the dependent variables, are derived. Mattingly demonstrates that a mode of operation that is different from the reference condition, may be analyzed and described by going through a specific procedure:

1. The four independent variables M_0, T_0, p_0 and T_{t4} are set for the new mode, called the performance condition.

2. Based on quantities for parameters known from the reference condition, the dependent variables are evaluated in a first approach to the performance condition.

3. These new dependent variable quantities form the next set of values for input. Most likely they deviate from the reference values, and they are probably not correct for the final performance condition.

4. The newly found quantities are used as input for a second round of calculations, and by iterations the engine parameters finally converge to describe a stable, well-balanced operation mode, the final performance condition. The requirement for accuracy is attached to the low pressure turbine temperature ratio τ_{TL} such that between two successive calculations it should not change more that 0.0001 (recommended by Mattingly).

   The other 10 dependent variables are:

   - bypass ratio
   - fan total pressure ratio,
   - fan total temperature ratio
   - LP compressor total pressure ratio
   - LP compressor total temperature ratio
   - HP compressor total pressure ratio
   - HP compressor total temperature ratio
   - LP turbine total pressure ratio
   - LP turbine total temperature ratio
   - exit Mach number core
   - exit Mach number bypass

5. Other parameters that are derived and found from the independent variables after iteration is completed are:

   - thrust
   - thrust specific fuel consumption
   - efficiencies (thermal, propulsive and overall efficiencies)
   - the remaining pressure and temperature ratios
   - exhaust nozzle pressures, and
   - HP and LP spool RPMs.

The equations, assumptions made, and the limitations to the Mattingly method are presented in a separate section, Section 3.3.2.

3.3.2 Basic equations for parametric cycle analysis

Assumption (by Mattingly) for Parametric Cycle Analysis:

1. Perfect gas upstream of main burner with constant properties γ_C, R_C, c_{pC}, etc.
2. Perfect gas downstream of main burner with constant properties γ_T, R_T, c_{pT}, etc.
3. All components are adiabatic.
4. The efficiencies of the compressor, fan and turbine are described through the use of (constant) polytropic efficiencies e_C, e_F and e_T, respectively.

Bypass uninstalled thrust:

$$F_F = \dot{m}_{a,F}(V_{19} - V_0) + A_{19}(p_{19} - p_0) \tag{3.6}$$

Core uninstalled thrust:

$$F_C = (\dot{m}_{a,9} V_9 - \dot{m}_{a,0} V_0) + A_9(p_9 - p_0) \tag{3.7}$$

Speed of sound:

$$a = (\gamma RT)^{\frac{1}{2}} \tag{3.8}$$

and Mach-number

$$M = \frac{V}{a} \tag{3.9}$$

yields (when γ and R are constant throughout the bypass stream):

$$\left(\frac{V_{19}}{a_0}\right)^2 = \left(\frac{T_{19}}{T_0}\right) M_{19}^2 \tag{3.10}$$

isentropic stagnation

$$\frac{p_t}{p} = \left(1 + \frac{(\gamma - 1)}{2} M^2\right)^{\frac{\gamma}{(\gamma-1)}} \tag{3.11}$$

$$\frac{T_t}{T} = \left(1 + \frac{(\gamma - 1)}{2} M^2\right) \tag{3.12}$$

Pressure and temperature ratios $\pi_{component}$ and $\tau_{component}$

$$p_{t19} = p_0 \pi_r \pi_D \pi_F \pi_{N'} \tag{3.13}$$

$$p_{t9} = p_0 \pi_r \pi_D \pi_{CL} \pi_{CH} \pi_B \pi_{TH} \pi_{TL} \pi_N \tag{3.14}$$

$$T_{t19} = T_0 \tau_r \tau_F \tau_{N'} \tag{3.15}$$

(assuming $\tau_{N'} = 1.00$)

$$T_{t9} = T_0 \tau_r \tau_D \tau_{CL} \tau_{CH} \tau_B \tau_{TH} \tau_{TL} \tau_N = T_0 \left(\frac{c_{pC}}{c_{pT}}\right) \tau_\lambda \tau_T \tag{3.16}$$

(assuming $\tau_N = 1.00$)

First law of thermodynamics, burner:

$$\dot{m}_{a,C}\, c_{pC}\, T_{t3} + \eta_B\, \dot{m}_f\, h_{PR} = \dot{m}_4\, c_{pT}\, T_{t4} \tag{3.17}$$

fuel-air ratio:

$$f = \frac{\dot{m}_f}{\dot{m}_{a,C}} \tag{3.18}$$

The power balance for the low pressure shaft (LP turbine and fan and LP compressor):

$$\dot{m}_{a,C}\, c_{pC} (T_{t2.5} - T_{t2}) + \dot{m}_{a,F}\, c_{pC} (T_{t13} - T_{t2}) = \eta_{mL}\, \dot{m}_4\, c_{pT} (T_{t4.5} - T_{t5}) \tag{3.19}$$

The power balance high pressure shaft (HP turbine and HP compressor):

$$\dot{m}_{a,C}\, c_{pC} (T_{t3} - T_{t2.5}) = \eta_{mH}\, \dot{m}_4\, c_{pT} (T_{t4} - T_{t4.5}) \tag{3.20}$$

Bypass ratio:

$$\alpha = \frac{\dot{m}_{a,F}}{\dot{m}_{a,C}} \tag{3.21}$$

Isentropic and polytropic relations, polytropic efficiencies

$$\pi_r = (\tau_r)^{\frac{\gamma_C}{\gamma_C - 1}} \tag{3.22}$$

$$\tau_r = \left(1 + \frac{(\gamma_C - 1)}{2} M_0^{\,2}\right) \tag{3.23}$$

$$\tau_F = (\pi_F)^{\frac{\gamma_C - 1}{\gamma_C \cdot e_F}} \tag{3.24}$$

$$\tau_C = (\pi_C)^{\frac{\gamma_C - 1}{\gamma_C \cdot e_C}} \qquad \text{(LP- and HP- compressors)} \tag{3.25}$$

$$\pi_T = (\tau_T)^{\frac{\gamma_T}{(\gamma_T - 1) e_T}} \qquad \text{(LP- and HP- turbines)} \tag{3.26}$$

Component efficiencies:

$$\eta_r = 1 \qquad \text{for } M_0 \le 1$$

$$= 1 - 0.075\,(M_0 - 1)^{1.35} \qquad \text{for } M_0 > 1 \tag{3.27}$$

$$\pi_D = \pi_{D,max}\, \eta_r \tag{3.28}$$

$$\eta_F = \frac{(\pi_F)^{\frac{\gamma_C - 1}{\gamma_C}} - 1}{\tau_F - 1} \tag{3.29}$$

$$\eta_C = \frac{(\pi_C)^{\frac{\gamma_C - 1}{\gamma_C}} - 1}{\tau_C - 1} \tag{3.30}$$

$$\eta_T = \frac{1 - \tau_T}{1 - (\tau_T)^{\frac{1}{e_T}}} \tag{3.31}$$

Further assumptions as applied for the "Engine Performance Analysis" (Mattingly):

1. The flow is choked at the high-pressure turbine entrance nozzle, low-pressure turbine entrance nozzle and the primary exit nozzle. Also the bypass duct nozzle for the turbofan is choked.

2. The total pressure ratios of the main burner, primary (core) exit nozzle and bypass stream exit nozzle (π_B, π_N and π_{FN}) do not change from their reference values.

3. The component efficiencies (η_C, η_F, η_B , η_{TH} , η_{TL} , η_{mH} and η_{mL}) do not change from their reference values.

4. Turbine cooling and leakage effects are neglected.

5. No power is removed from the turbine to drive accessories (or alternately, η_{mH} and η_{mL} account for the power removed and are still constant).

6. Gases are assumed calorically perfect both upstream and downstream of the main burner, and γ_T and c_{pT} do not vary with the power setting (T_{t4}).

7. The term unity plus the fuel/air ratio (1 + f) is considered a constant.

The enthalpy rises across the low pressure compressor and fan are proportional to the LP spool rotational speed squared:

$$c_{pC}(T_{t2.5} - T_{t2}) = K1 \cdot N1^2 \tag{3.32}$$

$$c_{pC}(T_{t13} - T_{t2}) = K2 \cdot N1^2 \tag{3.33}$$

hence:

$$(T_{t2.5} - T_{t2}) = K \cdot (T_{t13} - T_{t2}) \Rightarrow \tag{3.34}$$

$$\tau_{CL} - 1 = K \cdot (\tau_F - 1) \tag{3.35}$$

K1, K2 and K being the proportional constants.

From the dimensionless analysis we find:

$$\alpha \left(\frac{\pi_{CL}\pi_{CH}}{\pi_F} \right) \left(\frac{\tau_\lambda}{\tau_r \tau_F} \right)^{-\frac{1}{2}} \cdot \frac{1}{MFP(M_{19})} = \text{constant} \tag{3.36}$$

the mass flow parameter in station n being defined as:

$$MFP(M_n) \equiv \frac{\dot{m}_{a,n}\sqrt{T_{tn}}}{p_{tn}A_n} \tag{3.37}$$

$$\frac{(\tau_F - 1)}{(1-\tau_{TL})}(1+\alpha)\frac{\tau_r}{\tau_\lambda} = \text{constant} \tag{3.38}$$

$$\frac{\dot{m}_{a,0}}{(1+\alpha)p_0\pi_r\pi_D\pi_{CL}\pi_{CH}(T_{t4})^{-\frac{1}{2}}} = \text{constant} \tag{3.39}$$

$$\frac{(\tau_{CH}-1)\tau_r\tau_{CL}}{\frac{T_{t4}}{T_0}} = \text{constant} \tag{3.40}$$

$$\dot{m}_4 = \frac{p_{t4}}{\sqrt{T_{t4}}}A_4 \cdot MFP(M_4) = \dot{m}_{4.5} = \frac{p_{t4.5}}{\sqrt{T_{t4.5}}}A_{4.5} \cdot MFP(M_{4.5}) \tag{3.41}$$

Hence (from the last equation)

$$\frac{\frac{p_{t4}}{p_{t4.5}}}{\sqrt{\frac{T_{t4}}{T_{t4.5}}}} = \frac{\pi_{TH}}{\sqrt{\tau_{TH}}} = \text{constant} \tag{3.42}$$

as stations 4 and 4.5 are assumed to be choked, and the cross sectional areas are constant.

For constant η_{TH}

π_{TH}, τ_{TH}, $\dot{m}_{c4}$ and $\dot{m}_{c4.5}$ are constant

(subscript c for corrected mass flow rate), example:

$$\dot{m}_{c4} = \frac{\dot{m}_4\sqrt{\theta_4}}{\delta_4};\quad \theta_4 = \frac{T_{t4}}{T_{ref}} \text{ and } \delta_4 = \frac{p_{t4}}{p_{ref}}$$

Similarly assuming that $\dot{m}_{4.5} = \dot{m}_8$ and that the flow is choked in station 8 as well, we get:

$$\frac{\pi_{TL}}{\sqrt{\tau_{TL}}}\,MFP(M_8) = \text{constant} \tag{3.43}$$

The LP spool power balance may be rearranged to yield:

$$\frac{\tau_r\left[\left(\tau_{CL}-1\right)+\alpha\left(\tau_F-1\right)\right]}{\frac{T_{t4}}{T_0}\left(1-\tau_{TL}\right)} = \eta_{mL}\,(1+f)\,\tau_{TH} = \text{constant} \tag{3.44}$$

Finding certain expressions to be constant in a fairly wide range of operation give the opportunity to evaluate engine performance parameters as functions of their corresponding reference (R) parameter. Equations (3.45) – (3.47) demonstrate this clearly:

$$\tau_{CL} - 1 = K\cdot(\tau_F - 1) \Rightarrow \tag{3.45}$$

$$\frac{\tau_{CL}-1}{\tau_F-1} = K = \left[\frac{\tau_{CL}-1}{\tau_F-1}\right]_R \tag{3.46}$$

which yields

$$\tau_{CL} = 1 + \frac{\tau_F-1}{\tau_{F,R}-1}\left(\tau_{CL,R}-1\right) \tag{3.47}$$

In a similar way the performance parameters τ_{CH}, τ_F, α, π_{TL}, $\dot{m}_{a,0}$, N1 and N2 are found. The remaining parameters are evaluated according to their definitions and the isentropic / polytropic relations; π's evaluated on the basis of corresponding τ's and η's and fuel/air flow ratio f are examples.

3.3.3 Aircraft kinematics and kinetics

In their text book Mattingly et al. utilize a work-energy relation to quantify changes in speed and altitude during flight (Mattingly, J.D., Heiser, W.H., Daley, D.H., 1987). In the present case, with aircraft mass reduction due to fuel burn being taken into consideration, this energy approach did not seem reliable and an impulse-momentum equation was chosen.
The assumption here was that the airplane climb and descent paths follow sections of straight lines, the angles of climb and descent being constant within limited flight intervals. This way only the components of forces, speed and acceleration that act parallel to the flight path had to be taken into consideration. The law of momentum for the airplane in such a linear flight mode (scalar, parallel to flight path) will always be:

$$(F - D - G_p)dt = d(m\cdot V) \tag{3.48}$$

F being the thrust, D the drag, G_p is the component of gravity parallel to the flight path, m is total mass of the aircraft, and V is aircraft speed. Dividing by dt and differentiating, the equation yields:

$$F - D - G_p = m \cdot \frac{dV}{dt} + V \cdot \frac{dm}{dt} \tag{3.49}$$

and

$$F - D - mg \cdot \sin\beta = m \cdot \frac{dV}{dt} + V \cdot \frac{dm}{dt} \tag{3.50}$$

β being the angle of climb. $\frac{dV}{dt}$ is the acceleration of the aircraft along its path and $\frac{dm}{dt}$ in this case is the equivalent of time specific fuel consumption (negative).
Airplane drag is found based on the drag coefficient C_D:

$$D = C_D \cdot S \cdot \frac{1}{2} \rho V^2 \tag{3.52}$$

with a characteristic airplane area S and the ambient air density ρ. Finally the aircraft acceleration may be expressed:

$$a = \frac{1}{m} \cdot (F - C_D \cdot S \cdot \frac{1}{2} \rho V^2 - mg \cdot \sin\beta + V \cdot \frac{dm}{dt}) \tag{3.53}$$

The rate of change of altitude is the vertical component of aircraft speed:

$$\frac{dh}{dt} = V \cdot \sin\beta \tag{3.54}$$

3.3.4 Outline of the engine simulation model CODE1X

In the need for initial studies of aircraft fuel consumption and emissions during a flight cycle, a somewhat simple computer model was put together. Such a code should have the capacity first of all to estimate the total amount of fuel burned throughout a complete flight. Secondly it should calculate the fuel flow rate and the combustion chamber temperature at any point during the flight cycle.
This task was initiated by coding the algorithm for parametric off-design engine studies in Fortran, i.e. the algorithm as presented by Mattingly, limiting the code for separate exhaust two spool turbofan engines only. This new code was tested against the Mattingly code by doing equivalent simulations, and the agreement was satisfactory.
Next, to expand the code, a continuous flight path had to be simulated and an independent thrust setting parameter had to be defined. The input variables M_0, T_0, p_0 and T_{t4} all vary in flight. T_{t4} which may at first seem like a suitable power setting indicator, is dependent on the

other three and not a good choice. The pilot (or the auto-throttle) in modern civil transport aircraft rely on the N1 (LP spool speed) as an indication of engine thrust (information from Braathens, November 1997). Basically all the thrust comes from the fan (approximately 80 %), therefore the fan speed (= N1) is directly related to the thrust, everything else being constant.
The most sensible parameter to be used, at this point, as a power plant performance indicator seemed to be N1. The N1 may be assumed a constant over a particular flight interval. Typically for level cruise flight N1 is 75 % of full power speed, at take-off and climb-out the values are in the range of 95 % and 85 to 90 % respectively (Braathens). Variations up to ± 5 % are seen in real operation.
Program execution now starts with the input variables M_0, T_0 and p_0 being given and magnitude of N1 specified. Input variable T_{t4} is given a default start value. By varying T_{t4} incrementally (e.g. 1 Kelvin) in repeated runs, the correct T_{t4} for the required N1 is eventually found and the proper engine parameters are calculated.
Up to this point speed development had not been considered. Time is not a factor in the work by Urban or Mattingly. There is a brief comment by Wallentinsen in his thesis, of course he is right in saying that as time is not considered, there is really no capability in the method to analyze fully transient situations. Time is the crucial parameter in any non-stationary event.
External forces in addition to engine thrust, the main ones being the drag, the lift and the gravity force, all act on the aircraft. These forces together make the aircraft change its position and speed.
Quite simple aircraft kinematics and kinetics as used with the simplified model is explained in Section 3.3.3.
The thrust for a particular N1 and flight condition was found from the computer calculations procedure described. To relate the ambient condition to altitude, a subroutine module to calculate standard atmosphere was added to the program.
Equations of motion and aircraft characteristics were incorporated, and the code now became a useful tool for the calculation of the following parameters:

- ambient air density
- acceleration
- climb angle
- "accumulated" altitude
- accumulated loss of mass (fuel burned), and
- current air speed

During execution the program works with very short (user defined) time intervals. One to two seconds is practical. Over an interval the acceleration (and of course N1) is assumed constant. Aircraft motion is accumulated, and finally the code will test if the position is at the prescribed distance and altitude. One more interval in time and transfer is added if this is not the case.

An additional set of input parameters is now required, these are:

- initial altitude (start of flight sequence)
- final altitude (end of flight sequence)
- initial air speed or Mach number
- angle of climb
- aircraft total mass at start
- low pressure spool velocity N1 (in %)
- drag coefficient
- wing area or other characteristic area of the aircraft
- number of engines on aircraft

The most useful output parameters:

- speed at designated position
- thrust at designated position
- turbine inlet temperature at designated position
- acceleration at designated position
- aircraft total mass at designated position
- total fuel consumed during flight sequence
- time elapsed since sequence started
- momentary value of any of the above parameters at any point in the sequence.

Simulation of a flight sequence, that is a particular flight distance in which certain parameters are kept constant, was now possible. N1 and climb angle are the constant parameters in this case. Usually, in the present work, N1 was adjusted manually, and until flight time for a specific sequence was close to that in real flight.
A complete flight from acceleration to touch down was modeled by combining a proper set of sequences.
The parametric engine simulation algorithm does not converge for low N1s. Idle speed is about 30 %, and convergence in this code seems to be limited at approximately 50 % of full N1. Apparently Mattingly experienced the same problem as his graphs showing "partial-throttle characteristics" stop at 60 %.
A set of subroutines suggested by Mattingly adds a more sophisticated turbine calculation for the model. This is used for the evaluation of gas properties for air and exhaust mixtures at all temperatures. To keep the model in the present work as simple as possible, these subroutines were generally omitted. However, to improve convergence at low N1s, the subroutines were activated in some cases of descent and approach sequences ($\beta < 0.0°$).

The simplified code was named CODE1X, and the flow chart is shown in Figure 3.4. The size of the code, data files required and amount of manual work associated with operation of the program is discussed in Section 7.3. For a complete listing of the Fortran program Code1x.for see Appendix J.

3.3.5 Limitations of the simulation model CODE1X

The engine simulation part of CODE1X is developed for a two spool non afterburning turbofan engine only. A well defined reference condition for the engine is needed, and the low pressure spool rotational speed has to be known for all operational conditions.
Ambient conditions are evaluated by the program according to the standard atmosphere, and used in the engine and aircraft calculations, i.e. "hot day" or "cold day" flights can not be simulated by this tool.
The airplane drag coefficient is kept at a constant average value throughout each sequence of the flight, as explained in Section 4.3. That is of course a rough assumption. Drag coefficient quantities for the sequences and a corresponding reference surface area of the airplane must be known, along with the airplane take-off load. The code is designed for two engine aircraft only.
Mass reduction due to fuel burn is accounted for in the CODE1X. Therefore there should be no limit, within reasonable range, to the lengths of flights that can be modeled. Wind forces and other disturbing phenomena during flight are not considered. The validity of the model beyond the conventional civil transport maximum altitude has not been tested.
Emission calculations are not performed in this code, they have to be done manually, based on CODE1X output data.

3.4 Conclusions of the Preliminary Studies

It was shown quite easily, by means of a relatively simple computer code, that fuel consumption and gas temperatures vary with engine component efficiencies and pressure losses. Likewise it is demonstrated how fuel consumption and T_{t4} are more sensitive to turbine degradation than compressor degradation. Interpretations that are of particular interest in this work are that:

- engine parameters that are essential in forming of emissions are influenced by the status of the engine, and
- these parameters are equally or even more sensitive to turbine than compressor performance deterioration.

The parametric engine calculation principles and the architecture of a simplified modeling system are explained.

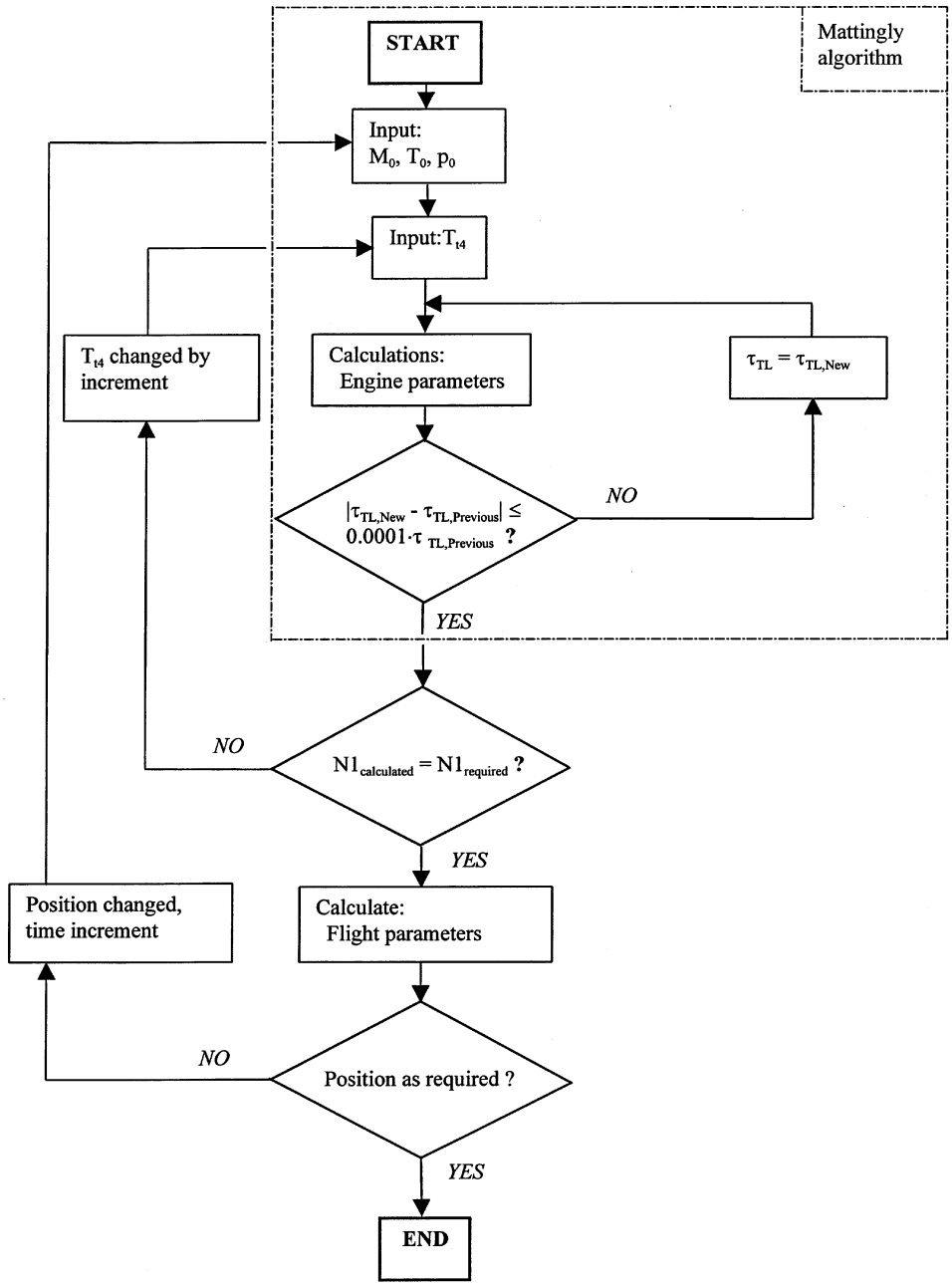

Figure 3.4 Flowchart, Simple (parametric) code *CODE1X.FOR*

4 MODELING THE OSLO – TRONDHEIM FLIGHT IN CODE1X

4.1 The CFM56-3C1 Engine Operating in Norway

The entire fleet of the Norwegian airline Braathens is composed of Boeing 737 airplanes, models -300, -400, -500 and -800. These are all powered by CFM56 engines.
The reasons for choosing Braathens of Norway as the cooperating airline in this research are four fold.

1. Braathens is the largest of Norwegian airlines serving mainly domestic destinations, hence a Braathens flight represents the typical domestic flight in this country.

2. The Braathens fleet is Boeing 737s only.

3. The Braathens' aircraft are all relatively new and modern.

4. Valuable points of contact in the Braathens company were available.

In the perspective of what is desirable for this work, namely to demonstrate relations between aircraft operation, engine performance deterioration and exhaust emissions, the CFM56-3C1 running on a Boeing 737-400 appeared to be the most suitable configuration for the study. The main reason for the choice is that the top rated engines in Braathens' fleet are used to power the 737-400s, as this is the Boeing 737-aircraft with the highest take-off thrust requirement. Thus the newest CFM56-3C1 engines are all found on the 737-400s of the company.
The CFM56-3C1 is a two spool turbofan engine rated at a maximum of 104 500 N (23 500 lbs) take-off thrust at sea level, 30 °C. The fan and the 3 stage low pressure compressor are driven by a 4 stage LP turbine and a single stage HP turbine drives the 9 stage HP compressor. The Braathens' CFM56-3C1 engines all have the conventional single stage

annular combustion chamber.
Bleed air for HP turbine and LP turbine cooling, HP turbine clearance control and external use is taken from the 5th stage of the HP compressor and the HP compressor discharge air.
The drive shaft for the accessory gear box is connected to the HP spindle.

4.2 Engine Design Condition

The design condition for the CFM56-3C1 engine in the parametric study is 104.5 kN static thrust at standard sea level atmosphere +15 K . In this condition the turbine inlet temperature is 1 640 K, air mass flow rate is 322 kg/s, bypass ratio is 5.0 and total pressure ratio is 25.6. Fuel heating value is chosen at $4.280 \cdot 10^7$ J/kg. Simplified air properties and engine design parameters are shown in Table 4.1 and Table 4.2 respectively.

Air Temperature	γ	c_p [$J \cdot kg^{-1} \cdot K^{-1}$]
Cold	1.40	1,040.0
Hot	1.33	1,172.0

Table 4.1 Simplified air properties used in the parametric study

Engine module	**Pressure** Ratio	**Temperature** Ratio	**Efficiencies**		
			Isentropic	Combustion	Mechanical
Diffuser (max)	0.999				
Fan	1.680		0.850		
HP compressor			0.877		
Combustion chamb.	0.9675			0.999	
HP turbine	0.228	0.729			
LP turbine	0.252	0.748	0.870		
Core nozzle	0.998				
Bypass nozzle	1.000				
HP spool					0.990
LP spool					0.990

Table 4.2 Engine design parameters for the CFM56-3C1 engine

Some of these data do not appear in engine specifications that are available. In such cases similar assumptions are made as for the Turbomatch modeling, later in this work. Certain pressure and temperature ratios and the air mass flow rate are as calculated by Turbomatch.

To make sure that the engine model is well balanced with the input data in the design condition, the model was run and deviations in calculated data from the inputs were studied. Performance parameter data should exactly match the reference data in this case. Two important modifications had to be made to achieve such balance. The main reason is assumed to be that cooling air and bleed air are not considered in this model. One consequence is that with a given bypass ratio the air flow through the combustion chamber is too large and with the turbine entry temperature set, the thrust will be higher than for the real engine. Secondly the temperature through the turbines of the real engine is reduced as the cooling air is mixed with the main core flow. Modifications to make up for these simplifications were to reduce the airflow and the turbine entry temperature while maintaining constant engine thrust close to 104.5 kN. Air mass flow reduction up to 10 %, and a T_{t4} variation in the range of +8 K to –58 K were tested, some of the test runs are shown in Appendix D.
Total air mass flow rate at 306 kg/s (5 % reduction) and turbine entry temperature around 1 615 K (25 K reduction) appear to be the correct quantities for a balanced design point. The resulting design condition as calculated is presented in the performance parameters column of Table D1, and the calculated data only show small deviations from the input set of parameters, referred to as the reference set.

4.3 Modeling the Aircraft and the Oslo – Trondheim Flight

The flight as described by Braathens (Appendix F) is divided into 9 sequences, covering acceleration and take-off through descent and approach and landing. Each sequence has the same distance, length in time, and the same change of altitude as used with the Turbomatch model. As explained earlier the low pressure RPM is kept constant within a sequence. Consequently the aircraft speed and accelerations will vary. This is of minor concern here if only the total time, change of altitude and speed at the end of sequence are correct.
In some cases the sequence final speed and total time are not matched exactly (figures appearing in *italics* in Table 4.3, target figures are shown in parentheses), the reason being either that the precise values cannot be hit with constant low pressure RPM, or the code does not converge for the very low thrust requirements. The latter is particularly the case in late descent and approach/landing sequences, deviations are quite small, however.
The aircraft reference area is calculated to be 202.85 m^2, calculations in Section 5.5.1. The total take-off weight for the aircraft with full rated, clean engines is 48 000 kg.
The drag coefficient is discussed extensively in the Section 5.5. In this simplified case constant average values for C_D over each flight sequence are used. The magnitudes of C_D correspond to those used in the Turbomatch modeling.

4.4 Engine Degradation

Two modes of engine degradation are studied:

1. referred to as "unclean 1"; fan and compressor pressure ratios are reduced by 1 %, total air mass flow is reduced by 1 % , fan and compressor isentropic efficiencies are reduced by 0.005 (0.5 % points, corresponds to the Turbomatch D1 fouling mode).

2. referred to as "unclean 2"; fan and compressor pressure ratios are reduced by 2 %, total air mass flow is reduced by 2 % , fan and compressor isentropic efficiencies by 0.01 (1 % point, corresponds to the Turbomatch D2 fouling mode).

Figures for the reduced parameters are directly input into the computer code CODE1X. These degradations are similar to those used in the Turbomatch model, the choice of degraded parameters is discussed in Section 5.6. With the Turbomatch model a third, more extreme fouling mode is studied as well. Due to convergence problems, this mode is not considered with the simplified model.

4.5 Calculation Procedure

For each flight sequence the start conditions, flight distance, climb angle and average drag coefficient are set. By manual iteration the suitable low pressure RPM is found such that the speed and flight time at the end of the sequence are correct. In a few cases a certain discrepancy has to be accepted, to stay within the range of model convergence, as already been discussed.
Accumulated fuel consumption and aircraft total mass are calculated. Take-off weight is slightly increased when deteriorated engines are in operation. This is done to achieve equal aircraft landing weights for all engine conditions.
As a control parameter the T_{t4} at the end of each sequence is presented.
Engine power setting, aircraft and flight parameters, and modeling results for the entire flight, are also presented in Table 4.3 below. All engine conditions *clean0*, *uncleanl* and *unclean2* appear in the same table.

Segment	N1	Altitude [m]		Speed [m/s]		Distance	Climb	Time	C_D	Fuelc.	T_{t4} [K]	A/C Mass
	[%]	start	end	start	end	[km]	[°]	[s]	average	[kg]	end	[kg] start
I (clean0)	80.2	12	12	10.3	*79* (72)	1.5	0.0	*31* (36)	0.102	58	1 402	48 000
(unclean1)	81.3	12	12	10.3	*79*	1.5	0.0	*31*	0.102	60	1 420	48 040
(unclean2)	82.8	12	12	10.3	*79*	1.5	0.0	*30*	0.102	60	1 442	48 080
II (clean0)	85.8	12	457	*79* (72)	107	4.3	5.9	*45* (48)	0.062	101	1 484	47 942
(unclean1)	86.8	12	457	*79*	107	4.3	5.9	*45*	0.062	103	1 500	47 980
(unclean2)	87.7	12	457	*79*	107	4.3	5.9	*45*	0.062	105	1 514	48 020
III_A (clean0)	87.0	457	2 071	107	*185* (220)	28.3	3.3	170	0.025	379	1 488	47 842
(unclean1)	87.9	457	2 071	107	*185*	28.3	3.3	170	0.025	387	1 502	47 877
(unclean2)	88.8	457	2 071	107	*185*	28.3	3.3	170	0.025	394	1 514	47 915
III_B(clean0)	88.5	2 071	11 278	*185* (220)	*208* (220)	161.7	3.3	*734* (730)	0.016	1 092	1 370	47 463
(unclean1)	89.5	2 071	11 278	*185*	*208*	161.7	3.3	*734*	0.016	1 115	1 382	47 491
(unclean2)	90.5	2 071	11 278	*185*	*208*	161.7	3.3	*734*	0.016	1 137	1 394	47 521
IV_A*(clean0)	88.5	11 278	11 278	*208*	220	5.5	0.0	26	0.0156	22	1 374	46 371
(unclean1)	89.5	11 278	11 278	*208*	220	5.5	0.0	26	0.0156	23	1 388	46 376
(unclean2)	90.5	11 278	11 278	*208*	220	5.5	0.0	26	0.0156	23	1 400	46 384
IV_B*(clean0)	74.3	11 278	11 278	220	220	83.5	0.0	380	0.0156	187	1 146	46 349
(unclean1)	75.0	11 278	11 278	220	220	83.5	0.0	380	0.0156	191	1 156	46 354
(unclean2)	75.9	11 278	11 278	220	220	83.5	0.0	380	0.0156	196	1 168	46 361
V_A (clean0)	50.0	11 278	5 628	220	*202* (220)	105.5	-3.1	*484* (480)	0.0175	102	806	46 162
(unclean1)	50.5	11 278	5 628	220	*202*	105.5	-3.1	*484*	0.0175	103	806	46 163
(unclean2)	50.9	11 278	5 628	220	*202*	105.5	-3.1	*484*	0.0175	103	808	46 165
V_B (clean0)	50.5	5 628	457	*202* (220)	*138* (82)	94.6	-3.1	*630* (627)	0.03	193	802	46 060
(unclean1)	51.0	5 628	457	*203*	*138*	94.6	-3.1	628	0.03	193	802	46 061
(unclean2)	51.4	5 628	457	*203*	*138*	94.6	-3.1	628	0.03	195	804	46 062
VI (clean0)	50.8	457	6	82	*87* (62)	9.3	-2.8	*110* (130)	0.075	38	784	45 868
(unclean1)	51.3	457	6	82	*87*	9.3	-2.8	*110*	0.075	38	786	45 868
(unclean2)	51.6	457	6	82	*87*	9.3	-2.8	*110*	0.075	39	788	45 868
Sum (clean0)						494.2		2 610		2 172		
(unclean1)						494.2		2 608		2 213 (= + 41)		
(unclean2)						494.2		2 607		2 252 (= + 80)		

Comments:
1. The cruise is divided into two sub-sequences IV_A and IV_B . *)
2. Final mass of aircraft in all three cases is 45 830 kg
3. The total time is 16 seconds too short

Table 4.3 Flight and weight data for the modeled flight Oslo – Trondheim; simple, CODE1X based model

4.6 Emission indexes

Emission indexes, emission quantity per mass of fuel, are usually empirically based. Authors such as Lefebvre (Lefebvre, A.H., 1983) suggest expressions to predict emissions from aircraft engines. Instead of using emission indexes found in the literature, which might well be justified with this simplified model, it has rather been chosen to make the emission calculations with indexes developed later in this work (see Section 5.7).

The following expressions are found to predict quantities of the emission components CO_2, H_2O, NO_X, CO and UHC from the CFM56-C1 engine correctly.

All flight conditions:

$$CO_{2\,EI} = 3.18 \text{ kg/kg}$$

$$H_2O_{EI} = 1.18 \text{ kg/kg}$$

$$NO_{X\,EI} = \frac{3.19 \cdot 10^{-9} \cdot P^{1.24} \cdot e^{0.01118 \cdot T_{st}}}{\dot{m}_A \cdot T_{t4} \cdot \left(\frac{\Delta P}{P}\right)^{0.223}} \quad [g/kg] \tag{4.1}$$

Climb and cruise:

$$CO_{EI} = \frac{23.2 \cdot \bar{f}^2 \cdot \dot{m}_a \cdot T_{t4} \cdot \left(\frac{\Delta P}{P}\right)^{0.629} \cdot P^{-0.822}}{e^{0.0048 \cdot T_{t4}}} \quad [g/kg] \tag{4.2}$$

$$UHC_{EI} = \frac{2{,}31 \cdot CO_{EI}^{\,0.399}}{\left(\frac{\Delta P}{P}\right)^{-0.389} \cdot P^{0.963}} \quad [g/kg] \tag{4.3}$$

Descent and approach:

$$CO_{EI} = \frac{1.08 \cdot 10^{7} \cdot \bar{f}^2 \cdot \dot{m}_a \cdot T_{t4} \cdot \left(\frac{\Delta P}{P}\right)^{0.355} \cdot P^{-3.04}}{e^{0.0123 \cdot T_{t4}}} \quad [g/kg] \tag{4.4}$$

$$UHC_{EI} = \frac{3.33 \cdot 10^{-5} \cdot CO_{EI}^{\,2.83}}{\left(\frac{\Delta P}{P}\right)^{-0.101} \cdot P^{-1.02}} \quad [g/kg] \tag{4.5}$$

Detailed emission quantity predictions from the parametric model are presented along with the discussion in Section 7.3.

4.7 Final Analyses and Presentations

Engine data and fuel consumption were calculated by the CODE1X code for 35 points during the flight, from acceleration and take-off to touch down, average time interval between points is 76 seconds. Based on these data, time specific emissions of CO_2, H_2O and NO_X were calculated (in Excel) for each point. For these final emission calculations, consumption and emissions per second were assumed constant throughout each interval, the mean of the start and end figures were used.
Time specific and accumulated quantities are presented. Also figures for emissions in particular altitude intervals are developed, see figures in Section 7.3.

Emissions of carbon monoxide and unburned hydrocarbons are not evaluated with this simplified model since the emission indexes for the two components, as presented above, when applied with the simple model predict CO and UHC emissions far beyond the realistic range, in descent and approach/landing in particular. The main reason seems to be as follows:
Emission index $NO_{X\,EI}$ is proportional to $\frac{1}{T_{t4}}$, while CO_{EI} and UHC_{EI} are both proportional to the expression $\frac{T_{t4}}{e^{0.0123T_{t4}}}$. A 10 % reduction in T_{t4} causes approximately a 200 % increase in $\frac{T_{t4}}{e^{0.0123T_{t4}}}$, in the actual temperature range. Because the simplified model predicts turbine entry temperatures at low power settings on the lower side compared to Turbomatch, the calculated NO_X quantities stay in a reasonable range, while the estimated CO and UHC emissions become extremely high.

5 FLIGHT MODELING USING *TURBOMATCH*

5.1 The Turbomatch Scheme for Gas Turbines

The Turbomatch software code was developed by the School of Mechanical Engineering at Cranfield University in England. The program was designed to perform design point and off-design calculations of all types of open cycle gas turbine engines. After continuous development for over 30 years Turbomatch is now an up-to-date simulation tool, and, according to Cranfield University, used by university people as well as external organizations. The reasons for choosing Turbomatch as the main engine simulation system in this study are the following:

1. the capability of this program to simulate
   - engine design and off-design conditions,
   - the effects of engine deterioration,
   - variable compressor geometry,
2. the flexibility of the program,
3. its reputation in academic and industrial environments,
4. reliability is documented over several years,
5. the relatively low user threshold.

The Turbomatch software is documented in ("The Turbomatch Scheme for Aero/Industrial Gas Turbine Engine Design Point/Off Design Performance calculation", Cranfield University, England). The code consists of a fixed set of pre-programmed units called "Bricks". The Turbomatch bricks correspond to engine modules (e.g. compressor, turbine), flow splitters and

mixers, bricks for arithmetical operations and final calculations and bricks to create suitable output. Station numbers are used to specify the location of engine modules.
The bricks are activated by writing so-called "Codewords", a codeword being a set of the brick name, interface parameters (called vector), definition of variables etc. Each brick category has its own requirements regarding codeword details.
The programming task is basically a process of choosing the correct combination of bricks, activating bricks in a suitable order to represent the engine, input quantities for the appropriate "brick data" variables (design condition) and finally listing the variable quantities for current operational conditions (off-design).
The fundamental aerodynamic and thermodynamic equations are the main calculating tools in Turbomatch. There are also 5 fixed and 5 variable geometry standard compressor and 6 fixed and 6 variable geometry turbine maps incorporated into the program. The user has to select among the maps for the components of the current engine. In each case the maps are scaled to match a set of parameters in the on-design condition of the engine and then used throughout the calculations.
Program execution is an iteration procedure through which all the engine components (bricks) are mutually balanced according to their predefined properties. For any extreme condition, convergence problems may be encountered. Attempts to specify engine operation beyond the limits of compressor maps (e.g. compressor stall) and turbine maps (e.g. turbine choking) will be interrupted.
Based on the design point condition for the engine, the Turbomatch is able to calculate engine performance and evaluate a number of engine parameters for off-design operating points as well. For the off-design conditions the user has to specify the operational environment, i.e. for aircraft applications the altitude, Mach-number, deviation from the standard atmosphere and certain engine settings like the opening of the bleed air valves and the angle of the variable stator vanes.
The size of the code, data files required and amount of manual work associated with operation of the program are discussed in Section 7.3.

5.2 Modeling the CFM56-3C1 Engine

The CFM56-3C1 engine was modeled quite simply, each component at a time, the steps of the airflow, going downstream, starting at the intake, splitting in the core and bypass flows and so on. One special issue had to be addressed as air is bled from the 5th stage of the HP compressor. A major decision was therefore to split the HP compressor between the 5th and the 6th stages, into two separate compressors, requiring equal rotational speeds for the two at all times.
A "throttle setting" parameter for the engine had to be defined to enable the user to control engine thrust. In this case the thrust is watched directly as calculations are executed, and one does not have to rely on a constant N1 as an indicator like with the CODE1X code. Therefore the turbine exit temperature (TET $\equiv T_{t4}$) was chosen as the engine power setting parameter. Secondly the T_{t4} has a close relation to the fuel flow and is also important in the process of forming certain emissions, hence, it is convenient to control this parameter.
Figure 5.1 is a schematic sketch of the CFM56-3C1 engine, as modeled in Turbomatch. All station numbers are shown on the sketch.

A listing of the Turbomatch user program for this particular engine, and two alternative output samples are attached in Appendix K.

5.2.1 Design condition

For a well-defined engine design condition several engine parameters have to be input to the program for the calculation of "design performance". This condition forms the basis for all off-design calculations.
No specific condition is said to be the design point for the CFM56 engine. The documentation on the engine that has been made available via Braathens and CFM International mostly presents data for the following conditions:

1. take-off, sea level, standard atmosphere (ISA) and 30 °C
2. maximum climb at 35 000 ft, 0.8 M, ISA
3. test cell operation / calibration (static)
4. engine shop testing (manuals including acceptance criteria for engine systems after overhaul)
   - plus a few single parameter quantities for other conditions.

All the necessary parameters are not covered completely for any of the conditions, at least not for the format specified in Turbomatch. The modeling task in the present work was based on the "take-off, sea level, ISA, 30 °C" condition which is by far the best documented. This is identical to the design condition defined for the simplified model calculations (CODE1X). Values of certain parameters in other conditions were useful in testing the accuracy and the quality of the calculations (CFM International: "CFM56-3 Service Bulletin, March 1984, Revision 3, September 1987") , (CFM International: "CFM56 Specific Operation Instructions, April 1988 and November 1992"). Performance data for the CFM56-3C1 (full rated i.e. clean) engine are presented in Tables 5.1 and 5.2.
For a few parameters minor variations in the quantities quoted in the various sources were found, for the take-off condition in particular; variations in by-pass ratio and overall pressure ratio are both in the range of ± 2 %.

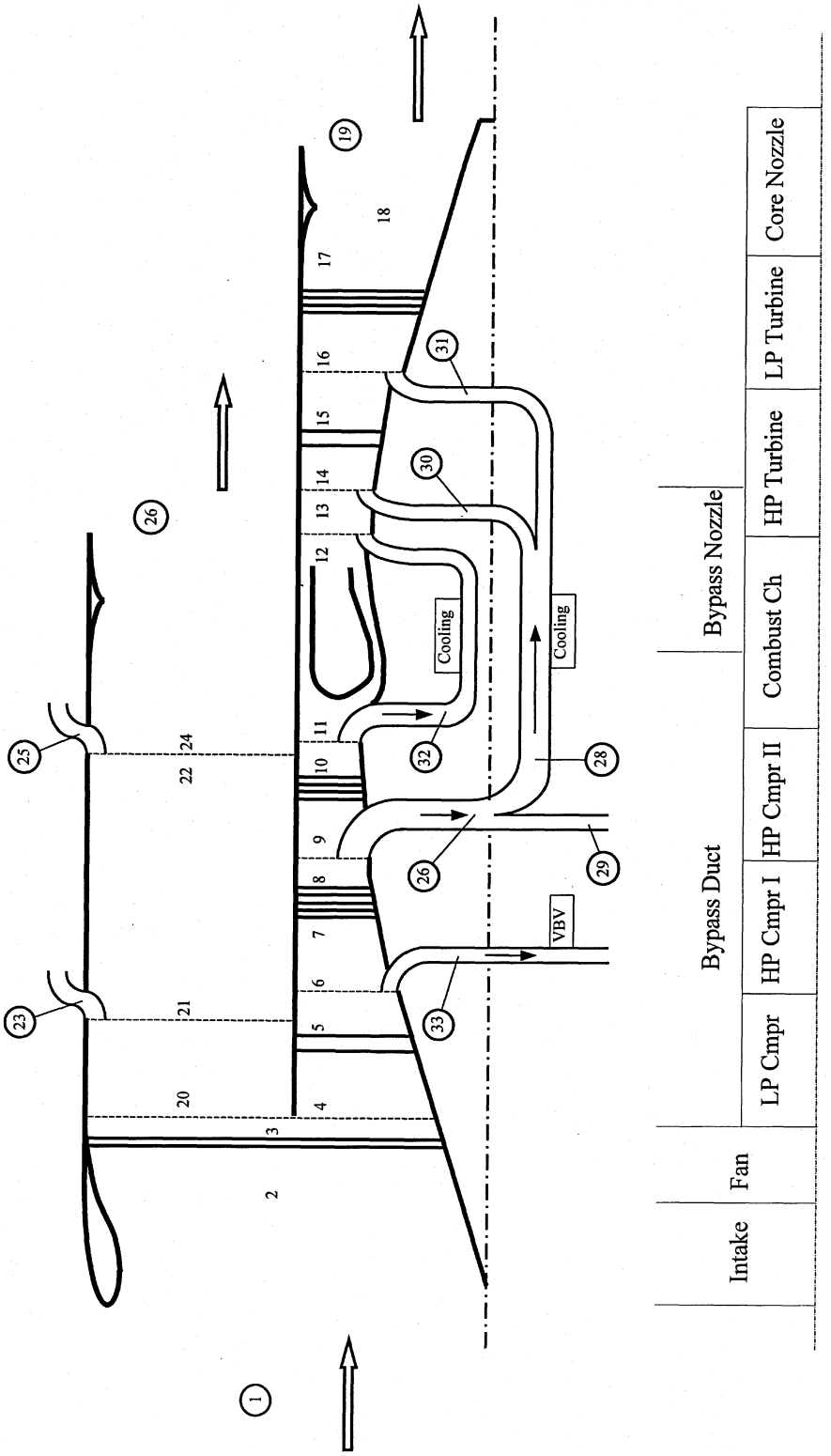

Figure 5.1 CFM56-3C1; Basic principles of the engine for Turbomatch modeling

Flight Condition	Thrust [kN]	By-pass ratio	O/A press. ratio	Air mass flow [kg/s]	Fuel flow [kg/s]	T_{t4} [K]	LP spool RPM	HP spool RPM
T/O sea level static, ISA +15K	104.5	5.0	25.5	322.1	1.154	1 640	4 959	14 250
Max. climb, M=0.8 10 688 m, ISA	24.64		30.6					
Climb out					0.954			
Approach					0.336			
Idle					0.124			

Table 5.1 CFM56-3C1 engine performance parameters as available for certain conditions.

Flight Condition	Thrust [kN]	Pressure ratios			
		Over all	Fan	LP compressor	HP compressor
T/O sea level static, ISA +15K	104.5	25.5	1.7	1.36	11.3

Table 5.2 Pressure ratios as available, CFM56-3C1 engine

The CFM56-3C1 turbofan engine is a fixed nozzle engine, i.e. the nozzles areas are constant at 0.294 m^2 and 0.736 m^2 for the core and the bypass nozzles respectively.
Graphs showing a range of correlations for data from test cell operation of the engine are available in (Duquesne, G., 1990).

5.2.2 Data used in the CFM56-3C1 Turbomatch model

Losses, efficiencies, etc.:

Since access was not available for all such information in detail for the real engine, most of these values were set based on examples and indications from the literature and from examples and recommendations in the Turbomatch manual. Bleed air quantities, except for the VBV (variable bleed valves) are estimated. All these data are considered design parameters and apply to the new and clean engine. The design point quantities are listed in Table 5.3.

Engine module	**Pressure losses [%]**	**Surge margins**	**Efficiencies**		**Air bleeds [%]**	**Power extraction [kW]**
			Isentropic	Com-bustion		
Bypass duct	0.25					
LP – HP compr. duct	1.80					
Combust. chamber	3.25			0.999		
Core exhaust duct	0.20					
Fan		0.85	0.850			
LP compressor		0.95	0.876			
HP compr. first 5 stg.		0.90	0.877			
HP compr. last 4 stg.		0.90	0.877			
HP turbine			0.883			100.0
LP turbine			0.870			0.0
Bypass duct upstream					0.83	
Bypass duct downstr.					0.93	
HP compr. 5^{th} stg. T/O					8.5 *	
HP com. 5^{th} stg. flight					10.0 *	
HP compr. discharge					4.5	

Table 5.3 Losses, margins and efficiencies for the CFM56-3C1 engine
*) HP compressor 5^{th} stage bleed air is for turbine cooling only at take-off and for turbine cooling and external use during flight.

Fuel quality:

The Turbomatch scheme does not give the user the opportunity to specify the heating value of the fuel. According to Cranfield University (R. Hales) the default calorific value of the fuel in Turbomatch is $4.3124 \cdot 10^7$ J/kg. This is 0.75 % higher than what is used in the CODE1X calculations for this study. Such a difference contributes to slightly lower predictions for fuel consumption by Turbomatch than by the simple model, for equivalent engine conditions.

VSVs and VBVs:

The engine is equipped with variable stator vanes (VSV) in the first four stages of the high pressure compressor and variable bleed valves (VBV) at the low pressure compressor discharge. These features are of major importance to the stability of the engine, at low RPMs in particular, and also have to be considered in this model.
Opening and closing of the VSV and the VBV are continuous functions of the high pressure spool rotational speed, N2. The position of the compressor guide vanes vary from what is set as 0.0 degree angle at full speed (above 12 500 RPM) to about 35 degrees at minimum speed (8 000 RPM) (CFM International: "CFM56-3/3B/3C Engine Shop Manual; Revision 46", May 1998).

The bleed valves are closed above 12 000 RPM, and 60 % open at low speed. Whether that percentage is equivalent to the current fraction of full opening bleed air flow is not obvious from the available sources.
For input to Turbomatch it was necessary to simplify these relations drastically and it was decided to use the following rules:

N2 range [RPM]	T_{t4} corresp. [K]	VSV angle [deg]	VBV bleed [% of air flow]
8 000 – 10 000	*950 – 1 150*	**30.0**	**25.0**
10 000 – 11 500	*1 150 – 1 300*	**20.0**	**15.0**
11 500 – 14 250	*1 300 – 1 700*	**0.0**	**0.0**

The ranges in the T_{t4} do not correspond exactly to the N2 intervals in all conditions. For modeling purposes though, the temperature was the most suitable and convenient parameter as the guiding variable for VSV and VBV, and was therefore used in this case.
Generally speaking, the settings of the VSV and the VBV that are different from zero apply only in the low thrust ranges.

Compressor and turbine characteristics:

The user of Turbomatch has to pick suitable non-dimensionalized compressor and turbine maps for the components of the engine. The manual offers advice on how to make the correct choice. Non-dimensional mass flow and speed for the turbines are set default.
The following selection of standardized compressor and turbine maps apply in this case (map numbers relate to the Turbomatch manual):

fan	compressor map no. 1
LP compressor	compressor map no. 2
HP compressor, first 5 stage	compressor map no. 4
HP compressor, last 4 stage.	compressor map no. 4
HP turbine	turbine map no. 5
LP turbine	turbine map no. 5

5.3 Running and Testing the CFM56-3C1 Turbomatch Program

5.3.1 Design point operation

For the take-off condition as described and defined here to be the design point condition, the Turbomatch calculates for the T_{t4} at 1 645 K:

thrust	104 243 N
fuel flow	1.1538 kg/s
core nozzles area	0.2890 m^2
bypass nozzles area	0.7361 m^2

which are close to the real engine figures.

For thrust there is a deviation from the real engine of 0.25 %. Calculated fuel flow is 0.02 % lower than specified. Core nozzles area is less than 2 % away from the actual engine and the bypass nozzle is correct.
The exhaust gas temperature (EGT) is measured continuously during the operation of the engine, the red line (maximum) being 930 °C. The EGT, the only internal hot section temperature seen by the pilot in flight, is measured between first and second stage of the low pressure turbine. Turbomatch does not present the temperature at this point in the engine. Assuming an equivalent reduction in total temperature over all the LP compressor stages, this EGT can easily be calculated manually. In the calculated design condition the EGT is approximately 835 °C.
By changing the most doubtful parameters such as quantities of bleed air and efficiencies, in minor intervals, one might achieve an even better agreement with the real engine parameters. Keeping in mind the slight discrepancies in some of the engine design parameters, this is not considered to be worthwhile. Secondly, in this work the main focus is on relative quantities, and therefore these small deviations are of no significance.

5.3.2 Off-design calculations, evaluation

By increasing altitude and Mach-number simultaneously in increments of 500 m and 0.05 respectively, the Turbomatch model eventually reaches engine performance at the maximum climb condition, 10 688 m (35 000 ft), M0.8. Parameters are set for full air bleed.
At this altitude and speed, with a TET at 1 554 K the engine is developing a net thrust 24 629 N, fuel flow at 0.495 kg/s and over all pressure ratio at 30.8. Thrust and pressure ratios show good correlation.
Other parameters in this condition are air mass flow at 138 kg/s, rotor speed N1 = 4 732 and rotor speed N2 = 13 617. EGT in the maximum climb condition (at altitude) is approximately 760 °C.
Finally the Turbomatch engine is returned to its original take-off condition, TET is again specified at 1 645 K, the hot day condition and bleed air are set properly, and the performance output is calculated as follows:

thrust:	104 267 N
bypass ratio:	4.99
over all pressure ratio:	25.62
air mass flow:	322.1 kg/s
fuel flow:	1.1548 kg/s
N1:	4 952 RPM
N2:	14 259 RPM

All these parameters are less than 0.02 % from their initial values, the take-off condition at the beginning of the calculations. Similar accuracy applies to other parameters as well.

5.3.3 Conclusions: engine modeling and testing

This is a reasonably good model for the CFM56-3C1 engine. It represents the engine with sufficient accuracy for take-off and maximum climb at 10 688 m, Mach 0.8 conditions. There are virtually no drifting or hysteresis phenomena during the program execution.

5.4 Modeling a Regular Braathens Flight from Oslo to Trondheim, Norway

5.4.1 The Oslo – Trondheim Flight

Detailed data for a representative flight from Oslo to Trondheim, standard day, take-off weight 48 000 kg (70 % of full load) with a Braathens Boeing 737-400 were supplied by Braathens, see Table 5.4. These data and some more details from a Boeing sample mission calculation (also Braathens) formed the basis for the flight specification in this work.

Mission segment	Time [s]	Distance [km]	Altitude (end) [m]	Speed (end) [m/s]	Flaps [deg]
Taxi-out	300	-	12	10.3	-
Acceleration	(incl. T/O)	(incl. T/O)	12	72.0	5
Take-off	114	4.3	457	108.0	5
Climb	864	213.0	11 278	220.0	-
Cruise	300	65.0	11 278	220.0	-
Descent	1 212	200.0	457	82.3	-;5
Appr. and Land.	120	9.3	6	61.7	5; 10; 15; 30
Taxi-in	300	-	6	10.3	-
SUM	**3 210**	**492**			

Table 5.4 Representative flight data for an Oslo – Trondheim flight, standard day, take-off weight 48 000 kg (70 % of full load) with a Braathens Boeing 737-400. Information from Braathens Flight Operations (Appendix F).

The necessary turbine entry temperature (throttle setting) in any point in flight was evaluated through an interpolation procedure (explained in Section 5.4.4) based on the thrust requirement in the particular point. Speed, acceleration and climb angle for the aircraft are among the parameters that have to be known to calculate the required thrust. Calculations are performed at a number of such points during the flight and the following assumptions and simplifications apply:

1. climb angle is constant over the main flight segments
2. aircraft acceleration is either constant or zero over major parts of flight segments
3. altitude and speed are according to the Braathens' route specification
4. total time and flight distances for each segment are according to the Braathens' description (a few minor exceptions are explained later).

The assumption regarding constant acceleration is a simplification and does not necessarily allow for stepwise constant low pressure rotational speed N1, as discussed earlier in this work. Speed developments for the two alternatives, the stepwise constant acceleration and the constant N1 are compared in Section 7.3.1 and appear on a graphical presentation in Figure 7.12. Deviations are not dramatic.
The taxiing sequence is included in the flight model, though this is omitted from the final analyses of the present work.
The mission segments and important details of the route are shown in Table I1, Appendix I.
For the accuracy in the present work a far more detailed mission description was used, each flight segment was divided into several sub-segments. Each of the sub-segments cover a time

span in the range of 30 seconds to two minutes. Flight and engine conditions were calculated for the start and end points for each sub-segment. All conditions at a sub-segment starting point were assumed constant and valid throughout the entire sub-segment.
New total mass of the aircraft was evaluated at each sub-segment end point and formed the mass for the following segment. The advantage of assuming parameters constant during a sub-segment is to calculate mass (i.e. fuel consumption) directly and thus avoid iterations. For further calculations average quantities for fuel consumption, emission indexes etc. were evaluated by linear interpolation between sub-segment start and end points.
Total number of points for calculation (sub-segments) is 35. The sub-segment details are presented in Table I2, Appendix I.

5.4.2 Acceleration and climb angle, special considerations and modifications

Aircraft accelerations and climb angle are essential parameters that do not appear in detail in the mission description from Braathens. Acceleration and climb angle relate directly to the gain of speed and altitude over time. For the climb and descent segments it can be shown quite easily, by the basic equations of motion, that the acceleration is not constant for the entire segment. For that reason the climb and the descent segments were split into sequences Climb I and Climb II, and Descent I and Descent II respectively. It was assumed that a constant acceleration causes the speed to reach a maximum climb speed during Climb I, and speed to stay constant during Climb II. The speed is constant in Descent I and acceleration is constant in Descent II. To keep the entire times and flight distances for climb and descent correct, the lengths of Climb I and Descent I were evaluated carefully. Climb angle is constant throughout the entire climb, and similarly for the entire descent segment.
For all the other flight segments acceleration and aircraft climb angle are not subject to variation within the segment.
With the simplifications described a certain inconsistency in the flight route was encountered. It was the aim to do the analyses for the Braathens mission, so some additional information was needed. To establish the most realistic mission specification a synthesis of the Braathens' Oslo - Trondheim flight and the Boeing sample mission calculation (Table F2) was made. In the Boeing case take-off weight is 31 % higher.
The following adjustments were made:

1. The runway is set to a length of 1 500 m.

2. Take-off time was reduced, the Braathens take-off distance and reasonable acceleration and climb rates are matched.

3. Braathens' climb distance cannot be achieved with reasonable average speed; excess take-off time is added to climb, the total climb distance is reduce to match climb angle.

4. Excess climb distance and corresponding time are added to cruise, cruise time is increased further to keep the cruise Mach number at 0.745 as specified.

5. Time for descent is reduced accordingly so that the entire flight time remains correct.

For all engine conditions (clean and unclean) it was found that at certain points the data did not include a sufficiently wide thrust range to respond to the acceleration and rate of climb requirements. The three points where this problem occurred are all transient points in the flight route:

1. Point 13, end of the sequence Climb I;
   change of acceleration (0.690 m/s^2 → 0.000 m/s^2)
2. Point 20, end of the sequence Climb II;
   change of climb angle (0.0570 m/m → 0.0000 m/m)
3. Point 26, start of the sequence Descent I;
   change of climb angle (0.0000 m/m → – 0.0547 m/m)

To complete the interpolation minor modifications to the acceleration and climb parameters were used as follows:

Point 13; acceleration	0.449 m/s^2
Point 20; climb angle	0.0520 m/m
Point 26; climb angle	– 0.0500 m/m

The modifications in points 13 and 20 are both conservative in the respect that they reduce fuel requirement and emissions. Secondly, all three reflect the transience, as the quantities lie between start and end values for the sequence, and thus give a more realistic picture of engine operation at these points.
The conditions at points 13 and 20 are just momentary conditions (time 0.0). The point 26 condition lasts 120 seconds, and for this particular point the reduction in the climb rate is accounted for in the succeeding points to keep the altitude and travel distance correct.
All these details are incorporated in the sub-segment list in Table I2 of Appendix I.
Extreme fouling (D3); special considerations:

A similar problem as described, though more pronounced, occurred at the last two points (19 and 20) of the Climb II sequence for this condition. To overcome this problem calculations were made for as high a climb angle as the data allowed, and the required parameters were evaluated by extrapolation based on increasing the climb angle. Except for the turbine entry temperature, which becomes unrealistically high, the parameters stay in a reasonable range.

Due to the high turbine entry temperatures this procedure may have caused an overestimated NO_X emission.

The extrapolated condition accounts for 15 % of the climb time, 5 % of total observed flight time with the extremely fouled engines only.

In two cases the D3 Turbomatch data did not reach the thrust requirement. These conditions are point 5 in acceleration, and descent 7 000 m – 4 000 m, points 29 – 32. For these conditions the D2 data were used. The fuel flow calculated on the basis of D2

data was then corrected by a percentage similar to the difference between D2 and D3 averaged over adjacent points, 5.5 % and 2.4 % respectively. In this way aircraft mass reduction was estimated, and the basis for emissions was quantified as correctly as possible. All remaining parameters were left as calculated from D2 data.
Roughly 30 % of the acceleration and take-off time, and 22 % of descent time, in extreme fouling condition, were effected by the adjustments.

5.4.3 Set of calculation

With the time and resources available, it was decided that the most convenient way to investigate the model engine performance in all flight conditions necessary was to build up a large set of data and later on interpolate in this database. All realistic combinations of three governing parameters, airspeed, altitude and turbine inlet temperatures for the engine, were run in the Turbomatch code, and subsequently all input and calculated data stored. The ranges of the governing parameters were established on the basis of easily available airline and manufacturer data, Appendix F and (CFM International: "CFM56-3 Basic Engine"), (CFM International: "CFM56-3 Engine Family", Company brochure CFMI-1234 (6/98)), (CFM International: "Durable Engines, Reliability at its Finest", Company brochure CFMI-1215 (9/96)), (CFM International: "Technology Continually Improving the CFM56 Engine", Company brochure CFMI-1217 (9/96)). Increments were chosen as small as possible without causing the number of combinations to exceed the practical size (computer storage capacity). All the discrete values of airspeed, altitude and turbine inlet temperature that are run, appear in Table I3 of Appendix I. There is one separate data subset for each flight sequence.
Further complete sets of data were generated for each of the three conditions of deteriorated engines. Some additional data subsets had to be generated for the extreme fouling to assure sufficient thrust in this condition, and in other cases to stay inside the ranges of Turbomatch convergence.

5.4.4 Interpolations

One combination of speed, altitude and turbine inlet temperature is for this particular study identified as one engine operation condition. More than 32 000 engine operation conditions form the total set of data. The data supplied by Turbomatch is in a format that is readable from a Fortran program.
Engine parameters for each distinct point in flight operation were found by interpolation in these large data sets, and a Fortran program was written to perform the interpolations through the following steps:

1. input by user, the altitude, Mach number, thrust requirement (and, if necessary, the flight sequence),

2. find the two Mach numbers, larger and smaller, closest to the operation Mach number, in the data subset (Mach numbers in the data sets are standardized),

3. find the two altitudes adjacent to operation altitude (larger and smaller, altitudes in the data sets are standardized),

4. for each of the four combinations of speeds and altitudes now at hand, find the two conditions closest to operation thrust performance.

5. Hence 8 engine conditions are sorted out from the data set. Using linear interpolation between these conditions, all relevant parameters for the current engine operation condition are evaluated.

5.4.5 Limitations

As Turbomatch does not provide sufficiently low net thrust at close to zero speed on the ground, the idle and taxiing sequences were not incorporated in the model. The fuel consumption during these sequences is very small, according to available data, typically Table F2, Appendix F, a one minute taxiing requires less than 13 kg fuel, and secondly all emissions occur on the ground. For those reasons the taxiing and ground idle conditions are not of really great significance in the present work.

5.5 Modeling the Boeing 737-400 Aircraft

5.5.1 Lift and drag, clean aircraft

There is a need to know the relations between the weight of the aircraft and the thrust from the engines at all points in flight. One fundamental source for this information is the aircraft drag polar. The drag polar is an expression of how the drag coefficient C_D varies with the lift coefficient C_L at different flight Mach numbers. The Boeing 737-400 clean aircraft drag polar was used (Figure F3, Appendix F).
Minor drag components, like those from antennas and other small equipment, are not included in the clean aircraft drag polar. Access was not available for such detailed information, and therefore predictions of fuel consumption that are slightly on the low side will be accepted throughout the study. This possible discrepancy applies in all flight conditions, and relative variations in fuel flow and emission quantities are not effected.
References like Roskam, J., 1989 suggest that the drag polar curve does not vary with speed for Mach-numbers lower than 0.70. In the present case it is assumed that this is valid for the Boeing 737-400, and thus the M0.70 drag polar is used for all Mach-numbers $M < 0.70$.
Standard definitions of lift and drag coefficients are

$$C_L = \frac{L}{\frac{1}{2} \rho V_0^2 S_{ref}} \tag{5.1}$$

$$C_D = \frac{D}{\frac{1}{2}\rho V_0^2 S_{ref}} \tag{5.2}$$

L and D are the total lift and total drag of the aircraft, ρ is air density, V_0 is ambient speed, and S_{ref} is a reference area of the airplane. Lift is equivalent to total weight W of the aircraft in level flight. Now the correct size of S_{ref} to be used with the available B737-400 drag polar had to be found. One flight case of the B737-400 is described (Braathens, CFMI, Appendix H) as follows:

> The take-off weight was 556.2 kN. Fuel used in taxi-out, take-off and climb was 979.3 kg and in the cruise segment 912.6 kg. Cruise altitude was 7 620 m, cruise Mach-number 0.72, and approximate thrust (2 engines) in cruise was 37.65 kN.

From these case data it was derived that the average aircraft weight in cruise was 542.1 kN and consequently $\frac{D}{W} = \frac{C_D}{C_L} = 0.0695$. The drag polar graph for M = 0.72 now reveals in this average cruise condition that the lift and drag coefficients were 0.196 and 0.0136 respectively.

Assuming cruise speed and flight altitude are both constant, the drag was replaced by the thrust F. Further by using data for standard atmosphere for 7 620 m altitude and setting speed equal to Mach number times the speed of sound, the reference area is evaluated from the C_D equation:

$$S_{ref} = \frac{F}{\frac{1}{2}\rho (M \cdot a)^2 C_D} = 202.9\ m^2 \tag{5.3}$$

Gross wing area of the Boeing 737-400, according to "Janes' All the World's Aircraft 1990-91", is 105.4 m^2, and wetted area for similar airplanes is roughly five times the wing area (Roskam, J., Lan, Ch.-T.E., 1997), i.e. 500 m^2 for the Boeing 737-400. These are both areas of great influence for the lift and drag of the airplane, and the reference area calculated above, being in the same range, is reasonable and was used in this work.

5.5.2 Drag due to flaps, landing gear and ground friction

In take-off and landing segments, the use of flaps and the deployed landing gear causes considerable increase in the total drag of the aircraft. The drag polar expresses the so-called clean aircraft drag, which does not account for such extra drag components. While on the ground, friction from the runway surface is added to the drag, and at low speed the ground friction is the major drag component.
To make a rough estimate of the lift-off drag, the conservative assumption is made that net engine thrust is F = 150 kN. Acceleration *a* immediately after lift-off, the incidence angle β of the aircraft and the aircraft mass m, hence the lift L for this moment, are all known quantities. The drag D was found from Equation (5.4) and the figures in Table 5.5.

$$D = F - m \cdot a - m \cdot g \cdot \sin \beta \tag{5.4}$$

Knowing the ambient airspeed and air density at this point, the lift and drag coefficients were evaluated from Equations (5.1) and (5.2), see Table 5.5.

For the next two points in the take-off segment, i.e. at altitudes 213 m and 457 m, the net engine thrust is reduced typically by 3 % and 10 % respectively, mainly due to higher ram drag. The lift is unchanged, and so are the acceleration and the climb angle. The ambient airspeed is increasing while air density falls slowly. The assumption is that at 213 m altitude the landing gear is down and 5° flaps are set while at 457 m altitude the landing gear is up and flaps still at 5°. Lift and drag forces and the calculated coefficients are presented in Table 5.5.

The lift-off point is totally out of range of the clean aircraft drag polar graph that is accessible. In the next two points the lift coefficient is within limits of the graph, and corresponding clean aircraft drag coefficients are 0.0235 and 0.0177. Differences from the total drag coefficients calculated above indicate the drag increase due to landing gear and flaps settings, $\Delta C_{D,g,f}$ and $\Delta C_{D,f}$. The sizes of these increments, as used for the take-off sequence, are listed in Table 5.5.

From Braathens' Flight Route Description it is evident that a flaps setting of 5° is used during take-off, and similar setting during the end of the descent segment.

In the second half of the descent (below 5 000 m = 16 400 ft) the thrust requirement has to be very low or zero, to keep deceleration and rate of climb as prescribed when clean airplane drag coefficient is used. The engine power setting in this segment is said to be "flight idle". Turbomatch model does not work successfully for close to zero net thrust, and therefore the thrust requirement had to be increased to stay within the range of the model. This may be interpreted as successively increasing flaps setting from 0° to 5° and eventually lowering the landing gear. To account for additional drag at low altitudes of descent and approach increments $\Delta C_{D,f}$ and $\Delta C_{D,gf}$ were used.

In the approach/landing segment, flaps setting is increased gradually from 5° to 30°. Referring to similar condition in take-off, C_D is increased accordingly. For the last three points of the flight particular quantities for the drag coefficient have been used.

Aerodynamic lift and drag are negligible during taxiing. In acceleration the aerodynamic forces increase successively. For aerodynamic lift and drag on the ground, coefficients $C_{L,AG}$ and $C_{D,AG}$ equivalent to those in the lift-off conditions were used.

All these coefficients and increments are shown in Table 5.5

Altitude [m]	Condition	Lift [kN]	Drag [kN]	Speed [m/s]	$\Delta C_{D,g,f}$ and $\Delta C_{D,f}$	Coefficients of total lift and drag			
						C_L	C_D	$C_{L,AG}$	$C_{D,AG}$
12	*Acceleration*							0.728	0.102
12	*Lift-off*	468.0	65.8	72	0.040	0.728	0.102		
213	*Take-off*		60.8	90	0.040	0.475	0.062		
457	*Take-off*		50.8	108	0.020	0.337	0.037		
4 228	*Descent*				0.001				
3 059	*Descent*				0.0025				
2 058	*Descent*				0.0075				
1 231	*Descent*				0.015				
577	*Descent*				0.030				
457	*Approach*				0.040		0.060		
215	*Approach*						0.075		
6	*Approach*						0.100		

Table 5.5 Drag coefficient due to landing gear and flaps, aerodynamic lift and drag close to the ground and during ground acceleration. The Boeing 737-400 in Oslo – Trondheim flight.

On the ground, during taxiing and acceleration, ground friction represents a major resistance component to the motion of the aircraft. According to Roskam (Roskam, J., 1989) the friction coefficient μ on a concrete runway is in the range of 0.02 — 0.03, independent of speed. In this work therefore $\mu = 0.025$ has been used. The ground friction is

$$R = \mu \cdot (m \cdot g - L) \tag{5.5}$$

and on the ground the horizontal Newton's second law (Equations (5.6 and (5.7)) is used to calculate the necessary thrust F.

$$F - R - D = m \cdot a \Rightarrow \tag{5.6}$$

$$F = \mu \cdot (m \cdot g - C_{L,AG} \cdot \frac{1}{2} \cdot \rho \cdot V_0^2 \cdot S_{ref}) + C_{D,AG} \cdot \frac{1}{2} \cdot \rho \cdot V_0^2 \cdot S_{ref} + m \cdot a \tag{5.7}$$

5.5.3 Evaluation of the Turbomatch based Model and Calculations

The CFM56-3C1 engine is represented very accurately in the Turbomatch Scheme, as concluded in Section 5.3.3. The flight route Oslo – Trondheim is modeled according to a realistic Braathens' flight, given a particular take-off weight and cruise altitude.

The clean aircraft drag polar is assumed to represent total drag of the real aircraft, except for the flaps, landing gear and ground friction drag. This assumption implies a small under-estimation of the aircraft drag.
To find how well the simulated flight of this work corresponds to a real case, the calculated fuel consumption as an indicator, is compared to the estimates of the aircraft and the engine manufacturer:

1. the mission calculations from Boeing, see Table F2 of Appendix F, and
2. the CFM estimates, copied in Appendix H (figures for one engine).

The comparisons are demonstrated in Table 5.6. Major reasons for the discrepancies are that the two other cases both deviate slightly from the Braathens' Oslo – Trondheim flight with respect to take-off weight, cruise altitude and cruise speed.
Data from the Turbomatch based calculations however appear to be quite reasonable, and close to industry data for the 500 km flight.

	Boeing estimates	**CFM estimates**	**Turbomatch / Braathens**
Take-off weight [kg]	62 800	56 700	48 000
Cruise altitude [m]	9450 / 10 670	7620	11 278
Cruise Mach no. / speed [m/s]	0.74 / 223	0.72 / 223	0.745 / 220
Climb fuel consumption [kg]	1242	829	1228
Fuel flow in cruise, both engines [kg/s]	0.682	0.761	0.525
Total fuel consumption, 500 km flight [kg]	2212	2021	1948

Table 5.6 Fuel consumption, different estimates for a 500 km Boeing 737-400 flight, two engines (the cruise segment of Boeing data adjusted to correct length by the author).

5.6 Modes of Engine Deterioration

In the present study deterioration due to fouling of the cold end of the engine, that is the fan and compressor sections, is considered.
From the literature it is evident that in general compressor fouling has an effect on the entire compressor map (Section 6.3 of this work) so the following parameters are affected:

- the compressor pressure ratio
- the compressor isentropic efficiency
- the compressor air flow (non-dimensional)
- the compressor surge margin.

According to references (Diakunchak, I.S., 1991), (Saravanamuttoo, I.H., Lakshminarasimha, A.N., 1985), (Grewal, M.S., 1988), (Cabrejas Morales, J.C., 1998), (Ul Hag, I., Saravanamuttoo, H.I.H., 1993), when degrading is in progress these properties all vary at the same time. The drop in pressure ratio is of the same magnitude as the reduction in the non-dimensional air flow and is twice to three times that of the drop in isentropic efficiency.
Turbomatch allows for changes in pressure ratio, isentropic efficiency and non-dimensional air flow for the off-design, deteriorated conditions.
Input to the Turbomatch model for different degrees of degradation (reductions in the parameters) is done through the so-called scaling factors. The scaling factors at the design condition were all set as default at 1.00.
The first task then was to reveal the relation between a reduction in each scaling factor and the consequences for the related property. This was done by running the clean engine in its design condition, only varying one scaling factor at the time, and reading the variation in the corresponding parameter. For the modeling of the degraded engine it was then known where to set the scaling factors to achieve proper and correct reductions in the compressor properties (changes to the compressor maps).
This was carried out for the fan and all the compressors in the engine. For details from this study see Appendix G.
An engine degradation parameter Φ is defined, related to the percentage point reduction in isentropic efficiency, e.g. if the isentropic efficiency falls from 0.800 to 0.795 (a reduction of 0.5 percentage points) Φ is equivalent to 0.5. A drop in efficiency of aircraft engine components due to normal wear may reach 2.5 %, see Section 3.2. For the present study, one mild, one moderate and one extreme state of fouling are defined and considered. The degraded engine conditions are identified as D1, D2 and D3 while the full performance (new and clean) engine is in C0 condition, see specifications in Table 5.7.

Property increment	**C0; $\Phi = 0.0$**				**D1; $\Phi = 0.5$**				**D2; $\Phi = 1.0$**				**D3; $\Phi = 3.0$**			
	Fan	**CL**	**CH 1**	**CH 2**	**Fan**	**CL**	**CH 1**	**CH 2**	**Fan**	**CL**	**CH 1**	**CH 2**	**Fan**	**CL**	**CH 1**	**CH 2**
$\Delta\pi_F$, $\Delta\pi_C$ [%]	0.0	0.0	0.0	0.0	–1.0	–1.0	–1.0	–1.0	–2.0	–2.0	–2.0	–2.0	–3.0	–6.0	–6.0	–6.0
$\Delta\eta_F$, $\Delta\eta_C$ [pts.]	0.0	0.0	0.0	0.0	–0.5	–0.5	–0.5	–0.5	–1.0	–1.0	–1.0	–1.0	–3.0	–3.0	–3.0	–3.0
$\Delta\dot{m}_{a,F}$, $\Delta\dot{m}_{a,C}$ [%]	0.0	0.0	0.0	0.0	–1.0	–1.0	–1.0	–1.0	–2.0	–2.0	–2.0	–2.0	–3.0	–6.0	–6.0	–6.0

Table 5.7 Component property reduction in percent and percentage points, pressure ratio, efficiency and mass flow rate, clean engine and all three modes of fouling

5.6.1 Special considerations regarding the extreme condition

1. Reasons for not reducing the fan pressure ratio and air flow capacity to the same extent as for the other three compressors are:

- the fan is exposed to rain and other precipitation that will wash and clean the blades, and consequently the fan is less prone to fouling
- any fouling on the fan has less consequences for the flow than in the rest of the compressor stages, the reason being the coarse geometry of the fan
- still, the fan is frequently dented and buckled by foreign objects so a reduction in efficiency is reasonable.

2. Certain convergence problems were encountered for the extreme condition. The results are assumed to still be valid and useful, as they are found through interpolations in the modeling results. In the interpolation process one single data point is just one eighth of the basis for a calculated engine condition, and thus the influence is minor. Secondly, by interpolation a certain level of inaccuracy has to be accepted.

3. In the introductory chapter it was explained that the new, fully efficient engines are used on the Boeing 737-400. The reason is that the deteriorated CFM56-3C1 engines are not capable of the high thrust performance required by the Boeing 737-400 within the acceptable EGT limits. The D3 condition is therefore of theoretical value only, as an indication of engine behavior with increasing degree of fouling.

5.6.2 Engine performance, consequences of cold end fouling

When all the scaling factors are changed at the same time, for all the four compressor modules, the performance of the engine changes considerably. A selected set of engine parameters at specific operational conditions for the clean and deteriorated engine is presented as a demonstration in Table 5.8.

5.7 Emission Indexes

5.7.1 General relations

Components usually considered in the exhaust from turbofan aircraft engines are carbon dioxide, water vapor, nitrogen oxides, carbon monoxide and unburned hydrocarbon (CO_2, H_2O, NO_X, CO and UHC). CO_2 and H_2O are dominant in quantity. NO_X is usually subject to great attention because of its detrimental effect to the environment.
Jet fuel with an average composition $C_{16}H_{29}$ (Statoil, ICAO) in complete combustion will give 3.18 kg CO_2 and 1.18 kg H_2O per kg fuel.

Condition	T_{t4}[K]	ΔT_{t4}[%]	$\dot{m}_f$ [kg/s]	$\Delta\dot{m}_f$ [%]	TSFC[kg·s^{-1}·kN^{-1}]	ΔTSFC [%]
1. Max take-off (0.0 m, M0.0, ISA); 104.5 kN thrust:						
Clean	1 579	*	1.126	*	0.01078	*
D1	1 626	3.0	1.168	3.7	0.01118	3.7
D2	1 671	5.8	1.209	7.4	0.01157	7.3
D3		—	*Out of range*		—	
2. Take-off (0.0 m, M0.0, ISA); 94.0 kN:						
Clean	1 513	*	0.974	*	0.01036	*
D1	1 536	1.5	0.995	2.2	0.01059	2.2
D2	1 570	3.8	1.022	4.9	0.01087	4.9
D3	1 737	14.8	1.125	15.5	0.01197	15.5
3. Max climb (10 688.0 m, M0.8, ISA); 24.65 kN:						
Clean	1 555	*	0.496	*	0.02012	*
D1	1 597	2.7	0.509	2.6	0.02065	2.6
D2	1 640	5.5	0.523	5.4	0.02122	5.5
D3		—	*Out of range*		—	
4. Climb (10 688.0 m, M0.8, ISA); 23.00 kN:						
Clean	1 499	*	0.455	*	0.01978	*
D1	1 540	2.7	0.467	2.6	0.02030	2.6
D2	1 580	5.4	0.479	5.3	0.02083	5.3
D3	1 751	16.8	0.517	13.6	0.02248	13.7

Table 5.8 Turbine entry temperature, fuel flow and thrust specific fuel consumption, variations with engine fouling. (Thrust specific fuel consumption of course increases by an equivalent amount as does the fuel flow, when thrust is kept constant.)

CO and UHC are minor fractions of the exhaust gas. For a CFM56 engine CO mass flow is typically $\frac{1}{1000}$ and UHC $\frac{1}{10\,000}$ of the CO_2 flow. NO_X amounts to approximately $\frac{1}{500}$ compared to CO_2, roughly 5 g NO_X released per kg fuel.
In the present work the emissions of CO_2, H_2O, NO_X, CO and UHC have been studied in detail.

Emission indexes, CO_2 and H_2O
The quantity (mass) of one gaseous component formed during the combustion of 1 kg fuel in an engine is traditionally defined as the emission index for that particular component and

engine. In the present study, for the case of aircraft gas turbine engines the fuel composition (C/H-ratio) was assumed constant.
Particularly for the carbon dioxide and water emission estimates, complete combustion was assumed. Hence, the emission indexes for CO_2 and H_2O are constants:

$$CO_{2\,EI} = 3.18 \text{ kg/kg}$$

$$H_2O_{\,EI} = 1.18 \text{ kg/kg}$$

Emission index, NO_X (in general)
Empirical models for predicting emissions of nitric oxides have been developed by Lefebvre (Lefebvre, A.H., 1983). According to Lefebvre the quantity of NO produced is dependent on four different factors:

1. dilution air flow downstream of the combustion zone
2. mean residence time in the combustion zone
3. chemical reaction rate
4. mixing rate,

and a general expression of volume fraction of NO in the exhaust flow is suggested as follows:

$$NO = \frac{A \cdot V_B \cdot P^y \cdot e^{z \cdot T_{pz}}}{\dot{m}_a \cdot T_{pz} \cdot \left(\frac{\Delta P}{P}\right)^x} \quad [\text{ppmV}] \tag{5.8}$$

V_B is combustor volume, P is maximum pressure in the combustor, T_{pz} is primary zone temperature, $\dot{m}_a$ is air mass flow rate and ΔP is pressure drop across the combustor.
A, x, y and z are constants. Lefebvre suggests x = 0.5, y = 1.2 and z = 0.009.

In his MSc thesis Le Dilosquer (Le Dilosquer, M., 1993) refers to other publications by Lefebvre where semi-empirical prediction of NO_X production is modeled according to the following:

$$NO_X = \frac{9 \cdot 10^{-8} \cdot V_B \cdot P^{1.25} \cdot e^{0.01 \cdot T_{st}}}{\dot{m}_a \cdot T_{pz}} \quad [\text{g/kg}] \tag{5.9}$$

T_{st} is stoichiometric flame temperature.

Assuming that in the NO_X, mass fraction $\frac{NO}{NO_2}$ is close to constant, the molecular mass of NO_X is then constant, and NO_X mass fraction is proportional to the volume fraction in a gas mixture.
Secondly the combustion zone volume V_B for one particular engine is assumed constant.
The stoichiometric flame temperature T_{st} is approximately 2 600 K at 800 K inlet temperature T_{in} and pressure P_{in} = 1.0 MPa. T_{st} is independent of pressure for P_{in} > 1.0 MPa, and ΔT_{st} is proportional to ΔT_{in} by the factor 0.5 (Lefebvre, A.H., 1983).
The primary zone temperature T_{pz} is not easily available and not supplied by Turbomatch. The turbine entry temperature T_{t4} is calculated in Turbomatch. T_{t4} is to some extent dependent on T_{pz} and in this particular case the two were assumed proportional.
Based on these considerations a slightly modified, and in this case more convenient prediction model for NO_X has been used. This NO_X emission index is a synthesis of the two by Lefebvre:

$$NO_{X\,EI} = \frac{K \cdot P^y \cdot e^{z \cdot T_{st}}}{\dot{m}_a \cdot T_{t4} \cdot \left(\frac{\Delta P}{P}\right)^x} \quad [g/kg] \tag{5.10}$$

K is constant.

Emission index, CO (in general)
Lefebvre argues further that the quantity of CO produced is dependent on the same four different factors as for NO.
Volume fraction of CO in the exhaust flow according to Lefebvre can generally be expressed as:

$$CO = \frac{C \cdot \bar{f}^2 \cdot \dot{m}_a \cdot T_{pz} \cdot \left(\frac{\Delta P}{P}\right)^b \cdot P^c}{V_B \cdot e^{d \cdot T_{pz}}} \quad [ppmV] \tag{5.11}$$

$\bar{f}$ is the fraction of total air participating in combustion. In stoichiometric combustion of a mass flow $\dot{m}_f$ of the fuel $C_{16}H_{29}$ the air flow participating in the combustion process is

$$\bar{\dot{m}}_a = 14.4 \cdot \dot{m}_f \tag{5.12}$$

Hence, the fraction of total air participating in the combustion then is

$$\bar{f} = \frac{\bar{\dot{m}}_a}{\dot{m}_a} = 14.4 \cdot \frac{\dot{m}_f}{\dot{m}_a} \tag{5.13}$$

C, b, c and d are constants.

Le Dilosquer (Le Dilosquer, M., 1993) and Lee, Le Dilosquer, Singh and Rycroft (Lee, S.H., Le Dilosquer, M., Singh, R., Rycroft, M.J., 1996) are suggesting semi-empirical prediction of CO production as follows:

$$CO = \frac{X \cdot \dot{m}_a \cdot T_{pz} \cdot e^{-0.00345 \cdot T_{pz}}}{(V_B - V_E) \cdot \left(\frac{\Delta P_L}{P}\right)^{0.5} \cdot P^{1.5}} \quad [g/kg] \tag{5.14}$$

ΔP_L is the pressure drop across the combustor liner and V_E is the part of V_B in which fuel evaporation takes place, X is a constant.

Lefebvre correctly points out that "A more rigorous analysis would involve the effects of atomization and droplet evaporation as well". In the present case there was no access to sufficient detailed information such as liner pressure drop and fuel evaporation volume, neither to data for the combustion process of the CFM56 engine, to utilize the latter of the two expressions. Turbomatch does not calculate these parameters either. Therefore, in this case the same assumptions were made as with the NO_X emission index, saying that the combustion-zone volume V_C for one particular engine is constant, and the primary zone temperature T_{pz} is proportional to the turbine entry temperature T_{t4}.
Based on the emission factor from Lefebvre a CO emission index in a general expression is suggested as follows.

$$CO_{EI} = \frac{L \cdot \bar{f}^2 \cdot \dot{m}_a \cdot T_{t4} \cdot \left(\frac{\Delta P}{P}\right)^b \cdot P^c}{e^{d \cdot T_{t4}}} \quad [g/kg] \tag{5.15}$$

L is constant.

Emission index, UHC (in general)
Lefebvre in his book does not present a procedure for UHC and smoke estimations " ... because the highly complex and unknown nature of the hydrocarbon oxidation reaction makes it impossible to derive satisfactory models for UHC and smoke".
Le Dilosquer (Le Dilosquer, M., 1993) suggests a relation between the CO_{EI} and a UHC emission index UHC_{EI} that corresponds well with a similar emission index presented in Lee, S.H., Le Dilosquer, M., Singh, R., Rycroft, M.J., 1996;

$$UHC_{EI} = K \cdot \frac{CO_{EI}}{\left(\frac{\Delta P_L}{P}\right)^{0.5} \cdot P} \quad [g/kg] \tag{5.16}$$

with K as a constant.

By replacing the pressure drop ΔP_L across the combustor liner by ΔP, which is the pressure drop across the combustor, and assuming that they behave similarly, the following expression was obtained and used in this work:

$$UHC_{EI} = \frac{M \cdot CO_{EI}^{\ r}}{\left(\frac{\Delta P}{P}\right)^{s} \cdot P^{t}} \quad [g/kg] \tag{5.17}$$

M, r, s and t are constants.

5.7.2 Emission index evaluations

Estimates from the engine manufacturer for fuel flow and emissions are presented in Appendix H. Most extensive data are available for the CFM56-3B1 engine (Tables H1.b, H2, H4.b, H5 etc.) rather than the CFM56-3C1. Data to compare the two engines on similar type aircraft (B737), at slightly different take-off weight, are shown in Tables H1.a, H4.a and H7.a of Appendix H. These emission data form the basis to quantify emission indexes at certain points during the flight cycle.
When studying the data it is observed that

- in climb and cruise the average CFM56-3C1 fuel consumption is 7.9 % *higher* than for CFM56-3B1, and in descent, figures for fuel consumption are equivalent.
- in climb and cruise the average $NO_{X\,EI}$ is 7.7 % and 4.3 % *higher* for CFM56-3C1 than CFM56-3B1, and in descent the engines show similar $NO_{X\,EI}$.
- in climb and cruise the average CO_{EI} is 6.2 % and 8.8 % *lower* for CFM56-3C1 than CFM56-3B1, and in descent the engines CO_{EI}'s are similar.
- in climb and cruise the average UHC_{EI} is 6.5 % and 2.6 % *lower* for CFM56-3C1 than CFM56-3B1, and in descent the engines have similar UHC_{EI}.

It was assumed that these relations are valid in any point within the particular segments of flight, they have been used as correction factors to estimate the fuel flow and NO_X, CO and UHC for the CFM56-3C1 based on data for the CFM56-3B1 engine.
Time specific fuel consumption and emission figures for the CFM56-3B1 engine are known for specific flight conditions. To find corresponding points in the flight envelope for the CFM56-3C1 engine similarities in flight altitude, the Mach number and the adjusted fuel consumption have been used. Given these parameters the corresponding point in the Turbomatch output file is found, and other parameters such as air mass flow, pressures, pressure loss and temperatures are read. The final data are collected in Appendix H, Tables H3, H6 and H9.
The four unknown constants in Equation (5.10) have thus been found by choosing five different flight conditions from Table H2 and demanding the correct (estimated) emission indexes as in Table H3. Equation (5.18) below fits the four conditions in climb and cruise for the CFM56-3C1 engine's NO_X emission index within less than ±1.5 % discrepancy. A separate emission index for the descent phase might have been evaluated since the equation as found overestimates the descent NO_X rate by about 40 %. This is considered of minor importance though, since very little NO_X is formed in this sequence, the rate being only 2.5 %

of what is maximum during climb, and even this equation predicts only 6 – 7 % of the total NO_X to be released during the descent phase (also discussed in Section 7.1.2).

$$NO_{X\,EI} = \frac{3.19 \cdot 10^{-9} \cdot P^{1.24} \cdot e^{0.01118 \cdot T_{st}}}{\dot{m}_a \cdot T_{t4} \cdot \left(\frac{\Delta P}{P}\right)^{0.223}} \quad [g/kg] \tag{5.18}$$

In the Equation (5.18) P is the maximum pressure in the combustor, ΔP is the pressure drop across the combustor, T_{st} is the stoichiometric flame temperature, T_{t4} is the turbine entry temperature, and $\dot{m}_a$ is the total air mass flow rate through the combustor.
In a similar way the constants in Equations (5.15) and (5.17) were evaluated to find the applicable emission indexes for CO and UHC. Expression for climb and cruise CO_{EI} and UHC_{EI} appear to be totally useless at low power settings (predicting only 1 – 2 % of what is indicated in the CFM data). This was found unacceptable, and separate sets of constants were evaluated for the descent and approach equations. Expressions for CO and UHC emission indexes then became;

in climb and cruise:

$$CO_{EI} = \frac{23.2 \cdot \bar{f}^2 \cdot \dot{m}_a \cdot T_{t4} \cdot \left(\frac{\Delta P}{P}\right)^{0.629} \cdot P^{-0.823}}{e^{0.00480 \cdot T_{t4}}} \quad [g/kg] \tag{5.19}$$

$$UHC_{EI} = \frac{2.31 \cdot CO_{EI}^{\,0.399}}{\left(\frac{\Delta P}{P}\right)^{-0.389} \cdot P^{0.963}} \quad [g/kg] \tag{5.20}$$

in descent and approach:

$$CO_{EI} = \frac{1.08 \cdot 10^{7} \cdot \bar{f}^2 \cdot \dot{m}_a \cdot T_{t4} \cdot \left(\frac{\Delta P}{P}\right)^{0.355} \cdot P^{-3.04}}{e^{0.0123 \cdot T_{t4}}} \quad [g/kg] \tag{5.21}$$

$$UHC_{EI} = \frac{3.33 \cdot 10^{-5} \cdot CO_{EI}^{\,2.83}}{\left(\frac{\Delta P}{P}\right)^{-0.101} \cdot P^{-1.02}} \quad [g/kg] \tag{5.22}$$

In the Equations (5.19), (5.20), (5.21) and (5.22) the variables P, ΔP, T_{st}, T_{t4} and $\dot{m}_a$ are the same as in the Equation (5.18). $\bar{f}$ is the fraction of total air participating in the combustion.

6 COMPRESSOR FOULING – LITERATURE REVIEW

6.1 Introduction

6.1.1 General description of the fouling process and cleaning

For modern gas turbine engines, "... performance deteriorates progressively with increasing operating time" and "In all cases, by far the largest contributor to engine performance deterioration is compressor fouling." (Diakunchak, I.S., 1993). One of the major causes for deterioration is said to be engine, compressor and hot end, fouling. Compressor fouling in industrial gas turbines has been outlined in the literature.
Particulate material, aerosols and other pollutants in the inlet air will adhere to the compressor flow path surfaces, and thereby change the flow cross sectional areas, the airfoil shapes etc. Dust pollen and other dust material, salt, oil mists, industrial and traffic pollutants are examples of fouling that during operation will eventually accumulate in the compressor.
The mechanism of fouling was described as early as 1955 by Fuks, as mentioned in Zaita, A.V., Buley, G., Karlson, G., 1998.
The fouling may to some extent be removed, in some cases completely, by the process called compressor washing. Washing is usually performed regularly on stationary gas turbine engines, and some aircraft engines, either with the engine being shut down, or while running at part load. Washing with the engine running, the so-called on-line cleaning, is normally done with water or a water-based mixture, while some other cleaning solutions are used on a cold engine, the crank wash compressor cleaning (Thames, J.M, Stegmaier, J.W. Ford, J.J. Jr., 1989). A certain performance recovery is usually achieved by compressor cleaning on gas turbine engines.

6.1.2 Relevance to aircraft; the present work

All compressors are susceptible to fouling, according to Saravanamutto and Lakshminarasimha (Saravanamuttoo, I.H., Lakshminarasimha, A.N., 1985). Compressor design and coating are factors that effect the rate of fouling and its influence on engine performance. In reference Lakshminarasimha, A.N. et al., 1994, gas turbine performance deterioration is said to have "emerged as a very important topic of research" because of its impact on aircraft operation, economy and safety.
Performance of aircraft gas turbine engines is of greater significance to this work than that of industrial gas turbines. Knowledge related to stationary turbines is still somewhat relevant and is considered in this review. Fouling and subsequent washing of aircraft engine compressors is less documented in the literature than what is the case for stationary engines.
The airline companies Braathens of Norway and Scandinavian Airlines (SAS) had a procedure for washing their Pratt & Whitney JT8D engines once they operated those engines. The CFM56-3's and -7's on the companies' B737s are reported never to be washed in operation. Widerøe's Flyveselskap, when the company operated Twin Otters in the 1980s, washed the Pratt & Whitney PT6 engines on the airplanes. Their Dash 8's of today are washed regularly as well (Kåre Pedersen, Widerøe, 03/02/2000). Norwegian Helicopter Service has all its Super Puma helicopter engines washed daily after the last flight of the day, in an on-line wash, washing while the engine is running idle.

6.2 The Fouling Mechanism, Reasons for Compressor Fouling

6.2.1 General aspects

The performance of gas turbine engines, the compressors in particular, deteriorate because of fouling, erosion and rubbing wear (Saravanamuttoo, I.H., Lakshminarasimha, A.N., 1985). Compressor fouling is one major factor in this picture. The fouling is caused by small particles and aerosols flying in the air. When sucked into the compressor ducts, portions of this material stick to the surfaces of blades and vanes. Dirt, dust, pollen, insects, oil and water vapor, seawater salt, sticky industrial chemicals, unburned hydrocarbon, soot particles, etc. are examples of such material, and it seems reasonable that presence of oily evaporation and the humidity of the air influence the adhesion of the particles (Tarabin, A.P. et al., 1998).
The deposition of the particles mainly occurs on surfaces facing the flow, though it "is also present on the leeward side of the blade profile as a result of whirls and turbulence" (Zaita, A.V., Buley, G., Karlson, G., 1998). The particles that adhere to the surfaces and to each other form a deposit and thus the airfoil shapes are altered, surfaces get rougher and the flow cross sectional areas are reduced.
To illustrate the magnitude of the phenomenon an example from (Lakshminarasimha, A.N. et al., 1994) states that since gas turbines use roughly half a tonne of air for each horsepower output, for every 24 hours of operation, even with only one part per million particles in the air entering the compressor, a 7 355 kW (10 000 horsepower) unit will ingest 5 kg of foreign material in a single day.
Not necessarily all the particles that hit the compressor inner surfaces adhere to it (Tarabin, A.P. et al., 1998).

Engine erosion is not the specific issue of this chapter, still, it is quite closely related to fouling as much of the ingested material may cause erosion, mechanically and chemically on engine parts, and cause performance reduction to compressors and other components.
A sudden fouling of the front end of the engines, typically on aircraft gas turbines, may occur when passing through, for example, a storm of hail or sand. In such instances the engine will virtually clog up, and the performance of course drops drastically. In such instances, when the fouling material is hard and sharp like sand or ash, serious erosion of the engine components is likely as well. This kind of instantaneous fouling is not within the scope of this work, except for the long-term erosion consequences that will arise from it.

6.2.2 Operational procedures

Very little documentation on how fouling relates to the engine operation is found. Tarabrin et. al. (Tarabin, A.P. et al., 1998) in their model find that the sensitivity to fouling increases with the stage head, and that the degree of particle deposition increases with higher blade angle of attack. Aside from the fact that the stage pressure heads and blade angles are parameters designed into the compressor, it can be concluded that fouling is dependent on the compressor loading; the heavier the compressor is loaded the more fouling is likely to form.
Operating a gas turbine engine such that oil spill from bearings, exhaust gases and foreign objects from the ground are sucked into the air intake will contribute to additional fouling. Aircraft engines are particularly prone to such fouling when on the ground, during engine reverse when air, exhaust, and dirt are blown forward, and when conditions are such that a ground vortex is formed.
Sand and dirt from the runway which are likely to enter the compressor during these modes of operation, appear to be the reason for compressor erosion rather than fouling.

6.2.3 Local conditions, operation site

It is obvious that the presence of airborne particles at the location where an engine operates is quite essential when it comes to the tendency of fouling occurrence. Hydrocarbons and droplets, aerosols of other substances are formed in considerable amounts on busy motorways and many industrialized areas. Airborne salt is present close to and above oceans, sandy material in desert areas. Pollen and other plant material (resin) are found widespread in the atmosphere, some even at higher altitudes. Rain, snow, hail and the general humidity of the air varies of course with time and location. Volcanic eruptions, when they happen, force large amounts of ash into the air. Volcanic ash is reported to foul jet engines very quickly, and it is extremely erosive, four times more than quartz sand (Tabakoff, W., Hamed, A., 1990). Volcanic ash in large quantities is considered quite insignificant to Norwegian air traffic, and it is not given a lot of attention in this work.
The "local" or site conditions are an important factor when it comes to the level of fouling experienced by an engine (Aker, G.F., Saravanamuttoo, H.I.H., 1989). For aircraft engines the operation site is not an unambiguous parameter, a range of conditions for air contamination and engine conditions apply for each individual flight.

The majority of Norwegian airports are located at low altitude and close to the sea. During the long winter season runway preparation in icy and snowy conditions has to be performed. Due to the lack of a dense population and widespread, polluting industry, the air above the lowest altitudes should be quite clean. The vegetation, especially in the northern part of the country is modest.

6.3 Consequences on Engine Performance

6.3.1 Location of fouling occurrence

The front end of the compressor is most vulnerable to fouling, conditions seem to be such that material coming through the air intake is caught quite early. According to Zaita, A.V., Buely, G., Karlson, G., 1998 and Aker, G.F., Saravanamuttoo, H.I.H., 1989 fouling is observed to progress up to 40 - 50 % into the compressor, and the front stages are affected the most. Lakshminarasimha and Saravanamutto (Lakshminarasimha, A.N., Saravanamuttoo, I.H., 1986) however state that fouling may also deposit in the later stages due to the higher temperatures and a certain baking process. Possible oil leaks into the compressor flow may contribute to a high pressure end fouling of the compressor.
Rotor- and stator vanes are prone to fouling, so is the inside of the air intake and compressor casing. As mentioned already, surfaces facing the flow will normally pick up a thicker layer of deposits than other surfaces.
Combustion chamber and turbines are to some extent subjects of fouling, caused by fuel-born material and non-gas combustion products such as sulfur and metal compounds. This is not an issue of this study. Neither is the clogging of filters and traps on marine and industrial gas turbine engines. Aircraft engines basically suck the air unfiltered through the inlet and into the compressor section. The exception to this is the fact that in the air inlet to some turboprop and turboshaft engines traps are fitted to separate heavier solid particles from the airstream.

6.3.2 Fouling on compressor components

When deposits build up on the surfaces in the compressor, shapes are changed, the flow cross sectional areas get smaller and the surfaces themselves get rougher. Aerodynamic shapes and angles of attack of the vanes and blades are altered (Zaita, A.V., Buely, G., Karlson, G., 1998) as indicated in Figure 6.1. The compressor characteristics are changed from their design conditions, and the performance is reduced. This may, to some extent, though not completely, be accounted for by the use of adjustable guide vanes.

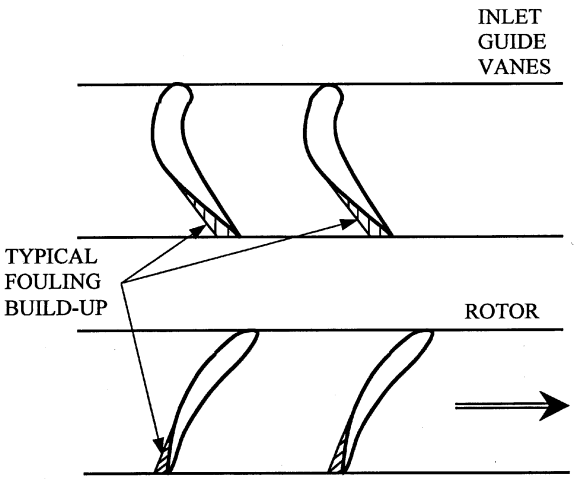

Figure 6.1 Fouling build-up in an axial compressor, from (Lakshminarasimha, A.N., Saravanamuttoo, I.H., 1986)

6.3.3 Compressor module performance, influence from fouling

The literature describes consequences of compressor fouling as a decrease in mass flow rate, efficiency, pressure ratio, and surge margin (Zaita, A.V., Buely, G., Karlson, G., 1998), and thus a drop in power output (Aker, G.F.,Saravanamuttoo, H.I.H., 1989). For a gas turbine engine the fouling severity is more noticeable at higher speeds than at lower off-design speeds because the reduction of the compressor mass flow rate is greater at higher speed (Lakshminarasimha, A.N. et al., 1994).

A somewhat contradictory statement regarding reduction of the compressor stall margin is presented in modeling results (Lakshminarasimha, A.N., Saravanamuttoo, I.H., 1986) saying: "As can be seen, fouling tends to unload the fouled stage, moving the peak line to lower mass flows, and increase the range of unstalled operation."

A couple of examples to quantify typical changes in gas turbine engine parameters due to fouling are quoted in Zaita, A.V., Buely, G., Karlson, G., 1998: a 5 % drop in mass flow rate, 2.5 % drop efficiency, and 10 % drop in output as suggested by Diakonchak, and a 5 % drop in mass flow along with 13 % drop in output and increased heat rate by 5.5 % are figures from General Electric. The last set of data is also presented in Stalder, J.-P., 1998 with reference to Hoeft (1993). In general a major part of performance loss in gas turbine engines is caused by compressor fouling, 70 – 85 % according to Diakunchak (Diakunchak, I.S., 1993).

6.3.4 Performance characteristics for the degraded compressor

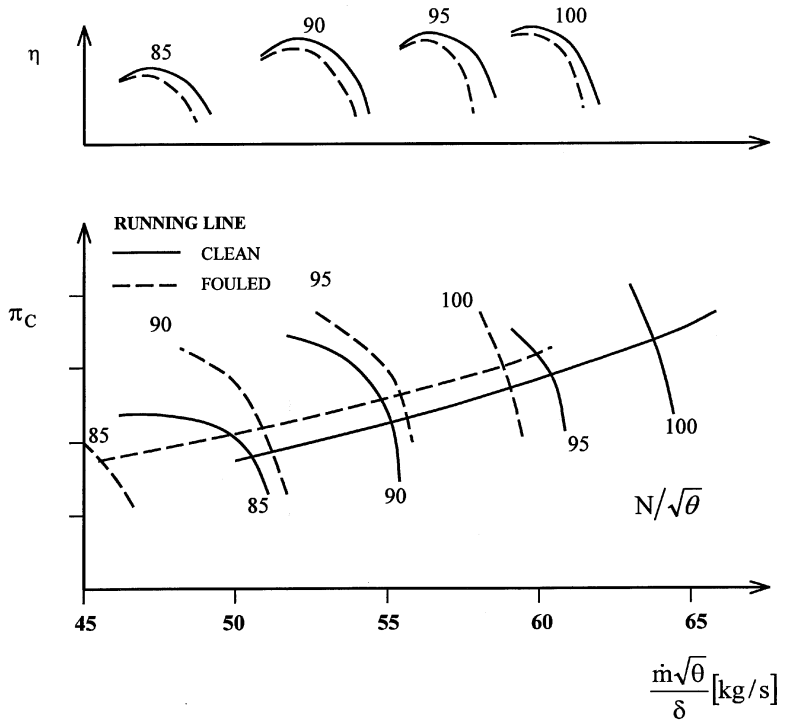

Figure 6.2 Compressor characteristics, clean and fouled compressor (Saravanamuttoo, I.H., Lakshminarasimha, A.N., 1985), (Lakshminarasimha, A.N. et al., 1994), (Lakshminarasimha, A.N., Saravanamuttoo, I.H., 1986)

A typical graph showing the compressor characteristics, parameters as functions of non-dimensional mass flow rate $\frac{\dot{m}\sqrt{\theta}}{\delta}$, is shown in Figure 6.2. For the same compressor in a fouled condition, the characteristic is moved to the left and down relative to the axes. This implies that to obtain pressure ratio and mass flow rate, the fouled compressor has to run at a higher speed and, according to most sources, closer to the surge limit. The efficiency η is also reduced. Consequently, more power is required to operate the compressor with a satisfactorily output, and thus fuel flow will eventually have to increase.

6.3.5 Interactions to other engine components and the overall engine performance

The compressor stages themselves interact, as explained by Lakshmiarasimha, Boyce and Meher-Homji in Lakshminarasimha, A.N. et al., 1994: "... front stages have a greater impact on overall compressor performance compared to rear stages, as front stages affect all the stages following it." Furthermore it is easily understood that a degraded compressor will affect the working conditions of components downstream and to those supplying power to the compressor. The turbine develops power in accordance with the following, and is heavily dependent on the air mass flow rate and entry temperature (Lakshminarasimha, A.N. et al., 1994):

$$P_T = \dot{m} \cdot c_p \cdot T_4 \cdot \left[1 - \frac{1}{\left(\frac{p_4}{p_5} \right)^{\frac{\gamma-1}{\gamma}}} \right] \tag{6.1}$$

Further from Lakshmiarasimha, Boyce and Meher-Homji: "The pressure ... entering the turbine is essentially the compressor discharge pressure minus the pressure drop in the combustion chamber. As the mass flow rate and the compressor delivery pressure drop due to deterioration, the work output of the turbine drops. In order to maintain the power output, the fuel control system will increase the fuel flow rate and hence the turbine inlet temperature. Since deterioration also causes the compressor efficiency to drop, the turbine work to maintain the same flow rate and compressor delivery pressure increases. These factors reduce the life of the hot section components."
The modeling results in Figures 8 and 9 in the paper (Lakshminarasimha, A.N. et al., 1994) (reproduced in Figures 6.3 and 6.4) compare gas turbine engine performance with a clean engine and same engine running with a fouled compressor corresponding to a 3 % reduction in air flow capacity of the compressor.
Figure 6.3 shows how modeling results indicate a reduced power output from a gas turbine engine due to fouling. The strongest impact from compressor fouling occurs in the upper speed range. The authors state that "The significant drop in power observed is primarily due to a reduction in air flow capacity of the compressor." From a rough copy of the graph it appears that a 3 % drop in output power at 100 % speed should be expected for the fouled engine.

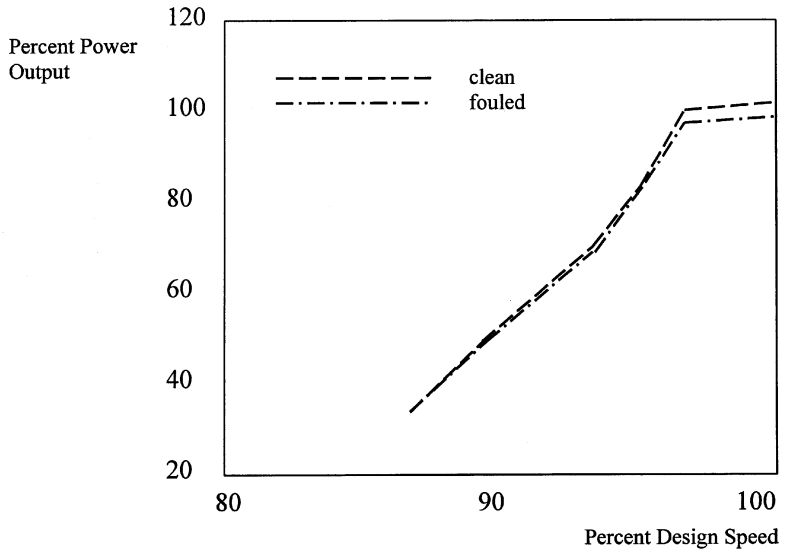

Figure 6.3 Effect of fouling on power; fouling corresponding to a 3 % reduction in air flow capacity of the compressor (Lakshminarasimha, A.N. et al., 1994)

In Figure 9 in the same paper (reproduced in Figure 6.4) there seems to be a mismatch with scale and units on the ordinate axis. It is obvious from the text that the axis range should be 100 % - 140 % (rather than 1.0 % - 1.4 %). Then it can easily be concluded, for the particular model engine and degree of fouling, that one will see a 3 % increase in specific fuel consumption throughout the speed range of roughly 87 % to 100 % of full RPM. Increased fuel consumption at a given power output means higher combustion temperatures and turbine entry temperature. As pointed out in Lakshminarasimha, A.N. et al., 1994, this implies reduced operation life for many of the hot section components.

It is probable that the changes in the conditions of operation for the combustor and turbine imply that these components operate at reduced efficiencies, as in the fouled compressor conditions they work outside their optimum/design-conditions. However this is not specifically commented on in the paper.

Basically it is a consequence of the thermodynamic laws, and it is a well-known fact, in the aircraft industry at least, that with engine deterioration the peak temperatures (EGT, TET etc.) go up as does the fuel consumption for fixed thrust performance.

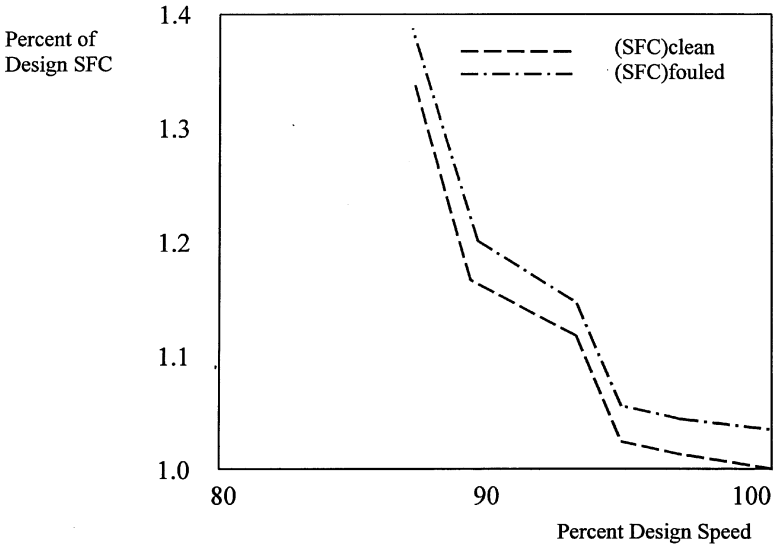

Figure 6.4 Effect of fouling on SFC; fouling corresponding to a 3 % reduction in air flow capacity of the compressor (Lakshminarasimha, A.N. et al., 1994)

6.3.6 Aircraft compressor fouling with time

Aker and Saravanamutto in their paper of 1989 (Aker, G.F.,Saravanamuttoo, H.I.H., 1989) suggest that the time since overhaul, the time between washes, and the severity of blade erosion and wear are important factors in compressor fouling and the drop in efficiency. Time for deposits to accumulate in the engine is essential.

Axial compressor fouling accumulates quite fast on clean components. Due to aerodynamic forces the accumulation seems to level off with time/cycles and more or less stop at a certain value. This is stated in Zaita, A.V., Buely, G., Karlson, G., 1998 that also quotes Schurovsky and Levikin (1986): "The behavior of compressor fouling is similar to the exponential law: After 1 000 – 2 000 operational hours the engine performance stabilization was noted because there took place the stabilization of thickness and the form of deposits."

Data presented in (Meher-Homji, C.B., 1990) also referred to in (Lakshminarasimha, A.N. et al., 1994) illustrate effects on fouling on an industrial gas turbine engine compressor. The graph copied in Figure 6.5 shows how compressor efficiency and engine heat rate develop with time over a 40 day-operation period, starting with a clean engine. The heat rate is the heat input required to produce a unit quantity of power (Cohen et al., 1996)

Lakshmiarasimha, Boyce and Meher-Homji (Lakshminarasimha, A.N. et al., 1994) present the modeling result from a preliminary model of the large turbofan aircraft engine JT9D, showing reduction in flow and efficiency of the high pressure and low pressure compressors due to in service deterioration over 6000 flight cycles. It should be emphasized that this does

include degrading factors other than just fouling. The graphs are reproduced in Figures 6.6 and 6.7.

All references agree that there is a considerable reduction in engine performance during operation. The losses in performance seem to grow exponentially with service time. The performance degradation that is caused by fouling apparently reaches a maximum level after approximately one month's operation for industrial engines, according to Figure 6.5 (Meher-Homji, C.B., 1990), (Lakshminarasimha, A.N. et al., 1994).

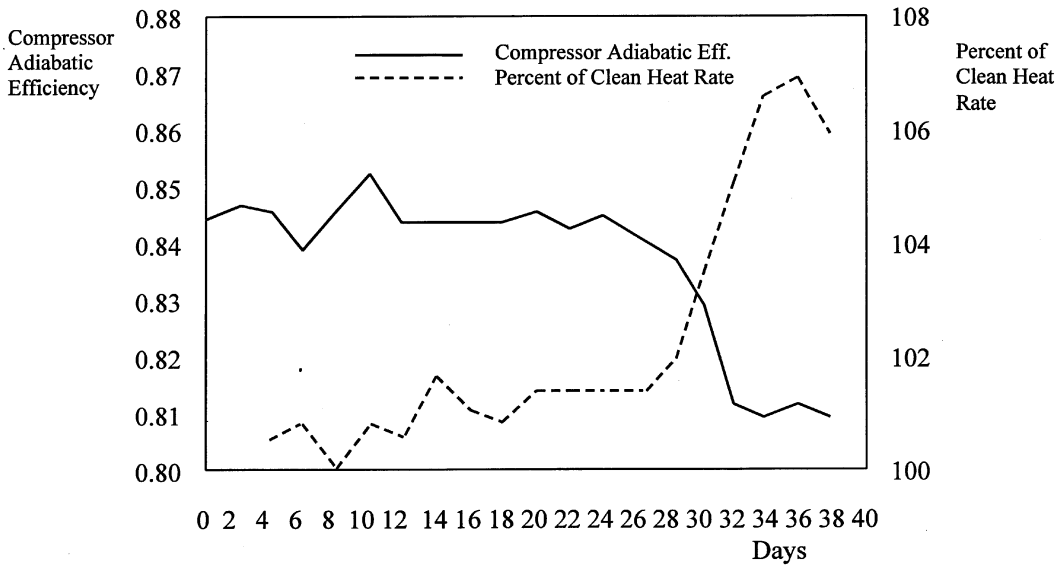

Figure 6.5 Effect of fouling on an industrial gas turbine (Meher-Homji, C.B., 1990), (Lakshminarasimha, A.N. et al., 1994)

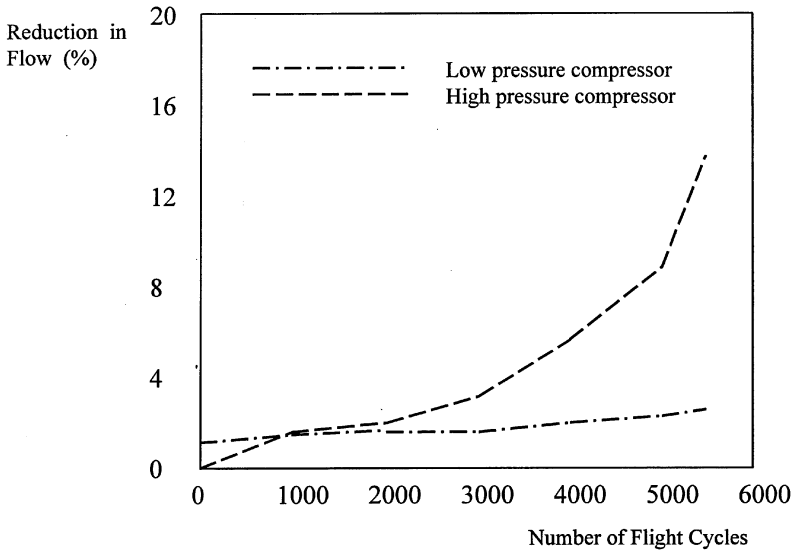

Figure 6.6 Preliminary model of JT9D performance deterioration – reduction in flow of the HP and LP compressor (Lakshminarasimha, A.N. et al., 1994)

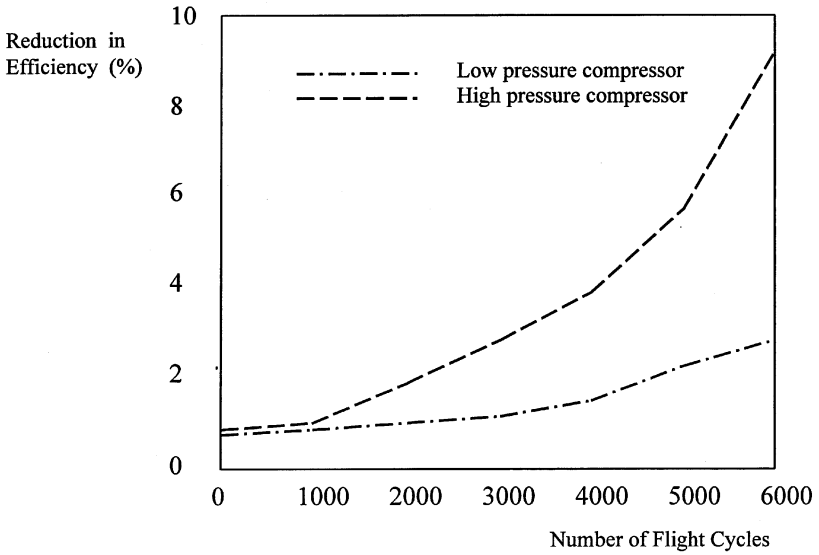

Figure 6.7 Preliminary model of JT9D performance deterioration – reduction in efficiency of the HP and LP compressor (Lakshminarasimha, A.N. et al., 1994)

6.3.7 Fouling of stationary, offshore and aircraft gas turbine engines

It is already explained how compressor fouling depends on the air quality at the operation site. Stationary engines, marine and offshore engines are to some extent protected from ingestion of foreign material by filters and traps, while most aircraft engines are not. Aero engine compressors, on the other hand, operate in a more friendly atmosphere while flying at high altitudes, and, according to (Lakshminarasimha, A.N., Saravanamuttoo, I.H., 1986), it may be expected that fouling is only a problem at lower altitudes and on the ground. Specific conditions like flying through clouds of volcanic ash are exceptions. Marine engines, and this also applies to offshore operated engines, are exposed to airborne salt spray (Lakshminarasimha, A.N., Saravanamuttoo, I.H., 1986).
Referring to Seddigh and Saravanamuttoo (Seddigh, F., Saravanamuttoo, H.I.H., 1991), Tarabin, A.P. et al., 1998 states that the performance of a smaller engine shows more deterioration by fouling than larger engines.
Further, according to (Aker, G.F., Saravanamuttoo, H.I.H., 1989), "the effect of fouling on a compressor stage is proportional to stage loading ", therefore one assumes that high performance aeroderivative gas turbine engines may suffer more performance losses from fouling than industrial engines.
Lakshmiarasimha, Boyce and Meher-Homji (Lakshminarasimha, A.N. et al., 1994) say that aircraft engines are affected more by fouling and particle ingestion than other gas turbine applications. Particularly during take-off, at high power setting, and with a ground vortex pointing into the engine inlet, the conditions favor dust and particle ingestion and compressor fouling.
No data that actually quantifies differences in fouling susceptibility for types of engines and applications are found in the literature. A qualitative set of conclusions based on what is found, is that smaller aircraft engines operating close to the ground much of the time (short-haul flight; frequent take-off and landings) are more prone to fouling than most other gas turbine engines. Heavily contaminated air (sand, volcanic ash, salt) is an additional threat to fouling and erosion to any compressor and gas turbine engine operating in such an environment, regardless its size and application.

6.3.8 Modeling compressor fouling

In (Zaita, A.V., Buely, G., Karlson, G., 1998) Zaita, Buely and Karlson say that "A well defined methodology to predict engine performance deterioration has not been developed." However, some attempts to model the fouling process and consequences analytically are described in the literature. Other references (Lakshminarasimha, A.N., Saravanamuttoo, I.H., 1986), (Adams, J., Schmitt-Wittrock, P., 1981) and (Tarabin, A.P. et al., 1998) present different approaches. A major obstacle in predicting performance deterioration is that the users do not have access to the compressor performance map or stage characteristics (Lakshminarasimha, A.N. et al., 1994).

Lakshminarasimha and Saravanamutto:
The so-called Stage Stacking Techniques are presented in (Lakshminarasimha, A.N., Saravanamuttoo, I.H., 1986) by Lakshminarasimha and Saravanamutto as a tool for predicting

compressor fouling. The main idea is that the performance of a complete compressor may be calculated one step (equals one compressor stage) at a time, knowing all stage performance curves, main geometry parameters and compressor inlet total pressure and temperature beforehand. Based on stage pressure and temperature ratios π_i and τ_i, total performance (i.e. overall performance) parameters for the compressor, the total of n stages then becomes:

overall pressure ratio:

$$\pi_{oa} = \pi_1 \cdot \pi_2 \cdot \ldots \cdot \pi_n = \prod_{i=1}^{n} \pi_i \tag{6.2}$$

overall temperature ratio:

$$\tau_{oa} = \prod_{i=1}^{n} \tau_i \tag{6.3}$$

efficiency:

$$\eta_{oa} = \frac{(\pi_{oa})^{\frac{\gamma-1}{\gamma}} - 1}{\tau_{oa} - 1} \tag{6.4}$$

The important advantage of this model appears to be that whenever one of the stages is changed e.g. by fouling, the influence on the operational conditions for the other stages, at least those downstream, is predicted and accounted for. Regardless of the degree of deterioration of one compressor stage, its performance will to some extent be influenced by the proceeding stages and eventually impact the total performance of the compressor.
The fouling of a compressor stage is quantified in two parameters:

1. change in rotor inlet angle due to fouling; $\Delta\beta_{1f}$ in terms of reduction in flow coefficient $\frac{\Delta\phi}{\phi}$, flow coefficient ϕ being the rotor inlet axial flow velocity divided by blade mean velocity, and

2. stage efficiency modified by use of an efficiency scaling factor K_f as follows:

$$\eta_f = \eta - K_f \cdot \eta_{ref} \tag{6.5}$$

η and η_f being clean and fouled efficiencies respectively, η_{ref} is design point efficiency.

The modified (fouled) stage characteristic can be calculated from the new velocity diagram and efficiency.

Lakshminarasimha and Saravanamutto in (Lakshminarasimha, A.N., Saravanamuttoo, I.H., 1986) do not suggest any quantities for realistic $\frac{\Delta\phi}{\phi}$ and K_f. Simulations are performed using $\frac{\Delta\phi}{\phi}$ = 3 % and K_f = 0 % as light fouling and $\frac{\Delta\phi}{\phi}$ = 8 % and K_f = 1 % as severe fouling of one compressor stage.
Modeling results are said to be reasonable for an actual five stage compressor.

Adams et al.:
Adams et al. in 1982 (Adams, J., Schmitt-Wittrock, P., 1981) define what they call the "Verschmutzungsgrad", the fouling intensity or the degree of fouling. To be able to optimize cleaning/washing intervals in a meaningful way, it is necessary to quantify such a parameter. The fouling intensity γ_v is an expression of compressor air flow rate reduction $(\dot{m}_a - \dot{m}_{a,f})$ with fouling relative to the unfouled mass flow rate at similar conditions, $\dot{m}_a$:

$$\gamma_v = \frac{\dot{m}_a - \dot{m}_{a,f}}{\dot{m}_a} \tag{6.6}$$

The paper explains how the degree of fouling may be expressed as

$$\gamma_v = 1 - \sqrt{\frac{\frac{\Delta p_f \cdot R_f}{p_f \cdot T_f}}{\frac{\Delta p \cdot R}{p \cdot T}}} \cdot \frac{\varepsilon_f \cdot T_f^*/T_0^*}{\varepsilon \cdot T^*/T_0^*} \tag{6.7}$$

Δp's are pressure differences, R's are gas constants for inlet humid air, p's and T's are pressures and temperatures of the inlet air. The ε's are called expansion numbers, and the fraction $\frac{T^*}{T_0^*}$ that may be read from a graph as functions of inlet air temperature, taking into account the fact that a change in inlet air density has some influence on the compressor efficiency.
Operational figures from one particular gas turbine at the Kraftwerks Emsland power station show that the degree of fouling, γ_v, typically grows from zero to 4.0 ± 0.75 during the first 1500 hours after clean engine start up. The rate of increase in γ_v is at its highest the first 500 hours. For this engine it is also found that increased specific fuel consumption with time (loss in fuel efficiency, $P_v(t)$) is directly related to the varying compressor fouling intensity:

$$P_v(t) = 1.44 \cdot \gamma_v(t) \tag{6.8}$$

Tarabrin, Schurovsky, Budrov and Stadler:
In Tarabin, A.P. et al., 1998 a model is presented to study the mechanism of fouling. The particles in the air that passes through the compressor, due to inertia forces, do not follow the

streamlines. They may collide with and stick to blade surfaces and also move to the periphery of the passage. A coefficient of entrainment, or a separation factor, E is determined by Fuks (1955) as follows:

$$E = \frac{\text{number of particles colliding with the surface of the body}}{\text{number of particles that could fall on the body surface if the streamlines were not deviated by the body}} \tag{6.9}$$

Figure 1 in Tarabin, A.P. et al., 1998 shows how particles tend to collide with a solid body in a flow. The graph is reproduced in Figure 6.8.

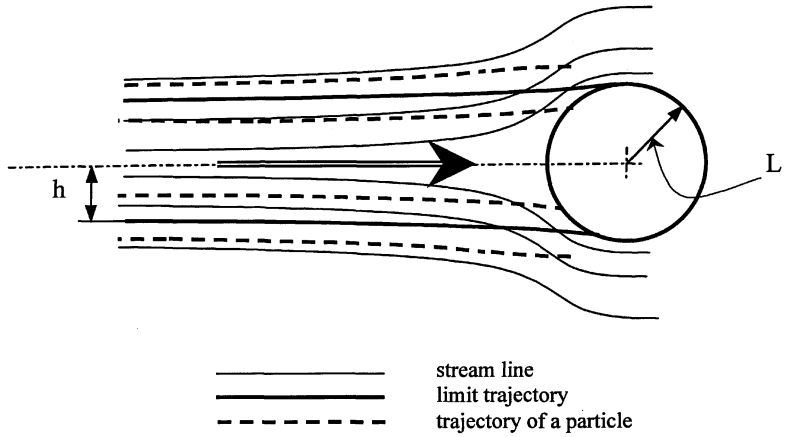

Figure 6.8 Inertial deposition of particles on cylinder surface (Tarabin, A.P. et al., 1998)

In this simple case the coefficient of entrainment can be expressed as

$$E = \frac{h}{L} \tag{6.10}$$

In general the coefficient of entrainment is a function of Stokes number, Reynolds number and particle diameter relative to a characteristic length in the cascade geometry.
The cascade coefficient of entrainment is finally presented in the form

$$E_c = (1 + 0.77/St_k)^{-1} \frac{b}{t} \frac{\sin(\Delta\beta/2)}{\sin\beta_1} \tag{6.11}$$

$\frac{b}{t}$ being the cascade solidity, i.e. blade cord divided by cascade pitch, the flow turning angle $\Delta\beta$ and the flow incidence angle to the cascade β_1.

The expressions referred to here are based on certain assumptions and simplifications, one important simplification being that all particles that collide with a surface stick to it. The Coriolis and centrifugal forces are not taken into consideration, but nevertheless the model gives useful guidance in studying how different parameters influence the sensitivity of compressors to fouling. These studies and further considerations result in an index of compressor sensitivity to fouling (ISF) to be:

$$ISF = \frac{\dot{m}_a \, c_p \Delta T_{t,stg}}{(1-\bar{r}_h^{\,2})D_c^{\,3}} 10^{-6} \tag{6.12}$$

where the mass flow rate $\dot{m}_a$, the average total temperature rise per stage $\Delta T_{t,stg}$, hub/tip diameter ratio of the first stage, $\bar{r}_h$ and tip diameter D_c are the main variables. It is demonstrated in the paper how the ISF is being used to compare the sensitivity to fouling for a number of real engine compressors.

ISF and the particle concentration and composition are assumed to be the essential factors to make some estimates of the influence of fouling on compressor performance. Two parameters are evaluated; the Δk_{Hf} (k_{Hf} is the so-called work done factor including fouling effect) and k_f (the factor of fouling). Based on real operational experience and data from different compressors operating in the same environment (concentration and fractional composition of aerosols) it is suggested that

$$\Delta k_{Hf} = m \cdot ISF \tag{6.13}$$

$$k_f = 1 + n \cdot ISF \tag{6.14}$$

with $m = 8 \times 10^{-4}$ and $n = 8 \times 10^{-3}$.

By using the relevant data for a compressor to evaluate the ISF, one will find it quite simple and convenient to calculate the reduction in work done, Δk_{Hf}, to be in the range of 0.000 – 0.010; to be a single digit percentage. The factor of fouling k_f is found as easily.

It is demonstrated in Tarabin, A.P. et al., 1998 that by simulating progressive fouling of the compressor, stage by stage, one may calculate the compressor performance characteristics at any state of fouling.

The paper states that the method can be used to estimate engine performance deterioration with fouling: "It allows one to determine not only a tendency but also a character and a degree of a change of the main parameters of a compressor and a gas turbine as a whole under fouling conditions."

6.3.9 Empirical and experimental data versus modeling results

Very few examples are presented in the literature that demonstrate the capability of theoretical models to predict engine fouling and related performance deterioration. As explained in (Lakshminarasimha, A.N., Saravanamuttoo, I.H., 1986), "... the trend of performance deterioration due to fouling is more important than the accuracy of the predicted results." Still the paper claims reasonable agreement between simulation and measurement characteristics for one particular compressor.
The modeling procedure in Adams, J., Schmitt-Wittrock, P., 1981 is performed to optimize compressor washing intervals, and real engines are used to adapt the model to real operation. No comparison of modeling results and measured operational data are presented.
In Tarabin, A.P. et al., 1998 the suggested model is applied to a small axial compressor, actually a GTE-150 LMZ scaled down by the ratio of 1:4.14. With 6 out of a total of 14 compressor stages fouled, which seems to be a fairly representative state of severe fouling, the model predicts a 4.5 percent reduction in inlet mass flow, 4 percent reduction in pressure ratio, and 2 percent reduction in compressor efficiency. These figures seem to correspond well with degradation in compressor performance as described elsewhere in the literature.
Papers that are referred to and discussed here are engine type specific and not general; in the sense that they do not claim or demonstrate the validity of models for a wide range of types and sizes of axial gas turbine engine compressors.

6.4 Compressor Cleaning / Washing

6.4.1 Methods and principles for cleaning axial compressors

Washing of axial compressors to remove fouling is a quite common operation in many different industries. The removal of the fouling material from the compressor surfaces at certain time intervals helps keep the engine performance closer to its design level. According to Tarabin, A.P. et al., 1998: "Performance deterioration due to fouling is for the most part recoverable." The frequency of cleaning is usually optimized to keep the pay off at its maximum, any shut-down time means loss in production as well.
The two main principles for washing are the on-line washing and off-line washing, as roughly explained in the introduction of this review. Off-line washing is also termed crank soak or simply crank wash. Components cleaning during main overhaul, shut down/disassembly, are usually included in off-line cleaning, though, in some cases (Thames, J.M, Stegmaier, J.W. Ford, J.J. Jr., 1989), defined as a third category of cleaning processes.
Stalder in (Stalder, J.-P., 1998) gives a comprehensive description of gas turbine compressor washing procedures and a presentation of some field experience. Basically it is all about industrial engines. Also Brittain (Brittain, D., 1983) from the Rivenaes company (now R-MC) explains how washes are performed for aero engines and offers examples. The R-MC, now a British owned company located in Bergen, Norway and London, sells compressor cleaning technology. The R-MC Internet pages */http://www.r-mc.com/aero.htm* (January 2000) have some information on aircraft gas turbine engine washing. A few other references explain the washing procedures and present figures from the operation.

Other methods than washing have also been applied for compressor cleaning over the years. Grit blasting, a process in which nut shells and rice hulls are sucked through the engine to scrape off dirt and deposits, is one example. Because of several disadvantages with this method, like solid material being left in the engine and in some instances clogging up passages, liquid washing is now the dominant cleaning method.

On-line washing

On-line washing is done with the engine running at a particular RPM, slightly above idle. The washing fluid is then sprayed into the air intake, through a manifold and a set of nozzles. On some engines the spray system is even permanently fitted. The spraying goes on for a limited time, typically 5 minutes, followed by a draining and drying run for another 15 or so minutes (Brittain, D., 1983).

Cleaning agents for on-line washing include water, water-soluble detergents and petroleum-based solvents (Thames, J.M, Stegmaier, J.W. Ford, J.J. Jr., 1989). The properties of the fluids have to be such that they neither extinguish the combustion nor cause any unfavorable increase in the temperature. They should be designed to fulfill the engine manufacturers' specification (Stalder, J.-P., 1998). The fluids can be composed to work efficiently on specific fouling material that may be dominant in the compressor.

The need for rinsing after a wash, usually with purified water, varies with the type of cleaning agent that has been used, and what remnants are likely to be on the inner surfaces.

This type of compressor cleaning does not necessarily totally remove all deposits from the flow surfaces, and it is most effective on the first stages of the compressor. It may have some effect down to the 6th stage, according to Stalder.

On-line washing is usually done quite frequently, typically from once a day to once a week.

Off-line cleaning (Crank cleaning)

For this type of cleaning the gas turbine engine has to be shut down and given sufficient time to cool. This may in itself be useful as shut downs and start-ups can positively affect compressor fouling by spalling off deposits (Stalder, J.-P., 1998). When the engine is cold, the cleaning solution is sprayed into the air intake while the engine is being run slowly by the starter, and after a while the compressor is rinsed with water and then allowed to dry (Thames, J.M, Stegmaier, J.W. Ford, J.J. Jr., 1989).

Off-line washing is quite time consuming, as both cooling time and time to dry after rinsing are required. This will easily amount to several hours total downtime.

According to Thames, Stegmaier and Ford the cleaning solution used in crank wash is in principle the same as with on-line washing.

This cleaning method is very efficient for removing all deposits on all the compressor stages. On the other hand, it is more costly as the engine has to be out of service for a much longer time than with on-line washing. Crank washing is done at intervals of approximately 3 – 4 months.

Optimum cleaning intervals

On-line and off-line cleaning are complementary (Stalder, J.-P., 1998). Frequent on-line cleaning extends the time interval between off-line cleaning operations. Power recovery after off-line washing is significantly higher than after an on-line washing.

Fouling material removed from the first stages in the compressor during an on-line wash may stick to surfaces further downstream, and thus require a crank wash to get it cleaned away completely (R-MC Power Recovery Ltd., 1998).
A graph showing the general benefit on performance from on-line washes is reproduced from (Thames, J.M, Stegmaier, J.W. Ford, J.J. Jr., 1989) in Figure 6.9. Apparently the time interval shown is between two crank washes, as a continuously declining line represents performance development without on-line washes. It is evident from the graph that with each on-line wash there is a performance recovery, though not entirely back to initial condition. This zigzag line however shows a far less average decline in performance than what is the case if on-line washing is omitted completely.

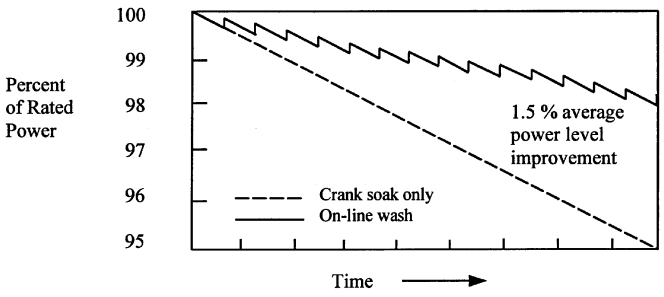

Figure 6.9 Typical gas turbine performance with compressor cleaning (Thames, J.M, Stegmaier, J.W. Ford, J.J. Jr., 1989)

Reliable procedures to find the optimum time interval between on-line washes and off-line washes are discussed in the literature. Adams et al. (Adams, J., Schmitt-Wittrock, P., 1981) suggest that on-line washing is to be performed once a week, and crank washes, Einweichreinigungen, in general when the degree of fouling (Section 6.3.8 of this work) is between 3 and 4 percent.
The criteria to determine optimum washing intervals are discussed by R-MC in (R-MC Power Recovery Ltd., 1998). For on-line washing, according to the paper, there are too many operation parameters to be monitored or considered, and "... time becomes an obvious choice for determining the frequency between on-line washes." Any recommendations regarding time intervals are not presented.
The R-MC criterion for off-line washing to be required (if off-line wash is not just carried out on an opportunity basis) is demonstrated in Figure 6.10 (R-MC Power Recovery Ltd., 1998).

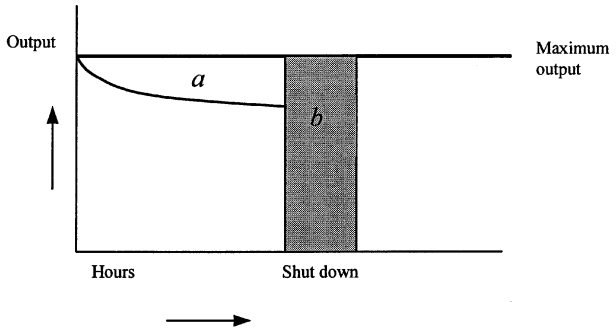

*"When **a** = **b** + **cost of fluid** + **cost of effluent disposal**, then wash is justified."*

Figure 6.10 Trend monitoring of output to determine time scale of off-line cleans (R-MC Power Recovery Ltd., 1998)

The interpretation of the graph is that wash is appropriate, called "cost justified", when the cost of accumulated loss in output due to fouling is equivalent to the cost of a shut down and an off-line wash.
The statement by Stalder (Stalder, J.-P., 1998) that more frequent on-line cleaning extends the time interval between off-line washes, as referred, demonstrates how a lifting of the performance curve shown in Figure 6.9, contributes to an elongation of the area *a* in Figure 6.10, and thus an extension of the time before shut down.

6.4.2 Washing agents

R-MC Power Recovery Ltd., 1998 gives a useful overview of the four main types of compressor cleaners, how they may be applied in on- and off-line cleaning and of their performance with respect to blade erosion, removing of fouling material and to the environment. The charts in Table 6.1 are reproduced from (R-MC Power Recovery Ltd., 1998).

On-line	Non-toxic	Biodegrad-able	Erosion	Organic	Inorganic	Rinse needed
Solids	Yes	?	Yes	Yes	Yes	No
Demineralized water	Yes	Yes	Yes	Yes	No	No
Solvents	No	?	No	Some	No	Yes
Surfactants/detergents	Yes	yes	Yes	yes	Yes	No

Off-line	Non-toxic	Biodegrad-able	Erosion	Organic	Inorganic	Rinse needed
Solids	N/A	N/A	N/A	N/A	N/A	N/A
Demineralized water	Yes	Yes	Yes	Yes	No	No
Solvents	No	?	No	Yes	No	Yes
Surfactants/detergents	Yes	Yes	Yes	Yes	Yes	No

Table 6.1 Compressor cleaners and their performance (R-MC Power Recovery Ltd., 1998)

The comments in (R-MC Power Recovery Ltd., 1998) to the charts may be summarized as follows:

Solids, more used in the past
- could not clean the forward facing parts of the compressor
- tendency to enter sight glasses and seals
- tendency to remove coatings

Demineralized water
- environmentally friendly
- large volumes required
- risk of surge and redeposition

Solvents, normally of hydrocarbon origin
- risk of flammability, environmental damage and health hazard
- potential for damaging rubber seals and coatings
- may cause overspeed in use

Surfactants / detergents
- dissolve oil and grease
- effective on all types of deposit
- can be heated to increase chemical efficiency

Kolkman in (Kolkman, H.J., 1992) explains how new compressor cleaners have been developed in the response of two concerns;

1. safety and environmental issues
2. corrosion inhibition.

These issues are of particular importance to the aircraft industry as soil pollution of airfields (e.g. by mineral oils) is regulated by authorities, and also that jet engines, unlike many other gas turbine engines, may not be operated immediately after washing, and therefore a certain risk of corrosion in the wet engine is obvious (Kolkman, H.J., 1992). The conclusion after tests is that the so-called ecologically sound cleaners are not as efficient as the old cleaners are. Corrosion inhibition however seemed to work as intended.

6.4.3 Areas of application, aircraft, offshore, other

General

Most of the literature regarding compressor fouling and subsequent cleaning either deals with industrial gas turbine engines, or comprises general, theoretical studies of the phenomena with no connection to fields of application.

Stationary gas turbine engines, most of them quite large, are typically found in electrical power stations based offshore on oil rigs, as well as on shore, and along pipelines (oil) for running pumping stations. The stationary engines are in two categories, the so-called industrial type engines; heavy duty, lower temperature engines and the aero derivatives; light weight, high performance engines. With the advantage of low weight the latter group of engines is particularly well suited to offshore installations. It has already been explained in this work how the aero derivative engines are more prone to fouling than the heavier engines.

Aircraft, automotive and marine gas turbine engines are less uniform in size and design and in their working environments.

Compressors on power plant and pipeline engines are washed extensively, research is concerned with the potential of performance recovery for these engines. According to R-MC's Internet information (http://www.r-mc.com/news.htm) R-MC products are approved for the Norwegian oil industry and used regularly today (1999) for cleaning the majority of turbines operating in the Norwegian offshore sector.

Regular cleaning of compressors on larger turbofan engines (aircraft) does not seem quite as common. One single case from 1999 is reported as a test; a CFM56 engine on a Boeing 737 being cleaned with an R-MC system and a certain performance improvement measured (R-MC).

Smaller aircraft engines, turboprops, helicopter turboshafts and auxiliary power units are, as already explained, more sensitive to fouling. Washing is done extensively for such categories of engines; as an example R-MC (Brittain, D., 1983) reports that 130 operators use their products for washing the Pratt & Whitney PT6 engines, in 1983.

CFM56 engines on Boeing 737-400 aircraft
The Boeing maintenance manual for the 737-400 engine (22) prescribes what is called an "Engine gas Path Cleaning". Particular incentives to perform such cleaning are not apparent, other than, as quoted: "For EGT recovery, it is recommended to perform the engine water rinse with pure water only. A detergent engine gas path is not recommended for EGT recovery. Engine washing with cleaning agent is recommended only when organic debris or oil deposits are present."
The two washing procedures described,

1. a detergent wash and subsequent water rinse, and
2. a water rinse with pure water only

both have to be performed on a cold engine, exhaust gas indication not more than 66 °C, the engine staying on the wing and run in the so-called Power Plant Dry-Motor procedure. The main steps in the washing procedure give an indication of the time frame of one engine wash: two minutes to apply the cleaning fluid, 5 minutes soaking, 5 minutes draining of the engine and then within no more than 30 minutes, operate the engine for 5 minutes at idle.

6.4.4 Engine performance improvements by compressor washing

Compressor deterioration is quantified by changes in the following parameters: air mass flow rate, pressure ratio and efficiency, in some cases also increasing specific fuel consumption for the engine. In operation the increasing EGT (exhaust gas temperature) is a common indication that the engine condition is not up to its standards. When performance is restored through compressor washing, improvements are recognized through engine parameters such as reduced EGT or TGT (turbine gas temperature), or extended TBO (time between overhauls) or engine output recovery.
One of the most recent articles presenting field data from washing is (Stalder, J.-P., 1998). A long-term test is reported on a 66 MW stationary gas turbine operation in a power station in The Netherlands. Over 18 months covering 8 089 operating hours 83 on-line washes and 5 off-line washes were performed. 72 of the 83 on-line washes gave a positive power recovery, average for all 83 was an increase in output by 712 kW, roughly 1 %. After off-line washes a power recovery in the range of 1 – 1.8 MW was observed, that is 2 – 3 %.
R-MC in (R-MC Power Recovery Ltd., 1998) explains the benefits of their washing system on turboprop aircraft engines. The British Civil Aviation Authority extended the TBO for Pratt & Whitney PT6 engines by 28 % after the system was introduced (1983). According to the same source, Air UK showed that in cases of severe contamination of their Rolls-Royce Dart engines, the use of R-MC can restore turbine gas temperature by 5 °C to 6 °C. The R-MC washing of a CFM56 engine on a Boeing 737 mentioned in the previous section gave an EGT improvement of 20 °C.
The fact that "More than 10 % of output power can be lost in matter of weeks as a result of fouling" (Diakunchak, I.S., 1993) and "On many turbines a 10°C increment in EGT reduces the hot section life by 50 %" (R-MC Power Recovery Ltd., 1998) put the importance of the performance recovery that these parameter improvements indicate into perspective.

6.4.5 Negative consequences from compressor washing

There are certain risks of engine damage associated with compressor washing, particularly the on-line washing that is performed quite frequently:

- corrosion, which may be avoided by either drying the engine properly, or by using cleaners with corrosion inhibition (Kolkman, H.J., 1992),
- washing a compressor too often (Zaita, A.V., Buely, G., Karlson, G., 1998), and incorrect atomization of the cleaning fluid (R-MC Power Recovery Ltd., 1998) may increase engine erosion,
- re-deposition of the fouling material further downstream when the washing fluid evaporates is an unwanted effect (R-MC Power Recovery Ltd., 1998),
- a non-uniform distribution of fluid may cause compressor surge during the washing process (R-MC Power Recovery Ltd., 1998),
- ice formation during washing is undesirable (R-MC Power Recovery Ltd., 1998).

Possible negative safety and environmental consequences (Kolkman, H.J., 1992) are mentioned in Section 4.2.

6.5 Engine Fouling and Engine Erosion; Relative Importance to Performance Deterioration

The statement by Diakunchak (Diakunchak, I.S., 1993) that usually about 70 to 85 % of engine performance loss is attributed to compressor fouling is already quoted. This implies that there are other phenomena causing performance loss, and the percentage may not be representative for all types of gas turbine engines and all kinds of operating environment.
Dust, sand and other material that is ingested into the engine does not necessarily stick to compressor blades or other surfaces but still does damage by causing erosion. Like with general wear and tear on components, performance recovery after erosion requires refurbishment or replacement of the damaged parts.
Fouling of the larger high bypass turbofan engines is not focused on or documented extensively in the literature, a single case of flying through clouds of volcanic ash is one exception. In general larger gas turbine engines are less prone to fouling than the smaller engines. These conclusions are reasons to believe that phenomena other than fouling are at least as important for performance deterioration of this category of engines.
In this perspective and for the purpose of this work it is of interest to quantify the potential of ingested material and subsequent erosion, causing performance deterioration. Data regarding the CFM56, a medium-sized series of turbofan engines is of particular interest.
A test documented in Peterson, R.C., 1986 shows how the modifications to the CFM56-2 engine, originally flown on DC-8 airplanes, improve engine tolerances against ground particle ingestion and erosion. The modifications were incorporated in the CFM56-3 engine, the case

engine in this thesis, and "... their effectiveness has been demonstrated in initial service experience." (Peterson, R.C., 1986)

Figure 6.11 below is reproduced from (Peterson, R.C., 1986), it clearly shows how operating procedures and engine improvements reduce the deterioration of performance from dust ingestion on the CFM56-2 engine. However, the lowest curve that more or less applies to the CFM56-3 engine as well, is of special interest in the present work. The EGT and the fuel flow increase linearly during the first 1 800 hours of operation for new engine, and at that point increases of 10 °C and 1 % are observed for the two parameters respectively.

Figure 2 in (Lakshminarasimha, A.N. et al., 1994), also in Figure 6.5 of the present work, shows heat rate development due to fouling for an industrial gas turbine engine over 40 days of operation after cleaning. The first 30 days, equivalent to 720 hours of operation, the heat rate increases, almost linearly with time, by approximately 2 %. The heat rate is close to proportional to specific fuel consumption and thus the fuel flow at a fixed power setting, and the example from (Lakshminarasimha, A.N. et al., 1994) is comparable to the CFM56-2 (similar to CFM56-3) case. Fuel flow growth rate due to erosion is roughly 0.56 % per 1 000 hours for the CFM56 engines while the heat rate growth caused by fouling for the industrial gas turbine is 2.7 % per 1 000 hours during the first 500 – 1 000 hours of operation after clean/new engine. While the consequence on fuel flow from erosion seems to level off after approximately 1 800 hours (75 days), the change of heat rate due to fouling grows exponentially and then levels off at around 40 days of operation with no cleaning, as seen already. The two developments, according to the graphs, stabilize at 1 % higher fuel flow from erosion for the CFM56 engine and at roughly 6 % additional heat rate from fouling for the industrial gas turbine.

Assuming erosion to be the most important reason for engine deterioration next to fouling, the two single cases studied in this chapter confirm the figures stated by Diakunchak regarding relative importance of fouling to the drop in performance. It ought to be obvious that if engine design, the air quality, or operation in general prevent or rule out particle ingestion and fouling, this conclusion is not relevant.

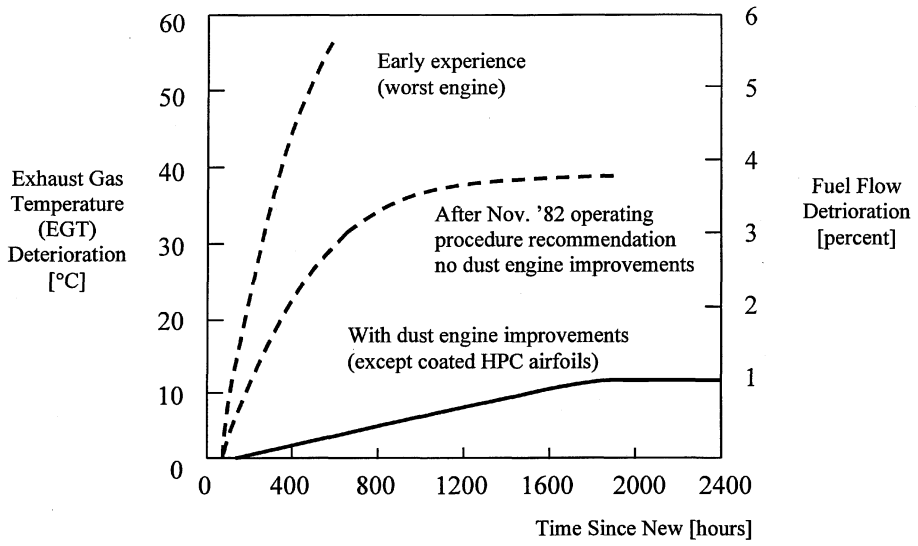

Figure 6.11 CFM56-2/DC-8-70 Performance Deterioration, copied from (Peterson, R.C., 1986), two upper curves drawn in broken lines by the author.

6.6 Norwegian Airlines and Engine Fouling; Discussion and Conclusions

The engine washing practice for some types of aircraft in the major Norwegian civil airlines in domestic service was highlighted in Section 6.1.2:

- Helicopter Service (HS) have all their Super Puma helicopter engines washed on-line every day after operation. Scheduled off-line washing is performed every 50 hours (R. Bergstrøm, Helicopter Service).

- Widerøe's Flyveselskap washed the turboprop engines on Twin Otter airplanes regularly (Brittain, D., 1983).

- Braathens do not perform any regular on-line cleaning on CFM56-3/-7 engines; washing has been done occasionally with no performance recovery reported. The low bypass turbofans JT8, in operation with Braathens until 1995, were cleaned and a certain performance recovery reported (J. B. Egeland, Braathens).

- CFM56 engines on Scandinavian Airlines' Boeing 737s are not washed on-line on a regular basis. The company still has a large number of Pratt & Whitney JT8s in operation, that are washed regularly (H. Pettersen, SAS).

HS helicopters are in service between the Norwegian coast and the North Sea oil installations. Widerøe's smaller aircraft (Twin Otters and Dash 8) airplanes are serving many small community airports, in most cases located close to the coastline, on short-haul flights which implies considerable low altitude flying near the ocean. Considering the fact that Braathens' and SAS' domestic destinations are airports that HS and Widerøe operate from, their larger aircraft are definitely exposed at times to fouling conditions, in landing and take-off in particular. The fact that engines on older version airplanes, flying basically the same traffic pattern as their more recent models, had to be cleaned lends weight to this assumption.

7 PRESENTATION OF RESULTS; EMISSIONS DURING THE SHORT-HAUL FLIGHT PATTERN

7.1 Clean Engines

7.1.1 Time specific fuel consumption and emissions

Time specific fuel consumption and emissions that are presented in this study from the Turbomatch calculations are sub-segment average quantities rather than discrete point values. This is done mainly to dampen certain peaks of the curves caused by the discontinuous developments of the climb angle and acceleration of the basic data. Each sub-segment is in the range of 30 to 120 seconds, i.e. 1.0 – 4.5 % of the mission.
It has been explained in Section 5.4.1 that average quantities for fuel consumption, emission indexes etc. for a sub-segment were evaluated by linear interpolation between the sub-segment start and end point quantities.

Fuel consumption:
For the Boeing 737-400 flying a short-haul flight (45 – 50 minutes) according to the calculations, in general the highest fuel consumption occurs at take-off. From that point on the acceleration, the climb angle and drag coefficient are all reduced and fuel consumption falls accordingly. During early climb (first 3 minutes) the speed is more than doubled while air density falls by approximately 15 %. Even with a reduction in the drag coefficient, we see an increasing demand for thrust, and fuel consumption increases.
In this model, acceleration is reduced at lift-off, and, of course, the climb angle gets a particular value larger than zero. Less than a minute later the acceleration is further reduced, and so is the climb angle. Additional drag from landing gear and flaps is assumed zero beyond this point and a considerable drop in thrust and fuel flow is observed. During the following 170 seconds the speed is more than doubled, drag will increase again, and a peak in the fuel flow at around 250 seconds from lift-off is seen. Throughout the remaining climb the speed

and climb angle are assumed constant while air density diminishes so that thrust and consequently fuel consumption fall continuously (see Figure 7.1).
Fuel consumption is constant during the cruise sequence and drops considerably at the beginning of descent.
In the first 8 minutes of descent there is a slight increase in fuel flow because the speed is kept constant, the remaining 10 – 11 minutes the airplane is set to decelerate and the drag coefficient increases, consequently the fuel consumption is more or less constant.
In the approach and landing phase the drag increases due to the use of flaps and the landing gear being lowered. Thrust is slightly higher than in the late descent phase.

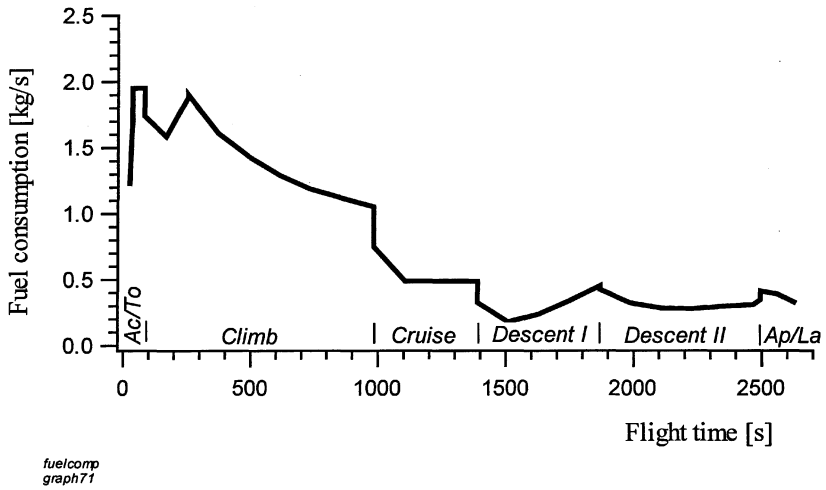

Figure 7.1 Time specific fuel consumption during the complete flight cycle Oslo – Trondheim, clean engines (Turbomatch model).

It has been explained already how the flight route model was simplified by keeping the acceleration constant over segments of the flight path. Sudden changes in acceleration are a major reason for discontinuities in the thrust requirement and hence fuel consumption in the present data, typically the peak on the curve around mid-descent (between Descent I and Descent II). Discontinuities like these may not be found pronounced to a similar extent in a real flight situation.

CO_2 and H_2O emissions:
The emission coefficients of CO_2 and H_2O state that the emission quantity is strictly proportional to fuel consumption, as presented in the graphs in Figures B3 and B4, Appendix B.

NO_X emissions:
The time specific NO_X emissions graph (Figure 7.2) shows certain similarities in shape to the specific fuel consumption (and emissions of CO_2 and H_2O). Significant quantitative differences appear though; NO_X production rate in cruise and descent are roughly 10 % and 3.5 % of maximum NO_X occurring in early climb while time specific fuel consumption in cruise and descent are 25 % and 15 % of maximum climb figures, respectively. The descent NO_X production rate as calculated is on the high side as already explained in Section 5.7.2.

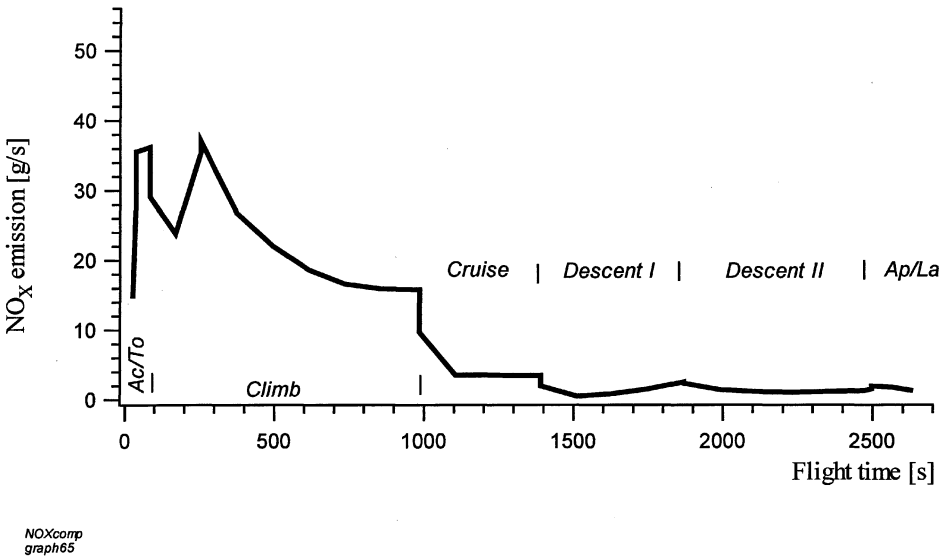

Figure 7.2 NO_X emission per second during the complete flight cycle Oslo – Trondheim, clean engines (Turbomatch model).

CO and UHC emissions:
CO and UHC appear in the exhaust when combustion is incomplete, that is when the temperature is low and/or the air speed in the combustion chamber is high such that cooling of the burning gases is too fast for the chemical reactions to end fully. We therefore find very little CO and UHC during the high thrust segments of the flight and the large amounts occur in the descent and approach/landing phases. The extreme peaks in early descent, 10 times and 400 times the climb and cruise figures for CO and UHC, correspond well to the real engine emission date as presented in Tables H5 and H8 (Appendix H).
The dips between Descent I and Descent II (Figure 7.3) are assumed to be directly connected to the peaks in fuel consumption and more intense combustion in that part of the flight, as explained earlier.

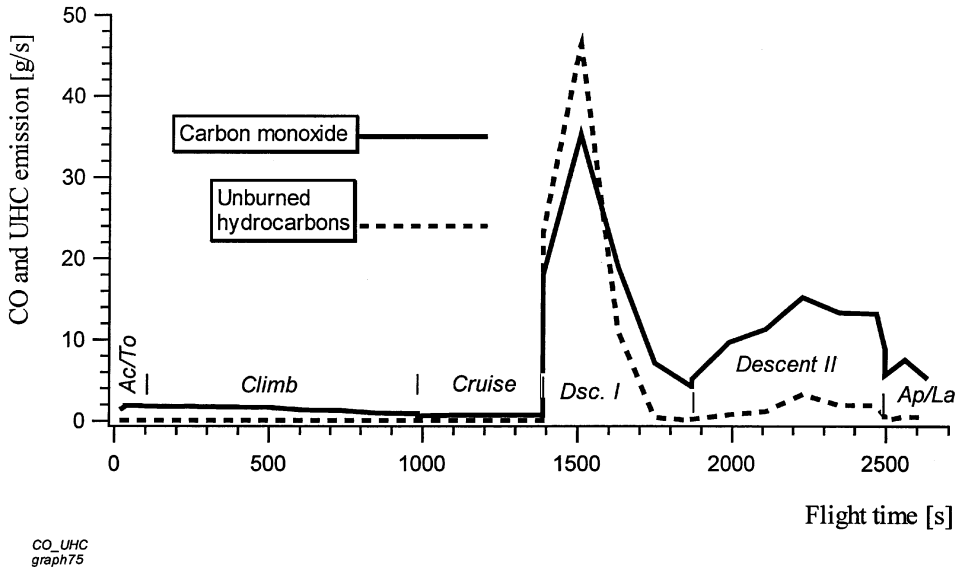

Figure 7.3 CO emissions and UHC emission per second during the complete flight cycle Oslo – Trondheim, clean engines (Turbomatch model).

7.1.2 Emissions per sequence

Based on the time-specific figures, accumulated consumption and emissions were evaluated quite easily, Table 7.1. Acceleration, take-off and climb, in this particular case, occur roughly during the first 16 – 17 minutes (1000 seconds). 1371 kg fuel is burned during the first 980 seconds, this accounts for 70 % of total fuel consumption. 10 % of all fuel is used in cruise, and the remaining 20 % in descent and approach. Equivalent figures apply for CO_2 and H_2O emissions.

21.5 kg NO_X, which is 87.5 % of the total, is released in take-off and climb, only 5.8 % in cruise sequence. The descent fraction of total NO_X is moderately overestimated at 6.7 % (Section 5.7.2).

Carbon monoxide is formed at a relatively constant rate during descent, and basically all CO, close to 90%, during that phase.

Consumption and emissions	Flight sequences fractions of total [%]		
	Acceleration, take-off and climb	Cruise	Descent and approach
Fuel consumption, CO_2 and H_2O	*70.0*	*10.0*	*20.0*
NO_X	*87.5*	*5.8*	*6.7*
CO	*7.8*	*1.5*	*≈90*
UHC	*< 1.0*	*< 0.5*	*≈100*

Table 7.1 Fractions of total consumption and emissions during the major sequences of flight Oslo – Trondheim, clean engines (Turbomatch model)

Similarly, we find that almost all the unburned hydrocarbons appear in the exhaust stream at low power settings. By studying the expressions for CO and UHC emission coefficients for descent and approach, it is evident that CO emission quantity is proportional to maximum engine pressure in the power of –3.4 and UHC quantity is proportional to the same pressure in the power of –8.7. Consequently, as engine pressure varies with ambient pressure, UHC falls off quite steeply with dropping altitude; the graph shows 85 % of all UHC is formed during the first 5 – 6 minutes of the descent.
From the data generated in this work it is evident that the take-off and climb (40 % of the total trip) are the most intense sequences when it comes to CO_2, H_2O and NO_X emissions, while the early descent is when CO and UHC rates are on their highest. The cruise phase that accounts for nearly 20 % of the total travel distance does not contribute to air pollution with a corresponding percentage.
A characteristic feature of short-haul flights where climb and descent together form the major part of the route, is that it is clear that only a small fraction of total emissions is formed during cruise. For a complete set of graphs showing accumulated fuel consumption and emissions, also see Appendix B.

7.1.3 Emissions at different altitudes

It has been explained earlier how the atmosphere as a recipient is able to cope with polluting gases differently depending on what altitude the pollutants are present. Regulations that impose limitations on what are legal emissions from aircraft engines are only concerned with emissions close to airports, that is at low altitudes. The present analyses have demonstrated how, for a typical short-haul flight, emissions are released at all levels. Graphs have been produced for five different ranges of altitude; below 1 000 meters, 1 000 – 4 000 meters, 4 000 – 7 000 meters, 7 000 – 10 000 meters, and above 10 000 meters. For the present case flight, engine performance with new and clean engines, the figures are as presented in Table 7.2, and

graphically in Appendix B. The percentage of total emissions released per 100 meters altitude change is calculated (average for each of the introduced altitude ranges) and shown in the graph of Figure 7.4.

Altitude [m]	CO_2 and H_2O[%] fraction of the total 6 200 kg and 2 300 kg	NO_X [%] fraction of the total 24.6 kg	CO [%] fraction of the total 17.8 kg	UHC [%] fraction of the total 6.9 kg
below 1 000	*17.3*	*18.1*	*12.8*	*2.8*
1 000 – 4 000	*27.6*	*32.0*	*32.5*	*14.8*
4 000 – 7 000	*21.3*	*20.9*	*12.2*	*2.2*
7 000 – 10 000	*17.5*	*16.8*	*19.6*	*21.4*
above 10 000	*16.3*	*12.2*	*22.8*	*58.9*

Table 7.2 Distribution in percent of the total flight emissions into the altitude domains

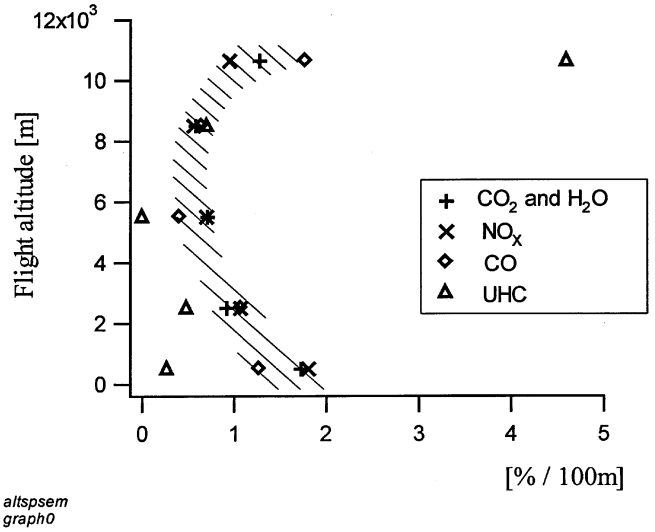

Figure 7.4 Variations of emissions per 100 m altitude of the atmosphere, percent of total emissions released during Oslo – Trondheim flight

The general picture is that at low altitude roughly 1.5 % of all CO_2, H_2O, NO_X and CO is dropped per 100 m altitude range. Above 10 000 meters the similar figure is also 1.5 % while at intermediate altitudes, 0.5 – 1.0 % per 100 meter is typical. The UHC deviates significantly from this trend, comments to this are found later in this chapter.
Studies of the coarser distributions from Table 7.2 reveal the following:

CO_2 and H_2O emissions:
Except for the lower altitude, 1 000 – 4 000 m, carbon dioxide and water vapor is evenly emitted at all altitude levels. The large portion, 27.6 %, between 1 000 and 4 000 m almost entirely comes from the early climb phase. Adding the close to the ground portion, 17.3 % of the total, leaves more than 40 % of these emissions within a 70 km radius of the airport.
It has been discussed already how effects of exhaust emissions may be quite different in the stratosphere to what they are closer to the ground. Just over 16 % or $\frac{1}{6}$ of all CO_2 and H_2O which amounts to 1 010 kg and 375 kg respectively, is released in the stratosphere (assuming the tropopause is at around 10 000 meter altitude during the standard flight of this study). As explained earlier, the exact location of the tropopause may change with latitude, and over the year. Still one obvious conclusion is that for flights in the range of 500 km, the impact on the stratosphere is minor. Though this greatly depends on the tropopause altitude. The CO_2 and H_2O stratospheric emission may change by several tens of percent either way with such variations.

NO_X emissions:
The 4.5 kg (18 %) NO_X formed below 1 000 m altitude is mostly released less then 10 km from the runway. Close to one third of all nitric oxides from this flight is produced in the 1 000 – 4 000 m range altitude, almost entirely during climb. Adding these two portions makes close to 50 % of all NO_X being emitted less than 70 km from the airport.
Assuming the tropopause to be at 10 000m altitude, 12 – 13 % (3.0 kg) of all NO_X will end up in the stratosphere, and consequently the remaining 87 – 88 % in the weather regime, the troposphere.

CO emissions:
The most intense CO production occurs during the first 3 minutes and the last 6 minutes of the descent (Figure 7.3). Early descent causes 4 kg stratosphere carbon monoxide and due to the final descent sequence almost one third of all CO ends up between altitudes of 1 000 and 4 000 meters. Aside from these details the CO is evenly distributed at all levels of the troposphere.

UHC emissions:
Since the most significant quantities of unburned hydrocarbons appear in the exhaust stream at the low thrust and high altitude portions of the flight, around 60 % of all UHC is left at stratosphere altitude, and 80 % (5.5 kg) above 7 000 m.
Virtually no unburned hydrocarbons, only 3 % of the total, are released in the vicinity of the airport, i.e. below 1 000 m.

7.2 Deteriorated Engine Performance; Compressor and Fan Fouling

7.2.1 Modeling the deteriorated engine

Clean engines and three different degrees of engine cold end fouling, also identified as modes, have been studied. The flight route is similar for flights with all engine conditions. Extra take-off weight is added to account for the increased fuel requirement. Landing weight is the same for all flights.
For specification of the engine deterioration, the way it is represented in this work is shown in Section 5.6. The three fouling modes are identified as D1, D2 and D3 and represent degrading of all the compressor modules of the engines, i.e. reduction in pressure increase, isentropic efficiency and air mass flow; details in Table 5.2. The engine degradation parameter Φ is defined and quantified in Section 5.6.

7.2.2 Time specific fuel consumption and emissions

All the calculated data are presented in graphs in the Appendix B. For the particular purpose of discussing ranges of variations in time-specific fuel consumption and emissions for each sequence of the flight, a certain selections of points along the time scale are chosen. The points, in seconds from the start of acceleration, are:

take-off	36	60		(start / late)
climb	84	374	734	(start / early / late)
cruise	1 224			(mid cruise)
descent	1 629	2 109	2 469	(early / mid / end)
app/land	2 561			(mid approach)

The consumption and emission figures presented in Tables 7.3, 7.4, 7.5 and 7.6 represent the single values and ranges of variation found for these points.

Fuel consumption, degraded engines:

	D1 ($\Phi = 0.5$)	**D2** ($\Phi = 1.0$)	**D3** ($\Phi = 3.0$)
take-off	1.5 - 2.0	3.0 - 4.8	11.7 - 14.3
climb	2.0 - 2.8	2.5 - 5.6	8.6 - 13.7
cruise	1.7	3.4	9.1
descent	0.6 - 0.8	1.2 - 1.7	3.7 - 5.3
app/land	0.4	1.2	4.5

Table 7.3 Percentage increase in time-specific fuel consumption and emissions of CO_2 and H_2O with cold end fouling, ranges of variation within each flight sequence.

The change in specific fuel consumption with engine deterioration as predicted by the model is presented in Table 7.3 above. The increase is roughly proportional to engine degradation as defined. This seems to be the case in all flight regimes. The proportionality coefficient however, varies with thrust setting, in general, such that at higher output relatively more fuel is required to make up for reduced engine performance. In take-off and climb, change in fuel flow is roughly 4 times the percentage of cold end degradation, in cruise the factor is 3, and in descent and approach we are seeing 1.5 as an average figure. Linearity is discussed further in Section 7.2.5.

CO_2 and H_2O emissions, degraded engines:

The figures for the relative increase in fuel consumption per second also apply for growth in CO_2 and H_2O emissions. We therefore see a significant jump in the two emissions when the fan and compressor performances deteriorate due to fouling.

NO_X emissions, degraded engines:

	D1 ($\Phi = 0.5$)	**D2** ($\Phi = 1.0$)	**D3** ($\Phi = 3.0$)
take-off	4.7 - 6.1	9.4 - 14.2	38.0 - 50.0
climb	3.7 - 10.6	7.3 - 20.5	26.9 - 59.7
cruise	2.9	3.9	23.5
descent	0.0 - 6.0	2.4 - 4.1	1.6 - 8.0
app/land	6.0	3.0	5.2

Table 7.4 Percentage increase in time specific emissions of NO_X with engine cold end fouling, ranges of variation within each flight sequence.

The equilibrium constant for the reaction

$$\frac{1}{2}N_2 + \frac{1}{2}O_2 \leftrightarrow NO \tag{7.1}$$

defined as $K_{p,NO} = \frac{p_{NO}}{p_{N_2}^{\frac{1}{2}} \cdot p_{O_2}^{\frac{1}{2}}}$ increases with temperature in the entire temperature range of interest (Kuo, K.K., 1986). This supports the calculated increase in NO_X with degradation, hence higher combustion temperatures.

The most significant relation of NO_X with engine fouling is observed for the high performance conditions, take-off and climb, the NO_X increase in percent is approximately 10 times the percentage point of degradation for these conditions (Table 7.4).

The data indicate that in cruise the NO_X production is quite sensitive to the initial degradation, then stays more or less constant with increasing fouling until, for the extreme engine mode D3, an extra 20 % NO_X per unit fuel is observed.

It has been explained earlier that due to model adjustments in certain conditions, an over-estimated NO_X should be expected. These modifications do not effect the cruise. More detailed calculations are needed to confirm whether there really is a certain range of degradation for which NO_X emission is almost independent of cold end fouling or not.

Cold end deterioration has some influence on NO_X formation during descent and approach, though correlation with the degree of fouling is not obvious. A different aspect is that the absolute time specific NO_X emission in these sequences, 1.5 – 2.0 g/s, is just 5 – 10 % of that of take-off and climb, and variations in such relatively small numbers is of little significance. The NO_X emission during descent and approach is released equally at all altitudes.

CO and UHC emissions, degraded engines:

	D1 ($\Phi = 0.5$)	**D2** ($\Phi = 1.0$)	**D3** ($\Phi = 3.0$)
take-off	–2.3 - –4.9	–3.4 - –9.2	– 24.2 - –35.1
climb	–2.5 - –10.3	–1.7 - –16.6	– 22.0 - – 45.3
cruise	+1.7	+8.8	–11.8
descent	–3.1 - –9.8	–5.3 - –10.8	– 21.7 - – 29.6
app/land	–12.0	–10.8	– 28.2

Table 7.5 Percentage changes in time specific emissions of CO with engine cold end fouling, ranges of variation within each flight sequence.

	D1 ($\Phi = 0.5$)	**D2** ($\Phi = 1.0$)	**D3** ($\Phi = 3.0$)
take-off	0.0 - –2.1	+1.4 - –2.3	–2.7 - –9.8
climb	–0.4 - –4.8	+1.7 - –5.3	–5.6 - –17.1
cruise	+3.8	+14.0	+6.6
descent	–9.6 - –27.7	–8.9 - –29.4	–55.2 - –75.7
app/land	–33.3	–30.6	–65.9

Table 7.6 Percentage changes in time specific of UHC with engine cold end fouling, ranges of variation within each flight sequence.

Variations in CO and UHC during acceleration, climb and cruise are quite insignificant because the absolute quantities of the emissions are extremely small in these sequences. Therefore the phenomenon that the emissions increase with fouling in cruise and in a few other cases, unlike everywhere else in the high performance regimes, is of academic interest, though not relevant in this case, and will not be discussed any further.

Flight condition and thrust requirement kept constant, the parameters that are most influential to CO and UHC forming will change with increasing compressor fouling. These parameters are the air mass flow rate, fuel-to-air ratio, maximum engine pressure, pressure change over combustion chamber, and turbine entry temperature. The following consequences are likely:

Reduced compressor performance means lower air mass flow, isentropic efficiency and compressor delivery pressure. To maintain engine performance, fuel flow is increased, and consequently we see higher turbine entry temperature. Air mass flow, fuel-to-air ratio, pressure and pressure losses will change and stabilize somewhere not too far from their initial (clean engine) magnitudes. Such variations are observed in the calculated data.

The emission index CO_{EI} for descent and approach is proportional to the functions of turbine entry temperature and maximum engine pressure, $\frac{T_{t4}}{e^{0.0123T_{t4}}}$ and $\frac{1}{P^{3.39}}$ respectively, the fuel-to-air ratio squared and the air mass flow through the combustion chamber. By studying the calculated data for clean engine and deteriorated engine mode D2, one finds that in most cases engine pressure is higher in the D2 mode. Most common is also that the air mass flow rate in the combustion chamber is lower and hence the fuel-to-air ratio is higher for the degraded engine in similar thrust conditions.
The turbine entry temperature T_{t4} and the engine pressure P are major parameters in estimating the emission indexes. Partial derivatives of CO emission index are

$$\frac{\partial(CO_{EI})}{\partial(T_{t4})} = K1 \cdot \frac{1 - 0.0123 \cdot T_{t4}}{e^{0.0123T_{t4}}} \tag{7.2}$$

$$\frac{\partial(CO_{EI})}{\partial(P)} = K2 \cdot (-3.39) \cdot \frac{1}{P^{4.39}} \tag{7.3}$$

K1 and K2 are positive constants.

The derivatives are negative for all T_{t4} larger than 82 K and for all P.

The trends are even more pronounced in the UHC_{EI} cases as the latter is proportional to $(CO_{EI})^{2.83}$.
These are strong indications as to why we should expect to find lower CO_{EI} and UHC_{EI} for increasing compressor fouling in lower engine thrust settings.
Emissions are also proportional to fuel flow, which is always higher for unclean engines, however, this obviously does not outweigh reductions in the emission indexes.

The equilibrium constant of the balance

$$CO + \frac{1}{2} O_2 \leftrightarrow CO_2 \tag{7.4}$$

is $K_{p,CO_2} = \frac{p_{CO_2}}{p_{CO} \cdot p_{O_2}^{\frac{1}{2}}} = \frac{p_{CO_2}}{p_{O_2}} \cdot \frac{1}{\frac{p_{CO}}{p_{O_2}^{\frac{1}{2}}}}$, and K_{p,CO_2} drops with increasing temperature, hence more CO should be expected in the high temperature range. This is in contrast to the calculated figures. Lefebvre in his book (Lefebvre, A.H., 1983) confirms that "...CO emissions are found to be much higher than predicted from equilibrium calculations and to be highest at low-power conditions, when peak temperatures are relatively low. This is in conflict with the predictions of equilibrium theory, and it suggests that much of the CO arises from incomplete combustion of the fuel." Based on such experience it should be expected that less CO is produced in a hotter, i.e. degraded engine. A similar tendency for the occurrence of

unburned hydrocarbons is likely since incomplete combustion of the fuel is also the reason for UHC forming.
The numbers in Tables 7.5 and 7.6 above reveal that in descent and approach, emission of carbon monoxide typically drops by 8 to 10 times the percentage of degradation. For unburned hydrocarbons the reduction is in the range of 20 to 30 times the degradation parameter Φ. This is the case for the two more severe degrees of degradation D2 and D3. With the least severe fouling D1 the reduction is relatively large and of the same magnitude as with mode D2. This is evident for both CO and UHC.
Considering the large variations in the numbers in this particular case, the basic trends and tendencies, rather than the details should be recognized.

7.2.3 Accumulated fuel consumption and emission

	C0	**D1**	**D2**	**D3**
Fuel consumption [kg]	1 948	1 986	2 023	2 141
change [kg]		**38**	**75**	**193**
change [%]		*1.9*	*3.9*	*9.9*
CO_2 emission [kg]	6 196	6 316	6 434	6 812
change [kg]		**120**	**238**	**616**
change [%]		*1.9*	*3.9*	*9.9*
H_2O emission [kg]	2 300	2 344	2 388	2 528
change [kg]		**44**	**88**	**228**
change [%]		*1.9*	*3.9*	*9.9*
NO_X emission [kg]	24.6	26.2	27.8	34.5
change [kg]		**1.6**	**3.2**	**9.9**
change [%]		*6.5*	*13.0*	*40.2*
CO emission [kg]	18.2	16.7	16.4	13.6
change [kg]		**–1.5**	**–1.8**	**–4.6**
change [%]		*–8.2*	*–9.9*	*–25.3*
UHC emission [kg]	8.2	5.9	5.7	2.7
change [kg]		**–2.3**	**–2.5**	**–5.5**
change [%]		*–28.0*	*–30.5*	*–67.1*

Table 7.7 Fuel consumption and exhaust emissions accumulated for entire flight, clean and deteriorated engines; deviation (absolute and percent) from clean engine conditions.

Accumulated fuel consumption and CO_2 and H_2O emissions:
Total fuel consumption and emissions of carbon dioxide and water vapor increase by close to 4 times the degradation percentage as defined. This translates to an extra CO_2 production of 616 kg and H_2O of 228 kg with 193 kg additional fuel burned in the most severe engine condition.

Accumulated NO_X emissions:
The quantity of NO_X emission accumulated over the whole flight, according to the present figures, increases linearly with degradation, proportional factor 13. Hence, in the $\Phi = 3.0$ degradation case, we see a 40 % higher total NO_X, the equivalent of an extra 10 kg on the Oslo – Trondheim flight.

Accumulated CO and UHC emissions:
The accumulated emission quantities fall with growing degradation such that the declining trend is at its steepest with little fouling and gets more moderate as engine condition deteriorates. Reductions in total accumulated CO and UHC emissions by $\frac{1}{4}$ and $\frac{2}{3}$ respectively are seen with the most dramatic fouling.

Fuel consumption and emissions, function of engine degradation Φ:

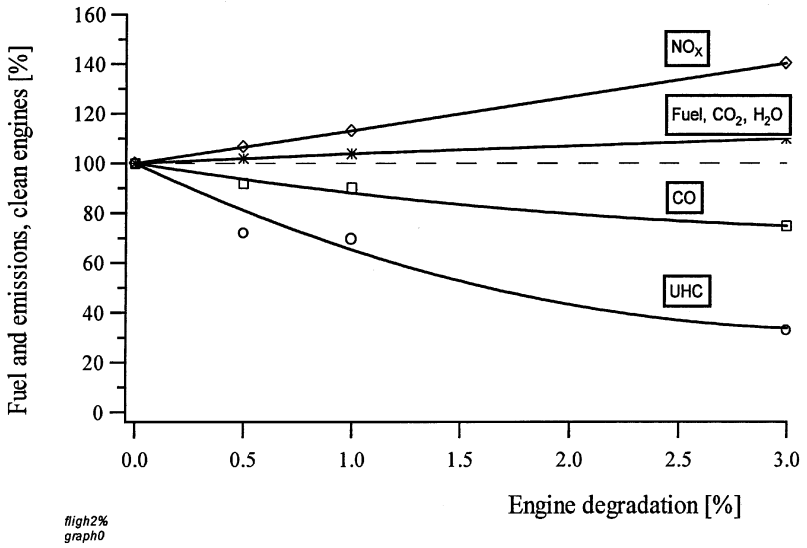

Figure 7.5 Changes in total fuel consumption and flight emissions with engine degradation due to fouling

The data from Table 7.7 is presented graphically in Figure 7.5. For the range of the engine degradation parameter Φ of the present study which is $0.0 \leq \Phi \leq 3.0$, the accumulated (total) fuel consumption, CO_2, H_2O and NO_X emissions vary almost linearly with Φ. This linear behavior is commented on already, it is also encountered in fractions of the flight, and for single operating points. The parameter Φ is proportional to the reduction in some important engine parameters, as defined in Section 5.6, and that is part of the reason for a close to linear connection. The physical side of the explanation is also evident:
The Turbomatch model finds, through iterations, the operation point of the engine in each flight condition and for the current fouling condition. The requirement that engine components match with respect to all interface parameters is met. When engine performance is reduced by fouling, and the thrust has to be kept unchanged or even increased, many parameters will have to vary. The picture is quite complex. However, by studying major parameters in the engine such as turbine entry temperature, overall pressure ratio, and core air mass flow rate for one particular flight condition (important parameters as explained in Section 2.5.3), support for linear behavior is found. As an example, calculated figures for these parameters in one particular point in cruise are shown in Table 7.8.

Engine Property	**C0;** Φ = 0.0	**D1;** Φ = 0.5	**D2;** Φ = 1.0	**D3;** Φ = 3.0
T_{t4} [K]	1 241	1 260 *+1.5%*	1 280 *+3.1%*	1 372 *+10.6%*
Overall Pressure ratio	21.95	21.94 *≈0%*	21.90 *−0.2%*	21.09 *−3.9%*
Core Mass Flow Rate [kg/s]	14.4	14.3 *−0.7%*	14.1 *−2.1%*	13.2 *−8.3%*

Table 7.8 Engine property change with fouling, turbine entry temperature, over all pressure ratio and core mass flow rate, cruise condition (point 22 of the model flight).

Change in fuel flow has to be proportional to temperature and mass flow changes. From the figures in the table it is clear that for the balanced engine temperature and air mass flow, changes are proportional to the degradation Φ. CO_2 and H_2O emissions are proportional to the fuel consumption. NO_X is highly dependent on the temperature, and as the residence time is influenced by the mass flow rate, NO_X is indirectly dependent on the mass flow of air through the combustor.
The rates at which CO and UHC are formed are affected by the primary zone combustion and other processes as well. An example is that quenching of the flame and hot gases by cooling air tends to freeze the two components before reactions are complete. Particularly the UHC content is difficult to predict, according to Lefebvre. A considerable drop in overall pressure

ratio is observed only for the most extreme fouling condition. This will influence the flow of cooling air and the atomization of the fuel in the combustion chamber, and consequently alter the conditions in favor of higher CO and UHC content.
Further studies have to be performed to clarify any simple relations with the degradation parameter.

7.2.4 Emissions at different altitudes

Quantities of all emissions from flights with the three modes of engine degradation were calculated for the different segments of the atmosphere as used earlier; below 1 000 meters, 1 000 – 4 000 meters, 4 000 – 7 000 meters, 7 000 – 10 000 meters and above 10 000 meters.

CO_2 and H_2O emissions:

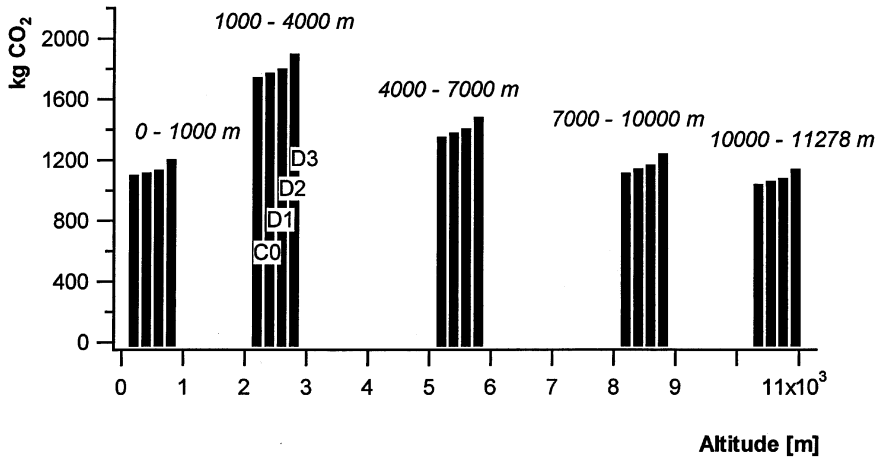

Figure 7.6 Quantities of CO_2 emissions in all altitude domains and, with clean engine (C0) and three degrees of fouling (D1, D2 and D3). (TURBOMATCH model)

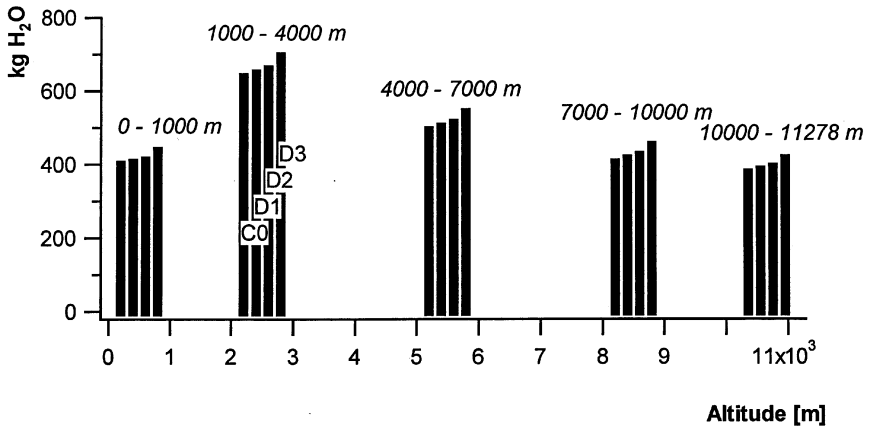

Figure 7.7 Quantities of H_2O emissions in all altitude domains and, with clean engine (C0) and three degrees of fouling (D1, D2 and D3). (TURBOMATCH model)

The relative growth in CO_2 and H_2O emissions with increasing engine degradation is shown graphically in Appendix C. Growth is strongest in the 7 000 m – 10 000 m domain and the weakest at low altitudes. Deviations from flight average growth are not large. Typically in the 1 % degradation (D2) the emission is close to 5 % higher between 7 000 m – 10 000 m and less than 3 % higher than the average growth below 1 000 m. The growth in accumulated flight emission of CO_2 and H_2O with 1 % degradation is 3.9 %. Since these emissions in general are quite low in early descent, the strongest emission increase at 7 000 m – 10 000 m altitude essentially happens in the late climb phase; at high thrust setting, high speed and low ambient temperature, pressure and air density. Part of the explanation of this phenomenon is probably that in this condition the compressors operate at high rotational speeds and pressure ratios and low entry temperatures, that is to the far right in the compressor maps, sample compressor map in Figure 7.8. In this part of the map the constant isentropic efficiency graphs are strongly curved and steep, and the isentropic efficiency is more sensitive to a small shift in the compressor operating point than elsewhere. Lower efficiency means increased fuel requirement, and thus higher CO_2 and H_2O emissions.

For the absolute magnitude of additional CO_2 and H_2O emissions the highest growth is in the 1 000 m – 4 000 m altitude range, though only marginally larger than for 4 000 m – 7 000 m and 7,000 m – 10,000 m, see Figures 7.6 and 7.7 and Appendix B. The general trend in the model data is quite clear: from the CO_2 and H_2O caused by cold end fouling of the turbojet engines, 67 – 70 % ends up evenly distributed between 1 000 and 10 000 m altitude, 12 – 16 % is left near the ground below 1 000 m and 17 – 18 % is dropped above 10 000 m, in the stratosphere.

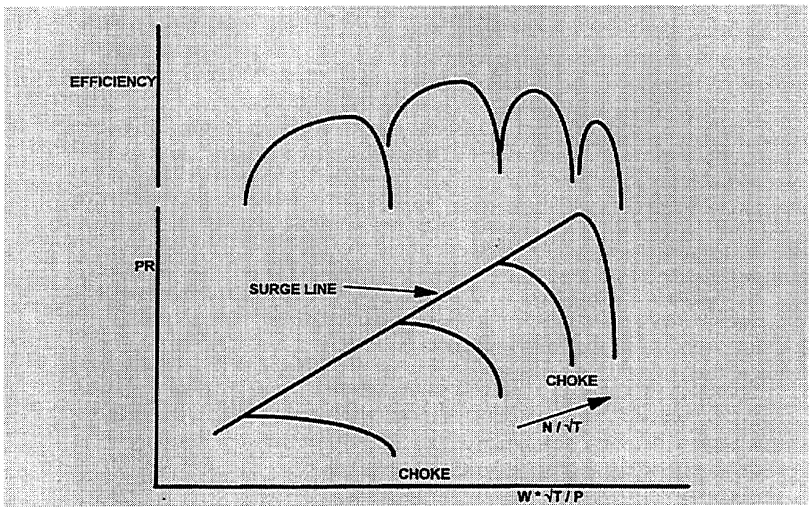

Figure 7.8 Sample compressor map. The steep efficiency curve at high rotational speed $N/\sqrt{T}$ appears quite clearly. (Walsh and Fletcher; Gas Turbine Performance)

NO_X emissions:

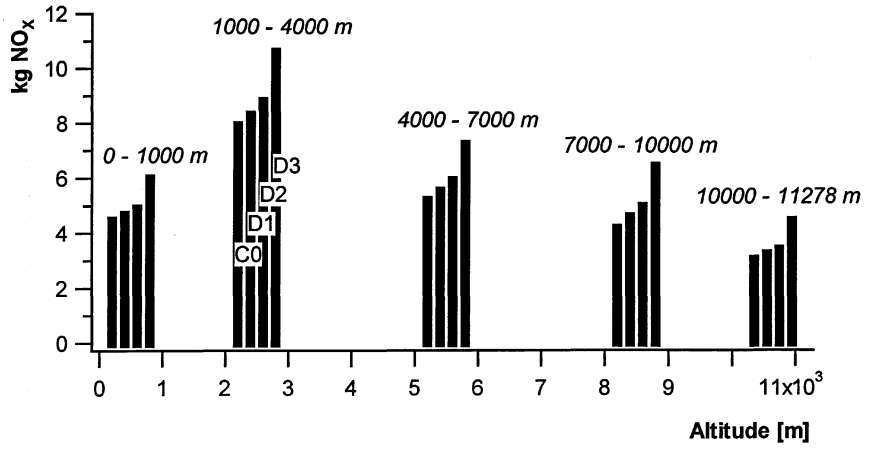

Figure 7.9 Quantities of NO_X emissions in all altitude domains and, with clean engine (C0) and three degrees of fouling (D1, D2 and D3). (TURBOMATCH model)

Probably related to the similar reason as discussed for CO_2 and H_2O emissions, the relative growth in NO_X emissions with increasing engine degradation is strongest in the 7 000 m – 10 000 m domain. Generally at these altitudes the figures show a relative increase in NO_X emission, twice that at altitudes under 1 000 m, see Figure C8 of Appendix C.
In the two severe modes of engine degradation most additional NO_X is formed in the 1 000 m – 4 000 m altitude regime. In general the 4 000 m – 7 000 m receives less additional NO_X then the adjacent regimes. The general trend in the model data is that from the additional NO_X caused by cold end fouling of the turbojet engines, 71 – 76 % ends up evenly distributed between 1 000 and 10 000 m altitude, 13 – 15 % is left near the ground below 1 000 m and 11 – 14 % is released above 10 000 m, in the stratosphere.

CO and UHC emissions:
Details of how these emissions vary with engine state at different altitudes is not clearly shown by the modeling data. Some trends seem clear though (see Figures 7.10 and 7.11):

1. Emissions of CO and UHC fall off with engine cold end fouling in all altitude regimes. These emissions are quite sensitive to light fouling, then appear to be independent as fouling builds up, and finally as degradation becomes most severe, emissions drop further, quite considerably. This is pointed out in Sections 7.2.2 and 7.2.3.

2. The magnitudes of emission reductions are small close to the ground and in the 4 000 m – 7 000 m altitude regime.

3. Within each of the other regimes the total quantity of CO drops approximately 0.3 kg (7 – 8 %) with moderate fouling and 1.2 kg (20 - 30 %) in the state of extreme fouling (this also applies in the stratosphere altitudes).

4. The relative reductions in CO and UHC is larger in the higher altitude regimes.

5. The absolute UHC reduction with increasing degradation is most significant in the higher altitudes. Total UHC emission in the stratosphere portion of the flight (above 10 000 m) drops more than 30 %, equivalent to 1.6 kg, with moderate fouling, and then another 30 % (1.6 kg) with extreme fouling of fan and compressors.

The reasons why the emissions of CO and UHC generally drop with increasing fouling the way they seem to do, is discussed already in this chapter.
In the 0 m – 1000 m and the 4 000 m – 7 000 m altitude regimes the relative drop in the two emissions are smaller than elsewhere, and so are the total emissions in these regimes (point 2 above). Therefore the calculated reductions are of less significance here. For the UHC in particular, the variations in these regimes are negligible compared to the overall magnitudes of the calculations.
At high altitudes, with low ambient temperature, the relative increase of T_{t4} to maintain thrust with fouling has to be bigger than at lower altitudes and higher ambient temperatures. This is a possible physical explanation to why we see larger drops due to fouling at higher altitudes for these emissions.

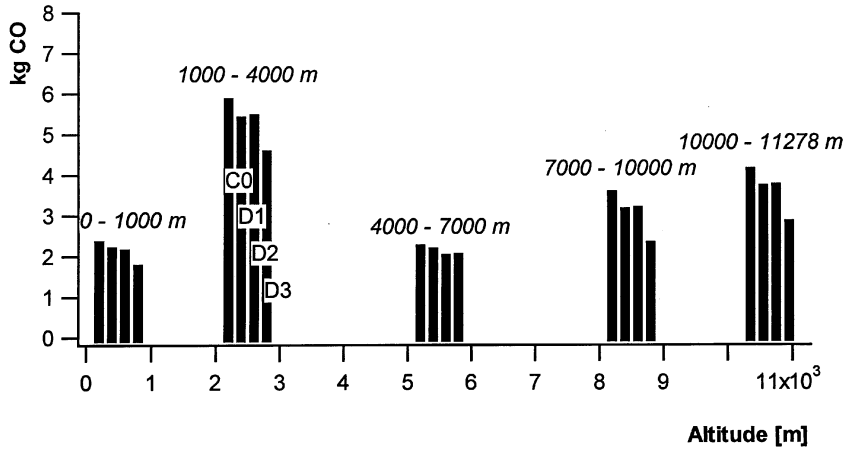

Figure 7.10 Quantities of CO emissions in all altitude domains and, with clean engine (C0) and three degrees of fouling (D1, D2 and D3). (TURBOMATCH model)

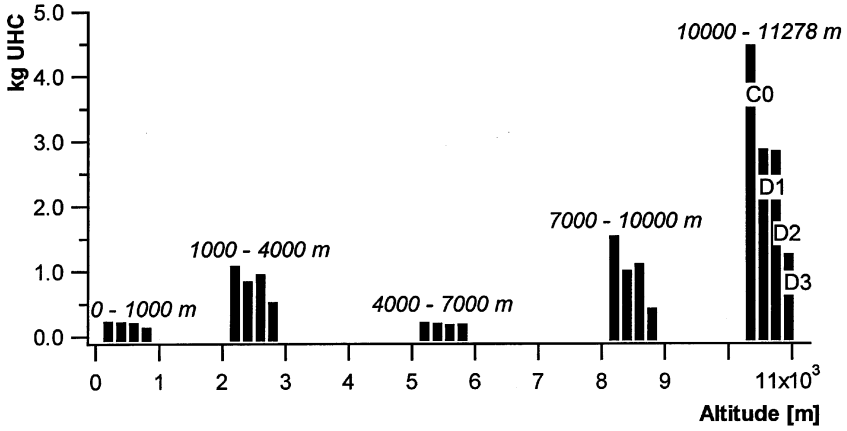

Figure 7.11 Quantities of UHC emissions in all altitude domains and, with clean engine (C0) and three degrees of fouling (D1, D2 and D3). (TURBOMATCH model)

7.3 The Simple Model; Evaluation of the CODE1X versus the Turbomatch-based Tool

7.3.1 General comments

Engine modeling is far more detailed and complex in Turbomatch than CODE1X. The representation of the aircraft that was used with the Turbomatch analyses is also much more advanced than in the CODE1X model. Boundary conditions, however, like flight distance, time, and altitude are similar in the two cases. The emission indexes used are identical in the two cases.

The size of the Turbomatch source code is around 660 kilobyte, a CFM56 engine representation adds another 30 kilobytes. For the studies of this work 32 000 engine conditions are calculated in Turbomatch, and the results from these calculations that are in a format readable from a Fortran code are 152 MB in total. A Fortran code of 15 kilobytes was used to select relevant data for each flight condition and do the interpolation. Turbomatch is (fall of year 2000) running successfully on a PC computer. Computer time for the simulation of one engine condition is not large. Setting up the input data for all 32 000 conditions is laborious and time-consuming as it has to be done manually. Emission calculations are done in Excel.

The entire CODE1X Fortran file is 60 kilobytes. Input data are given manually during program execution, and for the analyses of this work 250 conditions of engine operation were calculated. The total of output files is around 240 kilobytes and emission quantities are included. Thus the CODE1X model is approximately $\frac{1}{10}$ of the Turbomatch in size and handles only $\frac{1}{100}$ the amount of data for this particular study.

It is already explained that for the simple model the engine power setting is based on low pressure spool rotational speed, and aircraft drag coefficient is averaged over flight sequences. Another major difference in the two models is the speed development throughout the flight, shown in Figure 7.12. Due to the differences in acceleration and drag, fuel consumption and emissions for the simple model are likely to deviate from the Turbomatch-based figures.

The intentions here are to evaluate the simple (parametric) model to find whether it is capable of predicting meaningful quantities for the aircraft emissions CO_2, H_2O and NO_X in a short-haul flight, and secondly, to find if there is a reasonable correlation to figures from the comprehensive model when it comes to the consequences of engine cold end fouling.

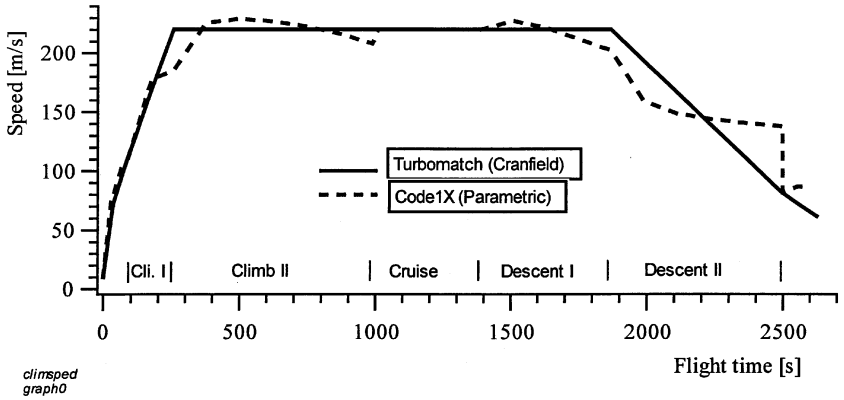

Figure 7.12 Flight speed development as used in the two models, Oslo – Trondheim flight

7.3.2 Clean engines

Carbon dioxide and water emissions are directly related to the fuel consumption. With the parametric model the speed during most of take-off and early climb is higher (causing more drag), and the speed increase is steeper (higher acceleration) then in the Turbomatch based model. Speed is also considerably much higher in the late descent phase. In these flight sequences the parametric model predicts higher fuel consumption and consequently higher CO_2 and H_2O emissions than Turbomatch. In late climb and mid-descent the opposite occurs.

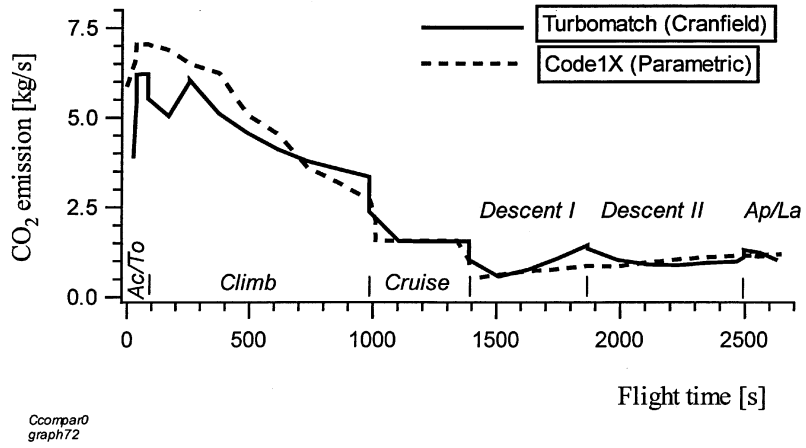

Figure 7.13 Time specific CO_2 emission development for the two models, Oslo – Trondheim flight, clean engines

The cruise speed is constant and similar for the two models, and fuel consumption and CO_2 and H_2O emission levels are the same as well. Time specific CO_2 emission is shown in Figure 7.13, H_2O and fuel flow in Appendix C.
In the majority of the flight time, specific fuel consumption and CO_2 and H_2O emissions in the parametric model deviate from the Turbomatch-based model typically within the limits of ± 10 %, in a few very short time periods by as much as 35 %.
Accumulated fuel consumption and emissions of CO_2 and H_2O follow well for the two models, the parametric model slightly higher, and the total quantities at the end of the flight is approximately 8.9 % higher for that model, CO_2 graphs in Figure 7.14, H_2O and fuel flow in Appendix C.

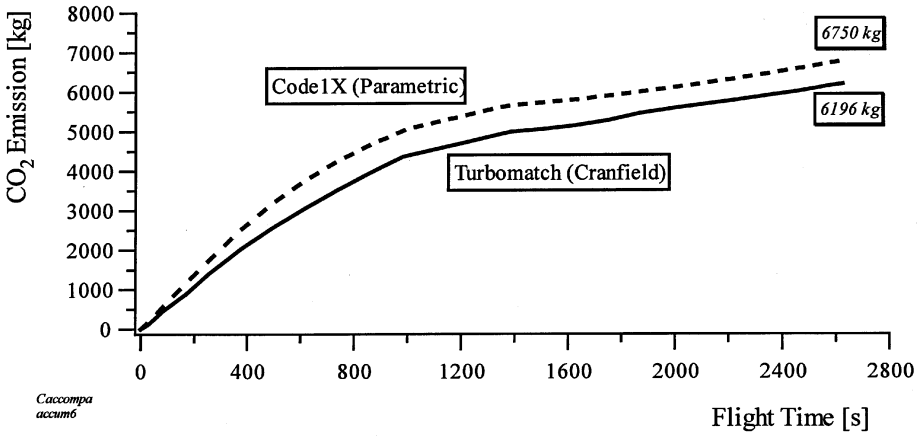

Figure 7.14 Accumulated CO_2 emission for the two models, Oslo – Trondheim flight, clean engines

Simple model emissions show good agreement at altitude levels 4 000 m and above, 8 % off from the Turbomatch based model at most. For the 0 – 1 000 m altitude range the parametric model over predicts carbon dioxide and water by 15 % and in the 1 000 – 4 000 m range by as much as 25 %. The obvious reason is the higher flight speeds in take-off and early climb for the simple model; CO_2 emission figures in graph Figure 7.15, H_2O in Appendix C.

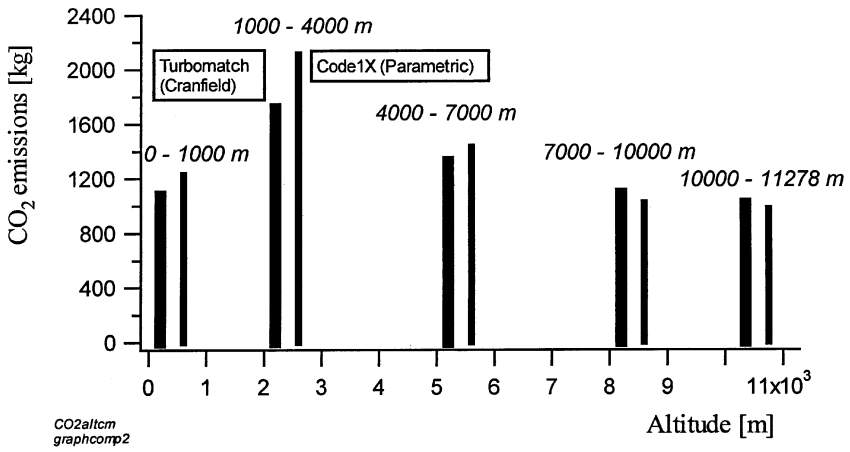

Figure 7.15 CO_2 emissions in domains of altitude for the two models, Oslo – Trondheim flight, clean engines

NO_X emissions as predicted by the simple model deviate slightly more from the Turbomatch-based figures, and mainly in the take-off and climb phases where the majority of the NO_X is released. In cruise the prediction is slightly on the low side, while total NO_X for the flight is 13 % higher when calculated in the parametric model.

Still, in relative numbers, there is an over-estimation of around 30 % NO_X at altitudes below 4 000 m and above 7 000 m the estimate is 20 – 30 % low. Higher figures at low altitude, like with CO_2, follow the higher flight speeds in take-off and early climb and higher thrusts and combustion zone temperatures. The fact that around 50 % of all NO_X is produced below 4 000 m, as already stated, then means that a 30 % deviation in these altitude ranges is quite a large portion of the total NO_X. Time specific NO_X and emissions per altitude domain are graphically presented in Figures 7.16 and 7.17.

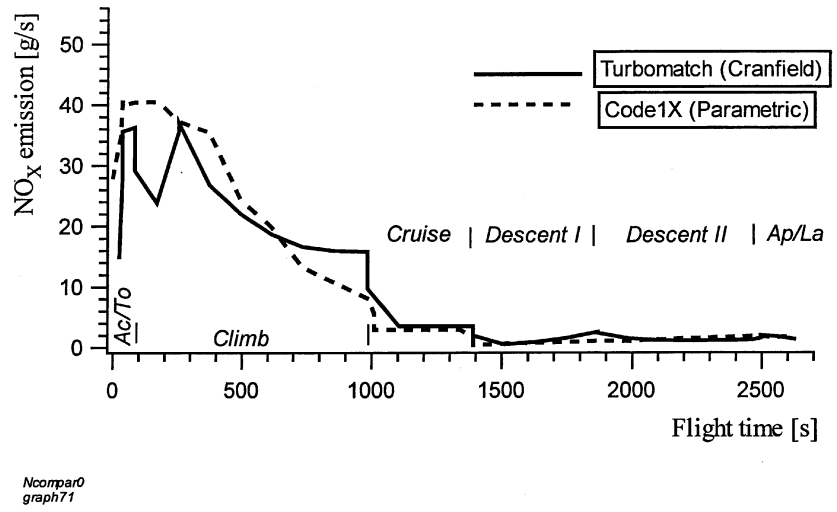

Figure 7.16 Time specific NO_X emission development for the two models, Oslo – Trondheim flight, clean engines

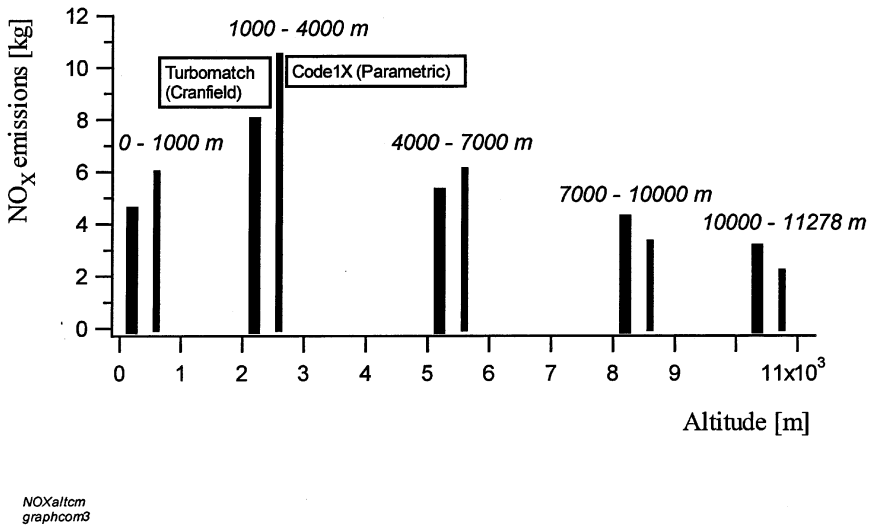

Figure 7.17 NO_X emissions in domains of altitude for the two models, Oslo – Trondheim flight, clean engines

7.3.3 Engine fouling consequences

Two modes of engine degradation are studied in the simple model; the modes are similar to the two less severe modes in the Turbomatch study.
In general the calculation procedures are less sophisticated in the simple model, with respect to component degradation as well. One particular detail is that Turbomatch will consider new quantities for compressor isentropic efficiencies by looking up the modified compressor maps (for the deteriorated fan and compressors) at every new point of operation, while the simple model is using the degraded compressor isentropic efficiencies as fixed quantities, once given by the operator. Secondly, in the Turbomatch case, the fan and compressors are modeled as four separate compressors, while with the parametric model, only two compressors are used; the fan including a low pressure unit and a high pressure compressor. From the long list of simplifications these are probably the more important when it comes to deviations in degraded engine performance and emissions.
The graphs representing time specific consumption and emissions for the Turbomatch and parametric models (Figures 7.18 and 7.19) clearly show that the increase due to cold end fouling is of the same magnitude.
In late climb, a major difference between the two models is obvious. As Turbomatch predicts additional emissions by fouling to increase with altitude, the parametric model is suggesting the opposite tendency. A different way of demonstrating the capacity of the parametric model to predict fouling consequences is seen in the graphs in Figures C7 and C8 of Appendix C, by showing the fuel consumption and emissions in the altitude domains. For CO_2 and H_2O, agreement is quite good for the two models at most altitudes, extreme deviations by the parametric model are the close to one and a half the Turbomatch estimate below 1 000 m and around $\frac{4}{5}$ between 7 000 m and 10 000 m.
Like Turbomatch the parametric model predicts an increasing NO_X emission with cold end fouling, agreement in quantity though, is not very good. At low altitude range the simple model suggests roughly two thirds, in intermediate ranges one half and above 7 000 m close to one third of the Turbomatch figures for percentage NO_X emission increase.

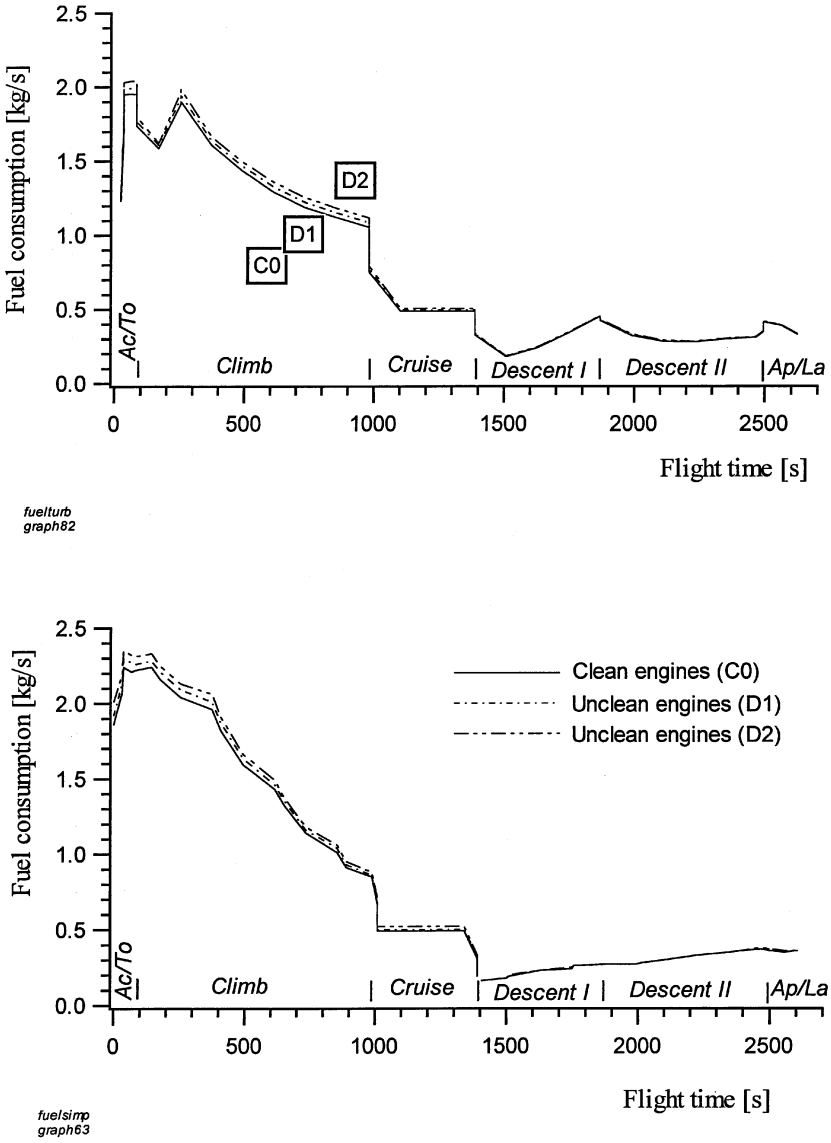

Figure 7.18 Specific fuel consumption with clean and degraded engines for the two models, Oslo – Trondheim flight, the simple model in the lower graph.

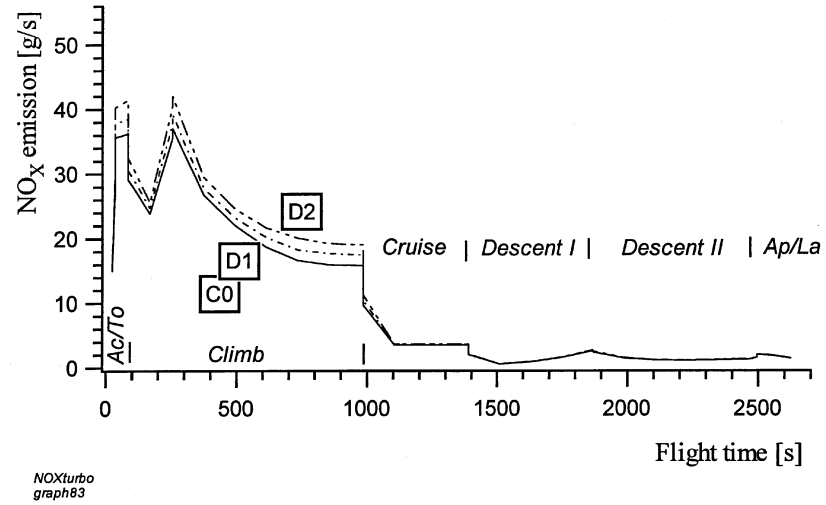

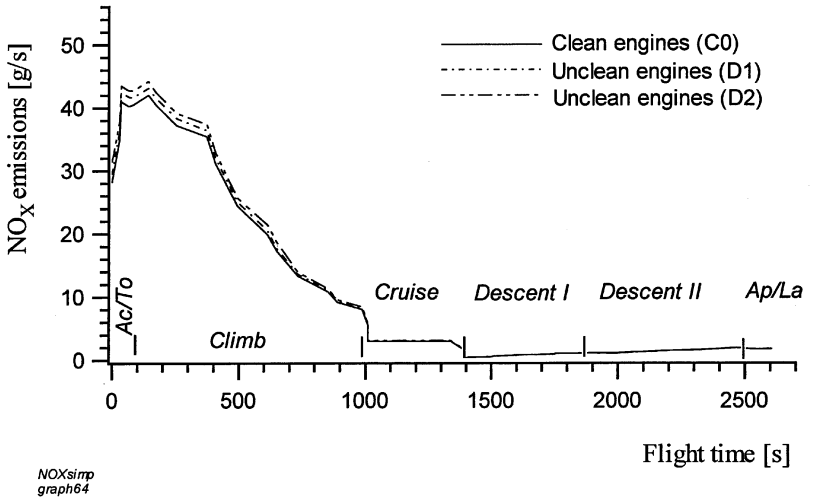

Figure 7.19 Time specific NO_X emissions with clean and degraded engines for the two models, Oslo – Trondheim flight, the simple model in the lower graph.

7.4 Emission Calculations, Summary and Conclusions

7.4.1 Short-haul flight emissions, variations with altitude

One major objective of this study has been to quantify amounts of emission gases released at all relevant altitude levels during a short-haul flight. For this purpose, the atmosphere was divided into five altitude domains:

- below 1 000 m; emission regulations already in effect
- three equally large altitude ranges:

  1 000 m – 4 000 m

  4 000 m – 7 000 m

  7 000 m – 10 000 m
- above 10 000 m; stratosphere emissions are of particular interest

Taxiing and ground idle are not included in the analyses. No additional flight time due to traffic delays or difficult weather conditions are considered.
Figure B1 presents the essence of the calculation.
Over the entire flight, assuming clean and new engines, a total of 6 200 kg carbon dioxide, 2 300 kg water vapor, 24.6 kg nitrogen oxides, 17.8 kg carbon monoxide and 6.9 kg unburned hydrocarbons are released.
Except for UHC, a major fraction of the emissions occur in the troposphere, only 16 % of CO_2 and H_2O, 12 % of the NO_X and 23 % of the CO are released above 10 000 m. Close to 60 % of all UHC ends up at this altitude, and UHC emission at 7 000 m and above is around 80 % of the total.
Emissions below 1 000 m are not a major portion of the total either; 17 % of all CO_2 and H_2O, 18 % of the NO_X, 13 % of the CO and 3 % of the UHC.
According to the calculations, close to one third of all CO_2, H_2O, NO_X and CO, are produced between 1 000 and 4 000 m. To regulate emissions at lower altitudes, close to the airport and the ground — and in the troposphere, an upper limit at 4 000 m altitude therefore seems quite sensible. That will include approximately 50 % of the major exhaust components on a short-haul flight, assuming current aircraft technology and operation.

7.4.2 The effect of engine cold end fouling on total flight emissions

An engine degradation parameter Φ, equivalent to the numerical quantity of the general drop in compressor isentropic efficiency, was defined. The range of the degradation parameter in the present studies is $0.0 \leq \Phi \leq 3.0$. The simultaneous degradation for all the compressor modules was assumed.
Results from the analyses quite clearly show that the total flight emission quantities of CO_2, H_2O and NO_X (the accumulated emissions) increased with engine degradation, while a considerable reduction was calculated for CO and UHC, as shown in Figure 7.5.

The total nitrogen oxide emission figure is quite sensitive to degradation; emission increases linearly in percent ten times the degradation parameter. Carbon dioxide and water total quantities are less effected by fouling, still a percentage increase of three times the degradation parameter was indicated.
The decline in the CO and UHC emissions with increasing degradation parameter is not at all linear. With only a modest degree of fouling, considerable reduction was estimated; $\Phi = 0.5$ causes reductions of 8 % and 28 % in CO and UHC respectively. For $0.5 < \Phi < 1.0$ these particular emissions seem to be independent of degradation, while for a more severe degradation, CO and UHC emissions fall drastically with increasing Φ; the calculations predicted large reductions for $\Phi = 3.0$.

7.4.3 The effect of engine cold end fouling on altitude emissions

Within all of the different altitude domains, emission quantities of CO_2, H_2O and NO_X increase almost proportionally with engine degradation (Figures B10 and B11). The most severe increase is observed in the 1 000 – 4 000 m range. Summing up the individual emissions for altitudes lower than 4 000 m reveals that roughly 40 % of engine fouling effects on emissions CO_2, H_2O and NO_X are observed at these low altitudes. (This amounts to 250 kg additional CO_2, 94 kg H_2O and 4.2 kg NO_X with $\Phi = 3.0$.) The CO_2 and NO_X figures quite clearly emphasize the importance of focusing on the lower 4 000 m at least, for emission release and emission abatement. This has already been suggested and is valid for additional emissions due to fouling, as well.
The effects of engine fouling on high altitude (stratosphere) CO_2, H_2O and NO_X emissions are significant, though not large. For the extreme condition $\Phi = 3.0$ an extra 102 kg CO_2, 38 kg H_2O and 1.4 kg NO_X are estimated.
For altitudes between 1 000 m and 10 000 m emissions are roughly $(20 \cdot \Phi)$ kg CO_2, $(6.5 \cdot \Phi)$ kg H_2O and $(0.25 \cdot \Phi)$ kg NO_X per 1 000 m.
Generally speaking, CO and UHC emissions quantities drop with increasing engine degradation Φ in all altitude domains. The major exception to this trend is that emissions seem to be constant or even increase with Φ between 0.5 and 1.0.
Aside from these trends, the following conclusion may be derived from the calculated figures:
CO and UHC dependence on fouling is first of all a high altitude phenomenon.
CO emissions below 4 000 m altitude are also reduced considerably with engine fouling; $\Phi = 3.0$ implies a more than 20 % reduction in CO in this range.
In the mid altitude range, 4 000 – 7 000 m, both emissions are basically independent of fouling, and so is low altitude UHC.
The very high portion of UHC released above 10 000 m is subject to considerable reduction, 2.85 kg (70 % reduction) with $\Phi = 3.0$.

8 CONCLUSIONS AND RECOMMENDATIONS FOR FURTHER WORK

1) The growth rate of commercial air traffic, particularly in the less industrialized regions of the world, and the detrimental influence that exhaust gases are believed to impede on the global environment, are incitements for this study. A review of the available literature shows that at the present time global traffic has doubled each 15 to 20 years, and in certain areas the rate is more than twice this average. It is also evident that the gas turbine-based engines are constantly becoming the more dominant means of propulsion. Whether exhaust gases are released at lower or higher altitudes is of great significance when it comes to environmental impacts and consequences like ozone layer depletion, green-house effect and acid precipitation.

2) The case flight of this study is a Boeing 737-400, engines CFM56-3C1, flying from Oslo to Trondheim, the approximate distance of 500 km. Two different computer models are used, the first one being a quite simple tool for turbofan engine analyses. This engine model is parametric, a straight-forward cycle analysis, based on the fundamental thermo- and aerodynamic equations. The aircraft model is simple as well and quite rough assumptions apply.
   Next, the case engine is modeled in the Turbomatch scheme, a well-reputed tool for gas turbine analyses and simulations that is ten times larger than the simple model. A more complex aircraft model based on Boeing data is programmed and connected. The representative Oslo – Trondheim flight is simulated independently in this modeling system as well. Exhaust emission indexes are developed and figures for fuel consumption and gaseous emissions for the case flight are evaluated.
   To facilitate further studies in this area, aircraft and mission modules should be written and connected to the Turbomatch software. This would save the users a great amount of manual data management and calculations.

3) The studies show that high power settings quite clearly contribute to high rates of carbon dioxide, water and nitric oxides, while at low power settings the carbon monoxide and unburned hydrocarbons (UHC) appear in the exhaust stream. The emissions that are released during the really short cruise sequence of this type of flight are not of major significance in the overall picture.
   Over the entire altitude range of operation for the case flight, i.e. sea level to 11 287 m, the distribution of the emissions vary from 0.5 % to 1.5 % of total emissions per each 100 m altitude increment. Percentages are on the higher side for the extreme high and low altitudes. The UHC is an exception with more than 50 % released around cruise altitude.
   Hence, in general emissions from short-haul jet transport flights are essentially tropospheric. In high latitude regions, however, more than half of all emissions end up in the stratosphere due to the low altitude tropopause in these areas.
   Further investigations should be done to obtain a more exact quantification of these tendencies. Particularly it is important to verify of the expressions for emission indexes, and focus on the low power settings where the engine models in this work do not always converge properly.
   A possible latitude differentiation of flight envelope adjustments should be looked into, particularly with respect to recommended cruise / maximum flight altitude and elimination of stratospheric flight.

4) Engine performance deterioration is simulated in the two models by reducing efficiencies, pressure ratios and air mass flow rates of fan and compressor sections. This particular mode of degradation is meant to represent mainly fouling of the forward part of the engine. An engine degradation parameter Φ, corresponding to the efficiency reduction, is introduced. Fuel consumption and emissions of CO_2, H_2O and NO_X appear to increase proportionally to Φ. Overall CO_2 and H_2O increase by as much as 10 % and NO_X by 40 % for the most extreme degradation and most severely in the late climb phase between 7 000 and 10 000 m altitude.
   Considerable drops in CO and UHC predictions are observed with increasing Φ. Even in the mildest state of engine degradation, the reductions are close to 10 % and 30 % respectively. The reductions are observed in all altitude ranges, less in the 0 – 1 000 m and 4 000 – 7 000 m domains, and for UHC most extreme at cruise altitude.
   The inevitable impact on aircraft emission level from engine degradation should be subject to the attention of further research. Engine cold end fouling may not be the most important cause of such degradation. Indications that turbine performance deterioration is more influential to the overall engine output should encourage studies of how engine hot end status relates to exhaust emissions. The results from the present work are indicative of the necessity for comprehensive studies, including field measurements, on how aircraft emissions vary with aging and time since engine cleaning and overhaul. The environmental aspect of maintenance strategy and policy are not to be neglected, also with respect to authority regulations.

5) The simple model presented in this work calculates the fuel consumption and exhaust emission quantities for the case flight successfully (the CO and UHC contents are not considered in this model). The deviations from the predictions of the larger model are in the order of 10 %. Hence, the smaller modeling system should be considered a really

useful tool for first estimates of whatever relevant consequences of engine status changes and flight modifications are being looked for.
To make full use of the code, it has to be extended to become more general with respect to what aircraft and engine categories are subjects of the study.
The user interface has not been elaborated to comply with current standards.

REFERENCES

Adams, J., Schmitt-Wittrock, P.: "Optimierung der Reinigungsinterwalle von Gasturbinen Verdichteren", Brennstoff, Wärme, Kraft: Zeitschrift für Energiewirtschaft, Deutscher Ingenieur-Verlag, Volume: 33, January 1981, pp. 25-31

Aker, G.F., Saravanamuttoo, H.I.H.: "Predicting Gas Turbine Performance Degradation due to Compressor Fouling using Computer Simulation Techniques", ASME, Journal of Engineering for Gas Turbines and Power, Volume 111, 1989, pp. 343-350

Archer L.J.: "Aircraft Emissions and the Environment: CO_X, SO_X, HO_X & NO_X", Oxford Institute for Energy Studies, Oxford, England, 1993

Brittain, D.: "Cleaning Gas Turbine Compressors. Some Service Experience with a Wet Wash System", Aircraft Engineering and Aerospace Technology, Bradford: MCB University Press, Volume: 55, January 1983, pp. 15-17

Cabrejas Morales, J.C.: "Gas Turbine Performance Simulation", Thesis, Cranfield University, School of Mechanical Engineering, and Universidad Politécnica de Madrid, Escuela Técnica Superior de Ingenieros Aeronáuticos, SOCRATES European Student Exchange Programme, 1998

CFM International: "CFM56-3 Service Bulletin, March 1984, Revision 3, September 1987"

CFM International: "CFM56 Specific Operation Instructions, April 1988 and November 1992"

CFM International: "CFM56-3/3B/3C Engine Shop Manual; Revision 46", May 1998

CFM International: "CFM56-3 Basic Engine"

CFM International: "CFM56-3 Engine Family", Company brochure CFMI-1234 (6/98)

CFM International: "Durable Engines, Reliability at its Finest", Company brochure CFMI-1215 (9/96)

CFM International: "Technology Continually Improving the CFM56 Engine", Company brochure CFMI-1217 (9/96)

Cohen, H., Rogers, G.F.C., Saravanamuttoo, H.I.H.: "Gas Turbine Theory", Addison Wesley Longman Limited, 1996

Cornish, J.L., Nicell, J.A., Groenewege, A.D.: "The Greening of Aviation", Transport Canada Publication no. TP 12543E, 1996

Correa, S.M.: "A Review of NO_X Formation Under Gas-Turbine Combustion Conditions", Combustion Science and Technology Vol. 87, 1992, pp. 329-362

Diakunchak, I.S.: "Performance Deterioration in Industrial Gas Turbines", ASME paper 91-GT-228, 36th International Gas Turbine and Aeroengine Congress and Exposition, Orlando, Florida, June 1991

Diakunchak, I.S.: "Performance Improvement in Industrial Gas Turbines", ASME paper 93-JPGC-GT-5, ASME/IEEE Power Generation Conference, Kansas City, USA, October 1993

Drolet, B. et al.: "The Euro-Québec Hydro-Hydrogen Pilot Project [EQHHPP]: Demonstration Phase", International Journal of Hydrogen Energy Vol.21, No.4, 1996

Duquesne, G.: "Correlation Report of Braathens SAFE Test Cell for CFM56-3 Engines", Reference KXTG No.09.057, CFM International/ Braathens SAFE, July 1990

French, T.: "Fanning the Flames", Airline Business, April 1988

Fuller, N.H.: "The Unducted Fan Engine: Was it a Bad Idea?", A Graduate Research Project, Embry-Riddle Aeronautical University, 1994

Gardner, R.M.: "Pollution from Aircraft", IEE colloquium / the Institute of Electrical Engineers, London, Volume 165, 1995, pp. 13/1-13/4

Grewal, M.S.: "Gas Turbine Engine Performance Deterioration Modelling and Analysis", Ph.D Thesis, Cranfield Institute of Technology, School of Mechanical Engineering, 1988

ICAO Journal, Volume 45 - No. 2, 1990, "Propfan Promises Fuel Efficiency, Low Noise Propulsion" pp. 13

ICAO Journal, Volume 51 - No. 6, 1996, "Annual Civil Aviation Report 1995", pp. 5-22

ICAO Journal, Volume 51 - No. 10, 1996, "Air Transport in Latin America and the Caribbean: a Story of Success and Failure" pp. 5-10

Intergovernmental Panel of Climate Change: "Aviation and the Global Atmosphere", Cambridge University Press, 1999

"The International Encyclopedia of Aircraft", Oriole Publishing Ltd., 1991

"Janes' All the Worlds Aircraft 1990-91", Edited by Lambert, M., Jane's Information Group

Jones, M.C.: "An Economical and Technical Assessment of the Advanced Propfan Aircraft", M.Sc. Thesis, Cranfield Institute of Technology, 1981

Knudsen, S., Strømsøe, S.: "Kartlegging av utslipp til luft fra norsk sivil luftfart", Norwegian Institute for Air Research, NILU OR: 88/90, Lillestrøm, Norway, 1990

Kolkman, H.J.: "Performance of Gas Turbine Compressor Cleaners", ASME paper 92-GT-360, the International Gas Turbine & Aeroengine Congress & Exposition, Cologne, Germany, June 1992

Kuo, K.K.: "Principals of Combustion", John Wiley & Sons, 1986

Lakshminarasimha, A.N., Saravanamuttoo, H.I.H.: "Prediction of Fouled Compressor Performance using Stage Stacking Techniques", Turbomachinery Performance Deterioration; Proceedings of the Fourth Joint Fluid Mechanics, Plasma dynamics, and Laser Conference, Atlanta , GA, May 1986, pp. 59-66

Lakshminarasimha, A.N., Boyce, M.P., Meher-Homji, C.B.: "Modeling and Analyses of Gas Turbine Performance Deterioration", ASME, Journal of Engineering for Gas Turbines and Power, Volume 116, 1994, pp. 46-52

Lambert, H.H.: "A Simulation Study of Turbofan Engine Deterioration Estimation Using Kalman Filtering Techniques", NASA-TM-104233, 1991

Le Dilosquer, M.: "Implications of Long range Civil Aircraft Flight Routes on Atmospheric Pollution", MSc thesis, Cranfield University 1993

Lee, S.H., Le Dilosquer, M., Singh, R., Rycroft, M.J.: "Further Considerations of Engine Emissions from Subsonic Aircraft at Cruise Altitude", Atmospheric Environment, Volume 30, No. 22, 1996, pp. 3689-3695

Lefebvre, A.H.: "Gas Turbine Combustion", Taylor & Francis, 1983

Luftfartsverket, "Civil Aviation Administration Annual Statistics 1994", Oslo, Norway 1995

Luftfartsverket, "Civil Aviation Administration Annual Statistics 1995", Oslo, Norway 1996

Luftfartsverket, "Civil Aviation Administration Annual Statistics 1996", Oslo, Norway 1997
Mattingly, J.D., Heiser, W.H., Daley, D.H.: "Aircraft Engine Design", AIAA Education Series, 1987

Mattingly, J.D.: "Elements of Gas Turbine Propulsion", McGraw-Hill, Inc., 1996

Meher-Homji, C.B.: "Gas Turbine Axial Compressor Fouling – a Unified Treatment of its Effects, Detection and Control", Proceedings of International Symposium on Gas turbines in Cogeneration, Repowering, and Peak-load Power Generation, New Orleans, LA, 1990, Volume: 5, pp. 179-190

Menon, S. et al.: "A New Unsteady Mixing Model to Predict NO_X Production During Rapid Mixing in a Dual-Stage Combustor", 30th Aerospace Sciences Meeting & Exhibit, 1992

Myers, L.P., Connors T.R.: "Flight Evaluation of an Extended Engine Life Mode on an F-15 Airplane", NASA-TM-104240, NASA-Dryden, 1992

Nelkin, D.: "Selling Science. How the Press Covers Science and Technology", W.H. Freeman and Company, 1994

Nüβer, H.-G, Schmitt, A., 1989.: "The Global Distribution of Air Traffic at High Altitudes, Related Fuel Consumptions and Trends", Proceedings of a DLR International Colloquium, Editor Schumann, U., Bonn, Germany, November 15/16, 1990, Springer-Verlag, pp. 1- 11

Pohl, H.W. et al.: "Hydrogen and other Alternative Fuels for Air and Ground Transportation", John Wiley & Sons, 1995

Price, T., Probert, D.: "Environmental Impacts of Air Traffic", Applied Energy, London, Volume 50, No. 2, 1995 pp. 133-162

Peterson R.C.: "Design Features for Performance Retention in the CFM56 Engine", Turbomachinery Performance Deterioration; Proceedings of the Fourth Joint Fluid Mechanics, Plasma dynamics, and Laser Conference, Atlanta , GA, May 1986, pp. 33-39

R-MC Power Recovery Ltd.: "Assessing the Latest Development in On- and Off-line Compressor Cleaning for Improved Operation Efficiency", Presented at Regent's Park Hilton, London, July 1998, Internet: http://www.r-mc.com/Tech%20paper.htm

Roskam, J.: "Airplane design", Roskam Aviation and Engineering Corporation, USA, 1989

Roskam, J., Lan, Ch.-T.E.: "Airplane Aerodynamics and Performance", DARcorporation, USA, 1997

Røkke, N.A.: "Experimental and Theoretical Studies of Environmental Aspects of Natural Gas Combustion", Doctoral Thesis, The Norwegian Institute of Technology, Division of Thermal Energy and Hydropower, 1994

Saravanamuttoo, I.H., Lakshminarasimha, A.N.: "A Preliminary Assessment of Compressor Fouling", ASME paper 85-GT-153, Turbomachinery International, September 1985, pp. 15-18

Seddigh, F., Saravanamuttoo, H.I.H.: "A Proposed Method for Assessing the Susceptibility of Axial Compressors to Fouling", ASME, Journal of Engineering for Gas Turbines and Power, Volume 113, 1991, pp. 595-601

Stalder, J.-P.: "Gas Turbine Compressor Washing, State of the Art – Field Experiences", ASME paper 98-GT-420, the International Gas Turbine & Aeroengine Congress & Exposition, Stockholm, Sweden, June 1998

Stewart, J.F.: "Integrated Flight Propulsion Control Research Results Using the NASA F-15 HIDEC Flight Research Facility", NASA-TM-4394, NASA-Dryden, 1992

Stinton, D.: "The Anatomy of the Aeroplane", Blachwell Science Ltd., 1998

Stordal, F., Pedersen, U.: "Regional and Global Air Pollution from Aircraft", Norwegian Institute for Air Research, NILU OR: 32/92, Lillestrøm, Norway, 1992

Tabakoff, W., Hamed, A.: "Jet Engine Performance Deterioration", Fluid Mechanics 3rd International Congress Papers, 1990, Volume 2, pp. 603-616

Tarabin, A.P., Schurovsky, V.A., Bodrov, A.I., Stakder, J.-P.: "An Analysis of Axial Compressor Fouling and Blade Cleaning Method", ASME, Journal of Turbomachinery, Volume 120, 1998, pp. 256-261

Thames, J.M, Stegmaier, J.W. Ford, J.J. Jr.: "On-line Compressor Washing, Practices and Benefits", ASME paper 89-GT-91, the Gas Turbine and Aeroengine Congress and Exposition, Toronto, Canada, June 1989

"The Turbomatch Scheme for Aero/Industrial Gas Turbine Engine Design Point/Off Design Performance calculation", Cranfield University, England

Torenbeek, E.: "Synthesis of Subsonic Airplane Design", Delft University Press and Kluwer Academic Publishers, 1982

Ul Hag, I., Saravanamuttoo, H.I.H.: "Axial Compressor Fouling Evaluation at High Speed Settings using an Aerothermodynamic Model", ASME paper 93-GT-407, the International Gas Turbine & Aeroengine Congress & Exposition, Cincinnati, Ohio, May 1993

Urban L.A.: "Gas Turbine Engine Parameter Interrelationships", Hamilton Standard Division of United Aircraft Corporation, 1969

Wallentinsen, Å.R.: "Utvikling av matematisk modell for beregning av gassturbinparametere under forskjellige driftsforhold", Master thesis, The Norwegian Institute of Technology, Dept. of Thermal Energy and Hydropower, 1980

Walsh, P.P., Fletcher, P.: "Gas Turbine Performance", Blackwell Science Ltd., 1998

Zaita, A.V., Buley, G., Karlson, G.: "Performance Deterioration Modeling in Aircraft Gas Turbine Engines", ASME, Journal of Engineering for Gas Turbines and Power, Volume 120, 1998, pp. 344-349

Zaralis, N., Joos F., Glaeser B., Ripplinger T.: "NO_X Reduction by Rich-Lean Combustion", AIAA, 28th Joint Propulsion Conference and Exhibit, 1992

Background Literature with No Specific Reference in the Text:

Anderson, J.D. Jr.: "Introduction to flight", McGraw-Hill, 2000

Brasseur, G.P. et al.: "European Scientific Assessment of the Atmospheric Effects of Aircraft Emissions", Atmospheric Environment Volume 32, No. 13, 1998, pp. 2329-2418

Cerri, G., Salvini, G., Procacci, F., Rispoll, F.: "Fouling and Air Bleed Extracted Flow Influence on Compressor Performance", ASME paper 93-GT-366, the International Gas Turbine & Aeroengine Congress & Exposition, Cincinnati, Ohio, May 1993

International Standards and Recommended Practices, "Environmental Protection, Volume II, Aircraft Engine Emissions", ICAO 1993

Latour, B.: "Science in Action", Harvard University Press, 1987

Lee, S.H. et al.: "Implications of NO_y Emissions from Subsonic Aircraft at Cruise Altitude", Proc. Instn. Mech Engrs., Volume 211, Part G, IMechE 1997, pp. 157-168

Spicer, C.W., Holdren, M.W., Riggin, R.M., Lyon, T.F.: "Chemical Composition and Photochemical Reactivity of Exhaust from Aircraft Turbine Engines", Ann. Geophysicae 12, 1994, pp. 944-955

Tabakoff, W., Lakshminarasimha, A.N., Pasin, M.: "Simulation of Compressor Performance Deterioration Due to Erosion", ASME paper 89-GT-182, 34th International Gas Turbine & Aeroengine Congress & Exhibition, Toronto, Canada, June 1989

LIST OF APPENDICES

APPENDIX A

ICAO – List of Contracting States

The International Civil Aviation Organization, ICAO, is since October 1947 a specialized agency of the United Nations linked to Economic and Social Council (ECOSOC).

185 Contracting States, the "ICAO members"
(http://www.icao.int/cgi/goto.pl?icao/en/about.htm, June 2000)

Islamic State of Afghanistan, Albania, Algeria,Angola, Antigua and Barbuda, Argentina, Armenia, Australia, Austria, Azerbaijan, The Bahamas, Bahrain, Bangladesh, Barbados, Belarus, Belgium, Belize, Benin, Bhutan, Bolivia, Bosnia and Herzegovina, Botswana, Brazil, Brunei Darussalam, Bulgaria, Burkina Faso, Burundi, Cambodia, Cameroon, Canada, Cape Verde, Central African Republic, Chad, Chile, China, Colombia, Comoros, Democratic Republic of the Congo, Republic of the Congo, Cook Islands, Costa Rica, Côte d'Ivoire, Croatia, Cuba, Cyprus, Czech Republic, Denmark, Djibouti, Dominican Republic, Ecuador, Egypt, El Salvador, Equatorial Guinea, Eritrea, Estonia, Ethiopia, Fiji, Finland, France, Gabon, The Gambia, Georgia, Germany, Ghana, Greece, Grenada, Guatemala, Guinea, Guinea-Bissau, Guyana, Haiti, Honduras, Hungary, Iceland, India, Indonesia, Islamic Republic of Iran, Iraq, Ireland, Israel, Italy, Jamaica, Japan, Jordan, Kazakhstan, Kenya, Kiribati, Democratic People's Republic of Korea, Republic of Korea, Kuwait, Kyrgyz Republic, Lao People's Democratic Republic, Latvia, Lebanon, Lesotho, Liberia, Libya, Lithuania, Luxembourg, former Yugoslav Republic of Macedonia, Madagascar, Malawi, Malaysia, Maldives, Mali, Malta, Marshall Islands, Mauritania, Mauritius, Mexico, Federated States of Micronesia, Moldova, Monaco, Mongolia, Morocco, Mozambique, Myanmar, Namibia, Nauru, Nepal, Netherlands, New Zealand, Nicaragua, Niger, Nigeria, Norway, Oman, Pakistan, Palau, Panama, Papua New Guinea, Paraguay, Peru, Philippines, Poland, Portugal, Qatar, Romania, Russian Federation, Rwanda, St. Lucia, St. Vincent and the Grenadines, Samoa, San Marino, São Tomé and Príncipe, Saudi Arabia, Senegal, Seychelles, Sierra Leone, Singapore, Slovak Republic, Slovenia, Solomon Islands, Somalia, South Africa, Spain, Sri Lanka, Sudan, Suriname, Swaziland, Sweden, Switzerland, Syrian Arab Republic, Tajikistan, Tanzania, Thailand, Togo, Tonga, Trinidad and Tobago, Tunisia, Turkey, Turkmenistan, Uganda, Ukraine, United Arab Emirates, United Kingdom, United States, Uruguay, Uzbekistan, Vanuatu, Venezuela, Vietnam, Republic of Yemen, Zambia, Zimbabwe

APPENDIX B

Supplementary Graphs from Modeling and Analyses

The Turbomatch-based Model

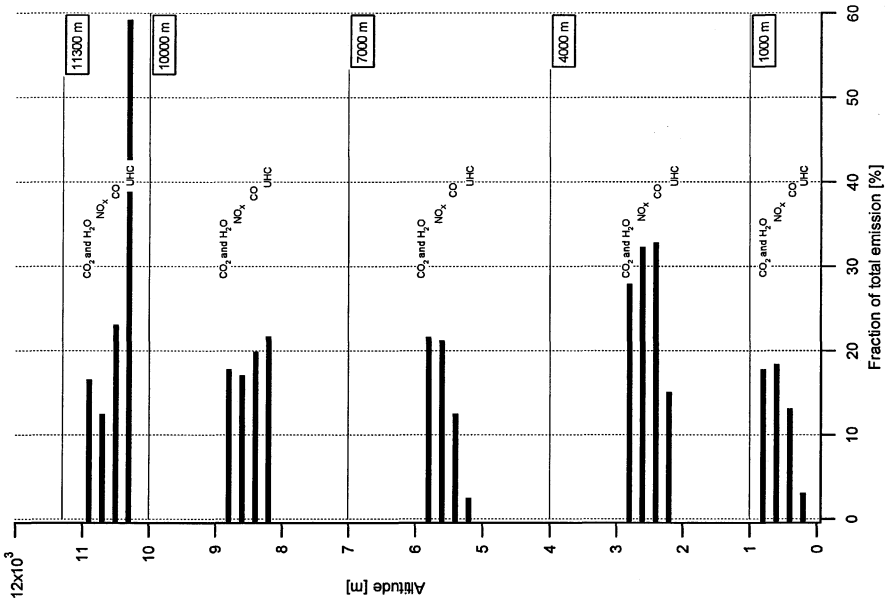

Figure B1 Fraction (%) of total emissions released into altitude domains, Boeing 737-400 flight Oslo-Trondheim

Total quantities:

CO_2: 6 196 kg H_2O: 2 300 kg
NO_X: 24.6 kg CO: 17.8 kg
UHC: 6.9 kg

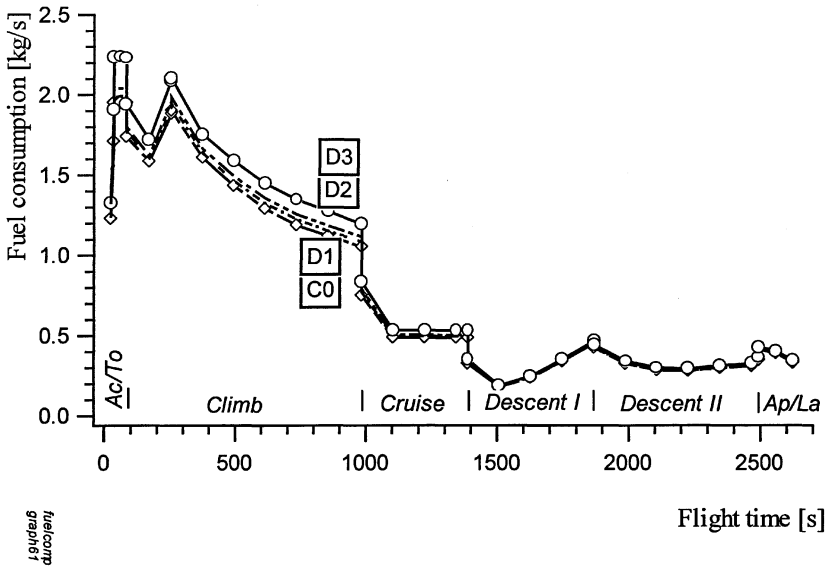

Figure B2 Time specific fuel consumption throughout the complete flight cycle. Clean (C0) and unclean (D1, D2, D3) engines; Turbomatch Model

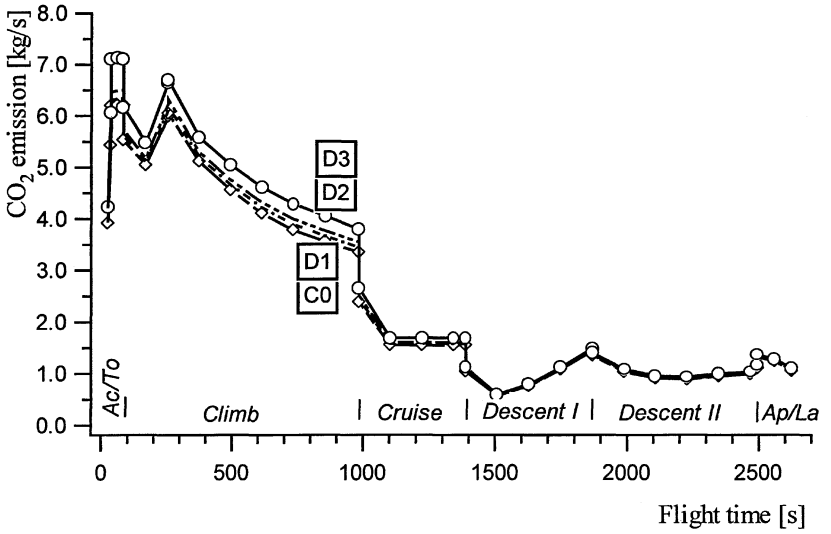

Figure B3 CO_2 emission per second throughout the complete flight cycle. Clean (C0) and unclean (D1, D2, D3) engines; Turbomatch Model

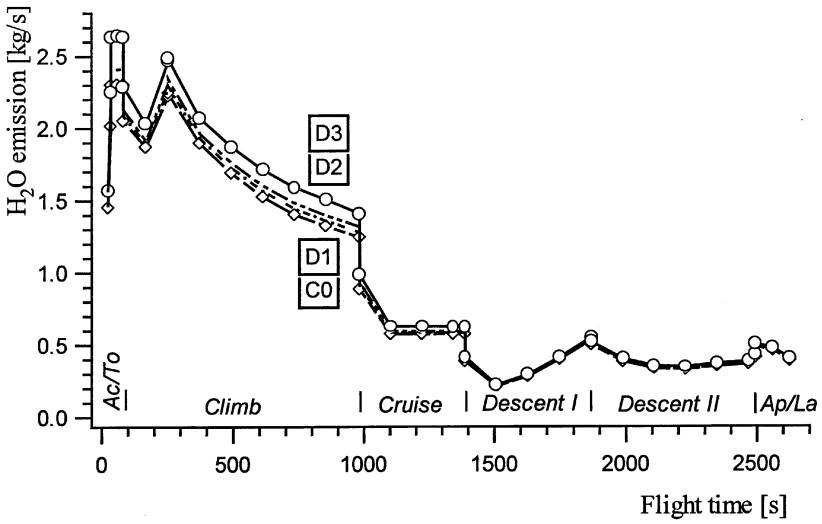

Figure B4 H_2O emission per second throughout the complete flight cycle. Clean (C0) and unclean (D1, D2, D3) engines; Turbomatch Model

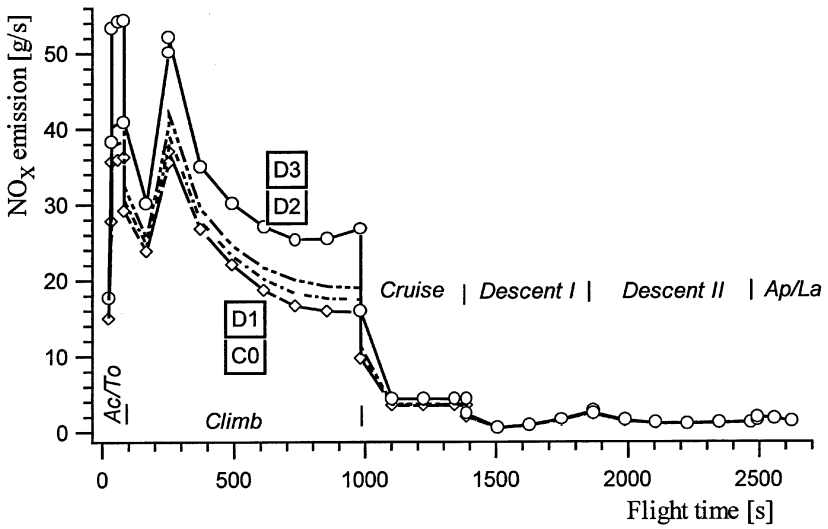

Figure B5 NO_X emission per second throughout the complete flight cycle. Clean (C0) and unclean (D1, D2, D3) engines; Turbomatch Model

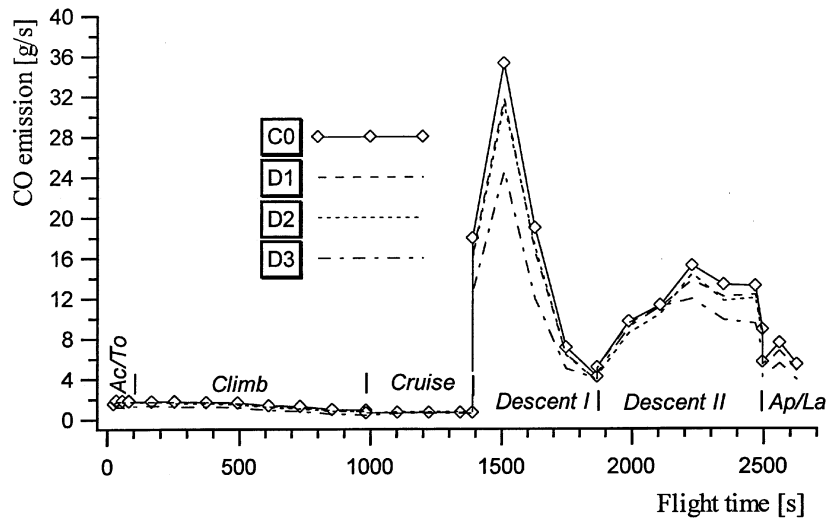

Figure B6 CO emission per second throughout the complete flight cycle. Clean (C0) and unclean (D1, D2, D3) engines; Turbomatch Model

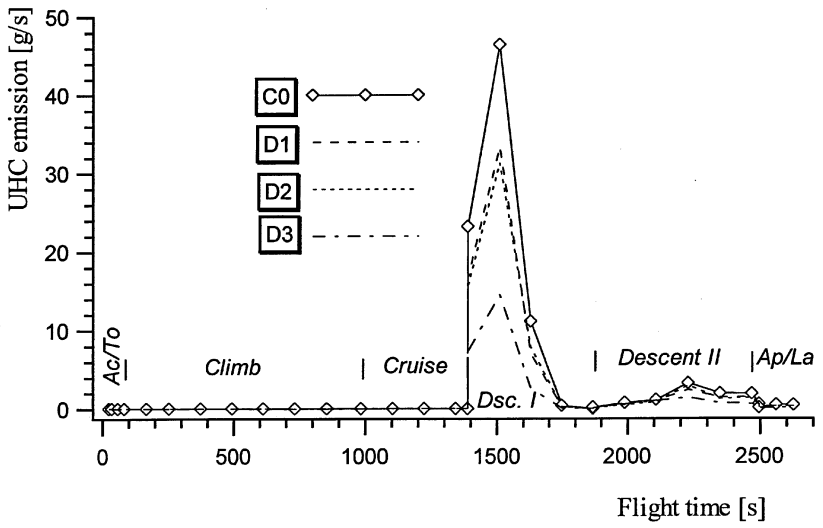

Figure B7 UHC emission per second throughout the complete flight cycle. Clean (C0) and unclean (D1, D2, D3) engines; Turbomatch Model

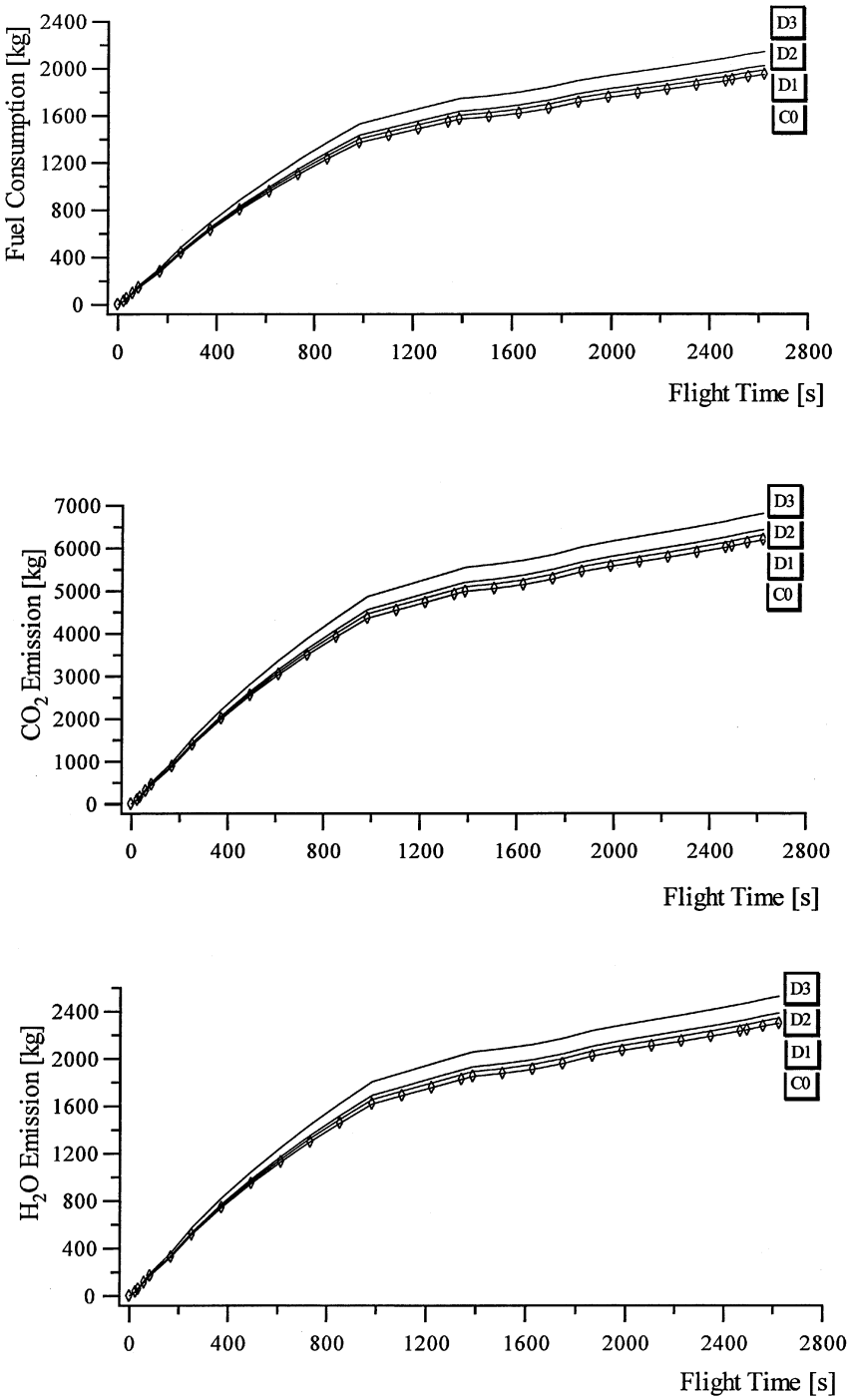

Figure B8 Accumulated fuel consumption (top) and emissions of CO_2 (middle) and H_2O (lower) during the flight.
Clean (C0) and unclean (D1, D2, D3) engines; Turbomatch Model

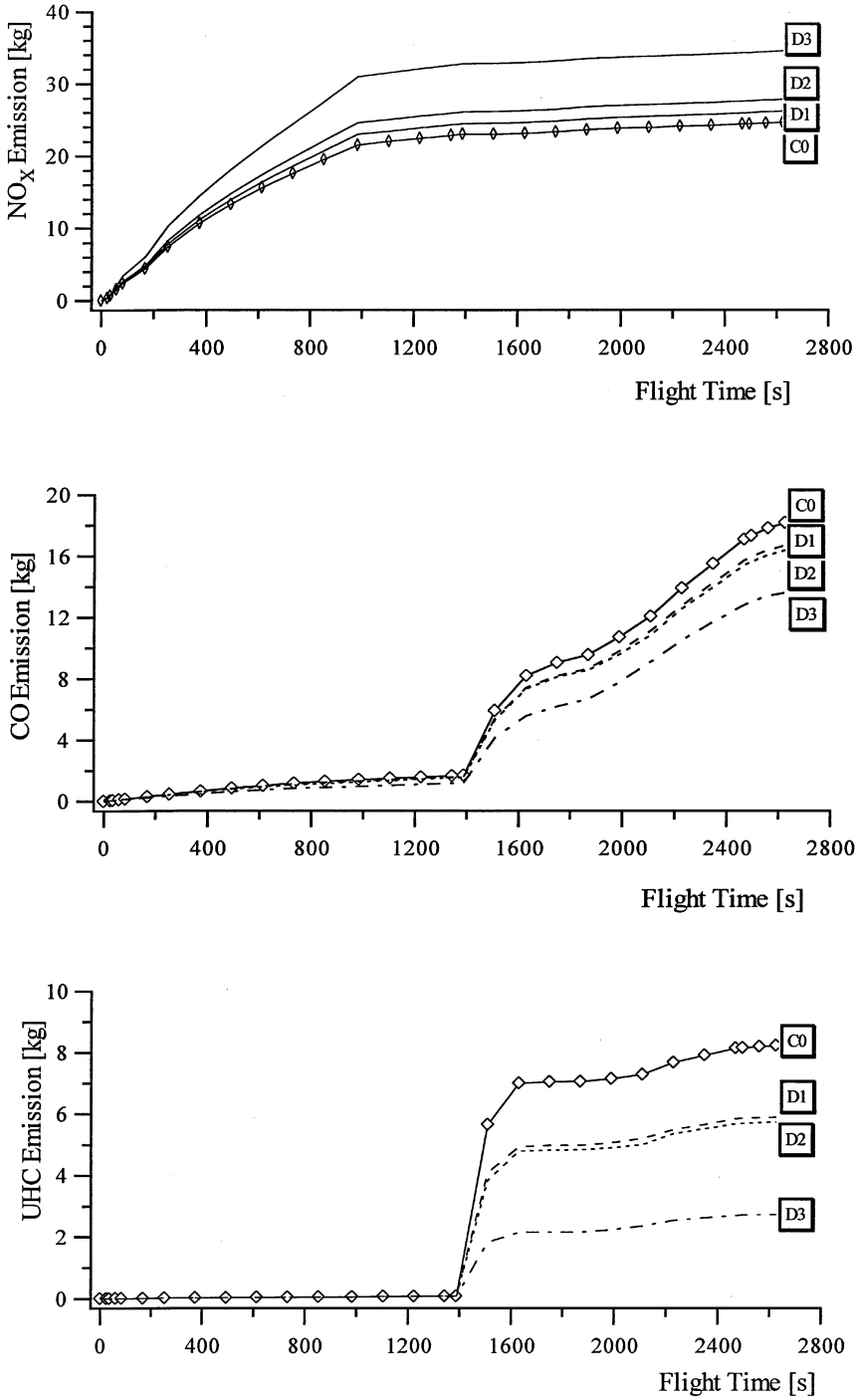

Figure B9 Accumulated emissions of NO_X (top) CO (middle) and UHC (lower) during the flight.
Clean (C0) and unclean (D1, D2, D3) engines; Turbomatch Model

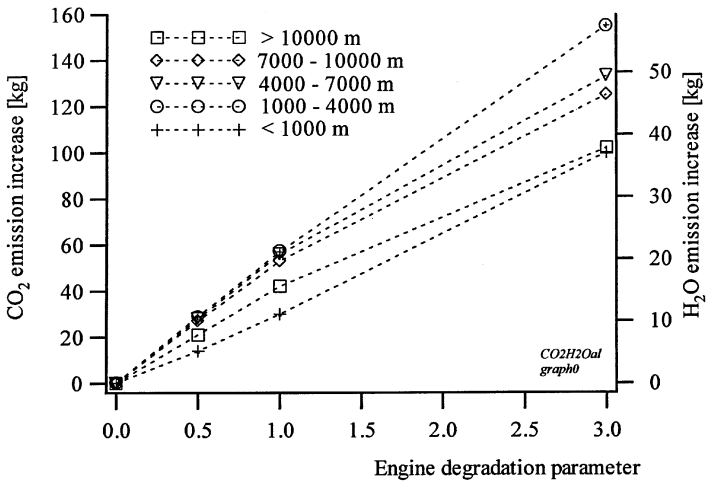

Figure B10 CO_2 and H_2O emission increase with engine degradation at all domains of flight altitude.
Total emissions, clean engines: CO_2: 6 200 kg and H_2O: 2 300 kg

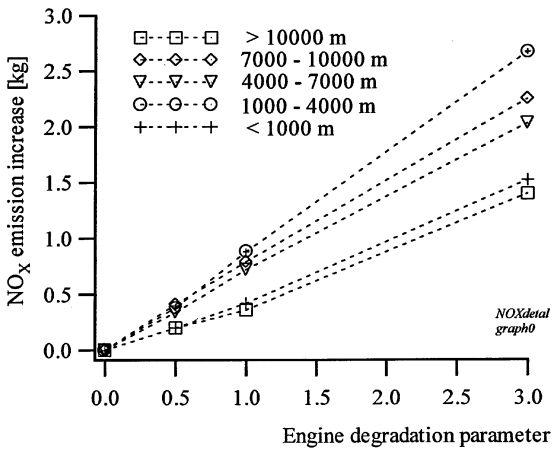

Figure B11 NO_X emission increase with engine degradation at all domains of flight altitude.
Total NO_X emissions, clean engines: 24.6 kg

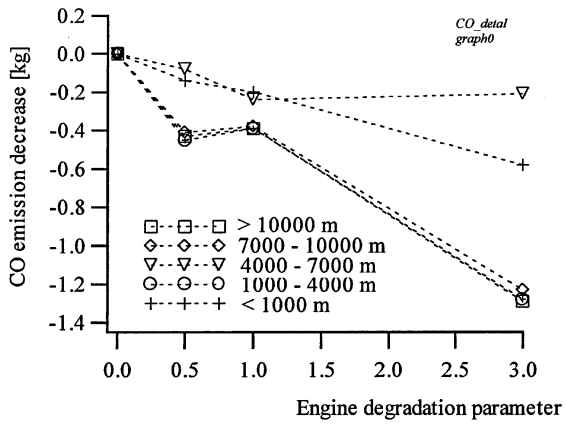

Figure B12 CO emission decrease with engine degradation at all domains of flight altitude.
Total CO emissions, clean engines: 17.8 kg

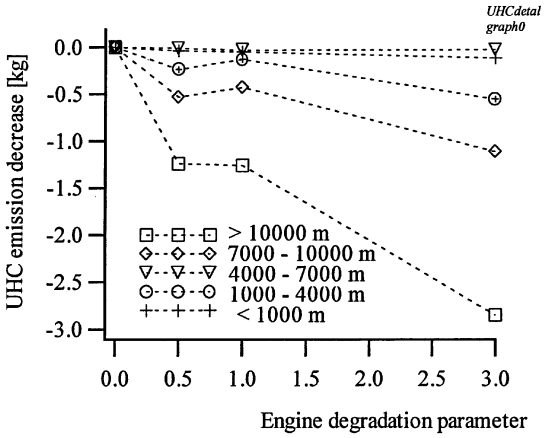

Figure B13 UHC emission decrease with engine degradation at all domains of flight altitude.
Total UHC emissions, clean engines: 6.9 kg

APPENDIX C

Supplementary Graphs from Modeling and Analyses

The Turbomatch *and Parametric* Models

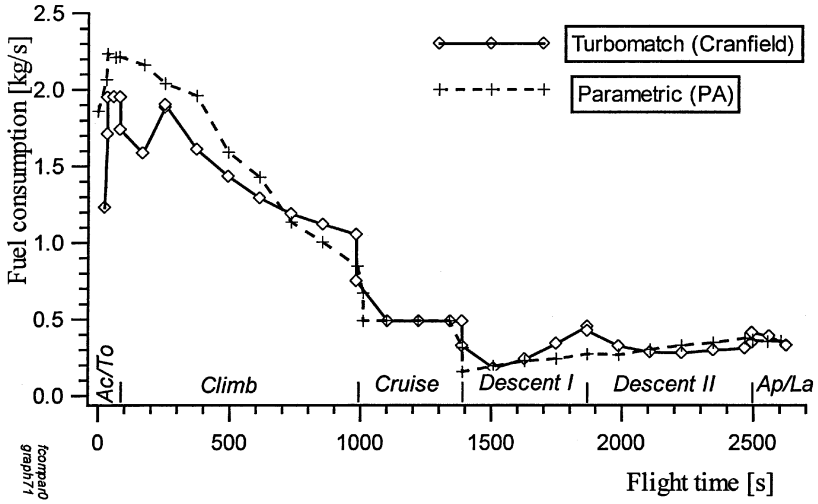

Figure C1 **Calculated time specific fuel consumption throughout the flight, the two models compared.**
Clean engines

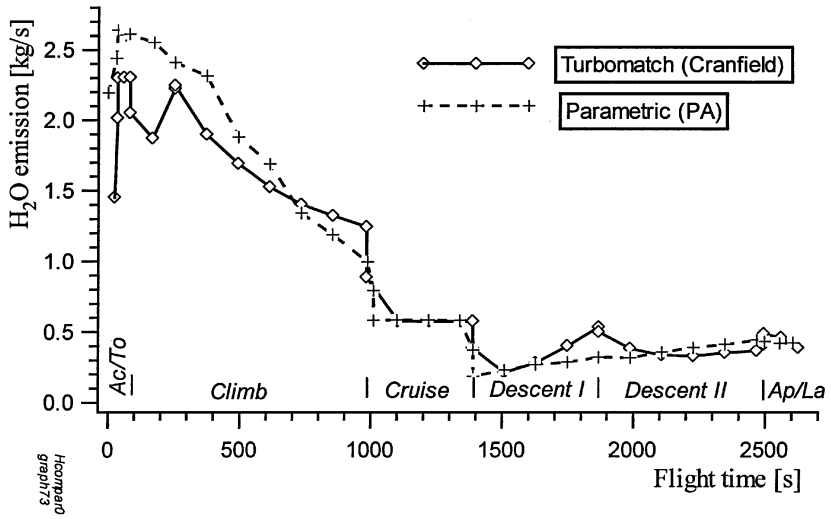

Figure C2 **Calculated H_2O emissions per second throughout the flight, the two models compared.**
Clean engines

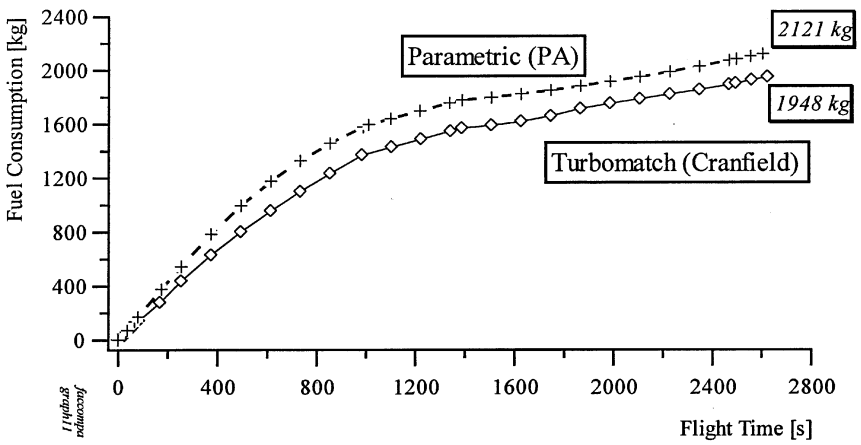

Figure C3 **Accumulated fuel consumption during the flight, calculated figures from the two models compared; Clean engines**

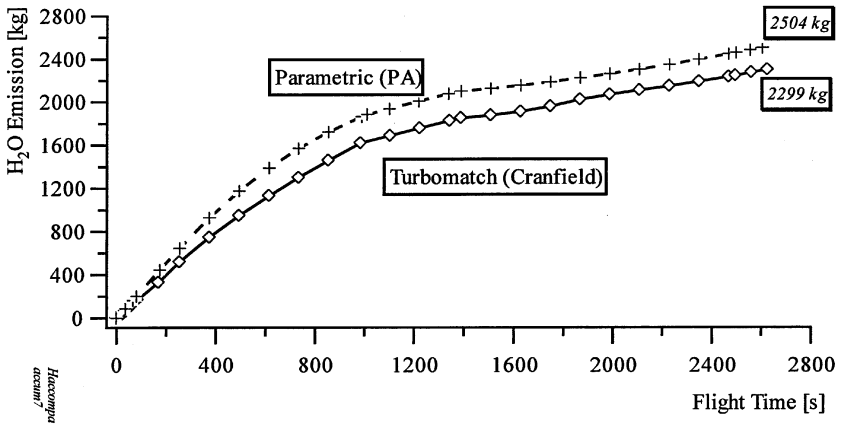

Figure C4 **Accumulated emissions of H_2O during the flight, calculated figures from the two models compared; Clean engines**

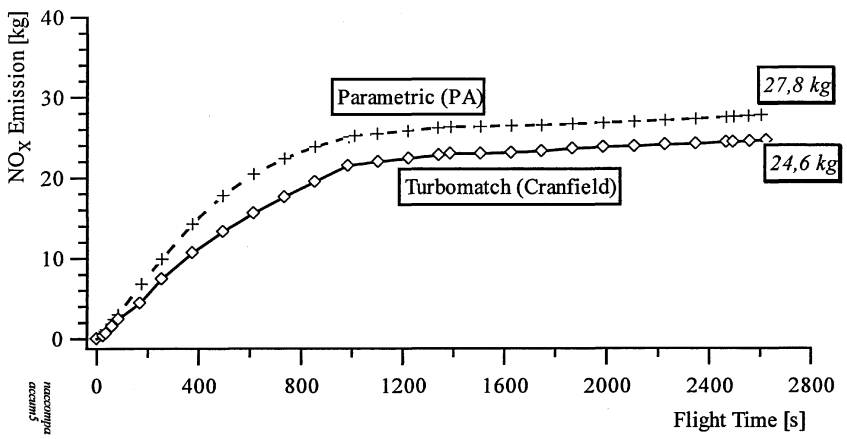

Figure C5 **Accumulated emissions of NO_X during the flight, calculated figures from the two models compared; Clean engines**

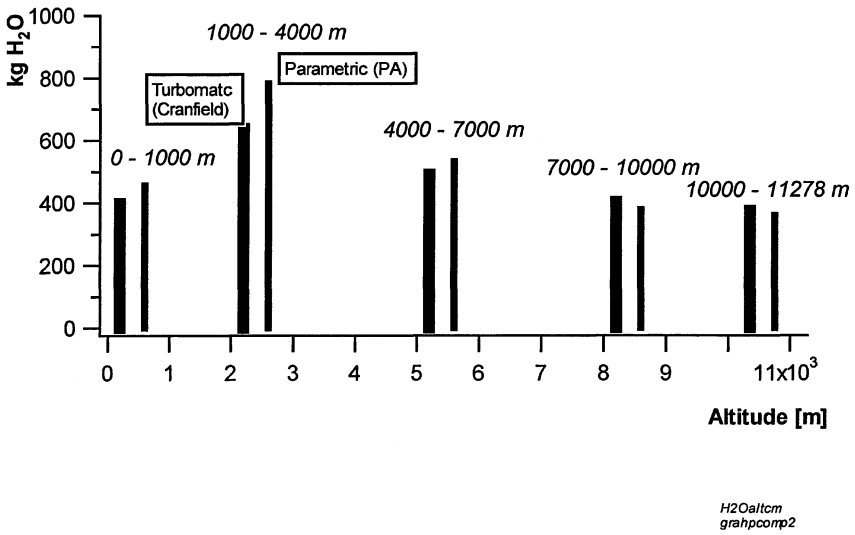

Figure C6 **Emissions of H_2O in altitude regimes of the Oslo – Trondheim flight, calculated figures from the two models compared; Clean engines**

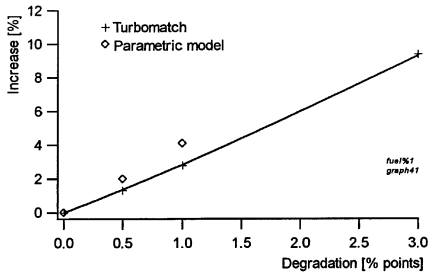

Percentage increase of fuel consumption, CO_2 and H_2O emissions as a function of engine cold section degradation. Altitude below 1000 m.

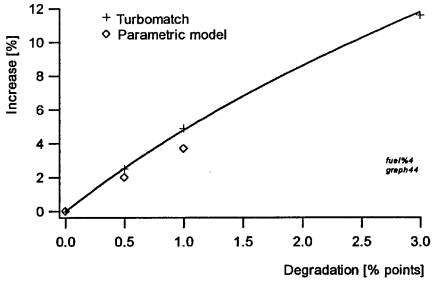

Percentage increase of fuel consumption, CO_2 and H_2O emissions as function of engine cold section degradation. Altitude 7000 m - 10000 m.

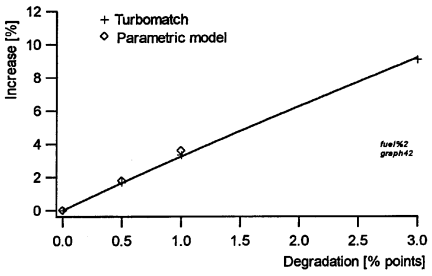

Percentage increase of fuel consumption, CO_2 and H_2O emissions as a function of engine cold section degradation. Altitude 1000 m - 4000 m.

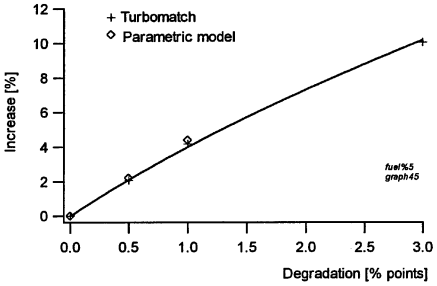

Percentage increase of fuel consumption, CO_2 and H_2O emissions as function of engine cold section degradation. Altitude 10000 m - 11278 m.

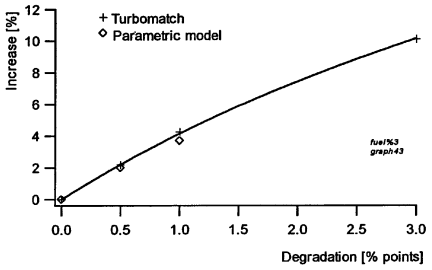

Percentage increase of fuel consumption, CO_2 and H_2O emissions as function of engine cold section degradation. Altitude 4000 m - 7000 m.

Figure C7 Increase of fuel consumption and emissions of CO_2 and H_2O with engine cold end degradation. Separate altitude regimes; calculated figures from the two models compared

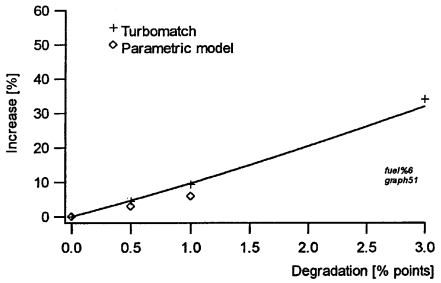

Percentage increase of NO_X emissions as function of engine cold section degradation. Altitude below 1000 m.

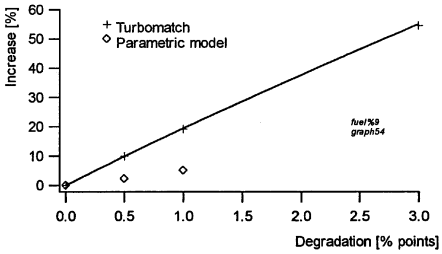

Percentage increase of NO_X emissions as function of engine cold section degradation. Altitude 7000 m - 10000 m.

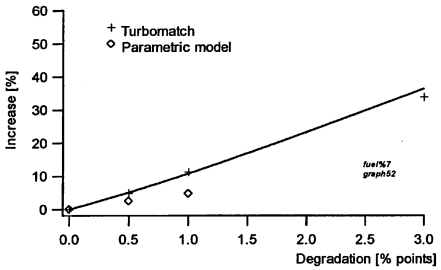

Percentage increase of NO_X emissions as function of engine cold section degradation. Altitude 1000 m - 4000 m.

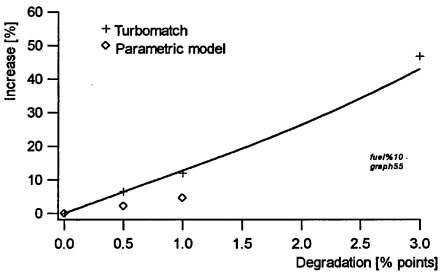

Percentage increase of NO_X emissions as function of engine cold section degradation. Altitude 10000 m - 11278 m.

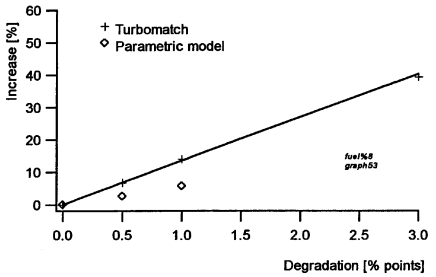

Percentage increase of NO_X emissions as function of engine cold section degradation. Altitude 4000 m - 7000 m.

Figure C8 **Increase of emissions of NO_X with engine cold end degradation. Separate altitude regimes; calculated figures from the two models compared**

APPENDIX D

Output from Calculations to Calibrate Performance Condition

Parametric Model

PERFORMACE DATA; SET NO. 1.1

* * Performance Conditions, Input:
T_0 [K]: **303.15** ; p_0 [Pa]: **0.1013E+06**; T_{t4} [K]: **1614.00**; M_0: **0.000**

* * Gas and Fuel Properties, Input:
c_{pC} [J·kg^{-1}·K^{-1}]:**1040.0** ; c_{pT} [J·kg^{-1}·K^{-1}]:**1172.00** ; γ_C: **1.40** ; γ_T: **1.33**

Fuel heating value [J/kg]: **$0.4280 \cdot 10^8$**

* *) *Performance parameters and reference parameters where they apply*:

PARAMETER	PERFORMANCE	REFERENCE
Ambient speed [m/s]	**0.0000**	**0.0000**
Ambient speed of sound [m/s]	355.1	
τ_r	1.0000	1.0000
τ_F	1.1858	1.1877
τ_{CH}	2.3400	2.3426
τ_{TH}	**0.7290**	**0.7290**
τ_{TL}	**0.7486**	**0.7480**
τ_λ	5.9998	6.0222
π_D	0.9990	0.9990
π_F	**1.6703**	**1.6790**
π_{CH}	**15.1778**	**15.2353**
π_B	0.9675	0.9675
π_{TH}	**0.2282**	**0.2282**
π_{TL}	**0.2529**	**0.2520**
Nozzle exit Mach-n., core, M_9	0.7355	0.7414
Nozzle exit Mach-n., byp., M_{19}	0.9061	0.8923
Nozz.ex. stgn.press. ,core [Pa]	142,975.9	143,774.0
Nozz.ex. stgn.press. ,byp. [Pa]	169,028.8	169,954.5
Air mass flow rate (total)[kg/s]	305.10	305.99
Specific thrust [N·kg^{-1}·s^{-1}]	341.5757	340.6316
Bypass ratio	**5.0269**	**5.0000**
Temp. relation core; T_9/T_0	2.6673	
Temp. relation bypass; T_{19}/T_0	1.0244	
Speed relation core; V_9/a_0	1.1582	
Speed relation bypass; V_{19}/a_0	0.9171	
RPM-LP-spool, rel. ref. condition	0.9946	
RPM-HP-spool, rel. ref. Condition	0.0000	
Thrust sp. fuel cons.[mg·N^{-1}·s^{-1}]	12.0864	
Fuel flow (one engine) [kg/s]	1.2596	
Thrust (one engine) [N]	**104,216.0**	

Table D1 Maximum take-off condition, static sea level, 30 °C. Testing of correlation with reference, and similar performance conditions
ΔT_{t4} = -25.0 K; $\Delta \dot{m}_a$ = -5.0 %

% %

P E R F O R M A C E   D A T A ;   SET NO. 1.1

* * Performance Conditions, Input:

T0 [K]: 303.15   ; p0 [Pa]: 0.1013E+06 ; Tt4 [K]: 1640.00 ; M0: 0.000

* * Gas and Fuel Properties, Input:

cpC [$J \cdot kg^{-1} \cdot K^{-1}$]: 1040.0 ; cpT [$J \cdot kg^{-1} \cdot K^{-1}$]:1172.00 ; gamC: 1.40 ; gamT: 1.33

Fuel heating value [J/kg]:   0.4280E+08

* * Performance paramerters, and reference parameters where they apply:

PARAMETER	PERFORMACE	REF.
Ambient speed [m/s]	0.0000	
Ambient speed of sound [m/s]	355.1	
tauR	1.0000	1.0000
tauF	1.1873	1.1877
tauCH	2.3431	2.3426
tauTH	0.7290	0.7290
tauTL	0.7480	0.7480
tau-LAMBDA	6.0965	6.0965
piD	0.9990	0.9990
piF	1.6773	1.6790
piCH	15.2447	15.2353
piB	0.9675	0.9675
piTH	0.2282	0.2282
piTL	0.2520	0.2520
Nozzle exit Mach-n., core, M9	0.7412	0.7414
Nozzle exit Mach-n., byp., M19	0.9100	0.8923
Nozz.ex. stgn.press. ,core [Pa]	143711.4	143774.0
Nozz.ex. stgn.press. ,byp. [Pa]	169742.4	169954.5
Air mass flow rate (total)[kg/s]	322.65	322.10
Specific thrust [N/(kg/s)]	343.8886	323.6000
Bypass ratio	5.0140	5.0000
Temp. relation core; T9/T0	2.7049	
Temp. relation bypass; T19/T0	1.0245	
Speed relation core; V9/a0	1.1754	
Speed relation bypass; V9/a0	0.9211	
RPM-LP-spool, rel. ref. condition	0.9990	
RPM-HP-spool, rel. ref. condition	0.0000	
Thrust sp. fuel cons.[(mg/s)/N]	12.3741	
Fuelflow ONE eng. [kg/s]	1.3730	
Thrust [N]	110955.5	

Table D2 Maximum take-off condition, static sea level, 30 °C. Testing of correlation with reference, and similar performance conditions

ΔT_{t4} = 0.0 K; $\Delta \dot{m}_a$ = 0.0 %

% %

P E R F O R M A C E   D A T A ;   SET NO. 1.1

* * Performance Conditions, Input:

T0 [K]: 303.15 ; p0 [Pa]: 0.1013E+06 ; Tt4 [K]: 1626.00 ; M0: 0.000

* * Gas and Fuel Properties, Input:

cpC [$J \cdot kg^{-1} \cdot K^{-1}$]: 1040.0 ; cpT [$J \cdot kg^{-1} \cdot K^{-1}$]:1172.00 ; gamC: 1.40 ; gamT: 1.33

Fuel heating value [J/kg]: 0.4280E+08

* * Performance paramerters, and reference parameters where they apply:

PARAMETER	PERFORMACE	REF.
Ambient speed [m/s]	0.0000	
Ambient speed of sound [m/s]	355.1	
tauR	1.0000	1.0000
tauF	1.1875	1.1877
tauCH	2.3436	2.3426
tauTH	0.7290	0.7290
tauTL	0.7480	0.7480
tau-LAMBDA	6.0445	6.0407
piD	0.9990	0.9990
piF	1.6784	1.6790
piCH	15.2564	15.2353
piB	0.9675	0.9675
piTH	0.2282	0.2282
piTL	0.2519	0.2520
Nozzle exit Mach-n., core, M9	0.7421	0.7414
Nozzle exit Mach-n., byp., M19	0.9106	0.8923
Nozz.ex. stgn.press. ,core [Pa]	143831.8	143774.0
Nozz.ex. stgn.press. ,byp. [Pa]	169852.3	169954.5
Air mass flow rate (total)[kg/s]	322.88	322.10
Specific thrust [N/(kg/s)]	343.8243	323.6000
Bypass ratio	5.0117	5.0000
Temp. relation core; T9/T0	2.6809	
Temp. relation bypass; T19/T0	1.0245	
Speed relation core; V9/a0	1.1717	
Speed relation bypass; V9/a0	0.9217	
RPM-LP-spool, rel. ref. condition	0.9996	
RPM-HP-spool, rel. ref. condition	0.0000	
Thrust sp. fuel cons.[(mg/s)/N]	12.1773	
Fuelflow ONE eng. [kg/s]	1.3519	
Thrust [N]	111014.5	

Table D3 Maximum take-off condition, static sea level, 30 °C. Testing of correlation with reference, and similar performance conditions

ΔT_{t4} = -15.0 K; $\Delta \dot{m}_a$ = 0.0 %

```
% % % % % % % % % % % % % % % % % % % % % % % % % % % % % % % % % % % % %

 P E R F O R M A C E   D A T A ;  SET NO. 1.1
                                          ===

 *  Performance  Conditions, Input:

T0 [K]:  303.15     ;  p0 [Pa]: 0.1013E+06 ;  Tt4 [K]: 1602.00 ;  M0:
0.000

 * *  Gas  and  Fuel  Properties,  Input:

  cpC [J·kg^-1·K^-1]: 1040.0 ;  cpT [J·kg^-1·K^-1]:1172.00 ;  gamC: 1.40       ;
gamT: 1.33

  Fuel heating value [J/kg]:     0.4280E+08

 * *  Performance paramerters, and reference parameters where they apply:
```

PARAMETER	PERFORMACE	REF.
Ambient speed [m/s]	0.0000	
Ambient speed of sound [m/s]	355.1	
tauR	1.0000	1.0000
tauF	1.1878	1.1877
tauCH	2.3443	2.3426
tauTH	0.7290	0.7290
tauTL	0.7479	0.7480
tau-LAMBDA	5.9552	5.9478
piD	0.9990	0.9990
piF	1.6790	1.6790
piCH	15.2712	15.2353
piB	0.9675	0.9675
piTH	0.2282	0.2282
piTL	0.2518	0.2520
Nozzle exit Mach-n., core, M9	0.7429	0.7414
Nozzle exit Mach-n., byp., M19	0.9110	0.8923
Nozz.ex. stgn.press. ,core [Pa]	143936.4	143774.0
Nozz.ex. stgn.press. ,byp. [Pa]	169914.4	169954.5
Air mass flow rate (total)[kg/s]	323.03	322.10
Specific thrust [N/(kg/s)]	343.4487	323.6000
Bypass ratio	5.0084	5.0000
Temp. relation core; T9/T0	2.6406	
Temp. relation bypass; T19/T0	1.0247	
Speed relation core; V9/a0	1.1641	
Speed relation bypass; V9/a0	0.9221	
RPM-LP-spool, rel. ref. condition	1.0000	
RPM-HP-spool, rel. ref. condition	0.0000	
Thrust sp. fuel cons.[(mg/s)/N]	11.8496	
Fuelflow ONE eng. [kg/s]	1.3147	
Thrust [N]	110945.5	

Table D4 Maximum take-off condition, static sea level, 30 °C. Testing of correlation with reference, and similar performance conditions

ΔT_{t4} **= -40.0 K;** $\Delta \dot{m}_a$ **= 0.0 %**

% %

P E R F O R M A C E   D A T A ;   SET NO. 1.1

===

* * Performance Conditions, Input:

T0 [K]: 303.15   ; p0 [Pa]: 0.1013E+06 ; Tt4 [K]: 1640.00 ; M0: 0.000

* * Gas and Fuel Properties, Input:

cpC [J·kg^{-1}·K^{-1}]: 1040.0 ; cpT [J·kg^{-1}·K^{-1}]:1172.00 ; gamC: 1.40   ; gamT: 1.33

Fuel heating value [J/kg]:   0.4280E+08

* * Performance paramerters, and reference parameters where they apply:

PARAMETER	PERFORMACE	REF.
Ambient speed [m/s]	0.0000	
Ambient speed of sound [m/s]	355.1	
tauR	1.0000	1.0000
tauF	1.1873	1.1877
tauCH	2.3431	2.3426
tauTH	0.7290	0.7290
tauTL	0.7480	0.7480
tau-LAMBDA	6.0965	6.0965
piD	0.9990	0.9990
piF	1.6773	1.6790
piCH	15.2447	15.2353
piB	0.9675	0.9675
piTH	0.2282	0.2282
piTL	0.2520	0.2520
Nozzle exit Mach-n., core, M9	0.7412	0.7414
Nozzle exit Mach-n., byp., M19	0.9100	0.8923
Nozz.ex. stgn.press. ,core [Pa]	143711.4	143774.0
Nozz.ex. stgn.press. ,byp. [Pa]	169742.4	169954.5
Air mass flow rate (total)[kg/s]	306.52	305.99
Specific thrust [N/(kg/s)]	343.8886	340.6316
Bypass ratio	5.0140	5.0000
Temp. relation core; T9/T0	2.7049	
Temp. relation bypass; T19/T0	1.0245	
Speed relation core; V9/a0	1.1754	
Speed relation bypass; V9/a0	0.9211	
RPM-LP-spool, rel. ref. condition	0.9990	
RPM-HP-spool, rel. ref. condition	0.0000	
Thrust sp. fuel cons.[(mg/s)/N]	12.3741	
Fuelflow ONE eng. [kg/s]	1.3043	
Thrust [N]	105407.7	

Table D5 Maximum take-off condition, static sea level, 30 °C. Testing of correlation with reference, and similar performance conditions

ΔT_{t4} = 0.0 K; $\Delta \dot{m}_a$ = -5.0 %

% %

P E R F O R M A C E   D A T A ;   SET NO. 1.1
===

* * Performance Conditions, Input:

T0 [K]: 303.15   ; p0 [Pa]: 0.1013E+06 ; Tt4 [K]: 1640.00 ; M0: 0.000

* * Gas and Fuel Properties, Input:

cpC [$J \cdot kg^{-1} \cdot K^{-1}$]: 1040.0 ; cpT [$J \cdot kg^{-1} \cdot K^{-1}$]:1172.00 ; gamC: 1.40   ; gamT: 1.33

Fuel heating value [J/kg]:   0.4280E+08

* * Performance paramerters, and reference parameters where they apply:

PARAMETER	PERFORMACE	REF.
Ambient speed [m/s]	0.0000	
Ambient speed of sound [m/s]	355.1	
tauR	1.0000	1.0000
tauF	1.1873	1.1877
tauCH	2.3431	2.3426
tauTH	0.7290	0.7290
tauTL	0.7480	0.7480
tau-LAMBDA	6.0965	6.0965
piD	0.9990	0.9990
piF	1.6773	1.6790
piCH	15.2447	15.2353
piB	0.9675	0.9675
piTH	0.2282	0.2282
piTL	0.2520	0.2520
Nozzle exit Mach-n., core, M9	0.7412	0.7414
Nozzle exit Mach-n., byp., M19	0.9100	0.8923
Nozz.ex. stgn.press. ,core [Pa]	143711.4	143774.0
Nozz.ex. stgn.press. ,byp. [Pa]	169742.4	169954.5
Air mass flow rate (total)[kg/s]	290.38	289.89
Specific thrust [N/(kg/s)]	343.8886	359.5556
Bypass ratio	5.0140	5.0000
Temp. relation core; T9/T0	2.7049	
Temp. relation bypass; T19/T0	1.0245	
Speed relation core; V9/a0	1.1754	
Speed relation bypass; V9/a0	0.9211	
RPM-LP-spool, rel. ref. condition	0.9990	
RPM-HP-spool, rel. ref. condition	0.0000	
Thrust sp. fuel cons.[(mg/s)/N]	12.3741	
Fuelflow ONE eng. [kg/s]	1.2357	
Thrust [N]	99860.0	

Table D6 Maximum take-off condition, static sea level, 30 °C. Testing of correlation with reference, and similar performance conditions

ΔT_{t4} = 0.0 K; $\Delta \dot{m}_a$ = -10.0 %

% %

P E R F O R M A C E   D A T A ; SET NO. 1.1

===

* * Performance Conditions, Input:

T0 [K]: 303.15 ; p0 [Pa]: 0.1013E+06 ; Tt4 [K]: 1630.00 ; M0: 0.000

* * Gas and Fuel Properties, Input:

cpC [J·kg^{-1}·K^{-1}]: 1040.0 ; cpT [J·kg^{-1}·K^{-1}]:1172.00 ; gamC: 1.40 ; gamT: 1.33

Fuel heating value [J/kg]: 0.4280E+08

* * Performance paramerters, and reference parameters where they apply:

PARAMETER	PERFORMACE	REF.
Ambient speed [m/s]	0.0000	
Ambient speed of sound [m/s]	355.1	
tauR	1.0000	1.0000
tauF	1.1873	1.1877
tauCH	2.3431	2.3426
tauTH	0.7290	0.7290
tauTL	0.7480	0.7480
tau-LAMBDA	6.0593	6.0593
piD	0.9990	0.9990
piF	1.6773	1.6790
piCH	15.2447	15.2353
piB	0.9675	0.9675
piTH	0.2282	0.2282
piTL	0.2520	0.2520
Nozzle exit Mach-n., core, M9	0.7412	0.7414
Nozzle exit Mach-n., byp., M19	0.9100	0.8923
Nozz.ex. stgn.press. ,core [Pa]	143711.5	143774.0
Nozz.ex. stgn.press. ,byp. [Pa]	169742.6	169954.5
Air mass flow rate (total)[kg/s]	316.20	315.66
Specific thrust [N/(kg/s)]	343.6512	330.2041
Bypass ratio	5.0140	5.0000
Temp. relation core; T9/T0	2.6884	
Temp. relation bypass; T19/T0	1.0245	
Speed relation core; V9/a0	1.1718	
Speed relation bypass; V9/a0	0.9211	
RPM-LP-spool, rel. ref. condition	0.9990	
RPM-HP-spool, rel. ref. condition	0.0000	
Thrust sp. fuel cons.[(mg/s)/N]	12.2403	
Fuelflow ONE eng. [kg/s]	1.3300	
Thrust [N]	108661.4	

Table D7 Maximum take-off condition, static sea level, 30 °C. Testing of correlation with reference, and similar performance conditions

ΔT_{t4} = -10.0 K; $\Delta \dot{m}_a$ = -2.0 %

APPENDIX E

Sample Outputs from the Mattingly Code, On-Design and Off-design Calculations

Case Engine similar to Pratt & Whitney JT9D

FILE: A:FANRUN11.DAT

ON-DESIGN CALCULATIONS

"New Engine"

TURBOFAN ENGINE WITH TWO EXHAUSTS & CONV. NOZZLES

********** **INPUT DATA** **********

MACH NO = .850	ALPHA = 5.000
ALT (FT) = 35000.	PI C` = 1.600
T0 (R) = 394.10	PI D (MAX) = 1.00
P0 (PSIA) = 3.4680	PI B = .95
DENSITY =.00073824	PI N = 1.00
(SLUG/CUFT)	PI N` = 1.00
EFFICIENCY	
CP C = .238 BTU/LBM-R	BURNER = .99
CP T = .295 BTU/LBM-R	MECH HI PR = .98
GAMMA C = 1.400	MECH LO PR = .99
GAMMA T = 1.300	LP COMPR (FAN) = .89 (EC`)
TT4 MAX = 2370. (R)	HP COMPR = .90 (ECH)
H - FUEL (BTU/LBM) = 18600.	HP TURBINE = .89 (ETH)
CTO LOW = .0100	LP TURBINE = .91 (ETL)
CTO HIGH = .0000	PWR MECH EFF L = .98
COOLING AIR #1 = 5.00 %	PWR MECH EFF H = .98
COOLING AIR #2 = 5.00 %	BLEED AIR = 1.00 %

********** **RESULTS** **********

TAU R = 1.145	A0 = 973.1 FT/SEC
PI R = 1.604	V0 = 827.1 FT/SEC
PI D = .995	MASS FLOW = 200.00 LBM/SEC
TAU L = 7.454	AREA ZERO = 10.180 SQFT
PTO LO= 197.93 KW	AREA ZERO* = 9.974 SQFT
PTO HI= .00 KW	
TAU C`= 1.163	PT5`/P0 = 2.553
ETA C`= .8825	TT5`/T0 = 1.331
PT9`/P9= 1.893	P0/P9` = .745
M9` = 1.000	V9`/V0 = 1.24
PI C = 25.00	TAU M1 = .9702
PI CH = 15.63	TAU M2 = .9805
TAU CH = 2.393	
ETA CH = .8565	
PI TH = .2124	
TAU TH = .7275	
ETA TH = .9067	
PI TL = .2904	
TAU TL = .7713	
ETA TL = .9212	
P0/P9 = .7876	
PT9/P0 = 1.8324	
F = .0226	V9/V0 = 1.90
FO = .0034	M9/M0 = 1.18
F/M = 15.209 LBF/LBM/S	A9/A0 = .1955
S = .7936 1/H	A9`/A0 = .5558
T9/T0 = 2.7912	THRUST = 3042. LBF

FILE: A:FANRUN12.DAT **ON-DESIGN** CALCULATIONS

"OLDER ENGINE"

- ***COMPRESSOR AND TURBINE EFFICIENCY REDUCED***
- ***AIRFLOW CONSTANT, Method A***

TURBOFAN ENGINE WITH TWO EXHAUSTS & CONV. NOZZLES

********** **INPUT DATA** **********	
MACH NO = .850	ALPHA = 5.000
ALT (FT) = 35000.	PI C` = 1.600
T0 (R) = 394.10	PI D (MAX) = 1.00
P0 (PSIA) = 3.4680	PI B = .95
DENSITY =.00073824	PI N = 1.00
(SLUG/CUFT)	PI N` = 1.00
EFFICIENCY	
CP C = .238 BTU/LBM-R	BURNER = .99
CP T = .295 BTU/LBM-R	MECH HI PR = .98
GAMMA C = 1.400	MECH LO PR = .99
GAMMA T = 1.300	LP COMPR (FAN) = .88 (EC`)
TT4 MAX = 2412. (R)	HP COMPR = .89 (ECH)
H - FUEL (BTU/LBM) = 18600.	HP TURBINE = .88 (ETH)
CTO LOW = .0100	LP TURBINE = .90 (ETL)
CTO HIGH = .0000	PWR MECH EFF L = .98
COOLING AIR #1 = 5.00 %	PWR MECH EFF H = .98
COOLING AIR #2 = 5.00 %	BLEED AIR = 1.00 %
********** **RESULTS** **********	
TAU R = 1.145	A0 = 973.1 FT/SEC
PI R = 1.604	V0 = 827.1 FT/SEC
PI D = .995	MASS FLOW = 200.00 LBM/SEC
TAU L = 7.586	AREA ZERO = 10.180 SQFT
PTO LO= 197.93 KW	AREA ZERO* = 9.974 SQFT
PTO HI= .00 KW	
TAU C`= 1.165	PT5`/P0 = 2.553
ETA C`= .8718	TT5`/T0 = 1.333
PT9`/P9= 1.893	P0/P9` = .745
M9` = 1.000	V9`/V0 = 1.24
PI C = 25.00	TAU M1 = .9701
PI CH = 15.63	TAU M2 = .9803
TAU CH = 2.417	
ETA CH = .8422	
PI TH = .2085	
TAU TH = .7273	
ETA TH = .8982	
PI TL = .2889	
TAU TL = .7727	
ETA TL = .9124	
P0/P9 = .8067	
PT9/P0 = 1.8324	
F = .0231	
FO = .0034	
F/M = 15.210 LBF/LBM/S	
S = .8118 1/H	
T9/T0 = 2.8442	A9/A0 = .2022
V9/V0 = 1.91	A9`/A0 = .5563
M9/M0 = 1.18	THRUST = 3042. LBF

FILE: A:FANRUN13.DAT **ON-DESIGN** CALCULATIONS

"OLDER ENGINE"

- ***COMPRESSOR AND TURBINE EFFICIENCY REDUCED***
- ***OPTIMUM T_{t4}, Method B***

TURBOFAN ENGINE WITH TWO EXHAUSTS & CONV. NOZZLES

********** **INPUT DATA** **********

MACH NO = .850	ALPHA = 5.000
ALT (FT) = 35000.	PI C` = 1.600
T0 (R) = 394.10	PI D (MAX) = 1.00
P0 (PSIA) = 3.4680	PI B = .95
DENSITY =.00073824	PI N = 1.00
(SLUG/CUFT)	PI N` = 1.00
EFFICIENCY	
CP C = .238 BTU/LBM-R	BURNER = .99
CP T = .295 BTU/LBM-R	MECH HI PR = .98
GAMMA C = 1.400	MECH LO PR = .99
GAMMA T = 1.300	LP COMPR (FAN) = .88 (EC`)
TT4 MAX = 2440. (R)	HP COMPR = .89 (ECH)
H - FUEL (BTU/LBM) = 18600.	HP TURBINE = .88 (ETH)
CTO LOW = .0100	LP TURBINE = .90 (ETL)
CTO HIGH = .0000	PWR MECH EFF L = .98
COOLING AIR #1 = 5.00 %	PWR MECH EFF H = .98
COOLING AIR #2 = 5.00 %	BLEED AIR = 1.00 %

********** **RESULTS** **********

TAU R = 1.145	A0 = 973.1 FT/SEC
PI R = 1.604	V0 = 827.1 FT/SEC
PI D = .995	MASS FLOW = 200.00 LBM/SEC
TAU L = 7.674	AREA ZERO = 10.180 SQFT
PTO LO= 197.93 KW	AREA ZERO* = 9.974 SQFT
PTO HI= .00 KW	
TAU C`= 1.165	PT5`/P0 = 2.553
ETA C`= .8718	TT5`/T0 = 1.333
PT9`/P9= 1.893	P0/P9` = .745
M9` = 1.000	V9`/V0 = 1.24
PI C = 25.00	TAU M1 = .9698
PI CH = 15.63	TAU M2 = .9799
TAU CH = 2.417	
ETA CH = .8422	
PI TH = .2130	
TAU TH = .7305	
ETA TH = .8980	
PI TL = .2953	
TAU TL = .7762	
ETA TL = .9122	
P0/P9 = .7724	
PT9/P0 = 1.8324	
F = .0236	
FO = .0035	
F/M = 15.529 LBF/LBM/S	
S = .8116 1/H	
T9/T0 = 2.9009	
V9/V0 = 1.93	
M9/M0 = 1.18	A9`/A0 = .5563
A9/A0 = .1956	THRUST = 3106. LBF

FILE: A:FANRUN14.DAT **ON-DESIGN** CALCULATIONS

"OLDER ENGINE"

- ***GENERALLY REDUCED EFFICIENCY***
- ***AIRFLOW CONSTANT*** *(Method A)*

TURBOFAN ENGINE WITH TWO EXHAUSTS & CONV. NOZZLES

********** **INPUT DATA** **********

MACH NO = .850	ALPHA = 5.000
ALT (FT) = 35000.	PI C` = 1.600
T0 (R) = 394.10	PI D (MAX) = .99
P0 (PSIA) = 3.4680	PI B = .95
DENSITY =.00073824	PI N = .99
(SLUG/CUFT)	PI N` = .99
EFFICIENCY	
CP C = .238 BTU/LBM-R	BURNER = .99
CP T = .295 BTU/LBM-R	MECH HI PR = .98
GAMMA C = 1.400	MECH LO PR = .99
GAMMA T = 1.300	LP COMPR (FAN) = .88 (EC`)
TT4 MAX = 2399. (R)	HP COMPR = .89 (ECH)
H - FUEL (BTU/LBM) = 18600.	HP TURBINE = .88 (ETH)
CTO LOW = .0100	LP TURBINE = .90 (ETL)
CTO HIGH = .0000	PWR MECH EFF L = .98
COOLING AIR #1 = 5.00 %	PWR MECH EFF H = .98
COOLING AIR #2 = 5.00 %	BLEED AIR = 1.00 %

********** **RESULTS** **********

TAU R = 1.145	A0 = 973.1 FT/SEC
PI R = 1.604	V0 = 827.1 FT/SEC
PI D = .994	MASS FLOW = 200.00 LBM/SEC
TAU L = 7.545	AREA ZERO = 10.180 SQFT
PTO LO= 197.93 KW	AREA ZERO* = 9.974 SQFT
PTO HI= .00 KW	
TAU C`= 1.164	PT5`/P0 = 2.551
ETA C`= .8771	TT5`/T0 = 1.332
PT9`/P9= 1.893	P0/P9` = .747
M9` = 1.000	V9`/V0 = 1.24
PI C = 25.00	TAU M1 = .9700
PI CH = 15.63	TAU M2 = .9803
TAU CH = 2.405	
ETA CH = .8493	
PI TH = .2110	
TAU TH = .7278	
ETA TH = .9024	
PI TL = .2904	
TAU TL = .7724	
ETA TL = .9168	
P0/P9 = .7952	
PT9/P0 = 1.8324	
F = .0230	
FO = .0034	
F/M = 15.216 LBF/LBM/S	
S = .8089 1/H	
T9/T0 = 2.8297	
V9/V0 = 1.91	
M9/M0 = 1.18	A9`/A0 = .5572
A9/A0 = .1988	THRUST = 3043. LBF

FILE: A:FANOFF12.DAT **OFF-DESIGN** CALCULATIONS

"OLDER ENGINE"

- ***COMPRESSOR AND TURBINE EFFICIENCY REDUCED***
- ***CONSTANT AIRFLOW AT DESIGNPOINT, Method A***
- ***THROTTLED FOR UNINSTALLED THRUST =11080 LBF***

***** FIXED AREA TURBINE - TURBOFAN ENGINE *****
CONVERGENT NOZZLE

INPUT CONSTANTS

PID MAX = .9950	CP C = .2380	CP T = .2950	ETA B = .9900
GAM C =1.4000	GAM T =1.3000	PI B = .9500	PI N = .9950
ETA C` = .8718	ETA CH = .8422	ETA TL = .9124	PI N` = .9950
PI TH = .2085	TAU TH = .7273	ETA MH = .9800	ETA ML = .9900
BLEED = 1.00%	COOL #1 = 5.00%	COOL #2 = 5.00 %	ETA MPL = .9800
PTO LOW = 716.KW	TAU M1 = .9701	TAU M2 = .9803	ETA MPH = .9800
PTO HI = 0.KW	PIC MAX = .00	PT3 MAX = .0	TT3 MAX = 0. R
RPML MAX= .0%	RPMH MAX= .0%		

PARAMETER	REFERENCE	OFF-DESIGN
M0	.85	.85
T0 (R)	394.1	394.1
P0 (PSIA)	3.468	3.468
ALT (FT)	35000.0	35000.0
TT4 (R)	2412.0	2417.3
PI R / TAU R	1.604/ 1.145	1.604/ 1.145
PI D	.995	.995
PI C / TAU C	25.000/ 2.815	25.124/ 2.820
PI C` / TAU C`	1.600/ 1.165	1.603/ 1.166
PI CH / TAU CH	15.625/ 2.417	15.670/ 2.419
PI TL / TAU TL	.2889/ .7727	.2889/ .7727
LP SPOOL - % REF RPM	100.00	100.21
HP SPOOL - % REF RPM	100.00	100.32
P0/P9	.807	.803
PT9/P9	1.832	1.832
P0/P9`	.745	.744
PT9`/P9`	1.893	1.893
Limit	None	
ALPHA	5.0000	4.9894

MDOT (LBM/S)	723.23	724.73
MDOT CORR (LBM/S)	1781.94	1785.64
AREA0 (SQFT)	36.81	36.890
AREA0*(SQFT)	36.07	36.14
F	.0231	.0232
FO (OVERALL)	.0034	.0034
T9/T0	2.8442	2.8504
V9/V0	1.9130	1.9151
M9/M0	1.1765	1.1765
A9/A0	.2022	.2018
T9`/T0	1.1110	1.1117
V9`/V0	1.2400	1.2404
M9`/M0	1.1765	1.1765
A9`/A0	.5563	.5551
S (1/H)	.8118	.8111
F/M (LBF/LBM/S)	15.21	15.29
FUEL FLOW (LB/H)	8930.	8989.
THRUST (LBF)	11000.	11082.
PROP EFF (%)	73.35	73.21
THERM EFF (%)	36.02	36.11

FILE: A:OFFRUN13.DAT **OFF-DESIGN** CALCULATIONS

"OLDER ENGINE"

- ***COMPRESSOR AND TURBINE EFFICIENCY REDUCED***
- ***OPTIMUM T_{t4} AT DESIGNPOINT, Method B***
- ***THROTTLED FOR UNINSTALLED THRUST =11080 LBF***

***** FIXED AREA TURBINE - TURBOFAN ENGINE *****
CONVERGENT NOZZLE

INPUT CONSTANTS

PID MAX = .9950	CP C = .2380	CP T = .2950	ETA B = .9900
GAM C =1.4000	GAM T =1.3000	PI B = .9500	PI N = .9950
ETA C` = .8718	ETA CH = .8422	ETA TL = .9122	PI N` = .9950
PI TH = .2130	TAU TH = .7305	ETA MH = .9800	ETA ML = .9900
BLEED = 1.00%	COOL #1 = 5.00%	COOL #2 = 5.00 %	ETA MPL = .9800
PTO LOW = 701.KW	TAU M1 = .9698	TAU M2 = .9799	ETA MPH = .9800
PTO HI = 0.KW	PIC MAX = .00	PT3 MAX = .0	TT3 MAX = 0. R
RPML MAX= .0%	RPMH MAX= .0%		

PARAMETER	REFERENCE	OFF-DESIGN
M0	.85	.85
T0 (R)	394.1	394.1
P0 (PSIA)	3.468	3.468
ALT (FT)	35000.0	35000.0
TT4 (R)	2440.0	2445.4
PI R / TAU R	1.604/ 1.145	1.604/ 1.145
PI D	.995	.995
PI C / TAU C	25.000/ 2.815	25.124/ 2.820
PI C` / TAU C`	1.600/ 1.165	1.603/ 1.166
PI CH / TAU CH	15.625/ 2.417	15.670/ 2.419
PI TL / TAU TL	.2953/ .7762	.2953/ .7762
LP SPOOL - % REF RPM	100.00	100.20
HP SPOOL - % REF RPM	100.00	100.32
P0/P9	.772	.769
PT9/P9	1.832	1.832
P0/P9`	.745	.744
PT9`/P9`	1.893	1.893
Limit	None	
ALPHA	5.0000	4.9893

MDOT (LBM/S)	708.37	709.84
MDOT CORR (LBM/S)	1745.34	1748.96
AREA0 (SQFT)	36.06	36.132
AREA0*(SQFT)	35.33	35.40
F	.0236	.0237
FO (OVERALL)	.0035	.0035
T9/T0	2.9009	2.9073
V9/V0	1.9320	1.9341
M9/M0	1.1765	1.1765
A9/A0	.1956	.1953
T9`/T0	1.1110	1.1117
V9`/V0	1.2400	1.2404
M9`/M0	1.1765	1.1765
A9`/A0	.5563	.5551
S (1/H)	.8116	.8110
F/M (LBF/LBM/S)	15.53	15.61
FUEL FLOW (LB/H)	8927.	8986.
THRUST (LBF)	11000.	11081.
PROP EFF (%)	72.36	72.22
THERM EFF (%)	36.47	36.56

FILE: A:OFFRUN14.DAT **OFF-DESIGN** CALCULATIONS

"OLDER ENGINE"

- ***GENERALLY REDUCED EFFICIENCY***
- ***CONSTANT AIRFLOW AT DESIGNPOINT***
- ***THROTTLED FOR UNINSTALLED THRUST =11069 LBF***

***** FIXED AREA TURBINE - TURBOFAN ENGINE *****
CONVERGENT NOZZLE

INPUT CONSTANTS

PID MAX = .9940	CP C = .2380	CP T = .2950	ETA B = .9880
GAM C =1.4000	GAM T =1.3000	PI B = .9490	PI N = .9940
ETA C` = .8771	ETA CH = .8493	ETA TL = .9168	PI N` = .9940
PI TH = .2110	TAU TH = .7278	ETA MH = .9780	ETA ML = .9880
BLEED = 1.00%	COOL #1 = 5.00%	COOL #2 = 5.00 %	ETA MPL = .9800
PTO LOW = 715.KW	TAU M1 = .9700	TAU M2 = .9803	ETA MPH = .9800
PTO HI = 0.KW	PIC MAX = .00	PT3 MAX = .0	TT3 MAX = 0. R
RPML MAX= .0%	RPMH MAX= .0%		

PARAMETER	**ERENCE**	**OFF-DESIGN**
M0	.85	.85
T0 (R)	394.1	394.1
P0 (PSIA)	3.468	3.468
ALT (FT)	35000.0	35000.0
TT4 (R)	2399.0	2403.4
PI R / TAU R	1.604/ 1.145	1.604/ 1.145
PI D	.994	.994
PI C / TAU C	25.000/ 2.799	25.104/ 2.803
PI C` / TAU C`	1.600/ 1.164	1.603/ 1.164
PI CH / TAU CH	15.625/ 2.405	15.663/ 2.407
PI TL / TAU TL	.2904/ .7724	.2904/ .7724
LP SPOOL - % REF RPM	100.00	100.17
HP SPOOL - % REF RPM	100.00	100.27
P0/P9	.795	.792
PT9/P9	1.832	1.832
P0/P9`	.747	.745
PT9`/P9`	1.893	1.893
Limit	None	
ALPHA	5.0000	4.9910

MDOT (LBM/S)	722.93	724.20
MDOT CORR (LBM/S)	1781.22	1784.33
AREA0 (SQFT)	36.80	36.863
AREA0*(SQFT)	36.05	36.12
F	.0230	.0231
FO (OVERALL)	.0034	.0034
T9/T0	2.8297	2.8350
V9/V0	1.9081	1.9099
M9/M0	1.1765	1.1765
A9/A0	.1988	.1985
T9`/T0	1.1100	1.1106
V9`/V0	1.2395	1.2398
M9`/M0	1.1765	1.1765
A9`/A0	.5572	.5562
S (1/H)	.8089	.8083
F/M (LBF/LBM/S)	15.22	15.28
FUEL FLOW (LB/H)	8898.	8947.
THRUST (LBF)	11000.	11069.
PROP EFF (%)	73.21	73.09
THERM EFF (%)	36.22	36.29

APPENDIX F

Engine, Aircraft and Operation Data

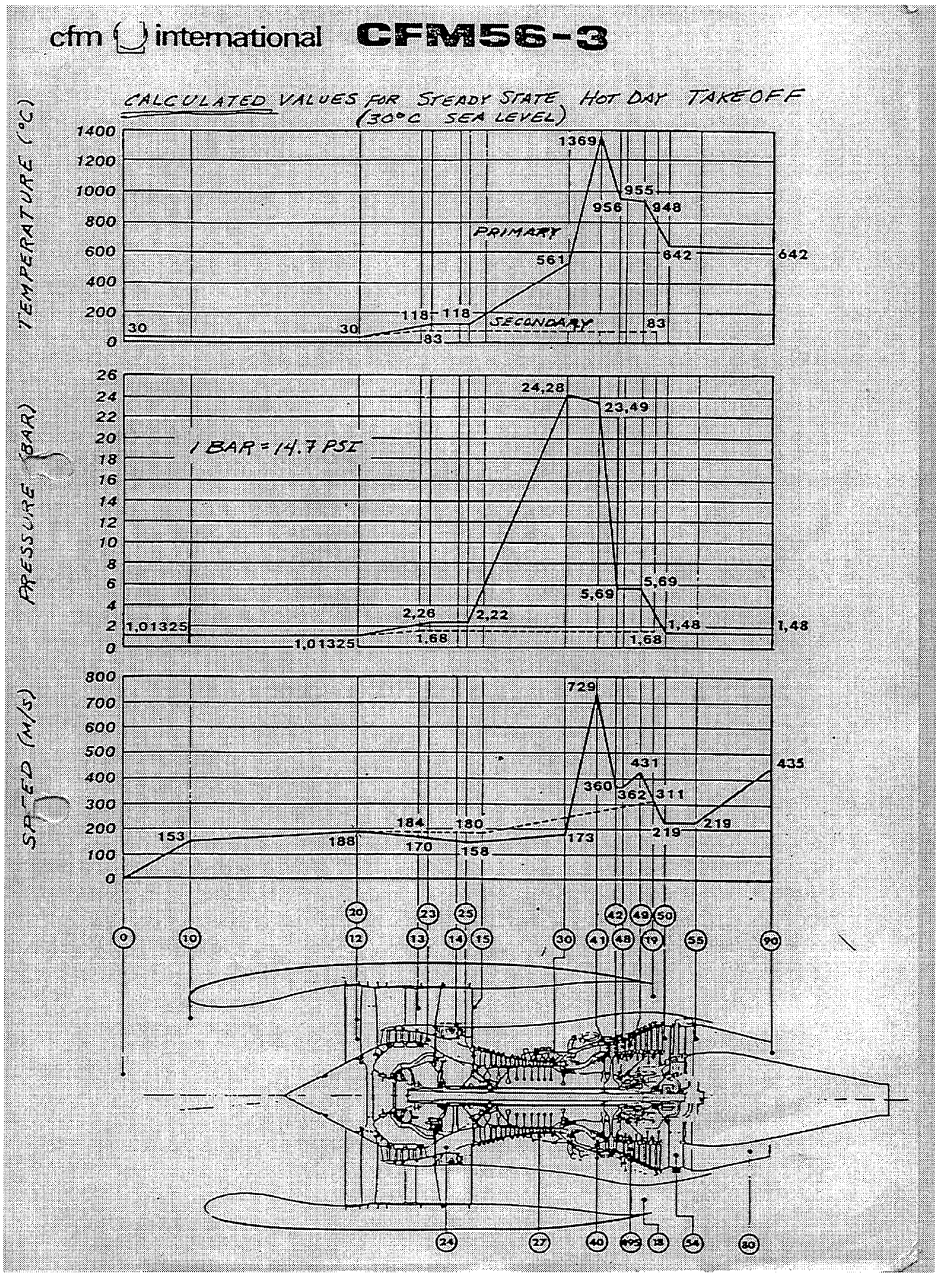

Figure F1 CFM56-3 Parameters Variation through the engine
Courtesy: CFM International

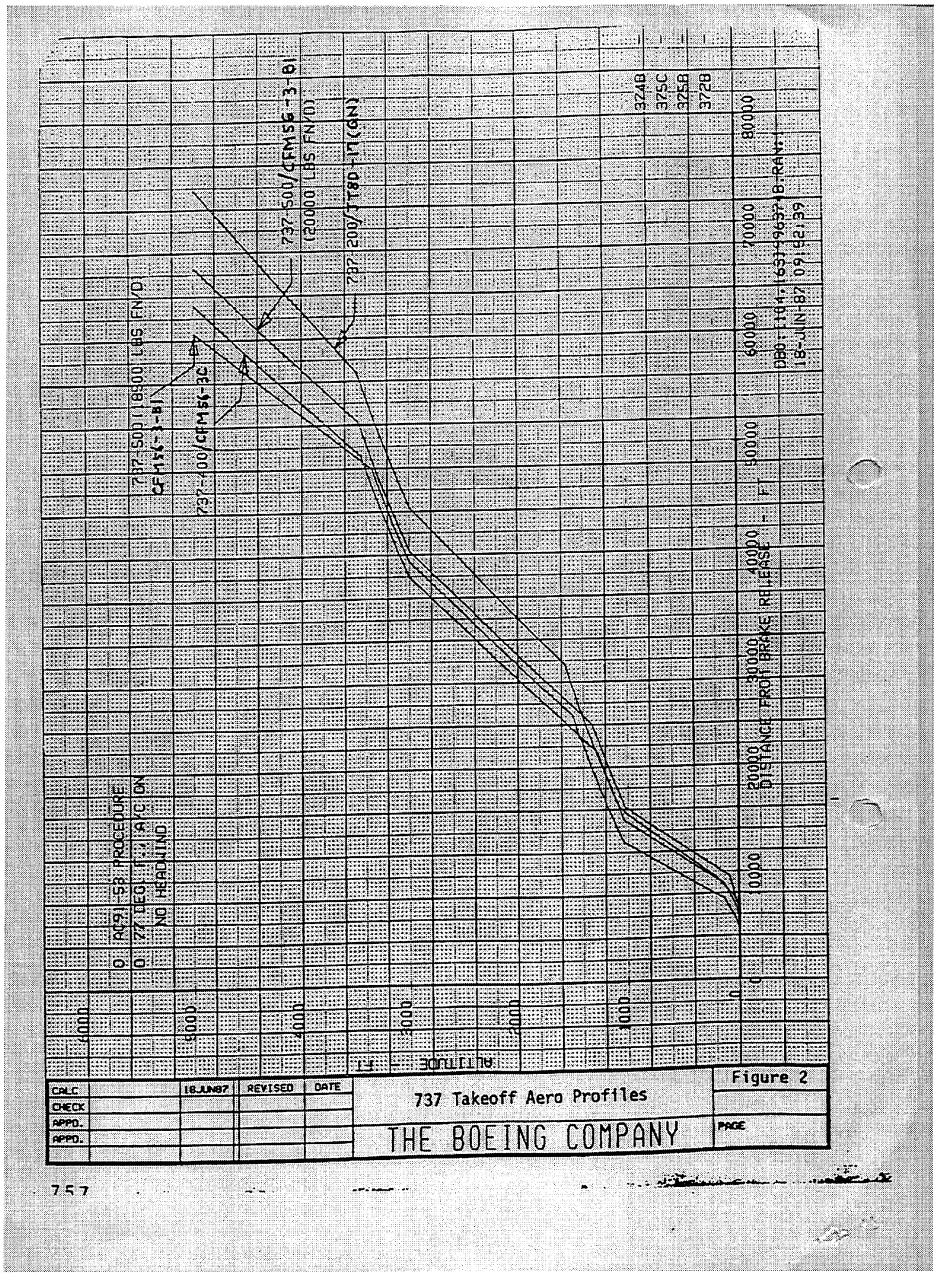

Figure F2 Takeoff Aero Profile for Boeing 737 Models
Courtesy: The Boeing Company

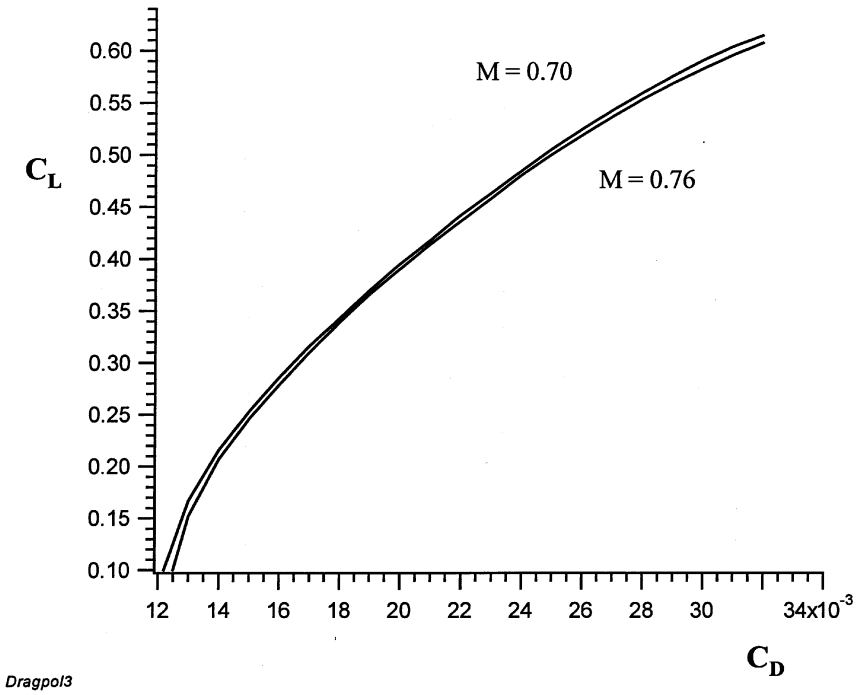

Figure F3 A Scetched Copy of the Boeing 737-400 Drag Polar
Courtesy: The Boeing Company

Basis: B737-400 CFM56-3C1 (23,5k)
48 tonnes take-off (approximately 70 % full load)
Fornebu – Vaernes
ISA weather conditions

Phase	Time (minutes)	Speed	Distance (nm)	Flap
Taxi-out	5	20 kts	-	-
Acceleration	1.9	20 – 140 kts	2.3	5
Take-off to 1500 ft		140 – 210 kts		5
Climb to FL370	14.4	210 – M.745	115	-
Cruise FL370	5	M.745 – M.745	35	-
Descent to 1500 ft	20.2	M.745 – 160 kts	108	- , 5
Approach	2.0	160 – 120 kts	5	5, 10, 15
Landing				30 (40)
Taxi-in	5	20 kts	-	-

Table F1 A Representaive Boeing 737-400 Braathens Flight Oslo – Trondheim, Norway
Courtesy: Braathens

SAMPLE CALCULATION
"DETAILED" MISSION CALCULATION METHOD

TYPICAL MISSION RULES

Taxi Weight	138,752 lb	Range	1,966 nm
Brake Release Gross Weight	138,500 lb	Fuel Load	33,652 lb
OEW + payload	105,100 lb	Block Time	4.986 hr
Type Cruise	LRC @ 31/35000 ft	Block Fuel	26,487 lb
Temperature	Standard Day	Trip Time	4.753 hr
Field Elevation	Sea Level	Trip Fuel	26,095 lb

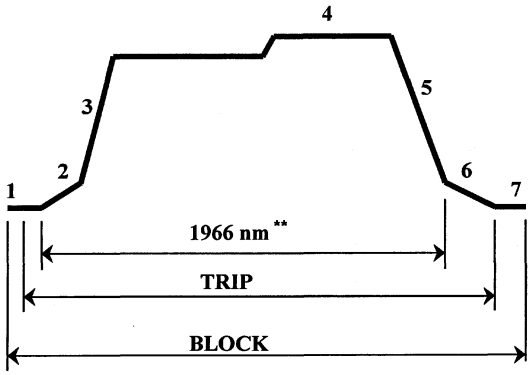

MISSION SEGMENT	Data From Page	Fuel Burned (lb)	Fuel Remaining (lb)	Weight @ End of Segment (lb)	Time (hr)	Distance (nm)
1. Taxi-out (9 min)	3-8	252	33,400	138,500	0.15	---
2. Takeoff Sea Level to 1,500 ft	4-25	494	32,906	138,006	0.03	4
3. Climb to 31,000 ft	6-3 6-4 6-5	2,740	30,156	135,256	0.234	85
4. Cruise at 31/35,000 ft	10-2 10-3	22,266	7,900	113,000	4.11	1,780
5. Descent to 1,500 ft	11-2 11-3	345	7,555	112,655	0.296	97
6. Approach and Land	3-8	250	7,305	112,405	0.083	---
7. Taxi-in (5 min)	3-8	140*	---	---	0.083	---
Trip Totals Block Totals		26,095 26,487			4.753 4.986	1,966
8. Reserve Fuel A. 5% Mission Fuel B. 200 nm Alternate C. ½ hr Hold @ 1,500 ft	 12-3 12-7	 1,305 3,600 2,400	 6,000 2,400 0	 111,000 107,500 105,100		
Total Reserve Fuel		7,305				

(Boeing No. D6-38193, Page 3-10)

* Taxi-in fuel is from reserves and is included in block fuel.
** No distance credit from brake release to 35 ft or approach and land.

Table F2 A Sample Mission Calculation for Boeing 737-400
Courtesy: The Boeing Company and Braathens

APPENDIX G

Scaling Factor Determination

Scaling Factor Adjustments for Prescribed Component performance reduction in Turbomatch.
Variations are Related to Changes in Pressure ratios, Efficiencies and Mass Flow Rate

Compressor no. 1; FAN

Pressure Ratio:

SFPR	PR_{DET}	PR_{CLE}	Reduction [%]
0.98	1.675	1.679	0.24
0.96	1.670		0.54
0.94	1.660		1.10
0.92	1.653		1.55
0.90	1.647		1.90
0.88	1.643		2.14
0.84	1.628		3.03

Isentropic Efficiency:

SFETA	ETA_{DET}	ETA_{CLE}	Reduction [pts.]
0.98	0.8357	0.850	1.44
0.96	0.8229		2.71
0.94	0.8095		4.05

Non dimensional Air Mass Flow:

SFWA	WA_{DET}	WA_{CLE}	Reduction [%]
0.98*	5599	5608	0.16
0.97	5560		0.85
0.96	5530		1.39
0.94	5472		2.43

*) Deviates from line through other points, well beyond any applied range.

Calculated Scaling factors for specific reductions in parameters,

Compressor no. 1; FAN:

ΔPR [%]	*SFPR*
-1.0	0.942
-2.0	0.895
-3.0	0.843

ΔETA [pts.]	*SFETA*
-0.5	0.993
-1.0	0.986
-3.0	0.958

ΔWA [%]	*SFWA*
-1.0	0.968
-2.0	0.948
-3.0	0.922

Compressor no. 2; LPC

Pressure Ratio:

SFPR	PR_{DET}	PR_{CLE}	Reduction [%]
0.98*	1.358	1.365	0.51
0.96	1.352		1.00
0.94	1.345		1.47
0.92	1.339		1.90

Isentropic Efficiency:

SFETA	ETA_{DET}	ETA_{CLE}	Reduction [pts.]
0.98	0.8586	0.876	1.7
0.96	0.8412		3.5
0.94	0.8240		5.2

Non dimensional Air Mass Flow:

SFWA	WA_{DET}	WA_{CLE}	Reduction [%]
0.98	604.1	606.8	0.44
0.96	600.5		1.03
0.94	593.2		2.25

*) Deviates from line through other points; $\sqrt{SFPR}$ fits and is used in this case.

Calculated Scaling factors for specific reductions in parameters:

ΔPR [%]	*SFPR*
-1.0	0.960
-2.0	0.918
-6.0	0.756

ΔETA [pts.]	*SFETA*
-0.5	0.994
-1.0	0.988
-3.0	0.964

ΔWA [%]	*SFWA*
-1.0	0.962
-2.0	0.944
-6.0	0.832

Compressor no. 3; HPC 1

Pressure Ratio:

SFPR	PR_{DET}	PR_{CLE}	Reduction [%]
0.98	3.825	3.840	0.39
0.96	3.808		0.83
0.94	3.775		1.69
0.92	3.745		2.47

Isentropic Efficiency:

SFETA	ETA_{DET}	ETA_{CLE}	Reduction [pts.]
0.99	0.863	0.877	1.4
0.98	0.849		2.8
0.96	0.821		5.6

Non dimensional Air Mass Flow:

SFWA	WA_{DET}	WA_{CLE}	Reduction [%]
0.98	472.1	475.8	0.78
0.96	467.5		1.74
0.94	462.4		2.81

Calculated Scaling factors for specific reductions in parameters:

ΔPR [%]	*SFPR*
-1.0	0.964
-2.0	0.932
-6.0	0.796

ΔETA [pts.]	*SFETA*
-0.5	0.9964
-1.0	0.994
-3.0	0.978

ΔWA [%]	*SFWA*
-1.0	0.976
-2.0	0.955
-6.0	0.865

Compressor no. 4; HPC 2

Pressure Ratio:

SFPR	PR_{DET}	PR_{CLE}	Reduction [%]
0.99	2.937	2.96	0.78
0.98	2.914		1.55
0.96	2.868		3.1
0.94	2.821		4.7

Isentropic Efficiency:

SFETA	ETA_{DET}	ETA_{CLE}	Reduction [pts.]
0.98	0.8623	0.877	1.5
0.96	0.8476		2.9
0.94	0.8327		4.4

Non dimensional Air Mass Flow:

SFWA	WA_{DET}	WA_{CLE}	Reduction [%]
0.99	138.8	139.8	0.73
0.98	137.2		1.85
0.96	133.1		4.82
0.94	129.5		7.39

Calculated Scaling factors for specific reductions in parameters:

ΔPR [%]	*SFPR*
-1.0	0.987
-2.0	0.974
-6.0	0.922

ΔETA [pts.]	*SFETA*
-0.5	0.993
-1.0	0.986
-3.0	0.958

ΔWA [%]	*SFWA*
-1.0	0.987
-2.0	0.978
-6.0	0.934

APPENDIX H

CFMI Fuel Consumption and Emission Estimates for the CFM56-3 Engine

NO_X Emissions

CFM56-3C1; TOGW 56700kg, Sea Level, ISA – 5 K:

Segment	Time [min]	Altitude [ft]	Mach no.	NO_X[kg]	Fuel used [kg]	*NO_X[kg/s]*	*Fuel [kg/s]*	*$NO_{X\,EI}$ [g/kg$_{fuel}$]*
T/O & Climbout	1.0	0 - 1500	0 - 0.39	1.075	62.6	*0.0179*	*1.043*	*17.17*
Climb	9.0	1500 - 25000	0.39 - 0.67	7.09	413.9	*0.0131*	*0.766*	*17.13*
Cruise	20.0	25000	0.72	5.122	456.3	*0.0043*	*0.380*	*11.23*
Descent	14.1	25000- 1500	0.60 - 0.39	0.274	77.8	*0.0003*	*0.092*	*3.52*

Table H1.a Average fuel consumption and NO_X production during flight segments for CFM56-3C1. Estimates by CFMI (Courtesy: CFM International and Braathens), columns in *italic* calculated and added by the author.

CFM56-3B1; TOGW 49000kg, Sea Level, ISA – 5 K:

Segment	Time [min]	Altitude [ft]	Mach no.	NO_X[kg]	Fuel used [kg]	*NO_X[kg/s]*	*Fuel [kg/s]*	*$NO_{X\,EI}$ [g/kg$_{fuel}$]*
T/O & Climbout	1.3	0 - 1500	0 - 0.39	0.9444	60.4	*0.0121*	*0.774*	*15.64*
Climb	8.2	1500 - 25000	0.39 - 0.67	5.564	349.5	*0.0113*	*0.710*	*15.91*
Cruise	20.9	25000	0.72	4.75	442.0	*0.0038*	*0.352*	*10.76*
Descent	14.0	25000- 1500	0.60 - 0.39	0.274	76.9	*0.0003*	*0.092*	*3.56*

Table H1.b Average fuel consumption and NO_X production during flight segments for CFM56-3B1. Estimates by CFMI (Courtesy: CFM International and Braathens), columns in *italic* calculated and added by the author.

Estimated Emissions for CFM56-3B1; TOGW 43000 kg, Sea Level, ISA – 10 K:

Condition	**Mach no.**	**Altitude [ft]**	**Fuel flow [kg/hr]**	**NO_X [kg/hr]**	***Fuel* *[kg/s]***	***NO_X* *[kg/s]***	***$NO_{X\,EI}$* *[g/kg$_{fuel}$]***
Takeoff	0.0	0.0	2535	32.9	*0.704*	*0.0091*	*12.98*
	0.0	0.0	2630	35.5	*0.731*	*0.0099*	*13.50*
	0.0	0.0	2728	38.3	*0.758*	*0.0106*	*10.37*
	0.0	0.0	2827	40.0	*0.785*	*0.0111*	*14.15*
	0.0	0.0	2928	43.0	*0.813*	*0.0119*	*14.68*
	0.0	0.0	3034	46.1	*0.843*	*0.0128*	*15.19*
	0.0	0.0	3148	49.7	*0.874*	*0.0138*	*15.78*
	0.0	0.0	3268	51.5	*0.908*	*0.0143*	*15.76*
Climb	**0.38**	**0.0**	**2775**	**39.4**	***0.771***	***0.0109***	***14.20***
	0.38	500.0	2754	39.0	*0.765*	*0.0108*	*14.16*
	0.41	5000.0	2469	34.7	*0.686*	*0.0096*	*14.05*
	0.45	10000.0	2933	43.7	*0.815*	*0.0121*	*14.90*
	0.51	10000.0	2515	36.7	*0.699*	*0.0102*	*14.59*
	0.55	**15000.0**	**2791**	**46.5**	***0.775***	***0.0129***	***16.66***
	0.61	20000.0	2423	36.5	*0.673*	*0.0101*	*15.06*
	0.67	**25000.0**	**2119**	**30.4**	***0.589***	***0.0084***	***14.34***
	0.74	**30000.0**	**1879**	**25.1**	***0.522***	***0.0070***	***13.36***
Cruise	**0.72**	**30000.0**	**1241**	**11.2**	***0.345***	***0.0031***	***9.02***
Descent	0.67	30000.0	159	0.3	*0.044*	$8 \cdot 10^{-5}$	*1.89*
Flight Idle	0.60	25000.0	171	0.3	*0.048*	$8 \cdot 10^{-5}$	*1.75*
	0.55	20000.0	201	0.4	*0.056*	$10 \cdot 10^{-5}$	*1.99*
	0.50	15000.0	235	0.6	*0.065*	$17 \cdot 10^{-5}$	*2.55**
	0.45	10000.0	272	0.7	*0.076*	$19 \cdot 10^{-5}$	*2.57*
	0.33	10000.0	274	0.7	*0.076*	$19 \cdot 10^{-5}$	*2.55*
	0.30	5000.0	316	0.8	*0.088*	$22 \cdot 10^{-5}$	*2.53*
Approach Idle	0.29	3000.0	420	1.6	*0.117*	$44 \cdot 10^{-5}$	*3.81*
	0.28	2000.0	434	1.7	*0.121*	$47 \cdot 10^{-5}$	*3.92*
	0.28	1000.0	449	1.8	*0.125*	$50 \cdot 10^{-5}$	*4.01*
	0.27	0.0	464	1.9	*0.129*	$52 \cdot 10^{-5}$	*4.09*
Ground Idle	0.0	0.0	397	1.1	*0.110*	$31 \cdot 10^{-5}$	*2.77*

Table H2 **Time specific fuel consumption and NO_X production during flight for CFM56-3B1. Estimates by CFMI (Courtesy: CFM International and Braathens), columns in *italic* calculated and added by the author.**

*) Test condition for descent.

Condition	Mach no.	Altitude [ft]	Fuel flow [kg/s]	$NO_{X\ EI}$ [g/kg_{fuel}]	T_{ET} [K]	ΔP_{Burner} [atm]	$P_{B,max}$ [atm]	Air $flow_B$ [kg/s]	T_{ST} [K]	Thrust [N]
Climb	0.38	0.0	0.8319	15.29	1437	0.68	20.93	40.9	2571	52200
	0.55	15000.0	0.8362	17.94	1568	0.64	18.92	35.7	2593	47100
	0.67	25000.0	0.6355	15.44	1548	0.46	14.40	27.4	2584	33800
	0.74	30000.0	0.5632	14.39	1547	0.42	12.46	24.0	2581	28800
Cruise	0.72	30000.0	0.3723	9.41	1328	0.34	9.82	20.2	2541	20300
Descent Flight Idle	0.50	15000.0	0.1170	2.55	924	0.13	4.53	10.3	2446	2800

Regarding underlined numbers:
Fuel consumption (CFMI calculations) at this particular point in descent is 0.065 kg/s, Turbomatch does not converge for such low fuel flow. 0.1170 kg/s corresponds to the net thrust requirement of 2800 N as calculated in the models of the present work.

Table H3 Estimated fuel consumption and NO_X production, other parameters calculated in Turbomatch, for CFM56-3C1. (Based on Table H2 figures)

CO emissions

CFM56-3C1; TOGW 56700kg, Sea Level, ISA – 5 K:

Segment	Time [min]	Altitude [ft]	Mach no.	CO[kg]	Fuel used [kg]	*CO[g/s]*	*Fuel [kg/s]*	*CO_{EI} [g/kg$_{fuel}$]*
T/O & Climbout	1.0	0 - 1500	0 - 0.39	0.052	62.6	*0.8667*	*1.043*	*0.831*
Climb	9.0	1500 - 25000	0.39 - 0.67	0.385	413.9	*0.7130*	*0.766*	*0.931*
Cruise	20.0	25000	0.72	0.920	456.3	*0.7667*	*0.380*	*2.018*
Descent	14.1	25000- 1500	0.60 - 0.39	2.659	77.8	*3.1430*	*0.092*	*34.16*

Table H4.a Average fuel consumption and CO production during flight segments for CFM56-3C1. Estimates by CFMI (Courtesy: CFM International and Braathens), columns in *italic* calculated and added by the author.

CFM56-3B1; TOGW 49000kg, Sea Level, ISA – 5 K:

Segment	Time [min]	Altitude [ft]	Mach no.	CO [kg]	Fuel used [kg]	*CO[g/s]*	*Fuel [kg/s]*	*CO_{EI} [g/kg$_{fuel}$]*
T/O & Climbout	1.3	0 - 1500	0 - 0.39	0.062	60.4	*0.7949*	*0.774*	*1.027*
Climb	8.2	1500 - 25000	0.39 - 0.67	0.347	349.5	*0.7053*	*0.710*	*0.993*
Cruise	20.9	25000	0.72	0.977	442.0	*0.7791*	*0.352*	*2.213*
Descent	14.0	25000- 1500	0.60 - 0.39	2.660	76.9	*3.1667*	*0.092*	*34.42*

Table H4.b Average fuel consumption and CO production during flight segments for CFM56-3B1. Estimates by CFMI (Courtesy: CFM International and Braathens), columns in *italic* calculated and added by the author.

Estimated Emissions for CFM56-3B1; TOGW 43000 kg, Sea Level, ISA – 10 K:

Condition	**Mach no.**	**Altitude [ft]**	**Fuel flow [kg/hr]**	**CO [kg/hr]**	***Fuel [kg/s]***	***CO [g/s]***	***CO_{EI} [g/kg$_{fuel}$]***
Takeoff	0.0	0.0	2535	3.8	*0.704*	*1.056*	*1.50*
	0.0	0.0	2630	3.7	*0.731*	*1.028*	*1.41*
	0.0	0.0	2728	3.5	*0.758*	*0.972*	*1.28*
	0.0	0.0	2827	3.4	*0.785*	*0.944*	*1.20*
	0.0	0.0	2928	3.5	*0.813*	*0.972*	*1.20*
	0.0	0.0	3034	3.3	*0.843*	*0.917*	*1.09*
	0.0	0.0	3148	3.1	*0.874*	*0.861*	*0.985*
	0.0	0.0	3268	3.3	*0.908*	*0.917*	*1.01*
Climb	**0.38**	**0.0**	**2775**	**3.3**	***0.771***	***0.917***	***1.19***
	0.38	500.0	2754	3.3	*0.765*	*0.917*	*1.20*
	0.41	5000.0	2469	2.7	*0.686*	*0.750*	*1.09*
	0.45	10000.0	2933	2.9	*0.815*	*0.806*	*0.989*
	0.51	10000.0	2515	2.3	*0.699*	*0.639*	*0.914*
	0.55	**15000.0**	**2791**	**2.5**	***0.775***	***0.694***	***0.896***
	0.61	20000.0	2423	2.2	*0.673*	*0.611*	*0.908*
	0.67	**25000.0**	**2119**	**1.9**	***0.589***	***0.528***	***0.896***
	0.74	**30000.0**	**1879**	**1.7**	***0.522***	***0.472***	***0.905***
Cruise							
	0.72	**30000.0**	**1241**	**1.9**	***0.345***	***0.528***	***1.530***
Descent	**0.67**	**30000.0**	**159**	**50.0**	***0.044***	***13.89***	***316.0***
Flight Idle	0.60	25000.0	171	62.7	*0.048*	*17.42*	*363.0*
	0.55	20000.0	201	44.8	*0.056*	*12.44*	*222.0*
	0.50	**15000.0**	**235**	**37.8**	***0.065***	***10.50***	***162.0***
	0.45	10000.0	272	32.3	*0.076*	*8.97*	*118.0*
	0.33	**10000.0**	**274**	**34.3**	***0.076***	***9.52***	***125.0***
	0.30	**5000.0**	**316**	**29.3**	***0.088***	***8.14***	***92.5***
Approach Idle	0.29	3000.0	420	17.6	*0.117*	*4.89*	*41.8*
	0.28	2000.0	434	16.9	*0.121*	*4.69*	*38.8*
	0.28	1000.0	449	16.3	*0.125*	*4.53*	*36.2*
	0.27	0.0	464	15.6	*0.129*	*4.33*	*33.6*
Ground Idle	0.0	0.0	397	27.5	*0.110*	*7.63*	*69.4*

Table H5 Time specific fuel consumption and CO production during flight for CFM56-3B1. Estimates by CFMI (Courtesy: CFM International and Braathens), columns in *italic* calculated and added by the author.

Condition	Mach no.	Altitude [ft]	Fuel flow [kg/s]	CO_{EI} [g/kg_{fuel}]	CO [g/s]	T_{ET} [K]	ΔP_{Burner} [atm]	$P_{B,max}$ [atm]	Air $flow_B$ [kg/s]	T_{ST} [K]	Thrust [N]
Climb	0.38	0.0	0.8319	1.12		1437	0.68	20.93	40.9	2571	52200
	0.55	15000.0	0.8362	0.84		1568	0.64	18.92	35.7	2593	47100
	0.67	25000.0	0.6355	0.84		1548	0.46	14.40	27.4	2584	33800
	0.74	30000.0	0.5632	0.85		1547	0.42	12.46	24.0	2581	28800
Cruise	0.72	30000.0	0.3723	1.40		1328	0.34	9.82	20.2	2541	20300
Descent Flight Idle	0.67	30000.0	0.0955	*145.0*	13.89	933	0.089	3.48	8.2		2200
	0.50	15000.0	0.1170	*89.7*	10.50	924	0.130	4.53	10.3		2800
	0.33	10000.0	0.1236	*77.0*	9.52	937	0.144	4.71	10.5		4750
	0.30	5000.0	0.1286	*63.3*	8.14	921	0.107	5.10	11.4		4850

Regarding underlined numbers:
Fuel consumption (CFMI calculations) at these particular points in descent are lower, Turbomatch does not converge for such low fuel flow. CO emissions are kept from the CFMI data at corresponding altitudes and Mach numbers and used to calculate emission indices (appear in italic print) for the lowest possible (ref. Turbomatch) thrust/fuel flow.

Table H6 Estimated fuel consumption and CO production, other parameters calculated in Turbomatch, for CFM56-3C1. (Based on Table H5 figures)

CFMI figures for UHC emissions

CFM56-3C1; TOGW 56700kg, Sea Level, ISA – 5 K:

Segment	Time [min]	Altitude [ft]	Mach no.	UHC[kg]	Fuel used [kg]	*UHC[g/s]*	*Fuel [kg/s]*	*UHC_{EI} [g/kg$_{fuel}$]*
T/O & Climbout	1.0	0 - 1500	0 - 0.39	0.0026	62.6	*0.0433*	*1.043*	*0.0415*
Climb	9.0	1500 - 25000	0.39 - 0.67	0.0208	413.9	*0.0385*	*0.766*	*0.0503*
Cruise	20.0	25000	0.72	0.0313	456.3	*0.0261*	*0.380*	*0.0687*
Descent	14.1	25000- 1500	0.60 - 0.39	0.1256	77.8	*0.1485*	*0.092*	*1.614*

Table H7.a Average fuel consumption and UHC production during flight segments for CFM56-3C1. Estimates by CFMI (Courtesy: CFM International and Braathens), columns in *italic* calculated and added by the author.

CFM56-3B1; TOGW 49000kg, Sea Level, ISA – 5 K:

Segment	Time [min]	Altitude [ft]	Mach no.	UHC [kg]	Fuel used [kg]	*UHC [g/s]*	*Fuel [kg/s]*	*UHC_{EI} [g/kg$_{fuel}$]*
T/O & Climbout	1.3	0 - 1500	0 - 0.39	0.0036	60.4	*0.0462*	*0.774*	*0.0597*
Climb	8.2	1500 - 25000	0.39 - 0.67	0.0188	349.5	*0.0382*	*0.710*	*0.0538*
Cruise	20.9	25000	0.72	0.0311	442.0	*0.0248*	*0.352*	*0.0705*
Descent	14.0	25000- 1500	0.60 - 0.39	0.1256	76.9	*0.1495*	*0.092*	*1.625*

Table H7.b Average fuel consumption and UHC production during flight segments for CFM56-3B1. Estimates by CFMI (Courtesy: CFM International and Braathens), columns in *italic* calculated and added by the author.

Estimated Emissions for CFM56-3B1; TOGW 43000 kg, Sea Level, ISA – 10 K:

Condition	**Mach no.**	**Altitude [ft]**	**Fuel flow [kg/hr]**	**UHC [kg/hr]**	***Fuel [kg/s]***	**UHC** *[g/s]*	**UHC** $_{EI}$
[g/kg$_{fuel}$]							
Takeoff	0.0	0.0	2535	0.1	*0.704*	*0.0278*	*0.039*
	0.0	0.0	2630	0.1	*0.731*	*0.0278*	*0.038*
	0.0	0.0	2728	0.1	*0.758*	*0.0278*	*0.037*
	0.0	0.0	2827	0.1	*0.785*	*0.0278*	*0.035*
	0.0	0.0	2928	0.1	*0.813*	*0.0278*	*0.034*
	0.0	0.0	3034	0.2	*0.843*	*0.0556*	*0.066*
	0.0	0.0	3148	0.2	*0.874*	*0.0556*	*0.064*
	0.0	0.0	3268	0.2	*0.908*	*0.0556*	*0.061*
Climb	**0.38**	**0.0**	**2775**	0.1	***0.771***	*0.0278*	***0.036***
	0.38	500.0	2754	0.1	*0.765*	*0.0278*	*0.036*
	0.41	5000.0	2469	0.1	*0.686*	*0.0278*	*0.041*
	0.45	10000.0	2933	0.1	*0.815*	*0.0278*	*0.034*
	0.51	10000.0	2515	0.1	*0.699*	*0.0278*	*0.040*
	0.55	**15000.0**	**2791**	0.1	***0.775***	*0.0278*	***0.036***
	0.61	20000.0	2423	0.1	*0.673*	*0.0278*	*0.041*
	0.67	**25000.0**	**2119**	0.1	***0.589***	*0.0278*	***0.047***
	0.74	**30000.0**	**1879**	0.1	***0.522***	*0.0278*	***0.053***
Cruise							
	0.72	**30000.0**	**1241**	0.1	***0.345***	*0.0278*	***0.081***
Descent	**0.67**	**30000.0**	**159**	**37.8**	***0.044***	***10.5***	***239.0***
Flight Idle	0.60	25000.0	171	42.6	*0.048*	*11.8*	*246.0*
	0.55	20000.0	201	26.1	*0.056*	*7.25*	*129.0*
	0.50	**15000.0**	**235**	**15.6**	***0.065***	***4.33***	***66.6***
	0.45	10000.0	272	9.6	*0.076*	*2.67*	*35.1*
	0.33	**10000.0**	**274**	**11.2**	***0.076***	***3.11***	***40.9***
	0.30	**5000.0**	**316**	**7.0**	***0.088***	***1.94***	***22.0***
Approach Idle	0.29	3000.0	420	1.6	*0.117*	*0.444*	*3.79*
	0.28	2000.0	434	1.4	*0.121*	*0.389*	*3.21*
	0.28	1000.0	449	1.3	*0.125*	*0.361*	*2.89*
	0.27	0.0	464	1.1	*0.129*	*0.306*	*2.37*
Ground Idle	0.0	0.0	397	5.7	*0.110*	*1.58*	*14.4*

Table H8 Time specific fuel consumption and UHC production during flight for CFM56-3B1. Estimates by CFMI (Courtesy: CFM International and Braathens), columns in *italic* calculated and added by the author.

Condition	Mach no.	Altitude [ft]	Fuel flow [kg/s]	UHC $_{EI}$ [g/kg$_{fuel}$]	UHC [g/s]	T_{ET} [K]	ΔP_{Burner} [atm]	$P_{B,max}$ [atm]	Air flow$_B$ [kg/s]	T_{ST} [K]	Thrust [N]
Climb	0.38	0.0	0.8319	0.034		1437	0.68	20.93	40.9	2571	52200
	0.55	15000.0	0.8362	0.034		1568	0.64	18.92	35.7	2593	47100
	0.67	25000.0	0.6355	0.044		1548	0.46	14.40	27.4	2584	33800
	0.74	30000.0	0.5632	0.050		1547	0.42	12.46	24.0	2581	28800
Cruise	0.72	30000.0	0.3723	0.079		1328	0.34	9.82	20.2	2541	20300
Descent Flight Idle	0.67	30000.0	0.0955	*109.9*	10.5	933	0.089	3.48	8.2		2200
	0.50	15000.0	0.1170	*37.0*	4.33	924	0.130	4.53	10.3		2800
	0.33	10000.0	0.1236	*25.2*	3.11	937	0.144	4.71	10.5		4750
	0.30	5000.0	0.1286	*15.1*	1.94	921	0.107	5.10	11.4		4850

Regarding underlined numbers:
Fuel consumption (CFMI calculations) at these particular points in descent are lower, Turbomatch does not converge for such low fuel flow. CO emissions are kept from the CFMI data at corresponding altitudes and Mach numbers and used to calculate emission indices (appear in italic print) for the lowest possible (ref. Turbomatch) thrust/fuel flow.

Table H9 Estimated fuel consumption and UHC production, other parameters calculated in Turbomatch, for CFM56-3C1. (Based on Table H8 figures)

APPENDIX I

Mission Specification and Details

The Braathens Flight Oslo – Trondheim, Boeing 737-400

Mission segment	Time [s]	Distance [km]	Altitude (end) [m]	Speed (end) [m/s]	Acceleration [m/s^2]	Climb Angle [m/m]	Flaps
Taxi-out	300	3,1	12	10,3	0,0	0,0	-
Acceleration	36	1,5	12	72,0	1,7	0,0	5
Take-off	48	4,3	457	108,0	*0,75*	*0,103*	5
Climb I	170	28,3	2019	220,0	0,69	*0,0570*	-
Climb II	730 (tot. 900)	161,7 (tot. 190)	11278	220,0	0,0	*0,0570*	-
Cruise	405	89,0	11278	220,0	0,00	0,0	-
Descent I	480	105,5	5570	220,0	0,0	-0,0541	-,5
Descent II	627 (tot. 1107)	94,5 (tot. 200)	457	82,3	-0,22	-0,0541	-,5
Approach and Land	130	9,3	6	61,7	-0,16	-0,0485	5,10,15,30
Taxi-in	300	3,1	6	10,3	0,00	0,0	-
SUM	**3226**	**500**					

Table I1 Mission Oslo – Trondheim, Outline

Table I2 Mission Oslo – Trondheim; Sub segments included

Mission segment	Time [s] (start/accum)	Distance [km]	Altitude (start)[m]	Speed (start) [m/s] (M)	Acceleration [m/s^2]	Climb Angle [m/m]	Density [kg/m^3]	Flaps	C_D (special)
Taxi-out	*300,0*	*3,1*	*12*	*10,3*	*0,0*	*0,0*		-	
Point 1	0,0 (0)	0,0	12	10,3 (0,030)	0,0	0,0	1,2236		
Point 2	120,0 (120)	1,24	12	10,3 (0,030)	0,0	0,0	1,2236		
Point 3	240,0 (240)	2,47	12	10,3 (0,030)	0,0	0,0	1,2236		
Point 4	300,0 (300)	3,1	12	10,3 (0,030)	0,0	0,0	1,2236		
Acceleration	*36*	*1,5*	*12*	*72,0*	*1,7*	*0,0*		*5*	
Point 5	**0,0 (300)**	**0,0**	**12**	**10,3 (0,030)**	**1,7**	**0,0**	**1,2236**		**0,102**
Point 6	**25,0 (325)**	**0,79**	**12**	**52,2 (0,155)**	**1,7**	**0,0**	**1,2236**		**0,102**
Point 7	**36,0 (336)**	**1,5**	**12**	**72,0 (0,212)**	**1,7**	**0,0**	**1,2236**		**0,102**
Take-off	*48*	*4,3*	*457*	*108,0*	*0,75*	*0,103*		*5*	
Point 8	**0,0 (336)**	**0,0**	**12**	**72,3 (0,213)**	**0,75**	**0,103**	**1,2236**		**0,102**
Point 9	**24,0 (360)**	**1,95**	**213**	**90,3 (0,226)**	**0,75**	**0,103**	**1,2002**		**0,062**
Point 10	**48,0 (384)**	**4,3**	**457**	**108,0 (0,319)**	**0,75**	**0,103**	**1,1722**		**0,037**
Climb I	*170*	*28,3*	*2019*	*220,0*	*0,69*	*0,0570*		-	
Point 11	**0,0 (384)**	**0,0**	**457**	**108,0 (0,319)**	**0,69**	**0,0570**	**1,1722**		**0,030**
Point 12	**85,0 (469)**	**11,7**	**1122**	**165,4 (0,465)**	**0,69**	**0,0570**	**1,0984**		
Point 13	**170,0 (554)**	**28,3**	**2071**	**220,0 (0,663)**	**0,449**	**0,0570**	**0,9994**		

Continued next page

Table I2 Mission Oslo – Trondheim; Sub segments included *(Continued)*

Mission segment	Time [s] (start/accum)	Distance [km]	Altitude (start)[m]	Speed (start) [m/s] (M)	Acceleration [m/s^2]	Climb Angle [m/m]	Density [kg/m^3]	Flaps	C_D (special)
Climb II	*730$^{(tot. 900)}$*	*161,7 $^{(tot. 190)}$*	*11278*	*220,0*	*0,0*	*0,0570*		-	
Point 14	0,0 (554)	0,0	2071	220,0 (0,663)	0,0	0,0570	0,9994		
Point 15	120,0 (674)	26,3	3522	220,0 (0,675)	0,0	0,0570	0,8614		
Point 16	240,0 (794)	52,8	5026	220,0 (0,686)	0,0	0,0570	0,7342		
Point 17	360,0 (914)	79,1	6529	220,0 (0,699)	0,0	0,0570	0,6220		
Point 18	480,0 (1034)	105,5	8033	220,0 (0,714)	0,0	0,0570	0,5234		
Point 19	600,0 (1154)	131,9	9536	220,0 (0,730)	0,0	0,0570	0,4372		
Point 20	730,0 (1284)	161,7	11278	220,0 (0,745)	0,0	0,0520	0,3486		
Cruise	*405*	*89,0*	*11278*	*220,0*	*0,00*	*0,0*		-	
Point 21	0,0 (1284)	0,0	11278	220,0 (0,745)	0,0	0,0	0,3486		
Point 22	120,0 (1404)	26,3	11278	220,0 (0,745)	0,0	0,0	0,3486		
Point 23	240,0 (1524)	52,8	11278	220,0 (0,745)	0,0	0,0	0,3486		
Point 24	360,0 (1644)	79,1	11278	220,0 (0,745)	0,0	0,0	0,3486		
Point 25	405,0 (1689)	89,0	11278	220,0 (0,745)	0,0	0,0	0,3486		
Descent I	*480*	*105,5*	*5628*	*220,0*	*0,0*	*-0,0547(-0,05)*		*-,5*	
Point 26	0,0 (1689)	0,0	11278	220,0 (0,745)	0,0	-0,0500	0,3486		
Point 27	120,0 (1809)	26,3	9963	220,0 (0,734)	0,0	-0,0547	0,4146		
Point 28	240,0 (1929)	52,8	8513	220,0 (0,720)	0,0	-0,0547	0,4943		
Point 29	360,0 (2049)	79,1	7073	220,0 (0,707)	0,0	-0,0547	0,5846		
Point 30	480,0 (2169)	105,5	5628	220,0 (0,693)	0,0	-0,0547	0,6874		

Continued next page

Table I2 Mission Oslo – Trondheim; Sub segments included (*Continued*)

Mission segment	Time [s] (start/accum)	Distance [km]	Altitude (start)[m]	Speed (start) [m/s] (M)	Acceleration [m/s^2]	Climb Angle [m/m]	Density [kg/m^3]	Flaps	C_D (special)
Descent II	*627 (tot. 1107)*	*94,5 (tot. 200)*	*457*	*82,3*	*-0,22*	*-0,0547*		*--,5*	
Point 31	**0,0 (2169)**	**0,0**	**5628**	**220,0 (0,693)**	**-0,22**	**-0,0547**	**0,6874**		
Point 32	**120,0 (2289)**	**24,8**	**4273**	**193,4 (0,599)**	**-0,22**	**-0,0547**	**0,7958**		***+0,0010***
Point 33	**240,0 (2409)**	**46,4**	**3093**	**167,0 (0,510)**	**-0,22**	**-0,0547**	**0,9005**		***+0,0025***
Point 34	**360,0 (2529)**	**64,9**	**2082**	**140,6 (0,424)**	**-0,22**	**-0,0547**	**0,9982**		***+0,0075***
Point 35	**480,0 (2649)**	**80,2**	**1246**	**114,2 (0,341)**	**-0,22**	**-0,0547**	**1,0850**		***+0,0150***
Point 36	**600,0 (2769)**	**92,3**	**584**	**87,8 (0,260)**	**-0,22**	**-0,0547**	**1,1578**		***+0,0300***
Point 37	**627,0 (2796)**	**94,6**	**457**	**81,9 (0,242)**	**-0,22**	**-0,0547**	**1,1722**		***+0,0400***
Approach and Land	*130*	*9,3*	*6*	*61,7*	*-0,16*	*-0,0485*		*5,10,15,30*	
Point 38	**0,0 (2796)**	**0,0**	**457**	**81,9 (0,242)**	**-0,16**	**-0,0485**	**1,1722**		***+0,0400***
Point 39	**65,0 (2861)**	**5,0**	**215**	**71,5 (0,211)**	**-0,16**	**-0,0485**	**1,1999**		**0,0750**
Point 40	130,0 (2926)	9,3	6	61,7 (0,181)	-0,16	-0,0485	1,2243		
Taxi-in	*300*	*3,1*	*6*	*10,3*	*0,00*	*0,0*		-	
Point 41	0,0 (2926)	0,0	6	10,3 (0,030)	0,0	0,0	1,2243		
Point 42	120,0 (3046)	1236	6	10,3 (0,030)	0,0	0,0	1,2243		
Point 43	240,0 (3166)	2472	6	10,3 (0,030)	0,0	0,0	1,2243		
Point 44	300,0 (3226)	3100	6	10,3 (0,030)	0,0	0,0	1,2243		
SUM	**3226**	**500**							

Table I3 Mission Oslo – Trondheim; Flight parameter increments and ranges used in Turbomatch calculations.

Sequence	Speeds [Mach number]	Altitude [m]	Power settings, T_{t4} [K]
Acceleration & Takeoff	0.0 / 0.05 / 0.1 / 0.15 / 0.2 / 0.25 / 0.3 / 0.35 / 0.4	0 / 100 / 200 / 300 / 400 / 500 1650 / 1700	1400 / 1450 / 1500 / 1550 / 1600 /
Acceleration & Takeoff (X- deteriorated)	0.0 / 0.05 / 0.1 / 0.15 / 0.2 / 0.25 / 0.3 / 0.35 / 0.4	0 / 100 / 200 / 300 / 400 / 500	1750 / 1800
Climb (I)	0.25 / 0.3 / 0.35 / 0.4 / 0.45 / 0.5 / 0.55 / 0.6 / 0.65 / 0.7 / 0.75 / 0.8	0 / 500 / 1000 / 1500 / 2000 / 2500 / 3000 / 3500 / 4000	1400 / 1450 / 1500 / 1550 / 1600 / 1650 / 1700
Climb (I) (X- deteriorated)	0.25 / 0.3 / 0.35 / 0.4 / 0.45 / 0.5 / 0.55 / 0.6 / 0.65 / 0.7 / 0.75 / 0.8	0 / 500 / 1000 / 1500 / 2000 / 2500 / 3000 / 3500 / 4000	1750 / 1800
Climb (II)	0.25 / 0.3 / 0.35 / 0.4 / 0.45 / 0.5 / 0.55 / 0.6 / 0.65 / 0.7 / 0.75 / 0.8	4000 / 4500 / 5000 / 5500 / 6000 / 6500 / 7000 / 7500 / 8000	1400 / 1450 / 1500 / 1550 / 1600 / 1650 / 1700
Climb (II) (X- deteriorated)	0.25 / 0.3 / 0.35 / 0.4 / 0.45 / 0.5 / 0.55 / 0.6 / 0.65 / 0.7 / 0.75 / 0.8	4000 / 4500 / 5000 / 5500 / 6000 / 6500 / 7000 / 7500 / 8000	1750 / 1800
Climb (III)	0.25 / 0.3 / 0.35 / 0.4 / 0.45 / 0.5 / 0.55 / 0.6 / 0.65 / 0.7 / 0.75 / 0.8	8000 / 8500 / 9000 /9500 / 10000 / 10500 / 11000 / 11500 / 12000	1400 / 1450 / 1500 / 1550 / 1600 / 1650 / 1700
Climb (III) (X- deteriorated)	0.25 / 0.3 / 0.35 / 0.4 / 0.45 / 0.5 / 0.55 / 0.6 / 0.65 / 0.7 / 0.75 / 0.8	8000 / 8500 / 9000 /9500 / 10000 / 10500 / 11000 / 11500 / 12000	1750 / 1800
Cruise	0.7 / 0.75 / 0.8	9000 / 9500 / 10000 / 10500 / 11000 / 11500 / 12000	1200 / 1250 / 1300 / 1350 / 1400 / 1450 / 1500
Cruise (X- deteriorated)	0.7 / 0.75 / 0.8	9000 / 9500 / 10000 / 10500 / 11000 / 11500 / 12000	1550 / 1600

Continued next page

Table I3 Mission Oslo – Trondheim; Flight parameter increments and ranges used in Turbomatch calculations (*Continued*)

Sequence	Speeds [Mach number]	Altitude [m]	Power settings, T_{t4} [K]
Descent (I)	0.75 / 0.7 / 0.65 / 0.6 / 0.55 / 0.5 / 0.45 / 0.4 / 0.35 / 0.3 / 0.25 / 0.2	8000 / 8500 / 9000 / 9500 /10000 /10500 / 11000 / 11500 / 12000	950 / 1000 / 1050 / 1100 / 1150 / 1200 / 1250 / 1300
Descent (II)	0.75 / 0.7 / 0.65 / 0.6 / 0.55 / 0.5 / 0.45 / 0.4 / 0.35 / 0.3 / 0.25 / 0.2	4000 / 4500 / 5000 / 5500 / 6000 / 6500 / 7000 / 7500 / 8000 /	950 / 1000 / 1050 / 1100 / 1150 / 1200 / 1250 / 1300
Descent (II), D3	*0.55 / 0.54 / 0.53 / 0.52 / 0.51 / 0.5 / 0.45 / 0.4 / 0.35 / 0.3 / 0.25 / 0.2*	*4000 / 4500 / 5000 / 5500 / 6000 / 6500 / 7000 / 7500 / 8000 /*	*950 / 1000 / 1050 / 1100 / 1150 / 1200 / 1250 / 1300*
Descent (III)	0.55 / 0.54 / 0.53 / 0.52 / 0.51 / 0.5 / 0.45 / 0.4 / 0.35 / 0.3 / 0.25 / 0.2	0 / 500 / 1000 / 1500 / 2000 / 2500 / 3000 / 3500 / 4000 /	950 / 1000 / 1050 / 1100 / 1150 / 1200 / 1250 / *1300*
Descent, Flight Idle	0.75 / 0.7 / 0.65 / 0.6 / 0.55 / 0.5 / 0.45 / 0.4 / 0.35 / 0.3 / 0.25 / 0.2	0 / 500 / 1000 / 1500 / 2000 / 2500 / 3000 / 3500 / 4000 / 4500 / 5000 / 5500 / 6000 / 6500 / 7000 / 7500 / 8000 / 8500 / 9000 / 9500 /10000 / 10500 / 11500 / 12000	920 / 935 / 950
Approach & Landing	0.0 / 0.1 / 0.2 / 0.3	0 / 100 / 200 / 300 / 400 / 500	925 / 950 / 1000 / 1050 / 1100 / 1150 / 1200
Taxing	0.0 / 0.02 / 0.04	0 / 15 / 30	920 / 935 / 950 / 1000 / 1050 / 1100 / 1150 / 1200 / 1250 / 1300 / 1350
Idle	0.0	0 / 50	850 / 900 / 950

APPENDIX J

The Paremetric Model CODE1X

Listing of Computer Code

The CODE1X Listingin *FORTRAN:*

```
CCCCCCCCCCCCCCCCCCCCCCCCCCCCCCCCCCCCCCCCCCCCCCCCCCCCCCCCCCCCCCCCCCCCCCCCCC
C                                                                     C
C      C l o s e   t o   B o e i n g 7 3 7 - 4 0 0 / 5 0 0            C
C                                                                     C
C      &   C F M 5 6 - 3 C - 1                                        C
C                                                                     C
CCCCCCCCCCCCCCCCCCCCCCCCCCCCCCCCCCCCCCCCCCCCCCCCCCCCCCCCCCCCCCCCCCCCCCCCCC

C  AIRCRAFT ENGINE PERFORMANCE PROGRAM; TURBOFAN ENGINE; SI-UNITS
C  TO CALCULATE FUEL CONSUMPTION OVER CLIMB SEQUENCE
C
C    SEPERAT LP COMPRESSOR STAGE

C  PERFORMANCE CONDITIONS:
C   ALL CONDITION VARIABLE NAMES STARTS WITH AN EXTRA "P"
      REAL PTEMPZRO,PPZRO,PTEMPT4,PMZRO,PETATH
C  REFERENCE QUANTITIES:
      REAL MZRO,MDTZRO,M45
      COMMON TEMPZRO,GAMC,CPC,GAMT,CPT,TEMPT4,MZRO,PIC,PIF,ALPHA,ETAF,ET
     1ACH,TAUTH,PITH,TAUTL,PITL,ETATL,ETAB,PIDMAX,PIB,PIN,PIFN,ETAMH,ETA
     2ML,PZRO,TAUF,TAUCL,PICL,ETACL,MDTZRO,FMDTZRO,F,HPR,WINGAREA,DRAGCO
     3EF,RN1FRAC,M45
C  QUANTITIES CALCULATED BASED ON REF VALUES
      REAL RC,RT,TAUR,PID,TAULMBD,PICH,TAUCH,M9,M19,PIR,TAUCL
      REAL MDOTTURB,MFP1,MFP45
C  QUANTITIES CALCULATED BASED ON PERFORMANCE VALUES
      REAL PAZRO,PVZRO,PTAUR,PPIR,PPID,PTAULMBD,PTAUTL
      REAL PTAUF,PPITL,PTAUCH,PPICH,PPIF,PPT19,PM19,PPT9,PM9,PALPHA
      REAL PMDTZRO,PF,PTMP9ZRO,PV9AZRO,PTMP19ZR,PV19AZRO,PFMDTZRO
      REAL PTSFC,THRUST,PNNLP,PPICL,PTAUCL
      REAL FTIME
      INTEGER ITIME


C
C  VALUES ASSIGNED TO ALL REF.-VARIABLES
C
      TEMPZRO=303.15
      PZRO=101325.0
      GAMC=1.4
      CPC=1040.0
      GAMT=1.33
      CPT=1172.0
      TEMPT4=1620.0
      MZRO=0.0
C  TOTAL PRESSURE ARTIO
      PIC=25.58

C  LOW SPOOL (= FAN AND LPC) PRESSURE RATIO
C       PICL=2.329
C  FAN RPESSURE RATIO ONLY
      PIF=1.679
      ALPHA=5.0
      ETAF=0.85
      ETACH=0.877
      TAUTH=0.729
      PITH=0.2282
      TAUTL=0.748
      PITL=0.2520
```

```
      ETATH=0.883
      ETATL=0.87
      ETAB=0.999
      PIDMAX=0.999
      PIB=0.9675
      PIN=0.998
      PIFN=1.0
      ETAMH=0.99
      ETAML=0.99

      corrfact=0.95

      MDTZRO=322.1
      mdtzro=mdtzro*corrfact
      FMDTZRO=323.6
      fmdtzro=fmdtzro/corrfact

      F=FMDTZRO*MDTZRO
      HPR=42.8E+06
      M45=1.0
C  AIRPLANE PARAMETERS
      WINGAREA=202.9
      DRAGCOEF=0.025
C  RN1FRAC DENOTES THE REFERENCE LP RPM (N1) IN PERCENT OF FULL SPEED

      RN1FRAC=92.0
C  SOME OTHER START VALUES
      FUELCONS=0.0
      TIME=0.0
      GRAVG=9.81
      IPRTCNT=0
    5 CONTINUE
      JPRTCNT=0
      CALL REFPRINT
      PRINT*,' Need to change any of reference engine data? (1/0)'
      READ*,IANS
C  IF DEMANDED NEW VALUES FOR REF VALUES GIVEN THROUGH "REFIN"
      IF(IANS.EQ.1)CALL REFIN
      IF(IANS.EQ.1)GOTO 5

C  WRITES ALL CURRENT REFERENCE DATA TO FILE "RESULTS2"
      IPRTCNT=IPRTCNT+1
      CALL REFFILE(IPRTCNT)
C
C  TAUF AND OTHER PARAMETERS FOR THE REFERENCE CONDITION HAVE TO
C  BE CALCULATED
C
      PIR=FPIR(MZRO,GAMC)
      TAUR=FTAUR(MZRO,GAMC)
      TAUF=1+(PIF**((GAMC-1)/GAMC)-1)/ETAF
      PICH=PIC/PIF
      TAUCH=1+(PICH**((GAMC-1)/GAMC)-1)/ETACH
      TAULMBD=FTAULMBD(CPC,CPT,TEMPT4,TEMPZRO)
      ETAR=1.00000
      IF(MZRO.GT.1.00000)ETAR=1-0.075*((MZRO-1)**1.35)
      PID=PIDMAX*ETAR
      RC=R(GAMC,CPC)
      RT=R(GAMT,CPT)
      TMPT3=TEMPZRO*TAUR*TAUF*TAUCH
      TMPT45=TEMPT4*TAUTH
      PT4=PZRO*PIR*PID*PIF*PICH*PIB
```

```
      PT45=PT4*PITH
      FUELAIR=(CPT*TEMPT4-CPC*TMPT3)/(ETAB*HPR-CPT*TEMPT4)
C  ASSUMING THAT HP TURBINE ENTRANCES, AND STATION 8 (CORE EXIT
C  NOZZLE) ARE CHOKED IN THE REFERENCE CONDITION
      CALL MASSFP(TEMPT4,FUELAIR,1.0,TMP4,MFP1)

      CALL MASSFP(TMPT45,FUELAIR,M45,TMP45,MFP45)
      MDOTTURB=(MDTZRO/(ALPHA+1))*(1+FUELAIR)

      AREA4=MDOTTURB*SQRT(TEMPT4)/(PT4*MFP1)
      AREA45=MDOTTURB*SQRT(TMPT45)/(PT45*MFP45)

C      PRINT*,' MFP1=',MFP1
C      PRINT*,' MFP45=',MFP45
C      PRINT*,' PT4=',PT4
C      PRINT*,' AREA4=',AREA4
C      PRINT*,' AREA45=',AREA45
C      PRINT*,' MDOTTURB=',MDOTTURB
C      PRINT*,' PT45=',PT45
C      PRINT*,' PT5=',PT5
C      PRINT*,' TEMPT4=',TEMPT4
C      PRINT*,' TMPT45=',TMPT45
C      PRINT*,' TMPT5=',TMPT5
C      PRINT*,' PITL=',PITL
C      PRINT*,' TAUTL=',TAUTL
C      PRINT*,' PITH=',PITH
C      PRINT*,' TAUTH=',TAUTH

C DEFAULT VALUES FOR PERFORMANCE/START VARIABLES AND PARAMETERS
C   AMBIENT TEMPERATURE:
      PTEMPZRO=303.15
C   AMBIENT PRESSURE:
      PPZRO=101325.0
C   ALTITUDE AT START
      PALTSTRT=0.00
C   DISTANCE VARIABLE SET TO ZERO
      WAY=0.0
C   ALTITUDE AFTER CLIMB/DESCENT
      PALTEND= 0.0
C   TOTAL DISTANCE [m] TO BE FLOWN
      PWAYEND=1.0
C   TURBINE INLET TEMPERATURE:
      PTEMPT4=1620.0
C   FLIGHT MACH-NUMBER:
      PMZRO=0.0000
C   SPEED AT START
      PVSTART=0.0000
C   LOAD (MASS [kg]) AT START
      PMASSTRT=48000.0
C  CLIMB/DESCENT ANGLE [degrees]
      BETA=0.0
C  N1, ASSUMED TO BE CONSTANT THROUGHOUT THIS SEQUENCE,
C  IN % OF FULL SPEED RPM FOR LP ROTOR
      PN1= 92.0
C
C  CALCULATE CERTAIN PARAMETERS FOR THE REF. CONDITION
C
      PT19=PZRO*FPIR(MZRO,GAMC)*PID*PIF*PIFN
      IF(PT19.LT.PZRO*((GAMC+1)/2)**(GAMC/(GAMC-1)))GOTO 99
      P19=PT19/((GAMC+1)/2)**(GAMC/(GAMC-1))
      GOTO 98
```

```
   99 CONTINUE
      P19=PZRO
   98 CONTINUE
      M19=SQRT((2/(GAMC-1))*(((PT19/P19)**((GAMC-1)/GAMC))-1))
      PT9=PZRO*FPIR(MZRO,GAMC)*PID*PIF*PICH*PIB*PITH*PITL*PIN
      IF(PT9.LT.PZRO*((GAMT+1)/2)**(GAMT/(GAMT-1)))GOTO 97
      P9=PT9/((GAMT+1)/2)**(GAMT/(GAMT-1))
      GOTO 96
   97 CONTINUE
      P9=PZRO
   96 CONTINUE
      M9=SQRT((2/(GAMT-1))*(((PT9/P9)**((GAMT-1)/GAMT))-1))
C
C   "INITIAL VALUES":
C

      PTAUF=TAUF
      PTAUCH=TAUCH
      PTAUTH=TAUTH
      PTAUTL=TAUTL
      PPIF=PIF
      PPICH=PICH
      PPIB=PIB
      PETATH=ETATH
      PPITH=PITH
      PPITL=PITL

C  INPUT NEW PERFORMANCE/START CONDITIONS, AMBIENT TEMP AND PRESSURE,
C  TEMPT4, INITIAL AND FINAL ALTITUDES, CLIMB ANGLE, FLIGHT MACH-NUMBER,
C  N1 AND MASS THROUGH "NEWPERF" (The Tempt4 is just a start value for
C  the iteration process!)

    6 CONTINUE
      PRINT*,' New Start (Performance) Conditions? (1/0)'
      READ*,JANS
      IF(JANS.EQ.1)CALL NEWSEQUE(PTEMPZRO,PPZRO,PTEMPT4,PMZRO,PALTSTRT,P
     1ALTEND,PWAYEND,PVSTART,PMASSTRT,BETA,PN1,DRAGCOEF)
      IF(ABS(PALTEND-PALTSTRT).GT.0.01.AND.PWAYEND.GT.0.01)BETA=ATAN((PA
     1LTEND-PALTSTRT)/PWAYEND)*360.0/6.2831853
      PALTI=PALTSTRT
      PRINT*,'Simple iteration? (0)'
      PRINT*,'Single point run? (1)'
      PRINT*,'Flight sequence? (any other number)'
      READ*,ISINGLE
      IF (ISINGLE.EQ.0.OR.ISINGLE.EQ.1)GOTO 59
      PMASS=PMASSTRT
C  LENGTH OF TIME INTERVALS FOR QUASI STATIONARY CONDITIONS DURING CLIMB
C  OR DESCENT, (1 - 2 sec WORKS ok:)
      PRINT*,' Time steps [seconds]?'
      READ*,DELTIME

   59 CONTINUE
C
C WITH UNCHANGED PERFORMANCE CONDITIONS CONTINUE HERE;
C
C  AMBIENT TEMP. AND PRES. WILL BE ADJUSTED TO THE SPECIFIED ALTITUDE
C  (STANDARD ATHMOSPHERE)
C  CALCULATE AMBIENT SPEED OF SOUND,AMBIENT AIRSPEED, TAU-R,
C    PI-R AND TAU-LAMBDA
C
      CALL ATMOSPH(PALTI,PTEMPZRO,PPZRO)
```

```
C  ***************************
C            PTEMPZRO=303.15
C  ***************************
      PAZRO=A(GAMC,RC,PTEMPZRO)
C IF START-MACH NUMBER > 0 AND SPEED = 0: NEW SPEED BASED ON M,
C SPEED > 0 IS THE GOVERNING PARAMETER
      IF(PMZRO.GT.0.00001.AND.PVSTART.LT.0.001)PVSTART=V(PAZRO,PMZRO)
      PVZRO=PVSTART
C NEW MACH NUMBER IN CASE IT DID NOT MATCH THE "GOVERNING SPEED"
      PMZRO=PVZRO/PAZRO

      GOTO 61

   60 CONTINUE
C FOR A NEW POINT IN FLIGHT:
      CALL ATMOSPH(PALTI,PTEMPZRO,PPZRO)
C  ***************************
C            PTEMPZRO=303.15
C  ***************************

      PAZRO=A(GAMC,RC,PTEMPZRO)
      PMZRO=PVZRO/PAZRO

   61 CONTINUE
      INUMBER=0

      PTT4INCR=0.00001
    7 CONTINUE
      INUMBER=INUMBER+1
      PTAUR=FTAUR(PMZRO,GAMC)
      ETAR=1.00000
      IF(PMZRO.GT.1.00000)ETAR=1-0.075*((PMZRO-1)**1.35)
      PPID=PIDMAX*ETAR
      PPIR=FPIR(PMZRO,GAMC)
      PTAULMBD=FTAULMBD(CPC,CPT,PTEMPT4,PTEMPZRO)
      WAYPRV=WAY
      PALTIPRV=PALTI
C
  100 CONTINUE
      PTAULMBD=FTAULMBD(CPC,CPT,PTEMPT4,PTEMPZRO)
C
C  ITERATION LOOP:
C  CALCULATES ENGINE PARAMETERS FOR A SPECIFIC POINT IN TIME, BASED ON
C  REFERENCE (DESIGN) CONDITION AND PERFORMANCE MACH-NUMBER, AMBIENT
C  CONDITION AND TUB. INL. TEMP. Tt4
C

      CALL       ITERATE(CPC,CPT,RC,RT,GAMC,GAMT,TAUR,TAULMBD,TAUF
     1,TAUCH,TAUTL,PIR,PID,PIF,      PICH,PITL,PIN,PIFN,PTAUR,PTAULMBD,PT
     2AUF,       PTAUCH,PTAUTH,PTAUTL,PPIR,PPID,PPIF,PPT4,  PPICH,PPIB,PP
     3ITH,PPITL,TEMPZRO,TEMPT4,PZRO     ,PTEMPZRO,PTEMPT4,PPZRO,PP9,PPT9,
     4PP19,PPT19,MZRO,M9,M19,PMZRO,PM9,PM19,ETAF,ETACL,ETACH,ETAB,ETATL,
     5ALPHA,PALPHA,IBADDATA,PMDTZRO,MDTZRO,PF,HPR,AREA4,AREA45,PETATH,TM
     6PT45,ETAML,BETA)

C  TO GIVE A NEW START:
      IF(IBADDATA.EQ.1)GOTO 5
C  STOP:
      IF(IBADDATA.EQ.10)GOTO 999

C  PNNLP is (N1/N1ref):
```

```
      PNNLP=SQRT(((PTEMPZRO*PTAUR)/(TEMPZRO*TAUR))*((PPIF**((GAMC-1)/GAM
     1C)-1)/(PIF**((GAMC-1)/GAMC)-1)))


C  PN1TEST is current N1 (%):
      PN1TEST=PNNLP*RN1FRAC

      IF(ISINGLE.EQ.0)GOTO 997

      PRVTT4IN=PTT4INCR

C  Generate Tt4 incremet (2K) to meet required N1:
      PTT4INCR=2.0*(PN1-PN1TEST)/ABS(PN1-PN1TEST)

C  The fluctuations of PN1 around PN1TEST may continue if the PN1TEST does
C  not hit close enough. Looping the program will be stopped if PN1TEST
C  fluctuates around PN1.

      IF(PTT4INCR/PRVTT4IN.GE.0.000000.OR.INUMBER.LT.10)GOTO 996
      PRINT*,' N1 does not hit the target value close enough for the pro
     1gram to stop. There is probably a fluctuation.'
      PRINT*,' Current N1 is:',PN1TEST
      PRINT*,' Target value: ',PN1
      PRINT*,' Execution continues, current N1 is used. Accepted? (1/0)'
      READ*,IBADHIT
      IF(IBADHIT.EQ.0)GOTO 999

  996 CONTINUE
      IF(ABS(PN1-PN1TEST).LT.0.1)GOTO 997
      PTEMPT4=PTEMPT4+PTT4INCR
      IF(INUMBER.LT.1000)GOTO 994
      PRINT*,' Number of loops in main program:',INUMBER
      GOTO 999
  994 CONTINUE

      GOTO 7
  997 CONTINUE
C
C  "REMAINING CALCULATIONS":
C
      PTMP9ZRO=((PTAULMBD*PTAUTH*PTAUTL)/((PPT9/PP9)**((GAMT-1)/GAMT)))*
     1(CPC/CPT)
      PTEMP9=PTEMPZRO*PTMP9ZRO
      PV9AZRO=PM9*SQRT((GAMT*RT*PTEMP9)/(GAMC*RC*PTEMPZRO))
      PTMP19ZR=PTAUR*PTAUF/((PPT19/PP19)**((GAMC-1)/GAMC))
      PV19AZRO=PM19*SQRT(PTMP19ZR)

      PFMDTZRO=(PAZRO/(1+PALPHA))*((1+PF)*PV9AZRO-PMZRO+(1+PF)*(RT/RC)*(
     1PTMP9ZRO/PV9AZRO)*((1-PPZRO/PP9)/GAMC))+(PAZRO*PALPHA/(1+PALPHA))*
     2(PV19AZRO-PMZRO+(PTMP19ZR/PV19AZRO)*((1-PPZRO/PP19)/GAMC))
C       print*,'2.: Pfmdtzro',Pfmdtzro
C       print*,'PAZRO,PALPHA,PF,PV9AZRO',PAZRO,PALPHA,PF,PV9AZRO
C       print*,'AZRO,ALPHA,FUELAIR,V9AZRO',AZRO,ALPHA,FUELAIR,V9AZRO
C       print*,'PMZRO,RT,RC,PTMP9ZRO,PPZRO',PMZRO,RT,RC,PTMP9ZRO,PPZRO
C       print*,'PP9,GAMC,PTMP19ZR',PP9,GAMC,PTMP19ZR
C       print*,'PV19AZRO,PP19',PV19AZRO,PP19

C  not yet: PTSFC IS CONVERTED TO (kg/hr)/N, AS SUPPOSED TO (kg/s)/N.
      PTSFC=(PF/((1+PALPHA)*PFMDTZRO))
      THRUST=PFMDTZRO*PMDTZRO
```

```
C      PRINT*,' Need print of all results? (1/0)'
C      READ*,JANS
C      IF (JANS.NE.1)GOTO 998

C      CALL TESTPRINT          (RC,RT,PAZRO,PVZRO,TAUR,PID,TAULMBD,TAUF,T
C     1AUCH,PIF,TAUTH,TAUTL,PIN,PIFN,PT9,PT19,PTAUR,PPID,PTAULMBD,PTAUF,P
C     2TAUCH,PICH,PPICH,PPIF,PTAUTL,M9,M19,PM9,PM19,PPT9,PPT19,ALPHA,PALP
C     3HA)

  998 CONTINUE

      CALL       EMISSIONS(PPT4,PPIB,PTEMPZRO,PTAUR,PTAUF,PTAUCH,PMDTZRO
     1,PALPHA,PTEMPT4,PF,PTSFC,THRUST,FUELFL,EMCO2,EMH2O,EMNOX,EMCOM1,EM
     2UHC1,EMCOM2,EMUHC2)

      JPRTCNT=JPRTCNT+1
C
C PRINT EVERY 30 SECONDS
C
      FTIME=TIME/30.0
      ITIME=TIME/30.0

      IF((FTIME-ITIME).LT.0.001)THEN
      CALL RESULTOUT           (pitl,RC,RT,PAZRO,PVZRO,TAUR,PID,TAULMBD,
     1TAUF,TAUCH,PIF,TAUTH,TAUTL,PIN,PIFN,PT9,PT19,PTAUR,PPID,PTAULMBD,P
     2TAUF,PTAUCH,PICH,PPICH,PPIF,PTAUTL,M9,M19,PM9,PM19,PPT9,PPT19,ALPH
     3A,PALPHA,PPITL,MDTZRO,PMDTZRO,PF,PTMP9ZRO,PTEMP9,PV9AZRO,PTMP19ZR,
     4PV19AZRO,PTSFC,THRUST,PNNLP,PNNHP,PTEMPZRO,PPZRO,PTEMPT4,PMZRO,CPC
     5,CPT,GAMC,GAMT,HPR,TAUCL,PTAUCL,  PTAUTH,PICL,PPICL,PIB,PPIB,PITH,P
     6PITH,PFMDTZRO,FMDTZRO,PPIN,PPIFN,IPRTCNT,JPRTCNT,FUELCONS,TIME,WAY
     7,FUELFL,EMCO2,EMH2O,EMNOX,EMCOM1,EMUHC1,EMCOM2,EMUHC2,BETA)
      CALL RESULTTWO           (pitl,RC,RT,PAZRO,PVZRO,TAUR,PID,TAULMBD,
     1TAUF,TAUCH,PIF,TAUTH,TAUTL,PIN,PIFN,PT9,PT19,PTAUR,PPID,PTAULMBD,P
     2TAUF,PTAUCH,PICH,PPICH,PPIF,PTAUTL,M9,M19,PM9,PM19,PPT9,PPT19,ALPH
     3A,PALPHA,PPITL,MDTZRO,PMDTZRO,PF,PTMP9ZRO,PTEMP9,PV9AZRO,PTMP19ZR,
     4PV19AZRO,PTSFC,THRUST,PNNLP,PNNHP,PTEMPZRO,PPZRO,PTEMPT4,PMZRO,CPC
     5,CPT,GAMC,GAMT,HPR,TAUCL,PTAUCL,  PTAUTH,PICL,PPICL,PIB,PPIB,PITH,P
     6PITH,PFMDTZRO,FMDTZRO,PPIN,PPIFN,IPRTCNT,JPRTCNT,FUELCONS,TIME,WAY
     7,FUELFL,EMCO2,EMH2O,EMNOX,EMCOM1,EMUHC1,EMCOM2,EMUHC2,BETA,PMASS)

      ENDIF

      IF(ISINGLE.EQ.0.OR.ISINGLE.EQ.1)GOTO 993

C  CALL OF SUBROUTINE TO EVALUATE NEW SPEED. ALTITUDE, ACCELERATION
C       MASS, FUEL CONSUMPTION, TIME ELAPSED

      CALL       LEGSTEP(PVZRO,PMZRO,PPZRO,PTEMPZRO,PALTI,THRUST,BETA,PA
     1CCEL,PTSFC,PMASS,WINGAREA,DRAGCOEF,RC,GRAVG,DELTIME,FUELCONS,TIME,
     2WAY)
      OPEN(UNIT=2,FILE='INCRFILE')
      WRITE(2,11)ITIME,PVZRO,PACCEL,FUELCONS,PALTI,(WAY/1000)
   11 FORMAT(' Time:',I6,' Speed',F8.0,' Accel.:',F8.5,' Fuelcon.:',F8.2
     1,'Curr. alt.:',F8.0,' Curr. dist.:',F8.0)

C  Counting the outer loop in main program:
      IOUTER=IOUTER+1

      IF(PWAYEND.LT.0.1)GOTO 991
C
```

```
C  IF FINAL DISTANCE IS NOT REACHED, GO FOR ONE MORE STEP IN TIME
C
      IF(ABS(WAY-PWAYEND).GT.1.0.AND.(WAY-PWAYEND)*(WAYPRV-PWAYEND).GT.0
     1.000000)GOTO 60
      GOTO 992
  991 CONTINUE
C
C  IF FINAL ALTITUDE IS NOT REACHED, GO FOR ONE MORE STEP IN TIME
C
      IF(ABS(PALTI-PALTEND).GT.1.0.AND.(PALTI-PALTEND)*(PALTIPRV-PALTEND
     1).GT.0.000000)GOTO 60
  992 CONTINUE
  993 CONTINUE
      PRINT*,' PALTSTRT:  ',PALTSTRT,'  PALTEND: ',PALTEND
      PRINT*,' THRUST: ',THRUST,'  PACCEL:  ',PACCEL
      PRINT*,' PMASS:  ',PMASS,'  FUELCONS:',FUELCONS
      PRINT*,' PWAYEND:',PWAYEND/1000.0,'  WAY     :',WAY/1000.0
      PRINT*,' TIME:   ',TIME,'  PTSFC [mg/Ns]:   ',PTSFC*1E6
      PRINT*,' PMZRO:  ',PMZRO,'  PVZRO:   ',PVZRO
      PRINT*,' PTEMPT4:',PTEMPT4,'  PPZRO:   ',PPZRO
C
C PRINT LAST CONDITION OF LEG
C
      CALL       RESULTOUT     (PITL,RC,RT,PAZRO,PVZRO,TAUR,PID,TAULMBD,
     1TAUF,TAUCH,PIF,TAUTH,TAUTL,PIN,PIFN,PT9,PT19,PTAUR,PPID,PTAULMBD,P
     2TAUF,PTAUCH,PICH,PPICH,PPIF,PTAUTL,M9,M19,PM9,PM19,PPT9,PPT19,ALPH
     3A,PALPHA,PPITL,MDTZRO,PMDTZRO,PF,PTMP9ZRO,PTEMP9,PV9AZRO,PTMP19ZR,
     4PV19AZRO,PTSFC,THRUST,PNNLP,PNNHP,PTEMPZRO,PPZRO,PTEMPT4,PMZRO,CPC
     5,CPT,GAMC,GAMT,HPR,TAUCL,PTAUCL,  PTAUTH,PICL,PPICL,PIB,PPIB,PITH,P
     6PITH,PFMDTZRO,FMDTZRO,PPIN,PPIFN,IPRTCNT,JPRTCNT,FUELCONS,TIME,WAY
     7,FUELFL,EMCO2,EMH2O,EMNOX,EMCOM1,EMUHC1,EMCOM2,EMUHC2,BETA)
      CALL       RESULTTWO     (PITL,RC,RT,PAZRO,PVZRO,TAUR,PID,TAULMBD,
     1TAUF,TAUCH,PIF,TAUTH,TAUTL,PIN,PIFN,PT9,PT19,PTAUR,PPID,PTAULMBD,P
     2TAUF,PTAUCH,PICH,PPICH,PPIF,PTAUTL,M9,M19,PM9,PM19,PPT9,PPT19,ALPH
     3A,PALPHA,PPITL,MDTZRO,PMDTZRO,PF,PTMP9ZRO,PTEMP9,PV9AZRO,PTMP19ZR,
     4PV19AZRO,PTSFC,THRUST,PNNLP,PNNHP,PTEMPZRO,PPZRO,PTEMPT4,PMZRO,CPC
     5,CPT,GAMC,GAMT,HPR,TAUCL,PTAUCL,  PTAUTH,PICL,PPICL,PIB,PPIB,PITH,P
     6PITH,PFMDTZRO,FMDTZRO,PPIN,PPIFN,IPRTCNT,JPRTCNT,FUELCONS,TIME,WAY
     7,FUELFL,EMCO2,EMH2O,EMNOX,EMCOM1,EMUHC1,EMCOM2,EMUHC2,BETA,PMASS)

      PRINT*,' The whole thing over again? (1) or'
      PRINT*,' continue on new flight sequence, start with current condi
     1tions (2)? (0=END)'
      READ*,NANSW
      IF(NANSW.EQ.1)GOTO 5
      IF(NANSW.EQ.2)GOTO 6
  999 CONTINUE
      PRINT*,'    M A I N   P R O G R A M   S T O P P E D  !!'
       END
C
C  END CORE PROGRAM
C               END CORE PROGRAM
C                           END CORE PROGRAM
C                                       END CORE PROGRAM
C                                                   END CORE PROGRAM
C  ***********************************************************************
C  ***********************************************************************
C  SUBROUTIENE TO PERFORM ITERATIONS, SOLVING THE SET OF CYCLE EQUATIONS
C  ***********************************************************************
      SUBROUTINE ITERATE(CPC,CPT,RC,RT,GAMC,GAMT,TAUR,TAULMBD,TAUF
     1,TAUCH,TAUTL,PIR,PID,PIF,      PICH,PITL,PIN,PIFN,PTAUR,PTAULMBD,PT
```

```
     2AUF,       PTAUCH,PTAUTH,PTAUTL,PPIR,PPID,PPIF,PPT4,  PPICH,PPIB,PP
     3ITH,PPITL,TEMPZRO,TEMPT4,PZRO     ,PTEMPZRO,PTEMPT4,PPZRO,PP9,PPT9,
     4PP19,PPT19,MZRO,M9,M19,PMZRO,PM9,PM19,ETAF,ETACL,ETACH,ETAB,ETATL,
     5ALPHA,PALPHA,IBADDATA,PMDTZRO,MDTZRO,PF,HPR,AREA4,AREA45,PETATH,TM
     6PT45,ETAML,BETA)
      REAL MZRO,M9,M19,MDTZRO
C      print*,'               I T E R A T E   iterate I T E R A T E'
C      print*,'               I T E R A T E   iterate I T E R A T E'
      IBADDATA=0

      APPROX=0.001
  499 CONTINUE
      JJ=0
  501
       DO 500 II=1,4
      PTAULMBD=FTAULMBD(CPC,CPT,PTEMPT4,PTEMPZRO)

      PTAUCH=1+(((PTEMPT4/PTEMPZRO)/(TEMPT4/TEMPZRO))*((FTAUR(MZRO,GAMC)
     1*TAUF)/(FTAUR(PMZRO,GAMC)*PTAUF))*(TAUCH-1))
      PPICH=(1+(PTAUCH-1)*ETACH)**(GAMC/(GAMC-1))
      PPIF=(1+(PTAUF-1)*ETAF)**(GAMC/(GAMC-1))

      PPT19=PPZRO*PPIR*PPID*PPIF*PIFN
C PID AND PIFN EQUIVALENT IN REF AND PERFORMANCE CONDITIONS

      IF(PPT19.LT.PPZRO*((GAMC+1)/2)**(GAMC/(GAMC-1)))GOTO 999

      PP19=PPT19/(((GAMC+1)/2)**(GAMC/(GAMC-1)))
      GOTO 998
  999 CONTINUE
      PP19=PPZRO
  998 CONTINUE

      IF(PPT19.GT.PP19)GOTO 994
      PRINT*,' Bypass nozzle exit total pressure is less than the nozzle
     1 exit static pressure!'
      PRINT*,' That is impossible. Modify input data.'
      PRINT*,' Modify = 1; Stop = 10'
      READ*,IBADDATA
      GOTO 502
  994 CONTINUE
      PM19=SQRT((2/(GAMT-1))*(((PPT19/PP19)**((GAMT-1)/GAMT))-1))
      PPT9=PPZRO*PPIR*PPID*PPIF*PPICH*PPIB*PPITH*PPITL*PIN

C PIB, AND PIN EQUIVALENT IN REF AND PERFORMANCE CONDITIONS

      IF(PPT9.LT.PPZRO*((GAMT+1)/2)**(GAMT/(GAMT-1)))GOTO 997
      PP9=PPT9/(((GAMT+1)/2)**(GAMT/(GAMT-1)))
      GOTO 996
  997 CONTINUE
      PP9=PPZRO
  996 CONTINUE

      IF(PPT9.GT.PP9)GOTO 995
      PRINT*,' Nozzle exit total pressure is less than the nozzle exit s
     1tatic pressure!'
      PRINT*,' That is impossible. Modify input data.'
      PRINT*,' Modify=1; Stop=10'
      READ*,IBADDATA
      GOTO 502
```

```
  995 CONTINUE
      PM9=SQRT((2/(GAMT-1))*(((PPT9/PP9)**((GAMT-1)/GAMT))-1))
      PALPHA=ALPHA*(PICH/PPICH)*SQRT((PTAULMBD/(PTAUR*PTAUF))/(FTAULMBD(
     1CPC,CPT,TEMPT4,TEMPZRO)/(FTAUR(MZRO,GAMC)*TAUF)))*AMFP(PM19,GAMT,R
     2T)/AMFP(M19,GAMT,RT)


      PTAUF=1+((1-PTAUTL)/(1-TAUTL))*((PTAULMBD/PTAUR)/(TAULMBD/TAUR))*(
     1(1+ALPHA)/(1+PALPHA))*(TAUF-1)
      PRVTAUTL=PTAUTL
      PTAUTL=1-ETATL*(1-PPITL**((GAMT-1)/GAMT))

      PPITL=PITL*SQRT(PTAUTL/TAUTL)*(AMFP(M9,GAMT,RT)/AMFP(PM9,GAMT,RT))
C###################
C      print*,'test iterate',ABS(ptautl-prvtautl),ptautl,prvtautl,approx

      PTAUTLDF=ABS(PTAUTL-PRVTAUTL)/PRVTAUTL

      PTMPT45=PTEMPT4*PTAUTH
      PPT4=PPZRO*PPIR*PPID*PPIF*PPICH*PPIB
      PPT45=PPT4*PPITH

      PMDTZRO=MDTZRO*((1+PALPHA)/(1+ALPHA))*((PPZRO*PPIR*PPID*PPIF *PPIC
     1H)/(PZRO*PIR*PID*PIF*PICH))*SQRT(TEMPT4/PTEMPT4)



      PF=(PTAULMBD-PTAUR*PTAUF *PTAUCH)/((HPR*ETAB)/(CPC*PTEMPZRO)-PTAUL
     1MBD)
      PMDT4=PMDTZRO*(PF+1)/(PALPHA+1)
      PMFP4=SQRT(PTEMPT4)*PMDT4/(PPT4*AREA4)
      PMFP45=SQRT(PTMPT45)*PMDT4/(PPT45*AREA45)
c      ibaddata=10
C      goto 502
      IF(PMFP4.GT.((SQRT(GAMT/RT))/((1+((GAMT-1)/2))**((GAMT+1)/(2*(GAMT
     1-1)))-1.0E-5)))GOTO 25
c      print*,'test8'
      CALL MACHNUMB(PMFP4,PM4,GAMT,RT)

      GOTO 26
   25 CONTINUE

      PM4=1.00000
   26 CONTINUE
      IF(PMFP45.GT.((SQRT(GAMT/RT))/((1+((GAMT-1)/2))**((GAMT+1)/(2*(GAM
     1T-1)))-1.0E-5)))GOTO 27

      CALL MACHNUMB(PMFP45,PM45,GAMT,RT)
      GOTO 28
   27 CONTINUE

      PM45=1.00000
   28 CONTINUE

      A4A45=AREA4/AREA45

      IF(BETA.LT.-0.01)THEN
      CALL TURB(PTEMPT4,PF,A4A45,PM4,PM45,PETATH,PTMPT45,PPITH,PTAUTH,PT
     1T45)
      ENDIF
```

```
C       IF(NJJ.GT.100)PTAUTL=PTAUTL-0.5*(PTAUTL-PRVTAUTL)

C       IF(PTAUTLDF.LT.0.001.AND.II.GT.2)GOTO 503

  500 CONTINUE
      JJ=JJ+1
      NJJ=4*JJ
C      PRINT*,NJJ,' iterations are performed'
c       BTAUTLDF=(PTAUTL-PRVTAUTL)/PRVTAUTL
c       print*,'Btautldf:',btautldf
      IF (PTAUTLDF.GT.APPROX.AND.NJJ.LE.1000)GOTO 501
      IF(NJJ.LE.1000)GOTO 503
      PRINT*,' No complete convergence with 1000 iterations! Want to'
      PRINT*,'    - continue iterations:                          (5)'
      PRINT*,'    - set easier requiremen, current:',APPROX
      PRINT*,'      and continue iterations:                      (6)'
      PRINT*,'    - give new data:                                (1)'
      PRINT*,'    - terminate:                                   (10)'
      READ*,IBADDATA
      IF(IBADDATA.EQ.6)PRINT*,' New limit for iteration?'
      IF(IBADDATA.EQ.6)READ*,APPROX
      IF(IBADDATA.EQ.5.OR.IBADDATA.EQ.6)GOTO 499
  503 CONTINUE
  502 CONTINUE

C      print*,' U t  a v  I t e r a t e !!'
      RETURN
      END

C  ***********************************************************************
C   SUBROUTINE TO CALCULATE PERFORMANCE over A LEG
C  ***********************************************************************
      SUBROUTINE LEGSTEP(PVZRO,PMZRO,PPZRO,PTEMPZRO,PALTI,THRUST,BETA,PA
     1CCEL,PTSFC,PMASS,WINGAREA,DRAGCOEF,RC,GRAVG,DELTIME,FUELCONS,TIME,
     2WAY)
C      print*,' legstep'

      ROAIR=PPZRO/(RC*PTEMPZRO)
C
C   CALCULATION FOR TWO ENGINES (THE WHOLE AIRCRAFT)
C
      PFUELFLW=2.0*PTSFC*THRUST
      DELFUEL=PFUELFLW*DELTIME
      DELMASS=0.0-DELFUEL
      PACCEL=(2.0*THRUST-0.5*DRAGCOEF*ROAIR*WINGAREA*(PVZRO**2.0)-PVZRO*
     1DELMASS-PMASS*GRAVG*SIN(6.2831853*BETA/360.0))/PMASS

c       print*,'  In Legstep: accel = ',paccel
C       print*,' Beta: & sinbeta: ',beta,SIN(6.2831853*BETA/360.0)
c       print*,'  Drag: ',0.5*DRAGCOEF*ROAIR*WINGAREA*(PVZRO**2.0)
c       print*,'  Grav.comp.:',PMASS*GRAVG*SIN(6.2831853*BETA/360.0)
c       print*,'2.*thrust,pvzro:',2.*thrust,pvzro
      PALTI=PALTI+(PVZRO*DELTIME+0.5*PACCEL*(DELTIME**2.0))*SIN(6.283185
     13*BETA/360.0)
      WAY=WAY+(PVZRO*DELTIME+0.5*PACCEL*(DELTIME**2.0))*COS(6.2831853*BE
     1TA/360)
      PVZRO=PVZRO+PACCEL*DELTIME
      FUELCONS=FUELCONS+DELFUEL
      PMASS=PMASS+DELMASS
      TIME=TIME+DELTIME
      ITIME=TIME
```

```
      TIMEHR=TIME/3600.0
      ITIMEHR=TIMEHR
      TIMEMIN=(TIMEHR-ITIMEHR)*60
      ITIMEMIN=TIMEMIN
      TIMESEC=(TIME-ITIMEHR*3600-ITIMEMIN*60)
      ITIMESEC=TIMESEC

      IF((ITIMEMIN.EQ.0.OR.ITIMEMIN.EQ.15.OR.ITIMEMIN.EQ.30.OR.ITIMEMIN.
     1EQ.45).AND.TIMESEC.LT.DELTIME)WRITE(6,10)ITIMEHR,ITIMEMIN,ITIMESEC
     2,PALTI,(WAY/1000.0)
   10 FORMAT(' Time elapsed:',I2,':',I2,':',I2,'  Curr. alt. [m]:',F8.0,
     1' Curr. dist. [km]:',F8.0)
      RETURN
      END

C  ***********************************************************************
C  SUBROUTINE TO ASK IF NEW REFERENCE DATA ARE REQUIRED
C  ***********************************************************************
      SUBROUTINE REFIN
      REAL MZRO,MDTZRO,M45
      COMMON TEMPZRO,GAMC,CPC,GAMT,CPT,TEMPT4,MZRO,PIC,PIF,ALPHA,ETAF,ET
     1ACH,TAUTH,PITH,TAUTL,PITL,ETATL,ETAB,PIDMAX,PIB,PIN,PIFN,ETAMH,ETA
     2ML,PZRO,TAUF,TAUCL,PICL,ETACL,MDTZRO,FMDTZRO,F,HPR,WINGAREA,DRAGCO
     3EF,RN1FRAC,M45

      CALL NEWREF(I,TEMPZRO,'TEMPZRO')
      IF(I.NE.1)GOTO 5
      CALL NEWREF(I,GAMC,'   GAMC')
      IF(I.NE.1)GOTO 5
      CALL NEWREF(I,CPC,'    CPC')
      IF(I.NE.1)GOTO 5
      CALL NEWREF(I,GAMT,'   GAMT')
      IF(I.NE.1)GOTO 5
      CALL NEWREF(I,CPT,'    CPT')
      IF(I.NE.1)GOTO 5
      CALL NEWREF(I,M45,'    M45')
      IF(I.NE.1)GOTO 5

      CALL NEWREF(I,TEMPT4,' TEMPT4')
      IF(I.NE.1)GOTO 5
      CALL NEWREF(I,MZRO,'   MZRO')
      IF(I.NE.1)GOTO 5
      CALL NEWREF(I,PIC,'    PIC')
      IF(I.NE.1)GOTO 5
      CALL NEWREF(I,PICL,'   PICL')
      IF(I.NE.1)GOTO 5
      CALL NEWREF(I,PIF,'    PIF')
      IF(I.NE.1)GOTO 5
      CALL NEWREF(I,ALPHA,'  ALPHA')
      IF(I.NE.1)GOTO 5
      CALL NEWREF(I,ETAF,'   ETAF')
      IF(I.NE.1)GOTO 5
      CALL NEWREF(I,ETACL,'  ETACL')
      IF(I.NE.1)GOTO 5
      CALL NEWREF(I,ETACH,'  ETACH')
      IF(I.NE.1)GOTO 5
      CALL NEWREF(I,TAUTH,'  TAUTH')
      IF(I.NE.1)GOTO 5
      CALL NEWREF(I,PITH,'   PITH')
      IF(I.NE.1)GOTO 5
      CALL NEWREF(I,TAUTL,'  TAUTL')
```

```
      IF(I.NE.1)GOTO 5
      CALL NEWREF(I,PITL,'   PITL')
      IF(I.NE.1)GOTO 5
      CALL NEWREF(I,ETATL,'  ETATL')
      IF(I.NE.1)GOTO 5
      CALL NEWREF(I,ETAB,'   ETAB')
      IF(I.NE.1)GOTO 5
      CALL NEWREF(I,PIDMAX,' PIDMAX')
      IF(I.NE.1)GOTO 5
      CALL NEWREF(I,PIB,'    PIB')
      IF(I.NE.1)GOTO 5
      CALL NEWREF(I,PIN,'    PIN')
      IF(I.NE.1)GOTO 5
      CALL NEWREF(I,PIFN,'   PIFN')
      IF(I.NE.1)GOTO 5
      CALL NEWREF(I,ETAMH,'  ETAMH')
      IF(I.NE.1)GOTO 5
      CALL NEWREF(I,ETAML,'  ETAML')
      IF(I.NE.1)GOTO 5
      CALL NEWREF(I,PZRO,'   PZRO')
      IF(I.NE.1)GOTO 5
      CALL NEWREF(I,MDTZRO,' MDTZRO')
      IF(I.NE.1)GOTO 5
      CALL NEWREF(I,FMDTZRO,'FMDTZRO')
      IF(I.NE.1)GOTO 5
      CALL NEWREF(I,F,'      F')
      IF(I.NE.1)GOTO 5
      CALL NEWREF(I,HPR,'    HPR')
      IF(I.NE.1)GOTO 5
      CALL NEWREF(I,WINGAREA,'WINGAREA')
      IF(I.NE.1)GOTO 5
      CALL NEWREF(I,DRAGCOEF,'DRAGCOEF')
      IF(I.NE.1)GOTO 5
      CALL NEWREF(I,RN1FRAC,'RN1FRAC')
      IF(I.NE.1)GOTO 5
    5 CONTINUE
      RETURN
      END
C  ***********************************************************************
C   SUBROTINE PRESENT OLD REFERECE VARIABLES AND READ NEW
C  ***********************************************************************
      SUBROUTINE NEWREF(IVAR,AVAR,BVAR)
      INTEGER IVAR
      REAL AVAR
      CHARACTER BVAR*7

      IVAR=1
      PRINT*,BVAR,' = ',AVAR,' Change? (1/0)'
      READ*,IANS
      IF(IANS.LT.1) GOTO 10
      PRINT*,' New value:'
      READ*,AVAR
      PRINT*,' More modifications in ref.data this run? (1/0)'
      READ*,IVAR
   10 CONTINUE
      RETURN
       END
C  ***********************************************************************
C   SUBROTINE PRESENTS PERFORMANCE VARIABLES IF ANY, AND READ NEW
C  ***********************************************************************
      SUBROUTINE NEWSEQUE(PTEMPZRO,PPZRO,PTEMPT4,PMZRO,PALTI,PALTEND,PWA
```

```
     1YEND,PVSTART,PMASSTRT,BETA,PN1,DRAGCOEF)
      CHARACTER TEXT1*32,TEXT2*32,TEXT3*32,TEXT4*32,TEXT5*32
      CHARACTER TEXT6*32,TEXT7*32,TEXT8*32,TEXT9*32,TEXT10*32,TEXT11*32
      CHARACTER TEXT12*32

      TEXT1='   Ambient Temperature [K]:    '
      TEXT2='   Ambient Pressure [Pa]:      '
      TEXT3='   Turbine inlet temp. [K]:    '
      TEXT4='   Initial Mach-number:        '
      TEXT5='   Initial Altitude [m]:       '

      TEXT6='   Final Altitude [m]:         '
      TEXT11='   Final Distance [km]:        '
      TEXT12='   Drag Coefficient:           '
      TEXT7='   Initial Speed  [m/s]:       '
      TEXT8='   Initial mass [kg]:          '
      TEXT9='   Climb Angel [degrees]:      '
      TEXT10='   Low Pressure speed [%]:     '
      PWAYEND=PWAYEND/1000.0
   90 CONTINUE
      PRINT*,' Performance conditions are as follows:'
      PRINT*,TEXT1,PTEMPZRO
      PRINT*,TEXT2,PPZRO
      PRINT*,TEXT5,PALTI
      PRINT*,TEXT3,PTEMPT4,' will change !'
      PRINT*,TEXT4,PMZRO,' used when speed is 0.00 !'
      PRINT*,TEXT6,PALTEND
      PRINT*,TEXT11,PWAYEND
      PRINT*,TEXT7,PVSTART
      PRINT*,TEXT8,PMASSTRT
      PRINT*,TEXT12,DRAGCOEF
      PRINT*,TEXT9,BETA,' should not be used'
c      PRINT*,'                                                    and chang
c     1e of altitude'
c      PRINT*,'                                                    are both
c     1diff. from  0.0'
      PRINT*,TEXT10,PN1
      PRINT*,'    '
      PRINT*,' Any modifications?  (1/0)'
      PRINT*,'    '
      PRINT*,'    (The code will calculate ambient temperature and pressu
     1re'
      PRINT*,'     unless altitude is set at 0.00000)'
      READ*,IANSW
      IF(IANSW.NE.1)GOTO 100
       CALL PERFREAD(PALTI,TEXT5)
      IF(PALTI.GT.0.001)GOTO 91
      CALL PERFREAD(PTEMPZRO,TEXT1)
      CALL PERFREAD(PPZRO,TEXT2)
   91 CONTINUE
      CALL ATMOSPH(PALTI,PTEMPZRO,PPZRO)
C  ****************************
C            PTEMPZRO=303.15
C  ****************************

      CALL PERFREAD(PVSTART,TEXT7)
      IF(PVSTART.GT.0.001)GOTO 92
      CALL PERFREAD(PMZRO,TEXT4)
   92 CONTINUE
      CALL PERFREAD(PTEMPT4,TEXT3)
      CALL PERFREAD(PALTEND,TEXT6)
```

```
      CALL PERFREAD(PWAYEND,TEXT11)
      CALL PERFREAD(PMASSTRT,TEXT8)
      CALL PERFREAD(DRAGCOEF,TEXT12)
      CALL PERFREAD(BETA,TEXT9)
      CALL PERFREAD(PN1,TEXT10)
      GOTO 90
  100 CONTINUE
      PWAYEND=PWAYEND*1000.0
      RETURN
      END
C  ***********************************************************************
C   SUBROTINE PRESENT PERFORMANECE VARIABLES AND READ NEW
C  ***********************************************************************
      SUBROUTINE PERFREAD(AVAR,BVAR)
      REAL AVAR
      CHARACTER BVAR*32

      PRINT*,BVAR,' = ',AVAR,' Change? (1/0)'
      READ*,IANS
      IF(IANS.LT.1) GOTO 10
      PRINT*,' New value:'
      READ*,AVAR
   10 CONTINUE
      RETURN
       END
C  ***********************************************************************
C  SUBROUTINE TO CALCULATE (INTERPOLATE) STANDARD ATMOSPHERE (SI-units)
C  ***********************************************************************
      SUBROUTINE ATMOSPH(PALTI,PTEMPZRO,PPZRO)
      REAL T(41),P(41)

      OPEN(UNIT=2,FILE='ATMOTEMP')
      OPEN(UNIT=3,FILE='ATMOPRES')
      DO 10 I=1,41
      READ(2,101)T(I)
      READ(3,101)P(I)
  101 FORMAT(F10.6)
   10 CONTINUE
      CLOSE(2)
      CLOSE(3)
      IALT=PALTI/1000.0
      PTEMPZRO=T(IALT+1)+((T(IALT+2)-T(IALT+1))/1000.0)*(PALTI/1000.0-AI
     1NT(PALTI/1000.0))*1000.0
      PTEMPZRO=PTEMPZRO*288.2
      PPZRO=P(IALT+1)+((P(IALT+2)-P(IALT+1))/1000.0)*(PALTI/1000.0-AINT(
     1PALTI/1000.0))*1000.0
      PPZRO=PPZRO*101300.0

      RETURN
      END
C  ***********************************************************************
C  SUBROUTINE TO CALCULATE (INTERATE) MACH-NUMBER BASED ON   M F P
C  ***********************************************************************
      SUBROUTINE MACHNUMB(MFP,AM,GAM,R)
      REAL MFP

      MFP=MFP*SQRT(R)
      AM=MFP*0.8
      IF(MFP.GT.0.55)AM=MFP
      AMFPPRV=0.000000
      i=0
```

```
  100 CONTINUE
        AM=AM+0.001

        AMFP=(AM*SQRT(GAM))/((1+((GAM-1)/2)*AM**2)**((GAM+1)/(2*(GAM-1))
     1))

       IF(ABS(MFP-AMFP).LT.(0.0001*MFP).OR.((MFP-AMFP)/(MFP-AMFPPRV)).LT.
     1-0.00001)GOTO 120
       IF(AM.gT.0.9999)GOTO 115

       AMFPPRV=AMFP
       i=i+1
       if(i.eq.10000)goto 110
       GOTO 100
  110 CONTINUE
       PRINT*,'MORE THAN 10000 IN "Machnumb", return! Read?'

       READ*,MMM
       goto 120
  115 CONTINUE
       PRINT*,'Mach GT 1.0, return! Read?'

       READ*,MMM
  120 continue
       MFP=MFP/SQRT(R)
       RETURN
       END



C   %%%%%%%%%%%%%%%%%%%%%%%%%%%%%%%%%%%%%%%%%%%%%%%%%%%%%%%%%%%%%%%%%%%%%
C   FUNCTIONS FOR BASIC CALCULATIONS:
C   %%%%%%%%%%%%%%%%%%%%%%%%%%%%%%%%%%%%%%%%%%%%%%%%%%%%%%%%%%%%%%%%%%%%%
       FUNCTION R(GAM,CP)
         R=(GAM-1)*CP/GAM
         RETURN
        END
C   %%%%%%%%%%%%%%%%%%%%%%%%%%%%%%%%%%%%%%%%%%%%%%%%%%%%%%%%%%%%%%%%%%%%%
       FUNCTION A(GAM,R,T)
         A=SQRT(GAM*R*T)
         RETURN
        END
C   %%%%%%%%%%%%%%%%%%%%%%%%%%%%%%%%%%%%%%%%%%%%%%%%%%%%%%%%%%%%%%%%%%%%%
       FUNCTION V(A,AM)
         V=A*AM
         RETURN
        END
C   %%%%%%%%%%%%%%%%%%%%%%%%%%%%%%%%%%%%%%%%%%%%%%%%%%%%%%%%%%%%%%%%%%%%%
       FUNCTION FTAUR(AM,GAM)
         FTAUR=1+((GAM-1)/2)*AM**2
         RETURN
        END
C   %%%%%%%%%%%%%%%%%%%%%%%%%%%%%%%%%%%%%%%%%%%%%%%%%%%%%%%%%%%%%%%%%%%%%
       FUNCTION FPIR(AM,GAM)
         FPIR=(1+((GAM-1)/2)*AM**2)**(GAM/(GAM-1))
         RETURN
        END
C   %%%%%%%%%%%%%%%%%%%%%%%%%%%%%%%%%%%%%%%%%%%%%%%%%%%%%%%%%%%%%%%%%%%%%
       FUNCTION FTAULMBD(CPC,CPT,TEMPT4,T)
         FTAULMBD=(CPT*TEMPT4)/(CPC*T)
```

```
         RETURN
        END
C   %%%%%%%%%%%%%%%%%%%%%%%%%%%%%%%%%%%%%%%%%%%%%%%%%%%%%%%%%%%%%%%%%%%%%%
C   VARIABLE AMFP IS THE "MFP"; MASS FLOW PARAMETER:
       FUNCTION AMFP(AM,GAM,R)
         AMFP=(AM*SQRT(GAM/R))/((1+((GAM-1)/2)*AM**2)**((GAM+1)/(2*(GAM-1
      1))))
       RETURN
        END
C   ********************************************************************
C   SUBROUTINE TO PRINT ALL PARAMETERS
C   ********************************************************************
       SUBROUTINE TESTPRINT          (RC,RT,PAZRO,PVZRO,TAUR,PID,TAULMBD,
      1TAUF,TAUCH,PIF,TAUTH,TAUTL,PIN,PIFN,PT9,PT19,PTAUR,PPID,PTAULMBD,P
      2TAUF,PTAUCH,PICH,PPICH,PPIF,PTAUTL,M9,M19,PM9,PM19,PPT9,PPT19,ALPH
      3A,PALPHA,PPITL,MDTZRO,PMDTZRO,PF,PTMP9ZRO,PTEMP9,PV9AZRO,PTMP19ZR,
      4PV19AZRO,PTSFC,THRUST,PNNLP,PNNHP)

       REAL RC,RT,PAZRO,PVZRO,TAUR,PID,TAULMBD,TAUF,TAUCH,PIF
       REAL TAUTH,TAUTL,PICH,PIN,PIFN,PT9,PT19,PTAUR,PPID,PTAULMBD,PTAUF
       REAL PTAUCH,PPICH,PPIF,PTAUTL,M9,M19,PM9,PM19,PPT9,PPT19
       REAL ALPHA,PALPHA,PPITL,MDTZRO,PMDTZRO,PF,PTMP9ZRO,PTEMP9,PV9AZRO
       REAL PTMP19ZR,PV19AZRO,PTSFC,THRUST,PNNLP,PNNHP
C       print*,'      testprint'
       PRINT*,' RC,  RT            :',RC,RT
       PRINT*,' (AZRO)   PAZRO     :',PAZRO
       PRINT*,' (VZRO)   PVZRO     :',PVZRO
       PRINT*,' TAUR,    PTAUR     :',TAUR,PTAUR
       PRINT*,' PID,     PPID      :',PID,PPID
       PRINT*,' TAULMBD, PTAULMBD :',TAULMBD,PTAULMBD
       PRINT*,' TAUTL,   PTAUTL    :',TAUTL,PTAUTL
       PRINT*,' TAUF,    PTAUF     :',TAUF,PTAUF
       PRINT*,' TAUCH,   PTAUFH    :',TAUCH,PTAUCH
       PRINT*,' PICH,    PPICH     ;',PICH,PPICH
       PRINT*,' PIF,     PPIF      :',PIF,PPIF
       PRINT*,' M9,      PM9       :',M9,PM9
       PRINT*,' PT9,     PPT9      :',PT9,PPT9
       PRINT*,' PIN,     PPIN      :',PIN
       PRINT*,' M19,     PM19      :',M19,PM19
       PRINT*,' PT19,    PPT19     :',PT19,PPT19
       PRINT*,' PIFN,    PPIFN     :',PIFN
       PRINT*,' ALPHA,   PALPHA    :',ALPHA,PALPHA

       RETURN
       END
C   ********************************************************************
C   SUBROUTINE TO PRINT ALL REFERENCE DATA TO SCREEN
C   ********************************************************************
       SUBROUTINE REFPRINT
       REAL MZRO,MDTZRO
       COMMON TEMPZRO,GAMC,CPC,GAMT,CPT,TEMPT4,MZRO,PIC,PIF,ALPHA,ETAF,ET
      1ACH,TAUTH,PITH,TAUTL,PITL,ETATL,ETAB,PIDMAX,PIB,PIN,PIFN,ETAMH,ETA
      2ML,PZRO,TAUF,TAUCL,PICL,ETACL,MDTZRO,FMDTZRO,F,HPR,WINGAREA,DRAGCO
      3EF,RN1FRAC,M45
C       print*,'      refprint'
       WRITE(6,112)
       WRITE(6,101)
       WRITE(6,100)
       WRITE(6,102)TEMPZRO,PZRO,TEMPT4,MZRO
       WRITE(6,100)
       WRITE(6,103)CPC,CPT,GAMC,GAMT
```

```
      WRITE(6,100)
      WRITE(6,104)HPR,RN1FRAC
      WRITE(6,100)
      WRITE(6,105)PIDMAX,PIC,PIF,PIB
      WRITE(6,100)
      WRITE(6,106)PICL,ETACL
      WRITE(6,100)
      WRITE(6,107)PITH,PITL,PIN,PIFN
      WRITE(6,100)
      WRITE(6,108)TAUTH,TAUTL,ETAF,ETACH
      WRITE(6,100)
      WRITE(6,109)ETAB,ETATL,ETAMH,ETAML
      WRITE(6,100)
      WRITE(6,110)MDTZRO,FMDTZRO
      WRITE(6,100)
      WRITE(6,111)ALPHA,WINGAREA
      WRITE(6,100)
      WRITE(6,121)DRAGCOEF,F
      WRITE(6,112)
  100 FORMAT('  ')
  101 FORMAT('  R E F E R E N C E   D A T A :')
  102 FORMAT('  T0 [K]:    ',F8.2,' ;   p0 [Pa]:   ',F8.2,' ;   Tt4 [K]:
     1',F8.2,' ;  M0: ',F6.3)
  103 FORMAT('  cpC [J/kgK]:',F7.1,' ;   cpT [J/kgK]:',F7.2,' ;   gamC:
     1     ',F5.2,' ;  gamT:',F5.2)
  104 FORMAT('  Fuel heating value [J/kg]:  ',E12.4,' ;      Low pressur
     1e speed [%]:',F7.3)
  105 FORMAT('  piDmax:',F6.4,' ;     piC:  ',F6.2,' ;     piF:  ',F6.2,
     1' ;     piB:  ',F6.2)
  106 FORMAT('  piCL:  ',F6.4,' ;     etaCL ',F6.2)
  107 FORMAT('  piTH:  ',F6.4,' ;     piTL: ',F6.4,' ;     piN:  ',F6.4,
     1' ;     piNf: ',F6.4)
  108 FORMAT('  tauTH :',F6.4,' ;     tauTL:',F6.4,' ;     etaF: ',F6.4,
     1' ;     etaCH:',F6.4)
  109 FORMAT('  etaB  :',F6.4,' ;     etaTL:',F6.4,' ;     etaMH:',F6.4,
     1' ;     etaML:',F6.4)
  110 FORMAT('  Air mass flow [kg/s]:',F8.2,' ;      Specific thrust [N/
     1Kg/s]:',F8.3)
  111 FORMAT('  alpha: ',F6.2,' ;       Wing area [m**2]:',F7.1)
  121 FORMAT('  Drag coeff.:',F7.4,' ; Thrust [N]:',F13.2)
  112 FORMAT(' %%%%%%%%%%%%%%%%%%%%%%%%%%%%%%%%%%%%%%%%%%%%%%%%%%%%%%%%%%%%%%%%
     1%%%%%%%%%%%%%%%%%%%%%%%%')
      RETURN
      END
C  ***********************************************************************
C  SUBROUTINE TO PRINT ALL RESULTS TO FILE "RESULTS1"
C  ***********************************************************************
      SUBROUTINE RESULTOUT     (pitl,RC,RT,PAZRO,PVZRO,TAUR,PID,TAULMBD,
     1TAUF,TAUCH,PIF,TAUTH,TAUTL,PIN,PIFN,PT9,PT19,PTAUR,PPID,PTAULMBD,P
     2TAUF,PTAUCH,PICH,PPICH,PPIF,PTAUTL,M9,M19,PM9,PM19,PPT9,PPT19,ALPH
     3A,PALPHA,PPITL,MDTZRO,PMDTZRO,PF,PTMP9ZRO,PTEMP9,PV9AZRO,PTMP19ZR,
     4PV19AZRO,PTSFC,THRUST,PNNLP,PNNHP,PTEMPZRO,PPZRO,PTEMPT4,PMZRO,CPC
     5,CPT,GAMC,GAMT,HPR,TAUCL,PTAUCL,  PTAUTH,PICL,PPICL,PIB,PPIB,PITH,P
     6PITH,PFMDTZRO,FMDTZRO,PPIN,PPIFN,IPRTCNT,JPRTCNT,FUELCONS,TIME,WAY
     7,FUELFL,EMCO2,EMH2O,EMNOX,EMCOM1,EMUHC1,EMCOM2,EMUHC2,BETA)

      REAL RC,RT,PAZRO,PVZRO,TAUR,PID,TAULMBD,TAUF,TAUCH,PIF,PITL
      REAL TAUTH,TAUTL,PICH,PIN,PIFN,PT9,PT19,PTAUR,PPID,PTAULMBD,PTAUF
      REAL PTAUCH,PPICH,PPIF,PTAUTL,M9,M19,PM9,PM19,PPT9,PPT19
      REAL ALPHA,PALPHA,PPITL,MDTZRO,PMDTZRO,PF,PTMP9ZRO,PTEMP9,PV9AZRO
      REAL PTMP19ZR,PV19AZRO,PTSFC,THRUST,PNNLP,PNNHP,PTEMPZRO,PPZRO
```

```
      REAL PTEMPT4,PMZRO,CPC,CPT,GAMC,GAMT,HPR,BETA
      REAL FUELFL,EMCO2,EMH2O,EMNOX,EMCOM1,EMUHC1,EMCOM2,EMUHC2

      RPRTCNT=JPRTCNT
      RPRTCNT=IPRTCNT+RPRTCNT/10

      OPEN(UNIT=1,FILE='RESULTS1')

      WRITE(1,250)
      WRITE(1,200)
      WRITE(1,201)RPRTCNT
      WRITE(1,199)
      WRITE(1,200)
      WRITE(1,202)
      WRITE(1,200)
      WRITE(1,203)PTEMPZRO,PPZRO,PTEMPT4,PMZRO
      WRITE(1,200)
      WRITE(1,204)
      WRITE(1,200)
      WRITE(1,205)CPC,CPT,GAMC,GAMT
      WRITE(1,200)
      WRITE(1,206)HPR
      WRITE(1,200)
      WRITE(1,207)
      WRITE(1,200)
      WRITE(1,208)
      WRITE(1,209)PVZRO
      WRITE(1,210)PAZRO
      WRITE(1,211)PTAUR,TAUR
C      WRITE(1,212)
      WRITE(1,213)PTAUF,TAUF
      WRITE(1,214)PTAUCH,TAUCH
      WRITE(1,215)PTAUTH,TAUTH
      WRITE(1,216)PTAUTL,TAUTL
      WRITE(1,217)PTAULMBD,TAULMBD
      WRITE(1,218)PPID,PID
C      WRITE(1,219)
      WRITE(1,220)PPIF,PIF
      WRITE(1,221)PPICH,PICH
      WRITE(1,222)PPIB,PIB
      WRITE(1,223)PPITH,PITH
      WRITE(1,224)PPITL,PITL
      WRITE(1,227)PM9,M9
      WRITE(1,228)PM19,M19
      WRITE(1,229)PPT9,PT9
      WRITE(1,230)PPT19,PT19
      WRITE(1,231)PMDTZRO,MDTZRO
      WRITE(1,233)PFMDTZRO,FMDTZRO
      WRITE(1,234)PALPHA,ALPHA
      WRITE(1,235)PTMP9ZRO
      WRITE(1,236)PTMP19ZR
      WRITE(1,237)PV9AZRO
      WRITE(1,238)PV19AZRO
      WRITE(1,239)PNNLP
      WRITE(1,240)PNNHP
      WRITE(1,232)PTSFC*1E+6
      WRITE(1,225)PTSFC*THRUST
      WRITE(1,241)THRUST
      WRITE(1,226)FUELCONS,TIME,WAY/1000.0
            WRITE(1,261)
            WRITE(1,262)FUELFL
```

```
         WRITE(1,263)EMCO2
         WRITE(1,264)EMH2O
         WRITE(1,265)EMNOX
      IF(BETA.LT.-0.001)THEN
         WRITE(1,266)EMCOM2,EMCOM1
         WRITE(1,267)EMUHC2,EMUHC1
      ELSE
         WRITE(1,266)EMCOM1,EMCOM2
         WRITE(1,267)EMUHC1,EMUHC2
      ENDIF


   WRITE(1,200)
   WRITE(1,250)


199 FORMAT('  ___________________________________                ===')
200 FORMAT('  ')
201 FORMAT('  P E R F O R M A C E   D A T A ;  SET NO.',F4
   1.1)
202 FORMAT(' * *  Performance  Conditions, Input:')
203 FORMAT('  T0 [K]:',F8.2,'     ;  p0 [Pa]:',E11.4,' ;  Tt4 [K]:',F8
   1.2,' ;  M0: ',F6.3)
204 FORMAT(' * *  Gas  and  Fuel  Properties,  Input:')
205 FORMAT('  cpC [J/kgK]:',F7.1,' ;  cpT [J/kgK]:',F7.2,' ;  gamC:',F
   15.2,'       ;  gamT:',F5.2)
206 FORMAT('  Fuel heating value [J/kg]:  ',E12.4)
207 FORMAT(' * *  Performance paramerters, and reference parameters wh
   1ere they apply:')
208 FORMAT('    PARAMETER                          PERFORMACE
   1   REF.')
209 FORMAT('    Ambient speed [m/s]              ',F12.4,'    ',F12.4)
210 FORMAT('    Ambient speed of sound [m/s]     ',F12.1,'    ',F12.1)
211 FORMAT('    tauR                             ',F12.4,'    ',F12.4)
212 FORMAT('    tauCL                            ',F12.4,'    ',F12.4)
213 FORMAT('    tauF                             ',F12.4,'    ',F12.4)

214 FORMAT('    tauCH                            ',F12.4,'    ',F12.4)
215 FORMAT('    tauTH                            ',F12.4,'    ',F12.4)
216 FORMAT('    tauTL                            ',F12.4,'    ',F12.4)
217 FORMAT('    tau-LAMBDA                       ',F12.4,'    ',F12.4)
218 FORMAT('    piD                              ',F12.4,'    ',F12.4)

219 FORMAT('    piCL                             ',F12.4,'    ',F12.4)
220 FORMAT('    piF                              ',F12.4,'    ',F12.4)
221 FORMAT('    piCH                             ',F12.4,'    ',F12.4)
222 FORMAT('    piB                              ',F12.4,'    ',F12.4)
223 FORMAT('    piTH                             ',F12.4,'    ',F12.4)

224 FORMAT('    piTL                             ',F12.4,'    ',F12.4)
225 FORMAT('    Fuelflow ONE eng. [kg/s]         ',F12.4,'    ',F12.4)
226 FORMAT('    Fuelc. A/C [kg]',F8.1,' Time [s]',F8.1,' Way [km]',F8.
   12)
227 FORMAT('    Nozzle exit Mach-n., core, M9    ',F12.4,'    ',F12.4)
228 FORMAT('    Nozzle exit Mach-n., byp., M19   ',F12.4,'    ',F12.4)

229 FORMAT('    Nozz.ex. stgn.press. ,core [Pa]  ',F12.1,'    ',F12.1)
230 FORMAT('    Nozz.ex. stgn.press. ,byp. [Pa]  ',F12.1,'    ',F12.1)
231 FORMAT('    Air mass flow rate (total)[kg/s] ',F12.2,'    ',F12.2)
232 FORMAT('    Thrust sp. fuel cons.[(mg/s)/N]  ',F12.4,'    ',F12.4)
233 FORMAT('    Specific thrust [N/(kg/s)]       ',F12.4,'    ',F12.4)
```

```
  234 FORMAT('    Bypass ratio                        ',F12.4,'    ',F12.4)

  235 FORMAT('    Temp. relation core; T9/T0          ',F12.4,'    ',F12.4)
  236 FORMAT('    Temp. relation bypass; T19/T0       ',F12.4,'    ',F12.4)
  237 FORMAT('    Speed relation core; V9/a0          ',F12.4,'    ',F12.4)
  238 FORMAT('    Speed relation bypass; V9/a0        ',F12.4,'    ',F12.4)
  239 FORMAT('    RPM-LP-spool, rel. ref. condition',F12.4,'    ',F12.4)

  240 FORMAT('    RPM-HP-spool, rel. ref. condition',F12.4,'    ',F12.4)
  241 FORMAT('    Thrust [N]                          ',F12.1,'    ',F12.1)

  261 FORMAT(' Fuel & Emissions, TWO ENGINES:')
  262 FORMAT('      Fuelflow  [kg/s]                   ',F12.4)
  263 FORMAT('      CO2     [kg/s]                     ',F12.4)
  264 FORMAT('      H20     [kg/s]                     ',F12.4)
  265 FORMAT('      NOX     [g/s]                      ',F12.4)
  266 FORMAT('      CO      [g/s]                      ',E12.4,'  (',E10.4
     1,')')
  267 FORMAT('      UHC     [g/s]                      ',E12.4,'  (',E10.4
     1,')')

  250 FORMAT(' % % % % % % % % % % % % % % % % % % % % % % % % % % % % % % % %
     1 % % % % % % % % % %')
   10 CONTINUE
      RETURN
      END
C  ***********************************************************************
C  SUBROUTINE TO PRINT ALL RESULTS TO DIFFERENT FORMAT FILE "RESULTS3"
C  ***********************************************************************
      SUBROUTINE RESULTTWO     (pitl,RC,RT,PAZRO,PVZRO,TAUR,PID,TAULMBD,
     1TAUF,TAUCH,PIF,TAUTH,TAUTL,PIN,PIFN,PT9,PT19,PTAUR,PPID,PTAULMBD,P
     2TAUF,PTAUCH,PICH,PPICH,PPIF,PTAUTL,M9,M19,PM9,PM19,PPT9,PPT19,ALPH
     3A,PALPHA,PPITL,MDTZRO,PMDTZRO,PF,PTMP9ZRO,PTEMP9,PV9AZRO,PTMP19ZR,
     4PV19AZRO,PTSFC,THRUST,PNNLP,PNNHP,PTEMPZRO,PPZRO,PTEMPT4,PMZRO,CPC
     5,CPT,GAMC,GAMT,HPR,TAUCL,PTAUCL,  PTAUTH,PICL,PPICL,PIB,PPIB,PITH,P
     6PITH,PFMDTZRO,FMDTZRO,PPIN,PPIFN,IPRTCNT,JPRTCNT,FUELCONS,TIME,WAY
     7,FUELFL,EMCO2,EMH2O,EMNOX,EMCOM1,EMUHC1,EMCOM2,EMUHC2,BETA,PMASS)

      REAL RC,RT,PAZRO,PVZRO,TAUR,PID,TAULMBD,TAUF,TAUCH,PIF,PITL
      REAL TAUTH,TAUTL,PICH,PIN,PIFN,PT9,PT19,PTAUR,PPID,PTAULMBD,PTAUF
      REAL PTAUCH,PPICH,PPIF,PTAUTL,M9,M19,PM9,PM19,PPT9,PPT19
      REAL ALPHA,PALPHA,PPITL,MDTZRO,PMDTZRO,PF,PTMP9ZRO,PTEMP9,PV9AZRO
      REAL PTMP19ZR,PV19AZRO,PTSFC,THRUST,PNNLP,PNNHP,PTEMPZRO,PPZRO
      REAL PTEMPT4,PMZRO,CPC,CPT,GAMC,GAMT,HPR,BETA,PMASS
      REAL FUELFL,EMCO2,EMH2O,EMNOX,EMCOM1,EMUHC1,EMCOM2,EMUHC2

      RPRTCNT=JPRTCNT
      RPRTCNT=IPRTCNT+RPRTCNT/10

      OPEN(UNIT=4,FILE='RESULTS3')

      WRITE(4,200)
      WRITE(4,201)RPRTCNT
      WRITE(4,200)
      WRITE(4,203)PTEMPZRO,PPZRO,PMZRO,PTEMPT4
      WRITE(4,200)
      WRITE(4,241)THRUST,PMASS
      WRITE(4,200)
      WRITE(4,226)FUELCONS,TIME,WAY/1000.0,PVZRO
      WRITE(4,200)
            WRITE(4,261)
```

```
            WRITE(4,262)FUELFL
            WRITE(4,263)EMCO2
            WRITE(4,264)EMH2O
            WRITE(4,265)EMNOX
          IF(BETA.LT.-0.001)THEN
            WRITE(4,266)EMCOM2,EMCOM1
            WRITE(4,267)EMUHC2,EMUHC1
          ELSE
            WRITE(4,266)EMCOM1,EMCOM2
            WRITE(4,267)EMUHC1,EMUHC2
          ENDIF


        WRITE(4,200)
        WRITE(4,250)

  199 FORMAT('  ___________________________________                ===')
  200 FORMAT('  ')
  201 FORMAT('  P E R F O R M A C E   D A T A ;  SET NO.',F4
     1.1)

  203 FORMAT('  T0 [K]:',F8.2,' ;  p0 [Pa]:',E11.4,' ;  M0: ',F6.3,' ;
     1Tt4 [K]:',F8.2)
  226 FORMAT('  Fuelc. A/C [kg]',F7.1,'; Time [s]',F6.1,'; Way [km]',F6.
     12,'; Speed [m/s]',F6.1)
  241 FORMAT('  Thrust [N]:              ',F12.1,' ;  A/C mass [kg]:
     1 ',F12.1)

  261 FORMAT('  Fuel & Emissions, TWO ENGINES:')
  262 FORMAT('       Fuelflow  [kg/s]                ',F12.4)
  263 FORMAT('       CO2       [kg/s]                ',F12.4)
  264 FORMAT('       H20       [kg/s]                ',F12.4)
  265 FORMAT('       NOX       [g/s]                 ',F12.4)
  266 FORMAT('       CO        [g/s]                 ',E12.4,'  (',E10.4
     1,')')
  267 FORMAT('       UHC       [g/s]                 ',E12.4,'  (',E10.4
     1,')')

  250 FORMAT(' % % % % % % % % % % % % % % % % % % % % % % % % % % % % % %
     1 % % % % % % % % % %')
   10 CONTINUE
      RETURN
      END

C  ***********************************************************************
C  SUBROUTINE TO WRITE ALL REFERENCE DATA TO FILE "RESLUTS2"
C  ***********************************************************************
      SUBROUTINE REFFILE(IPRTCNT)
      REAL MZRO,MDTZRO
      COMMON TEMPZRO,GAMC,CPC,GAMT,CPT,TEMPT4,MZRO,PIC,PIF,ALPHA,ETAF,ET
     1ACH,TAUTH,PITH,TAUTL,PITL,ETATL,ETAB,PIDMAX,PIB,PIN,PIFN,ETAMH,ETA
     2ML,PZRO,TAUF,TAUCL,PICL,ETACL,MDTZRO,FMDTZRO,F,HPR,WINGAREA,DRAGCO
     3EF,RN1FRAC,M45
C     reffile'
      OPEN(UNIT=1,FILE='RESULTS2')

      WRITE(1,112)
      WRITE(1,101)IPRTCNT
      WRITE(1,99)
      WRITE(1,100)
      WRITE(1,102)TEMPZRO,PZRO,TEMPT4,MZRO
```

```
      WRITE(1,100)
      WRITE(1,103)CPC,CPT,GAMC,GAMT
      WRITE(1,100)
      WRITE(1,104)HPR
      WRITE(1,100)
      WRITE(1,105)PIDMAX,PIC,PIF,PIB
      WRITE(1,100)
      WRITE(1,106)PICL,ETACL
      WRITE(1,100)
      WRITE(1,107)PITH,PITL,PIN,PIFN
      WRITE(1,100)
      WRITE(1,108)TAUTH,TAUTL,ETAF,ETACH
      WRITE(1,100)
      WRITE(1,109)ETAB,ETATL,ETAMH,ETAML
      WRITE(1,100)
      WRITE(1,110)MDTZRO,FMDTZRO
      WRITE(1,100)
      WRITE(1,111)ALPHA,F
      WRITE(1,112)
      WRITE(1,100)
   99 FORMAT('  ========================================')
  100 FORMAT('  ')
  101 FORMAT('  R E F E R E N C E   D A T A ;  SET NO.',I3)
  102 FORMAT('  T0 [K]:    ',F8.2,' ;   p0 [Pa]:   ',F8.2,' ;   Tt4 [K]:
     1',F8.2,' ;  M0: ',F6.3)
  103 FORMAT('  cpC [J/kgK]:',F7.1,' ;   cpT [J/kgK]:',F7.2,' ;   gamC:
     1     ',F5.2,' ;  gamT:',F5.2)
  104 FORMAT('  Fuel heating value [J/kg]:  ',E12.4)
  105 FORMAT('  piDmax:',F6.4,' ;     piC:  ',F6.2,' ;     piF:  ',F6.2,
     1' ;     piB:  ',F6.2)
  106 FORMAT('  piCL:  ',F6.4,' ;     etaCL ',F6.2)
  107 FORMAT('  piTH:  ',F6.4,' ;     piTL: ',F6.4,' ;     piN:  ',F6.4,
     1' ;     piNf: ',F6.4)
  108 FORMAT('  tauTH :',F6.4,' ;     tauTL:',F6.4,' ;     etaF: ',F6.4,
     1' ;     etaCH:',F6.4)
  109 FORMAT('  etaB  :',F6.4,' ;     etaTL:',F6.4,' ;     etaMH:',F6.4,
     1' ;     etaML:',F6.4)
  110 FORMAT('  Air mass flow [kg/s]:',F8.2,' ;      Specific thrust [N/
     1Kg/s]:',F8.3)
  111 FORMAT('  alpha:',F6.2,'                    ;      Thrust [N]:',F12.
     12)
  112 FORMAT(' %%%%%%%%%%%%%%%%%%%%%%%%%%%%%%%%%%%%%%%%%%%%%%%%%%%%%%%%%%%%
     1%%%%%%%%%%%%%%%%%%%%%%%%')
      RETURN
      END

C  ***********************************************************************
C  SUBROUTINE TO CALCULATE EMISSION QUANTITIES
C  ***********************************************************************

      SUBROUTINE EMISSIONS(PPT4,PPIB,PTEMPZRO,PTAUR,PTAUF,PTAUCH,PMDTZRO
     1,PALPHA,PTEMPT4,PF,PTSFC,THRUST,FUELFL,EMCO2,EMH2O,EMNOX,EMCOM1,EM
     2UHC1,EMCOM2,EMUHC2)
      REAL CO2EI,H2OEI,NOXEI,COEI1,COEI2,UHCEI1,UHCEI2,PTST,PMDOT
      REAL PTEMPT4,PPT4,PPIB,PTEMPZRO,PTAUR,PTAUF,PTAUCH,PMDTZRO,PALPHA
      REAL PF,PTSFC,THRUST,APPT3,APPT4,PTEMPT3
      REAL F,FUELFL,EMCO2,EMH2O,EMNOX,EMCOM1,EMUHC1,EMCOM2,EMUHC2

      APPT4=PPT4/0.1013E+06
      APPT3=APPT4/PPIB
```

```
      PTEMPT3=PTEMPZRO*PTAUR*PTAUF*PTAUCH

      PTST=2600.0+(PTEMPT3-800.0)*0.5
      PMDOT=PMDTZRO/(PALPHA+1.0)
      F=14.4*PF
      FUELFL=PTSFC*THRUST

      CO2EI=3.18
      H2OEI=1.18

      NOXEI=3.185E-09*APPT3**1.2435*EXP(0.011178*PTST)/(PMDOT*PTEMPT4*((
     1APPT3-APPT4)/APPT3)**0.22276)

      COEI1=23.15*F**2*PMDOT*PTEMPT4*((APPT3-APPT4)/APPT3)**0.6288*APPT3
     1**(-0.8225)/(EXP(0.004803*PTEMPT4))
      COEI2=1.084E+07*F**2*PMDOT*PTEMPT4*((APPT3-APPT4)/APPT3)**0.3550*A
     1PPT3**(-3.0359)/(EXP(0.01233*PTEMPT4))

      UHCEI1=2.306*COEI1**0.3985/(((APPT3-APPT4)/APPT3)**(-0.3886)*APPT3
     1**0.9628)
      UHCEI2=3.326E-05*COEI2**2.8318/(((APPT3-APPT4)/APPT3)**(-0.1009)*A
     1PPT3**(-1.0249))
C
C  For two engines
C

      EMCO2=2.0*CO2EI*FUELFL
      EMH2O=2.0*H2OEI*FUELFL
      EMNOX=2.0*NOXEI*FUELFL
      EMCOM1=2.0*COEI1*FUELFL
      EMUHC1=2.0*UHCEI1*FUELFL
      EMCOM2=2.0*COEI2*FUELFL
      EMUHC2=2.0*UHCEI2*FUELFL
      FUELFL=2.0*FUELFL
        RETURN
        END
C  ***********************************************************************
C  SUBROUTINE TO FIND PIT, TAUT, AND TT5
C
C   O.K. WITH SI UNITS
C   COPIED FROM MATTINGLY
C  ***********************************************************************
      SUBROUTINE TURB(TT4,F,A4A5,M4,M5,ETAT,TT5S,PIT,TAUT,TT5)
       REAL TT4,F,A4A5,M4,M5,ETAT,TT5S,PIT,TAUT,TT5,MFP4,MFP5,HT4,PRT4
       REAL PHIT4,CPT4,RT4,GAMT4,AT4,T4,T5,HT5,PRT5,PHIT5,CPT5
       REAL RT5,GAMT5,AT5,TT5I,HT5I,PRT5I,PHIT5I,CPT5I,RT5I,GAMT5I,AT5I
       REAL TT5N
C      print*,'                                        turb'

      CALL FAIR(1,TT4,HT4,PRT4,PHIT4,CPT4,RT4,GAMT4,AT4,F)


      CALL MASSFP(TT4,F,M4,T4,MFP4)

      TT5=TT5S
      I=0
   10 CONTINUE
      I=I+1

      CALL MASSFP(TT5,F,M5,T5,MFP5)
```

```
      CALL FAIR(1,TT5,HT5,PRT5,PHIT5,CPT5,RT5,GAMT5,AT5,F)

      PIT=(MFP4/MFP5)*A4A5*SQRT(TT5/TT4)
      PRT5I=PIT*PRT4

      CALL FAIR(3,TT5I,HT5I,PRT5I,PHIT5I,CPT5I,RT5I,GAMT5I,AT5I,F)

      HT5=HT4-ETAT*(HT4-HT5I)

      TAUT=HT5/HT4
C      PRINT*,'taut, etat, HT4, HT5I in TURB:',taut,etat,ht4,ht5i
      CALL FAIR(2,TT5N,HT5,PRT5,PHIT5,CPT5,RT5,GAMT5,AT5,F)
      TT5ERR=ABS(TT5-TT5N)
C      PRINT*,'TT5 & TT5N:',TT5,TT5N
      IF(TT5ERR.LT.0.1)GOTO 11
      TT5=TT5N
      IF(I.LT.1000)GOTO 10
      PRINT*,'MORE THAN 1000 IN "Turb", return! Read?'
      READ*,MMM
   11 CONTINUE
C

      RETURN
      END
C  ***********************************************************************
C  SUBROUTINE TO FIND RPOPERTIES OF FUEL/AIR MIXTURES USING PHIT,
C  PROCOM, AND TEMP.
C    UI=1: KNOWNS T,FA
C    UI=2: KNOWNS H,FA
C    UI=3: KNOWNS PR,FA
C    UI=4: KNOWNS PHI,FA
C  CALLED WITH ENGLISH UNITS AND WORKS IN ENGLISH UNITS EXCLUSIVELY
C
C   MODIFIED TO WORK IN SI UNITS
C   COPIED FROM MATTINGLY
C  ***********************************************************************
      SUBROUTINE FAIR(IU,T,H,PR,PHI,CP,R,GAM,A0,FA)
      INTEGER IU
      REAL T,H,PR,PHI,CP,R,GAM,A0,FA,PHI0,AMW,RX
C      print*,'       fair'

      PHI0=6608.7
      IF(IU.EQ.1)CALL PROCOM(FA,T,A0,GAM,CP,R,PHI,PR,H)

      IF(IU.NE.2)GOTO 10

      CALL TEMP(H,FA,T)

      CALL PROCOM(FA,T,A0,GAM,CP,R,PHI,PR,H)

   10 CONTINUE
      IF(IU.NE.3)GOTO 11

      AMW=28.97-0.946186*FA

      RX=8285.42/AMW


      PHI=RX*LOG(PR)+PHI0
      CALL PHIT(PHI,FA,T)
```

```
      CALL PROCOM(FA,T,A0,GAM,CP,R,PHI,PR,H)
   11 CONTINUE
      IF(IU.NE.4)GOTO 12
      CALL PHIT(PHI,FA,T)
      CALL PROCOM(FA,T,A0,GAM,CP,R,PHI,PR,H)
   12 CONTINUE

      RETURN
      END

C  ********************************************************************
C  SUBROUTINE TO FIND T USING PROCOM, GIVEN PHI ANDFUEL/AIR RATIO
C  CALLED WITH ENGLISH UNITS AND WORKS IN ENGLISH UNITS EXCLUSIVELY
C
C   MODIFIED TO WORK IN SI UNITS
C   COPIED FROM MATTINGLY
C  ********************************************************************
      SUBROUTINE PHIT(PHI,FA,T)
      REAL PHI,FA,T,TTO,PHIO,PHIN,DELT,SLOPE
      REAL DUM1,DUM2,DUM3,DUM4,DUM5,DUM6
C      print*,'     phit'
      TTO=PHI*0.1

      CALL PROCOM(FA,TTO,DUM1,DUM2,DUM3,DUM4,PHIO,DUM5,DUM6)

      DELT =14.0

  100 CONTINUE

      T=TTO+DELT

      CALL PROCOM(FA,T,DUM1,DUM2,DUM3,DUM4,PHIN,DUM5,DUM6)

      PHITEST=PHIN-PHIO

      IF(ABS(PHITEST).LT.0.1E-11)GOTO 110


        IF(ABS((PHIN-PHI)/PHI).LT.0.00000001)GOTO 109

          SLOPE=(TTO-T)/(PHIO-PHIN)

          DELT=SLOPE*(PHI-PHIN)

          PHIO=PHIN
          TTO=T
          GOTO 100
  109   CONTINUE
  110 CONTINUE
      RETURN
      END
C  ********************************************************************
C  SUBROUTINE TO FIND CP,HT,R,A,GAM,PHI, AND PR
C
C   COMMUNICATES IN SI UNITS (WORKS IN ENGLISH UNITS)
C   COPIED FROM MATTINGLY
C  ********************************************************************
      SUBROUTINE PROCOM(FAtransp,Ttransp,AX,GAM,CPX,RX,PHI,PR,HX)
      REAL FAtransp,FA,Ttransp,T,AX,GAM,CPX,RX,PHI,PR,HX
      DOUBLE PRECISION A0,A1,A2,A3,A4,A5,A6,A7,HREF,PHIREF,PHI0
      DOUBLE PRECISION A0F,A1F,A2F,A3F,A4F,A5F,A6F,A7F,HREFF,PHIREFF
```

```
      DOUBLE PRECISION CP,CPA,H,HA,PHIA,CPF,HF,PHIF,PHIB
C      print*,'                        p r o c o m'
      FA=FAtransp

C  Trans. from SI to eng. units

      T=Ttransp*1.8
      AX=AX*3.28
      CPX=CPX*2.388E-4
      RX=RX*2.388E-4
      PHI=PHI*2.388E-4
      HX=HX*4.299E-4

      A0=0.25020051
      A1=-0.000051536879
      A2=0.000000065519486
      A3=-6.7178376E-12
      A4=-1.5128259E-14
      A5=7.6215767E-18
      A6=-1.452677E-21
      A7=1.011554E-25
      HREF=-1.7558886
      PHIREF=0.0454323

      A0F=0.073816638
      A1F=0.001225863
      A2F=-0.0000013771901
      A3F=9.9686793E-10
      A4F=-4.2051104E-13
      A5F=1.0212913E-16
      A6F=-1.3335668E-20
      A7F=7.267871E-25
      HREFF=30.58153
      PHIREFF=0.6483398

      PHI0=1.5784181

      IF(FA.GT.0.067623)FA=0.067623
      IF(T.LT.300.0)T=300.0
      IF(T.GT.4000.0)T=4000.0
      IF(FA.LT.0.0)FA=0.00000

      CP=((A7*T+A6)*T+A5)*T+A4
      CPA=(((CP*T+A3)*T+A2)*T+A1)*T+A0
      H=((A7/8*T+A6/7)*T+A5/6)*T+A4/5
      HA=((((H*T+A3/4)*T+A2/3)*T+A1/2)*T+A0)*T+HREF

C PHIB IS INTRODUCED TO REPLACE PHI AS A TEMPORARY VARIABLE

      PHIB=((A7/7*T+A6/6)*T+A5/5)*T+A4/4
      PHIA=(((PHIB*T+A3/3)*T+A2/2)*T+A1)*T+A0*LOG(T)+PHIREF

      IF(FA.LE.0.0000)GOTO 10
      CP=((A7F*T+A6F)*T+A5F)*T+A4F
      CPF=(((CP*T+A3F)*T+A2F)*T+A1F)*T+A0F
      H=((A7F/8*T+A6F/7)*T+A5F/6)*T+A4F/5
      HF=((((H*T+A3F/4)*T+A2F/3)*T+A1F/2)*T+A0F)*T+HREFF
      PHIB=((A7F/7*T+A6F/6)*T+A5F/5)*T+A4F/4
      PHIF=(((PHIB*T+A3F/3)*T+A2F/2)*T+A1F)*T+A0F*LOG(T)+PHIREFF
   10 CONTINUE
```

```
      CPX=(CPA+FA*CPF)/(1.0+FA)
      HX=(HA+FA*HF)/(1.0+FA)
      PHI=(PHIA+FA*PHIF)/(1.0+FA)
      AMW=28.97-0.946186*FA
      RX=1.9857117/AMW
      GAM=CPX/(CPX-RX)
      AX=SQRT(GAM*RX*T*25039.775)
      PR=EXP((PHI-PHI0)/RX)

C  Trans. from eng. to SI units

      AX=AX/3.28
      CPX=CPX/2.388E-4
      RX=RX/2.388E-4
      PHI=PHI/2.388E-4
      HX=HX/4.299E-4

      RETURN

      END
C  ***********************************************************************
C  SUBROUTINE TO FIND T USING PROCOM, GIVEN H AND FUEL/AIR RATIO
C  CALLED WITH ENGLISH UNITS AND WORKS IN ENGLISH UNITS EXCLUSIVELYC
C
C   MODIFIED TO WORK IN SI UNITS
C   COPIED FROM MATTINGLY
C  ***********************************************************************
      SUBROUTINE TEMP(H,F,T)
      REAL H,F,T,H1,DELT,T2,CP,H2
      REAL DUM1,DUM2,DUM3,DUM4,DUM5,DUM6
C      print*,'   temp'
      T=H*0.000795
      CALL PROCOM(F,T,DUM1,DUM2,DUM3,DUM4,DUM5,DUM6,H1)

      DELT=15
      T2=T
      I=0
   10 CONTINUE
      I=I+1
      T=T2+DELT

      CALL PROCOM(F,T,DUM1,DUM2,CP,DUM3,DUM4,DUM5,H2)

      IF(ABS((H2-H1)/H).LT.0.000001)GOTO 11
      DELT=(H-H2)/CP
      H1=H2
      T2=T
      IF(I.LT.1000)GOTO 10
      PRINT*,'MORE THAN 1000 IN "Temp", return! Read?'
      READ*,MMM

   11 CONTINUE

      RETURN
      END
C  ***********************************************************************
C  SUBROUTINE TO FIND MFP AND T
C  CALLED WITH ENGLISH UNITS AND WORKS IN ENGLISH UNITS EXCLUSIVELY
C
C   O.K. WITH SI UNITS
C   COPIED FROM MATTINGLY
```

```
C  ***********************************************************************
      SUBROUTINE MASSFP(TT,F,M,T,MFP)
      REAL TT,F,M,T,MFP,HT,PRT,PHIT,CPT,RT,GAMT,AT,V,H,PR,PHI,CP,R,GAM,A
      REAL VN,VERR
C    THE HT IN THE NXT LINE IS QUESTIONABLE (SHOULD BE H?)
C       print*,'      massfp'
      CALL FAIR(1,TT,HT,PRT,PHIT,CPT,RT,GAMT,AT,F)
      V=M*AT*((1+(((GAMT-1)/2)*(M**2)))**(-0.5))
C  PREVIOUS LINE CORRECTED; "DENOMINATOR" RAISED TO THE POWER OF 0.5

      I=0
   10 CONTINUE
      I=I+1
      H=HT-(V**2)/2

      CALL FAIR(2,T,H,PR,PHI,CP,R,GAM,A,F)

      VN=M*A

      VERR=ABS((V-VN)/V)
      IF(VERR.LT.0.000001)GOTO 11
c bare for testing:
      b=V
      bn=VN
c slutt for test.
      V=VN
      IF(I.LT.1000)GOTO 10
      PRINT*,'MORE THAN 1000 IN "Massfp", return! Read?'
      print*,'(V-VN), V and VERR:',(b-bn),b,VERR,'VERR supposadly LT 0.0
     100001'
      READ*,MMM


   11 CONTINUE

      MFP=M*(PR/PRT)*SQRT((GAM*TT)/(R*T))

      RETURN
      END
```

APPENDIX K

The TURBOMATCH *CFM56-3C1* Program Setup and Output Samples

The TURBOMATCH *CFM56-3C1* program setup;
Flight condition data set for "*CRUISE*"

```
TURBOMATCH
Engine: CFM56-3C1
Based on data from Braathens/CFM, particularly the calculated CFM data for
"hot day takeoff" (+30 deg. C). Ambient temperatur is changed to ISA
condition
and TET adjusted accordingly to obtain the specified takeoff thrust.

Programmer: Paul Arentzen

File: CRUI.DAT      NB! Full print"

Modified  16/10/98
------------------------------------------------------------------------
--
////
OD SI KE VA FP
-1
-1
INTAKE S1-2       D1-4      R200
COMPRE S2-3       D5-11     R201     V5 V6     ! FAN
PREMAS S3,4,20    D12-15              V12       ! SPLIT INTO CORE AND BYPASS
FLOW
ARITHY            D151-155                      ! FAN SPEED = LP COMPR SPEED
PREMAS S20,23,21  D16-19                        ! BLEED AIR FROM BYPASS DUCT
DUCTER S21-22     D20-23    R203                ! BYPASS DUCT
PREMAS S22,25,24  D28-31                        ! BLEED AIR UPSTREAM OF BYPASS
NOZZLE
NOZCON S24,26,1   D36 R206                      ! BYPASS NOZZLE
COMPRE S4-5       D37-43    R207     V37       ! LP COMPRESSOR
ARITHY            D156-162                      ! SUM WORK FAN AND LP COMP
PREMAS S5,33,6    D24-27                        ! BLEED AIR (VBV)
DUCTER S6-7       D44-47    R209                ! LPC-HPC DUCT
COMPRE S7-8       D48-54    R210     V48 V49   ! HP COMPRESSOR FIRST 5 STAGES
PREMAS S8,27,9    D55-58                        ! 5TH STAGE BLEED
PREMAS S27,29,28  D59-62                        ! 5TH STAGE BLEED TO EXTERNAL
PREMAS S28,30,31  D63-66                        ! 5TH STAGE BLEED TO HPT & LPT
ARITHY            D163-167                      ! HP COMPR SPEED UNIFORM
COMPRE S9-10       D67-73    R212     V67       ! HP COMPRESSOR REMAINING 4
STAGES
ARITHY            D168-174                      ! SUM WORK COMPLETE HP COMPR
PREMAS S10,32,11   D74-77                       ! COMPR DISCH BLEED
BURNER S11-12     D78-80    R214
MIXEES S12,32,13                                ! MIXING OF HPT COOLING AIR
MIXEES S13,30,14
TURBIN S14-15     D81-88,213,89     V82         ! HP
MIXEES S15,31,16                                ! MIXING OF LPT COOLN AIR
TURBIN S16-17     D90-97,208,98     V91         ! LP
DUCTER S17-18     D99-102   R215                ! CORE EXHAUST DUCT
NOZCON S18-19,1   D103      R216                ! CORE
ARITHY            D175-181  R250                ! LP-SPOOL RPM
ARITHY            D183-189  R251                ! HP-SPOOL RPM
OUTPBD            D250,251
PERFOR S1,0,0     D104-107,206,200,214,216,0,0,0,0,0
CODEND
////
! INTAKE
1 0.0                !ALTITUDE
2 15.0               !S.I.A DEV (K), CFM EXAMPLE
```

```
3 0.0                   !MACHNUMBER
4 1.0                   !PRESSURE RECOV; ACCORDING TO CFM-CALC
! FAN
5 0.85                  !SURGE MAG; SEVERAL EXAMPLES
6 1.0                   !ROTATIONAL SPEED
7 1.679                 !PRESSURE RATIO; CFM
8 0.85                  !ISENTROPIC EFFICIENCY; SEVERAL EX
9 0.0                   !ERROR SELECTION
10 1.0                  !COMPRESSOR MAP
11 0.0                  !STATOR ANGLE
! SPLIT INTO CORE AND BYPASS FLOW (PREMAS)
12 0.1667               !CORE FLOW FRACTION; BYPASS 5.0
13 0.0                  !FLOW LOSS (DEL W)
14 1.0                  !PRESSURE RECOVERY (LAMB P)
15 0.0                  !PRES LOSS (DEL P)
! BLEED AIR FROM BYPASS DUCT (PREMAS)
16 0.0083               !BLEED FRACTION; ESTIMATE (used to be 0.02)
17 0.0                  !FLOW LOSS (DEL W)
18 1.0                  !PRESSURE RECOVERY (LAMB P)
19 0.0                  !PRESSURE LOSS (DEL P)
! BYPASS DUCT
20 0.0                  !NO HEATING
21 0.0025               !PRESSURE LOSS < 0.003 (CFM)
22 0.0                  !COMBUSTION EFFICIENCY
23 1.E6                 !NO FUEL FLOW
! BLEED AIR VBV
24 0.0                  !BLEED FRACTION**********
25 0.0                  !FLOW LOSS (DEL W)
26 1.0                  !PRESSURE RECOVERY (LAMB P)
27 0.0                  !PRESSURE LOSS (DEL P)
! BLEED AIR UPSTREAM OF BYPASS NOZZLE (PREMAS)
28 0.0093               !BLEED FRACTION; ESTIMATE (used to be 0.02)
29 0.0                  !FLOW LOSS (DEL W)
30 1.0                  !PRESSURE RECOVERY (LAMB P)
31 0.0                  !PRESSURE LOSS (DEL P)
! COOLING AIR DUMPED DOWNSTR. OF CORE N.
32 0.0                  !
33 0.05                 !
34 0.0                  ! NOT IN USE
35 1.E6                 !
! BYPASS NOZZLE
36 -1.0                 !FIXED GEOMETRY
! COMPRESSOR LP
37 0.95                 !SURGE MARG; EXAMPLE
38 1.0                  !ROTATIONAL SPEED
39 1.365                !PRESSURE RATIO; CFM
40 0.876                !ISENTROPIC EFFICIENCY; SEVERAL EX
41 1.0                  !ERROR SELECTION
42 2.0                  !COMPRESSOR MAP
43 0.0                  !STATOR ANGLE
! LPC-HPC DUCT
44 0.0                  !NO HEATING
45 0.018                !PRESSURE LOSS; CFM
46 0.0                  !COMBUSTION EFFICIENCY
47 1.E6                 !NO FUEL FLOW
!HP. COMPRESSOR FIRST 5 STAGES
48 0.9                  !SURGE MARG; ESTIMATE
49 1.0                  !ROTATIONAL SPEED
50 3.84                 !PRSSURE RATIO; CFM
51 0.877                !ISENTROPIC EFFICIENCY; SEVERAL EX
52 1.0                  !ERROR SELECTION
```

```
53 4.0                !COMPRESSOR MAP
54 0.0                !STATOR ANGLE**********
!5TH STAGE BLEED (PREMAS)
55 0.085             !BLEED FRACTION; ESTIMATE
56 0.0                !FLOW LOSS (DEL W)
57 1.0                !PRESSURE RECOVERY (LAMB P)
58 0.0                !PRESSURE LOSS (DEL P)
! 5TH STAGE BLEED TO EXTERNAL (PREMAS)
59 0.0               !BLEED FRACTION; ESTIMATE **********
60 0.0                !FLOW LOSS (DEL W)
61 1.0                !PRESSURE RECOVERY (LAMB P)
62 0.0                !PRESSURE LOSS (DEL P)
! 5TH STAGE BLEED TO HPT & LPT (PREMAS)
63 0.3               !BLEED FRACTION HPT; ESTIMATE
64 0.0                !FLOW LOSS (DEL W)
65 1.0                !PRESSURE RECOVERY (LAMB P)
66 0.0                !PRESSURE LOSS (DEL P)
! HP.COMPRESSOR, REMAINING 4 STAGES
67 0.9                !SURGE MAGINE; ESTIMATE
68 1.0                !ROTATIONAL SPEED
69 2.96               !PRSSURE RATIO; CFM
70 0.877              !ISENTROPIC EFFICIENCY; SEVERAL EX
71 1.0                !ERROR SELECTION
72 4.0                !COMPRESSOR MAP
73 0.0                !STATOR ANGLE
! COMPR. DISCH. BLEED (PREMAS)
74 0.045             !BLEED FRACTION ESTIMATE
75 0.0                !FLOW LOSS (DEL W)
76 1.0                !PRESSURE RECOVERY (LAMB P)
77 0.0                !PRESSURE LOSS (DEL P)
! BURNER
78 0.0325             !PRESSURE LOSS; CFM
79 0.999              !COMBUSTION EFFICIENCY; GUESS
80 -1.0               !FUEL FLOW TO BE CALCULATED
! TURBINE HP
81 1.0E5              !AUXILIARY WORK
82 -1.0               !REL NON-DIM INL MASS FLOW
83 -1.0               !REL NON-DIM SPEED
84 0.883              !ISENTROPIC EFFICIENCY (ESTIM)
85 -1.0               !COMPRESSOR  TURBINE
86 3.0                !COMPRESSOR NUMBER TO BE DRIVEN
87 5.0                !TURBINE MAP NUMBER
88 -1.0               !AUXWK IS ASSUMED CONSTANT
89 0.0                !NOZZLE GUIDE VANES, ANGLE (REL DP)
! TURBIN LP
90 0.0               !AUX WORK;EXAMPLE (used to be 2.E5)
91 -1.0               !REL NON-DIM INL MASS FLOW
92 -1.0               !REL NON-DIMS SPEED
93 0.87               !ISENTROPIC EFFICIENCY (used to be .9)
94 -0.1               !COMPRESSOR TURBINE
95 1.0                !COMPRESSOR NUMBER TO BE DRIVEN
96 5.0                !TURBINE MAP NUMBER
97 -1.0               !AUXWK IS ASSUMED CONSTANT
98 0.0                !NOZZLE GUIDE VANES, ANGLE (REL DP)
! CORE EXHAUST DUCT
99 0.0                !NO HEATING
100 0.002             !PRESS LOSS < 0.003; CFM
101 0.0               !COMBUSTION EFFICIENCY
102 1.E6              !NO FUEL FLOW
! NOZZLE
103 -1.0              !CONSTANT AREA
```

```
! PERFORMANCE
104 -1.0                ! = TURBOFAN
105 -1.0                ! = TURBOFAN
106 0.0                 ! = NO SCALING
107 0.0                 ! = TURBOFAN
! COMMON ROT. SPEED FOR FAN & LP
151 5.0
152 -1.0
153 38.0
154 -1.0
155 6.0
! SUM FAN AND LP. COMPR. WORK
156 1.0
157 -1.0
158 208.0
159 -1.0
160 201.0
161 -1.0
162 207.0
! HP.COMPR.SPEED UNIFORM
163 5.0
164 -1.0
165 68.0
166 -1.0
167 49.0
! SUM WORK FOR COMPLETE HP.COMPR
168 1.0
169 -1.0
170 213.0
171 -1.0
172 210.0
173 -1.0
174 212.0
! LOW PRESSURE SPOOL RPM (250)
175 3.0
176 -1.
177 250.
178 -1.
179 6.0
180 -1.
181 182.
182 4950.
! HIGH PRESSURE SPOOL RPM (251)
183 3.0
184 -1.
185 251.0
186 -1.
187 49.0
188 -1.
189 190.
190. 14250.
-1
1 2 322.1       ! MASS FLOW,  DP
12 6 1645.      ! TET  ,DP
-1
-1
12 6 1645.
-1
1 0.0         ! ALTITUDE [m] !J-U-S-T G-E-T-T-I-N-G I-N-T-O POSITION
3 0.0           ! MACH NUMBER
-1
```

```
12 6 1600.      ! TET,  OD
-1
1 1000.0         ! ALTITUDE [m]
3 0.1          ! MACH NUMBER
-1
12 6 1550.      ! TET,  OD
-1
1 2000.       ! ALTITUDE [m]
3 0.2          ! MACH NUMBER
-1
12 6 1500.     ! TET,  OD
-1
1 3000.       ! ALTITUDE [m]
3 0.3          ! MACH NUMBER
-1
12 6 1500.      ! TET,  OD
-1
1 4000.       ! ALTITUDE [m]
2 0.0
3 0.4          ! MACH NUMBER
55 0.1
59 0.2
-1
12 6 1500.    ! TET,  OD
-1
1 5000.       ! ALTITUDE [m
2 0.0
3 0.5          ! MACH NUMBER
55 0.1
59 0.2
-1
12 6 1500.      ! TET,  OD
-1
1 6000.       ! ALTITUDE [m]
2 0.0
3 0.6          ! MACH NUMBER
55 0.1
59 0.2
-1
12 6 1500.      ! TET,  OD
-1
1 7000.       ! ALTITUDE [m]
2 0.0
3 0.7          ! MACH NUMBER
24 0.0
54 0.0
55 0.1
59 0.2
-1
12 6 1500.      ! TET,  OD
-1
1 8000.    ! ALTITUDE [m]
2 0.0
3 0.7          ! MACH NUMBER
24 0.0
54 0.0
55 0.1
59 0.2
-1
12 6 1500.      ! TET,  OD
-1
```

```
1 9000.  ! ALTITUDE [m]   !F-I-R-S-T S-E-R-I-E-S O-F C-R-U-I-S-E
2 0.0
3 0.7         ! MACH NUMBER
24 0.0
54 0.0
55 0.1
59 0.2
-1
12 6 1500.
-1
1 9000.  ! ALTITUDE [m]   !F-I-R-S-T S-E-R-I-E-S O-F C-R-U-I-S-E
2 0.0
3 0.7         ! MACH NUMBER
24 0.0
54 0.0
55 0.1
59 0.2
-1
12 6 1450.    ! TET,  OD
-1
1 9000.  ! ALTITUDE [m]   !F-I-R-S-T S-E-R-I-E-S O-F C-R-U-I-S-E
2 0.0
3 0.7         ! MACH NUMBER
24 0.0
54 0.0
55 0.1
59 0.2
-1
12 6 1400. ! TET,  OD
-1
1 9000.  ! ALTITUDE [m]   !F-I-R-S-T S-E-R-I-E-S O-F C-R-U-I-S-E
2 0.0
3 0.7         ! MACH NUMBER
24 0.0
54 0.0
55 0.1
59 0.2
-1
12 6 1350.     ! TET,  OD
-1
1 9000.  ! ALTITUDE [m]   !F-I-R-S-T S-E-R-I-E-S O-F C-R-U-I-S-E
2 0.0
3 0.7         ! MACH NUMBER
24 0.0
54 0.0
55 0.1
59 0.2
-1
12 6 1300.
-1
1 9000.  ! ALTITUDE [m]   !F-I-R-S-T S-E-R-I-E-S O-F C-R-U-I-S-E
2 0.0
3 0.7         ! MACH NUMBER
24 0.0
54 0.0
55 0.1
59 0.2
-1
12 6 1250. ! TET,  OD
-1
1 9000.  ! ALTITUDE [m]   !F-I-R-S-T S-E-R-I-E-S O-F C-R-U-I-S-E
```

```
2 0.0
3 0.7          ! MACH NUMBER
24 0.0
54 0.0
55 0.1
59 0.2
-1
12 6 1200. ! TET,  OD
-1
-3
```

The TURBOMATCH sample output, category "2"
CFM56-3C1 in cruise,
altitude 9000 m; Mach number 0,7; turbine entry temperature 1500 K

```
 1 9000.  ! ALTITUDE [m]    !F-I-R-S-T S-E-R-I-E-S O-F C-R-U-I-S-E
 2 0.0
 3 0.7          ! MACH NUMBER
 24 0.0
 54 0.0
 55 0.1
 59 0.2
 ! OPEN
 -1
 12 6 1500.
 -1
                                                    Time Now 10:30:34

 ***********************************************
 BERR( 1) =   -0.12448E-01
 BERR( 2) =    0.61910E-02
 BERR( 3) =    0.91511E-03
 BERR( 4) =    0.46177E-02
 BERR( 5) =   -0.70560E-02
 BERR( 6) =   -0.12870E-02
 BERR( 7) =   -0.84739E-02
 BERR( 8) =    0.12618E-02
 BERR( 9) =   -0.70502E-02

 Loop   1
 BERR( 1) =    0.10667E-03
 BERR( 2) =    0.69400E-04
 BERR( 3) =   -0.21088E-05
 BERR( 4) =   -0.31323E-03
 BERR( 5) =    0.31443E-03
 BERR( 6) =   -0.36287E-03
 BERR( 7) =   -0.19343E-03
 BERR( 8) =    0.64313E-02
 BERR( 9) =   -0.14074E-02

 Loop   2
 BERR( 1) =    0.37137E-05
 BERR( 2) =   -0.13765E-04
 BERR( 3) =    0.26890E-05
 BERR( 4) =   -0.61178E-05
 BERR( 5) =    0.39002E-05
 BERR( 6) =   -0.22241E-04
 BERR( 7) =   -0.84063E-05
 BERR( 8) =    0.23530E-02
 BERR( 9) =   -0.16281E-03
1

      ***** OFF DESIGN ENGINE CALCULATIONS. Converged after   2 Loops *****
```

```
***** AMBIENT AND INLET PARAMETERS *****
Alt. =    9000.0      I.S.A. Dev. =     0.000       Mach No. =  0.70
Etar = 1.0000         Momentum Drag =  33289.33

***** COMPRESSOR  1 PARAMETERS *****
PRSF =  0.16642E+01     ETASF =  0.97626E+00     WASF =  0.55496E+00
Z = 0.87625             PR =    1.759            ETA = 0.81143
PCN =    0.9474         CN = 1.03865             COMWK =  0.85534E+07
STATOR ANGLE =    0.00

***** CONVERGENT NOZZLE  1 PARAMETERS *****
NCOSF =  0.10000E+01
Area =  0.7361          Exit Velocity =  320.57  Gross Thrust =  46377.13
Nozzle Coeff. =  0.97888E+00

***** COMPRESSOR  2 PARAMETERS *****
PRSF =  0.53363E+00     ETASF =  0.10683E+01     WASF =  0.12570E+00
Z = 0.93884             PR =    1.381            ETA = 0.86532
PCN =    0.9474         CN = 1.02636             COMWK =  0.93050E+06
STATOR ANGLE =    0.00

***** COMPRESSOR  3 PARAMETERS *****
PRSF =  0.26296E+01     ETASF =  0.10635E+01     WASF =  0.15996E+00
Z = 0.87998             PR =    3.909            ETA = 0.86559
PCN =    0.9461         CN = 1.02204             COMWK =  0.50858E+07
STATOR ANGLE =    0.00

***** COMPRESSOR  4 PARAMETERS *****
PRSF =  0.18148E+01     ETASF =  0.10635E+01     WASF =  0.46982E-01
Z = 0.91859             PR =    3.064            ETA = 0.85408
PCN =    0.9461         CN = 1.01458             COMWK =  0.56311E+07
STATOR ANGLE =    0.00

***** COMBUSTION CHAMBER PARAMETERS *****
ETASF =  0.99900E+00
ETA = 0.99900           DLP = 0.3861             WFB =    0.5183

***** TURBINE  1 PARAMETERS *****
CNSF =  0.87674E+02     ETASF =  0.10526E+01     TFSF =  0.26407E+01
DHSF =  0.50938E+05
TF =  220.048            ETA = 0.88527            CN =  2.180
AUXWK =  0.10000E+06     NGV ANGLE = 0.00

***** TURBINE  2 PARAMETERS *****
CNSF =  0.75799E+02     ETASF =  0.10371E+01     TFSF =  0.76353E+00
DHSF =  0.55247E+05
TF =  222.301            ETA = 0.87949            CN =  2.193
AUXWK =  0.00000E+00     NGV ANGLE = 0.00

***** CONVERGENT NOZZLE  2 PARAMETERS *****
NCOSF =  0.10000E+01
Area =  0.2890          Exit Velocity =  504.78  Gross Thrust =  14536.55
Nozzle Coeff. =  0.98086E+00

  BD(250) = 0.468979E+04   BD(251) = 0.134815E+05


Scale Factor on above Mass Flows, Areas, Thrusts & Powers =     1.0000
```

Station	F.A.R.	Mass Flow	Pstatic	Ptotal	Tstatic	Ttotal	Vel	Area
1	0.00000	156.472	0.30334	0.42088	229.65	252.24	212.7	******
2	0.00000	156.472	******	0.42088	******	252.24	******	******
3	0.00000	156.472	******	0.74016	******	306.74	******	******
4	0.00000	27.026	******	0.74016	******	306.74	******	******
5	0.00000	27.026	******	1.02239	******	340.99	******	******
6	0.00000	27.026	******	1.02239	******	340.99	******	******
7	0.00000	27.026	******	1.00398	******	340.99	******	******
8	0.00000	27.026	******	3.92498	******	525.73	******	******
9	0.00000	24.324	******	3.92498	******	525.73	******	******
10	0.00000	24.324	******	12.02494	******	744.31	******	******
11	0.00000	23.229	******	12.02494	******	744.31	******	******
12	0.02231	23.747	******	11.63881	******	1500.00	******	******
13	0.02131	24.842	******	11.63881	******	1469.37	******	******
14	0.02075	25.490	******	11.63881	******	1447.66	******	******
15	0.02075	25.490	******	3.03732	******	1102.15	******	******
16	0.01957	27.004	******	3.03732	******	1072.42	******	******
17	0.01957	27.004	******	0.63634	******	769.51	******	******
18	0.01957	27.004	******	0.63507	******	769.51	******	******
19	0.01957	27.004	0.34316	0.63507	654.59	769.51	504.8	0.2890
20	0.00000	129.445	******	0.74016	******	306.74	******	******
21	0.00000	128.371	******	0.74016	******	306.74	******	******
22	0.00000	128.371	******	0.73831	******	306.74	******	******
23	0.00000	1.074	******	0.74016	******	306.74	******	******
24	0.00000	127.177	******	0.73831	******	306.74	******	******
25	0.00000	1.194	******	0.73831	******	306.74	******	******
26	0.00000	127.177	0.39008	0.73831	255.52	306.74	320.6	0.7361
27	0.00000	2.703	******	3.92498	******	525.73	******	******
28	0.00000	2.162	******	3.92498	******	525.73	******	******
29	0.00000	0.541	******	3.92498	******	525.73	******	******
30	0.00000	0.649	******	3.92498	******	525.73	******	******
31	0.00000	1.513	******	3.92498	******	525.73	******	******
32	0.00000	1.095	******	12.02494	******	744.31	******	******
33	0.00000	0.000	******	0.00000	******	0.00	******	******

```
 Gross Thrust =  60913.68
Momentum Drag =  33289.33
   Net Thrust =  27624.34
    Fuel Flow =    0.5183
       s.f.c. =  18.76135
   Sp. Thrust =   176.545
         Time Now 10:30:34

**********************************************
```

The TURBOMATCH sample output, category "3" (readable from Fortran code)
CFM56-3C1 in cruise,
altitude 9000 m; Mach number 0,7; turbine entry temperature 1500 K

```
INTAKE
 0.90000E+04  0.00000E+00  0.70000E+00  0.10000E+01
COMPRE
 0.87625E+00  0.94743E+00  0.17586E+01  0.81143E+00  0.00000E+00            1
0.00000E+00
PREMAS
 0.17273E+00  0.00000E+00  0.10000E+01  0.00000E+00
PREMAS
 0.83000E-02  0.00000E+00  0.10000E+01  0.00000E+00
PREMAS
 0.93000E-02  0.00000E+00  0.10000E+01  0.00000E+00
NOZCON
 0.73607E+00
COMPRE
 0.93884E+00  0.94743E+00  0.13813E+01  0.86532E+00  0.10000E+01            2
0.00000E+00
PREMAS
 0.00000E+00  0.00000E+00  0.10000E+01  0.00000E+00
COMPRE
 0.87998E+00  0.94607E+00  0.39094E+01  0.86559E+00  0.10000E+01            4
0.00000E+00
PREMAS
 0.10000E+00  0.00000E+00  0.10000E+01  0.00000E+00
PREMAS
 0.20000E+00  0.00000E+00  0.10000E+01  0.00000E+00
PREMAS
 0.30000E+00  0.00000E+00  0.10000E+01  0.00000E+00
COMPRE
 0.91859E+00  0.94607E+00  0.30637E+01  0.85408E+00  0.10000E+01            4
0.00000E+00
PREMAS
 0.45000E-01  0.00000E+00  0.10000E+01  0.00000E+00
BURNER
 0.38613E+00  0.99900E+00  0.51827E+00
TURBIN
 0.10000E+06  0.22005E+03  0.21800E+01  0.88527E+00  0.94607E-04  0.30000E+01
5 -0.10000E+01  0.10717E+08  0.00000E+00
TURBIN
 0.00000E+00  0.22230E+03  0.21930E+01  0.87949E+00  0.94743E-04  0.10000E+01
5 -0.10000E+01  0.94839E+07  0.00000E+00
NOZCON
 0.28904E+00
PERFOR
-0.10000E+01 -0.10000E+01  0.10000E+01  0.27624E+05  0.46377E+05  0.33289E+05
0.51827E+00  0.14537E+05  0.00000E+00  0.00000E+00
 0.00000E+00  0.00000E+00  0.00000E+00
           1  0.00000E+00  0.15647E+03  0.30334E+00  0.42088E+00  0.22965E+03
0.25224E+03  0.21275E+03 -0.10000E-05
           2  0.00000E+00  0.15647E+03 -0.10000E-05  0.42088E+00 -0.10000E-05
0.25224E+03 -0.10000E-05 -0.10000E-05
           3  0.00000E+00  0.15647E+03 -0.10000E-05  0.74016E+00 -0.10000E-05
0.30674E+03 -0.10000E-05 -0.10000E-05
           4  0.00000E+00  0.27026E+02 -0.10000E-05  0.74016E+00 -0.10000E-05
0.30674E+03 -0.10000E-05 -0.10000E-05
           5  0.00000E+00  0.27026E+02 -0.10000E-05  0.10224E+01 -0.10000E-05
0.34099E+03 -0.10000E-05 -0.10000E-05
           6  0.00000E+00  0.27026E+02 -0.10000E-05  0.10224E+01 -0.10000E-05
0.34099E+03 -0.10000E-05 -0.10000E-05
```

```
           7  0.00000E+00  0.27026E+02 -0.10000E-05  0.10040E+01 -0.10000E-05
0.34099E+03 -0.10000E-05 -0.10000E-05
           8  0.00000E+00  0.27026E+02 -0.10000E-05  0.39250E+01 -0.10000E-05
0.52573E+03 -0.10000E-05 -0.10000E-05
           9  0.00000E+00  0.24324E+02 -0.10000E-05  0.39250E+01 -0.10000E-05
0.52573E+03 -0.10000E-05 -0.10000E-05
          10  0.00000E+00  0.24324E+02 -0.10000E-05  0.12025E+02 -0.10000E-05
0.74431E+03 -0.10000E-05 -0.10000E-05
          11  0.00000E+00  0.23229E+02 -0.10000E-05  0.12025E+02 -0.10000E-05
0.74431E+03 -0.10000E-05 -0.10000E-05
          12  0.22311E-01  0.23747E+02 -0.10000E-05  0.11639E+02 -0.10000E-05
0.15000E+04 -0.10000E-05 -0.10000E-05
          13  0.21307E-01  0.24842E+02 -0.10000E-05  0.11639E+02 -0.10000E-05
0.14694E+04 -0.10000E-05 -0.10000E-05
          14  0.20754E-01  0.25490E+02 -0.10000E-05  0.11639E+02 -0.10000E-05
0.14477E+04 -0.10000E-05 -0.10000E-05
          15  0.20754E-01  0.25490E+02 -0.10000E-05  0.30373E+01 -0.10000E-05
0.11022E+04 -0.10000E-05 -0.10000E-05
          16  0.19568E-01  0.27004E+02 -0.10000E-05  0.30373E+01 -0.10000E-05
0.10724E+04 -0.10000E-05 -0.10000E-05
          17  0.19568E-01  0.27004E+02 -0.10000E-05  0.63634E+00 -0.10000E-05
0.76951E+03 -0.10000E-05 -0.10000E-05
          18  0.19568E-01  0.27004E+02 -0.10000E-05  0.63507E+00 -0.10000E-05
0.76951E+03 -0.10000E-05 -0.10000E-05
          19  0.19568E-01  0.27004E+02  0.34316E+00  0.63507E+00  0.65459E+03
0.76951E+03  0.50478E+03  0.28904E+00
          20  0.00000E+00  0.12944E+03 -0.10000E-05  0.74016E+00 -0.10000E-05
0.30674E+03 -0.10000E-05 -0.10000E-05
          21  0.00000E+00  0.12837E+03 -0.10000E-05  0.74016E+00 -0.10000E-05
0.30674E+03 -0.10000E-05 -0.10000E-05
          22  0.00000E+00  0.12837E+03 -0.10000E-05  0.73831E+00 -0.10000E-05
0.30674E+03 -0.10000E-05 -0.10000E-05
          23  0.00000E+00  0.10744E+01 -0.10000E-05  0.74016E+00 -0.10000E-05
0.30674E+03 -0.10000E-05 -0.10000E-05
          24  0.00000E+00  0.12718E+03 -0.10000E-05  0.73831E+00 -0.10000E-05
0.30674E+03 -0.10000E-05 -0.10000E-05
          25  0.00000E+00  0.11938E+01 -0.10000E-05  0.73831E+00 -0.10000E-05
0.30674E+03 -0.10000E-05 -0.10000E-05
          26  0.00000E+00  0.12718E+03  0.39008E+00  0.73831E+00  0.25552E+03
0.30674E+03  0.32057E+03  0.73607E+00
          27  0.00000E+00  0.27026E+01 -0.10000E-05  0.39250E+01 -0.10000E-05
0.52573E+03 -0.10000E-05 -0.10000E-05
          28  0.00000E+00  0.21621E+01 -0.10000E-05  0.39250E+01 -0.10000E-05
0.52573E+03 -0.10000E-05 -0.10000E-05
          29  0.00000E+00  0.54053E+00  0.00000E+00  0.39250E+01  0.00000E+00
0.52573E+03  0.00000E+00 -0.10000E-05
          30  0.00000E+00  0.64863E+00 -0.10000E-05  0.39250E+01 -0.10000E-05
0.52573E+03 -0.10000E-05 -0.10000E-05
          31  0.00000E+00  0.15135E+01 -0.10000E-05  0.39250E+01 -0.10000E-05
0.52573E+03 -0.10000E-05 -0.10000E-05
          32  0.00000E+00  0.10946E+01 -0.10000E-05  0.12025E+02 -0.10000E-05
0.74431E+03 -0.10000E-05 -0.10000E-05
          33  0.00000E+00  0.00000E+00  0.00000E+00  0.00000E+00  0.00000E+00
0.00000E+00  0.00000E+00 -0.10000E-05
LOOPS
           2
```

APPENDIX L

Interpolation Routine for TURBOMATCH Data

Interpolation Routine for Turbomatch data

```
C  Programmer Paul Arentzen
□
C  Clean engine
□
C

      DIMENSION NR(44),ALT(44),RMACH(44),V(44),RO(44),TIME(44),ROC(44)
      DIMENSION MNR(36),AKS(44)
      OPEN(UNIT=3,FILE='ROUTDATA')
      DO 100 I=1,44
      READ(3,200)NR(I),ALT(I),RMACH(I),V(I),RO(I),TIME(I),ROC(I),AKS(I)
  100 CONTINUE
      CLOSE(3)
      MNR(1)=5
      MNR(2)=6
      MNR(3)=7
      MNR(4)=8
      MNR(5)=9
      MNR(6)=10
      MNR(7)=11
      MNR(8)=12
      MNR(9)=13
      MNR(10)=14
      MNR(11)=15
      MNR(12)=16
      MNR(13)=17
      MNR(14)=18
C changed from here13.01.99
      MNR(15)=19
      MNR(16)=20
      MNR(17)=21
      MNR(18)=22
      MNR(19)=23
C to here 13.01.99
      MNR(20)=24
C changed from here12.01.99
      MNR(21)=25
      MNR(22)=26
      MNR(23)=27
      MNR(24)=28
      MNR(25)=29
      MNR(26)=30
      MNR(27)=31
      MNR(28)=32
      MNR(29)=33
      MNR(30)=34
      MNR(31)=35
      MNR(32)=36
      MNR(33)=37
      MNR(34)=38
      MNR(35)=39
      MNR(36)=40
      AWING=202.85
      G=9.81
      FMY=0.025
      TOTFUEL=0.0
      PRINT*,' Give T/O-weight or Start weight [kg]'
      READ*,TOWEIGHT
      ACMASS=TOWEIGHT
```

```
      PRINT*,' Give start point in flight route (< 42)'
      READ*,NRSTART
      DO 110 NJ=1,35
      IF(MNR(NJ).EQ.NRSTART)THEN
       JSTART=NJ
       GOTO 111
      ENDIF
  110 CONTINUE
  111 CONTINUE
       OPEN(UNIT=1,FILE='RESULAA.DAT')
       OPEN(UNIT=7,FILE='RESULBB.DAT')

      WRITE(7,205)
      WRITE(7,206)
      WRITE(7,204)

      DO 150 J=JSTART,35

C old section from here
C
C     PRINT*,' Give start point in flight route (< 42)'
C     READ*,NRSTART
C       OPEN(UNIT=1,FILE='RESULAA.DAT')
C       OPEN(UNIT=7,FILE='RESULBB.DAT')
C
C      WRITE(7,205)
C      WRITE(7,206)
C      WRITE(7,204)

C      DO 150 J=1,33
C to here

C      IF(J.LE.4.OR.J.GE.41)THEN
C       ACTHRUST= ACMASS*G*FMY
C        GOTO 120
C     ENDIF
      IF(MNR(J).GE.5.AND.MNR(J).LE.7)THEN
       CL=0.728
       CD=0.102
       PRINT*,' Station no.: ',MNR(J)
       PRINT*,'     CL default =  ',CL, '     CD default =  ',CD
       ACLIFT=CL*(RO(MNR(J))*AWING*V(MNR(J))**2.0)/2.0
       ACDRAG=CD*(RO(MNR(J))*AWING*V(MNR(J))**2.0)/2.0
       ACTHRUST=ACDRAG+ACMASS*AKS(MNR(J))+(ACMASS*G-ACLIFT)*FMY
      ELSE
       ALFA=ATAN(ROC(MNR(J)))
       ACLIFT=ACMASS*G*COS(ALFA)
       CL=2.0*ACLIFT/(RO(MNR(J))*AWING*V(MNR(J))**2.0)
       CALL DRAGCOEF(CL,RMACH(MNR(J)),CD)
       IF(MNR(J).EQ.8)THEN
           CD=0.102
         ELSEIF(MNR(J).EQ.9)THEN
           CD=0.062
         ELSEIF(MNR(J).EQ.10)THEN
           CD=0.037
         ELSEIF(MNR(J).EQ.11)THEN
           CD=0.03
         ELSEIF(MNR(J).EQ.32)THEN
           CD=CD+0.001
         ELSEIF(MNR(J).EQ.33)THEN
```

```
          CD=CD+0.0025
        ELSEIF(MNR(J).EQ.34)THEN
          CD=CD+0.0075
        ELSEIF(MNR(J).EQ.35)THEN
          CD=CD+0.0150
        ELSEIF(MNR(J).EQ.36)THEN
          CD=CD+0.03
        ELSEIF(MNR(J).EQ.37)THEN
          CD=CD+0.04
        ELSEIF(MNR(J).EQ.38)THEN
          CD=CD+0.04
        ELSEIF(MNR(J).EQ.39)THEN
          CD=0.075
       ENDIF
       PRINT*,' Station no.: ', MNR(J)
       PRINT*,' Machnr. =  ',RMACH(MNR(J)),'  CL =  ',CL,'  CD = ',CD
       PRINT*,' Is CD-value OK? (1/0; 0 = STOP)'
       READ*,NANS
       IF(NANS.NE.1)THEN
         PRINT*,' Give CD in station', MNR(J),'! ( < 0.0 = STOP)'
         READ*,CD
       ENDIF
       IF(CD.LT.0.0)GOTO 160
       ACDRAG=(CD*RO(MNR(J))*AWING*V(MNR(J))**2.0)/2.0
       ACTHRUST=ACDRAG+ACMASS*(G*SIN(ALFA)+AKS(MNR(J))/COS(ALFA))
      ENDIF
  120 CONTINUE
      ENGTHRST=ACTHRUST/2.0
      PRINT*,' Engine thrust:',ENGTHRST
      CALL READTURB(NR(MNR(J)),RMACH(MNR(J)),ALT(MNR(J)),ENGTHRST,WFUEL)
       TOTFUEL= TOTFUEL+2.0*WFUEL*(TIME(MNR(J+1))-TIME(MNR(J)))
      ACMASS=ACMASS-2.0*WFUEL*(TIME(MNR(J+1))-TIME(MNR(J)))
      PRINT*,' ACMASS & WFUEL: ',ACMASS,WFUEL
      WRITE(1,201)NR(MNR(J+1)),ACMASS,TOTFUEL
      WRITE(1,202)(TOWEIGHT-ACMASS),((TOWEIGHT-ACMASS)/0.4536)
      WRITE(7,203)NR(MNR(J+1)),ACMASS,TOTFUEL
  150 CONTINUE

  200 FORMAT(I3,7E12.5)
  201 FORMAT('  Station:',I3,'  Current A/C mass:',F8.0,'  Fuel cons.:',
     1F7.1)
  202 FORMAT('      Cntr. fuel cons.:',F8.0,' kg',F8.0,' lbm')
  203 FORMAT(I3,2E13.5)
  204 FORMAT(' NO    ACMASS      TOTFUEL   ')
  205 FORMAT(' NO     ALT         MACH        THRUST      FLAMETEMP
     1  TET         WaINT       WaCOMB')
  206 FORMAT(' NO     Wf          BYP-RAT     F/A-RAT     Ptot u-COMB  P
     1tot d-COMB   Max P-RAT')
  160 CONTINUE
      CLOSE(1)
      CLOSE(7)
      END

C   Program name: READTURB.FOR
C
C  All the 8 parameters describing 33 stations in max 2000 conditions and
C    sevaral other parameters for those conditions are sorted out.
C
C  Program will read from a "Full Print" Turbomatch file type FOR004.DAT.
C  Name of the file needs to appear in the listing of the program, in
C  CHARACTER FILEIN.
```

```
C
C  The word STOPIT has to be put on the far end of that file if the
C    complete file is to be read.
C
C  The data that are found are printed to a file named MOD004.DAT
C
      SUBROUTINE READTURB(NR,RUNMACH,RUNALT,RUNTHRST,FINFUEL)
      DIMENSION RINTAKE(2000,4),PERFOR(2000,13)
      DIMENSION ALTI(2000),RMZERO(2000),TET(2000),AIRIN(2000)
      DIMENSION BYPASS(2000),AIRCOMB(2000),TTINCO(2000),PTDSCOMB(2000)
      DIMENSION FUELFL(2000),RMAXPT(2000),PRATIO(2000),FUELAIR(8)
      DIMENSION FAR(2000,33),RMASSFL(2000,33),PSTAT(2000,33)
      DIMENSION PTOTAL(2000,33)
      DIMENSION TSTATIC(2000,33),TTOTAL(2000,33),VELOS(2000,33)
      DIMENSION AREA(2000,33),GROSST(2000),RMOMDRAG(2000),RNETT(2000)
      CHARACTER FILENAME*9(44)

C  Address / station number
      DIMENSION ISTN(2000,33)
      CHARACTER DDUMP*6,FILEIN*12
      INTEGER I,J,K,L,ICOND,IDUMP
  999 CONTINUE
C
C Name of "read file":
C
      OPEN(UNIT=8,FILE='INFILEC0')
      DO 997 I=1,44
      READ(8,155)IDUMP,FILENAME(I)
  997 CONTINUE
      CLOSE(8)
  155 FORMAT(I3,A9)
      WRITE(6,151)FILENAME(NR)

  151 FORMAT(' Input file is  ',A9)
      PRINT*,' HAPPY?? (1/0)'
      READ*,IDUMP
      IF(IDUMP.EQ.1)THEN
        FILEIN=FILENAME(NR)
        GOTO 998
      ENDIF
      PRINT*,' Give input file (12 CHAR.) '
      READ(6,101)FILEIN
  998 CONTINUE
      WRITE(6,141)FILEIN

      OPEN(UNIT=2,FILE=FILEIN)
      ICOND=2000
      DO 10 I=1,ICOND
   49 CONTINUE
      READ(2,101)DDUMP
      IF(DDUMP.EQ.'STOPIT')GOTO 11
      IF(DDUMP.NE.'INTAKE'.AND.DDUMP.NE.'PERFOR')GOTO 50
      IF(DDUMP.EQ.'INTAKE')READ(2,113) RINTAKE(I,1), RINTAKE(I,2), RINTA
     1KE(I,3), RINTAKE(I,4)
      IF(DDUMP.EQ.'PERFOR')READ(2,114) PERFOR(I,1), PERFOR(I,2), PERFOR(
     1I,3), PERFOR(I,4), PERFOR(I,5), PERFOR(I,6), PERFOR(I,7), PERFOR(I
     2,8), PERFOR(I,9), PERFOR(I,10)
      IF(DDUMP.EQ.'PERFOR')READ(2,113)PERFOR(I,11), PERFOR(I,12),PERFOR(
     1I,10)
      IF(DDUMP.EQ.'PERFOR')GOTO 51
      GOTO 49
```

```
   50 CONTINUE
      READ(2,113)FDUMP
      GOTO 49
   51 CONTINUE
      II=I
      DO 8 J=1,33
      READ (2,100) ISTN(I,J),FAR(I,J),RMASSFL(I,J),PSTAT(I,J),PTOTAL(I,J
     1),TSTATIC(I,J),TTOTAL(I,J),VELOS(I,J),AREA(I,J)
    8 CONTINUE
      ALTI(I)=RINTAKE(I,1)
      RMZERO(I)= RINTAKE(I,3)
      AIRIN(I)=RMASSFL(I,1)
      AIRCOMB(I)=RMASSFL(I,11)
      BYPASS(I)=(RMASSFL(I,1)-RMASSFL(I,4))/ RMASSFL(I,4)
      TET(I)= TTOTAL(I,12)
      TTINCO(I)=TTOTAL(I,11)
      RMAXPT(I)= PTOTAL(I,10)
      PTDSCOMB(I)=PTOTAL(I,12)
      PRATIO(I)=PTOTAL(I,10)/PTOTAL(I,1)
      FUELFL(I)=PERFOR(I,7)
      GROSST(I)=PERFOR(I,5)+PERFOR(I,8)
      RMOMDRAG(I)=PERFOR(I,6)+PERFOR(I,9)
      RNETT(I)=GROSST(I)-RMOMDRAG(I)

   10 CONTINUE
   11 CONTINUE
      ICOND=II
      CLOSE(2)
      DMNEG=-10.000000
      DMPOS=10.000000
      DALTNEG=-20000.0
      DALTPOS=20000.0
C
C  Identifying adjacent points:
      DO 70 NN=1,ICOND
      DELM=RMZERO(NN)-RUNMACH
      DELALT=ALTI(NN)-RUNALT
      IF(DELM.LT.0.00000)THEN
        IF(DELM.GT.DMNEG)THEN
         DMNEG=DELM
        ENDIF
      ELSE
        IF(DELM.LT.DMPOS)THEN
         DMPOS=DELM
        ENDIF
      ENDIF
      IF(DELALT.LT.0.00000)THEN
        IF(DELALT.GT.DALTNEG)THEN
         DALTNEG=DELALT
        ENDIF
      ELSE
        IF(DELALT.LT.DALTPOS)THEN
         DALTPOS=DELALT
        ENDIF
      ENDIF

   70 CONTINUE

      RMLIMOV=RUNMACH+DMPOS
      RMLIMUN=RUNMACH+DMNEG
      RALIMOV=RUNALT+DALTPOS
```

```
      RALIMUN=RUNALT+DALTNEG

      WRITE(6,160) RMLIMOV,RMLIMUN
  160 FORMAT(' Mach over:      ',F8.4,' Mach under:      ',F8.4)
      WRITE(6,161) RALIMOV, RALIMUN
  161 FORMAT(' Altitude over: ',F10.1,' Altitude under: ',F10.1)


C
C  Name of file where all relevant parameters for 8 adjacent conditions
C  are stored:
C
      OPEN(UNIT=4,FILE=' TMPSTORE.DAT')
      DDUMP='NXTCON'

      DO 23 K=1,ICOND
      IF((ABS(RMLIMOV-RMZERO(K)).GT.0.001.AND.ABS(RMZERO(K)-RMLIMUN).GT.
     10.0001).OR.(ABS(RALIMOV-ALTI(K)).GT.0.0001.AND.ABS(ALTI(K)-RALIMUN
     2).GT.0.0001))GOTO 22
      WRITE (4,101)DDUMP

      WRITE(4,110) K,ALTI(K),RMZERO(K),TET(K),AIRIN(K),BYPASS(K),RMAXPT(
     1K),PRATIO(K)
      WRITE(4,112)K,GROSST(K),RMOMDRAG(K),RNETT(K),FUELFL(K)
      WRITE(4,115)K,AIRCOMB(K),TTINCO(K),PTDSCOMB(K)

      DO 21 L=1,33
      WRITE(4,111)    K,ISTN(K,L),FAR(K,L),RMASSFL(K,L),PSTAT(K,L),PTOTA
     1L(K,L),TSTATIC(K,L),TTOTAL(K,L),VELOS(K,L),AREA(K,L)
   21 CONTINUE
   22 CONTINUE
   23 CONTINUE
      DDUMP='STOPIT'
       WRITE (4,101)DDUMP
      CLOSE (4)
C
C Find proper thrust over/under
C
      CALL THRSTLIM(RUNTHRST,RMLIMOV,RMLIMUN,RALIMOV,RALIMUN)
      WRITE (6,170)
      WRITE (6,171)
      WRITE (6,172)
  170 FORMAT(' Interpolate for the specified condition?')
  171 FORMAT('  (If any of the thrust values listed are')
  172 FORMAT('   zero interpolation is of no value)')
      WRITE(6,106)
      WRITE(6,173)
  173 FORMAT (' Answer (1/0) !')
      READ(6,104)IANSWER
      IF(IANSWER.NE.1)GOTO 24

      OPEN(UNIT=5,FILE='MODTEMP.DAT')
      DO 300 J=1,8
      READ(5,107)I
      READ (5,110)I,ALTI(I),RMZERO(I),TET(I),AIRIN(I),BYPASS(I), RMAXPT(
     1I),PRATIO(I)
      READ (5,112)I,GROSST(I),RMOMDRAG(I),RNETT(I),FUELFL(I)
      READ(5,115)K,AIRCOMB(K),TTINCO(K),PTDSCOMB(K)
      DO 301 L=1,33
      READ (5,111)    I,ISTN(I,L),FAR(I,L),RMASSFL(I,L),PSTAT(I,L),PTOTA
     1L(I,L),TSTATIC(I,L),TTOTAL(I,L),VELOS(I,L),AREA(I,L)
```

```
  301 CONTINUE
      FUELAIR(I)=FAR(I,12)
  300 CONTINUE
      CLOSE(5)


C
C Interpolation routine
C flyttet til hovedprogram       OPEN(UNIT=1,FILE='RESULT.DAT')
      CALL INTERPOL(RUNMACH,RUNALT,RUNTHRST,TET,FINTMP)
      CALL INTERPOL(RUNMACH,RUNALT,RUNTHRST,AIRIN,FINAIR)
      CALL INTERPOL(RUNMACH,RUNALT,RUNTHRST,FUELFL,FINFUEL)
      CALL INTERPOL(RUNMACH,RUNALT,RUNTHRST,BYPASS,FINBYP)
      CALL INTERPOL(RUNMACH,RUNALT,RUNTHRST,FUELAIR,FINFAIR)
      CALL INTERPOL(RUNMACH,RUNALT,RUNTHRST,PRATIO,FINPRAT)
      CALL INTERPOL(RUNMACH,RUNALT,RUNTHRST,AIRCOMB,FINAIRC)
      CALL INTERPOL(RUNMACH,RUNALT,RUNTHRST,TTINCO,FINTTINC)
      CALL INTERPOL(RUNMACH,RUNALT,RUNTHRST,RMAXPT,FINPMAX)
      CALL INTERPOL(RUNMACH,RUNALT,RUNTHRST,PTDSCOMB,FINPDSC)

C  Estimating Stoichiometric Flame Temperature
C

      TSTOICH=2600.0+0.500*(FINTTINC-800.0)

      WRITE(6,106)
      WRITE(6,120)NR
      WRITE(6,121)
      WRITE(6,122)RUNALT
      WRITE(6,123)RUNMACH
      WRITE(6,124)RUNTHRST
      WRITE(6,106)
      WRITE(6,125)
      WRITE(6,132)TSTOICH
      WRITE(6,126)FINTMP
      WRITE(6,127)FINAIR
      WRITE(6,133)FINAIRC
      WRITE(6,128)FINFUEL
      WRITE(6,129)FINBYP
      WRITE(6,130)FINFAIR
      WRITE(6,134)FINPMAX
      WRITE(6,135)FINPDSC
      WRITE(6,131)FINPRAT
      WRITE(6,106)

      WRITE(1,106)
      WRITE(1,120)NR
      WRITE(1,121)
      WRITE(1,122)RUNALT
      WRITE(1,123)RUNMACH
      WRITE(1,124)RUNTHRST
      WRITE(1,106)
      WRITE(1,125)
      WRITE(1,132)TSTOICH
      WRITE(1,126)FINTMP
      WRITE(1,127)FINAIR
      WRITE(1,133)FINAIRC
      WRITE(1,128)FINFUEL
      WRITE(1,129)FINBYP
      WRITE(1,130)FINFAIR
      WRITE(1,134)FINPMAX
```

```
      WRITE(1,135)FINPDSC
      WRITE(1,131)FINPRAT
      WRITE(1,106)
      WRITE(7,142)NR,RUNALT,RUNMACH,RUNTHRST,TSTOICH,FINTMP,FINAIR,FINAI
     1RC
      WRITE(7,143) NR,FINFUEL,FINBYP,FINFAIR,FINPMAX,FINPDSC,FINPRAT
C        CLOSE(1)
  100 FORMAT(I12,8E13.5)
  101 FORMAT(A)
  102 FORMAT(I12)
  103 FORMAT(I1,F7.1)
  104 FORMAT(I2)
  105 FORMAT(2I2,F6.0)
  106 FORMAT('  ')
  107 FORMAT(I4)
  110 FORMAT(I4,F12.2,F8.5,2F8.1,3F8.3)
  111 FORMAT(I4,I3,8F12.6)
  112 FORMAT(I4,3F16.2,F16.5)
  113 FORMAT(E12.5,3E13.5)
  114 FORMAT(E12.5,9E13.5)
  115 FORMAT(I4,2F8.2,F8.1)

  120 FORMAT(' F I N A L   R E S U L T S; Station',I3)
  121 FORMAT('     CONDITION:')
  122 FORMAT('        Altitude=     ',F8.1,' m')
  123 FORMAT('        Mach number=    ',F6.3)
  124 FORMAT('        Thrustreq.= ',F10.1,' N')
  125 FORMAT('    INTERPOLATED QUANTITIES:')
  126 FORMAT('        TET=                    ',F8.1,' K')
  127 FORMAT('        Air Massfl. Intake=     ',F8.1,' kg/s')
  128 FORMAT('        Fuelflow=               ',F8.4,' kg/s')
  129 FORMAT('        Bypass ratio=           ',F8.3)
  130 FORMAT('        Fuel/Air ratio=         ',F8.5)
  131 FORMAT('        Max Press.ratio=        ',F8.3)
  132 FORMAT('        Stoich. Flame. Temp. =  ',F8.1,' K')
  133 FORMAT('        Air Massfl. Combustor = ',F8.1,' kg/s')
  134 FORMAT('        Ptot. Upst. Comb. =    ',F10.3,' atm')
  135 FORMAT('        Ptot. Dwnst. Comb. =   ',F10.3,' atm')
C 140 FORMAT(' Stop here? (1=STOP; 0=SAME INP.FILE; 2=NEW INP.FILE)')
  141 FORMAT(' File for input data:',A12)
  142 FORMAT(I3,7E13.5)
  143 FORMAT(I3,6E13.5)

   24 CONTINUE
C      WRITE(6,140)
C      READ*,ICONTIN
C      IF(ICONTIN.EQ.2)GOTO 999
C      IF(ICONTIN.EQ.0)GOTO 998
   25 CONTINUE
      RETURN
      END

      SUBROUTINE THRSTLIM(RUNTHRST,RMLIMOV,RMLIMUN,RALIMOV,RALIMUN)
      DIMENSION ALTI(50),RMZERO(50),TET(50),AIRIN(50),BYPASS(50)
      DIMENSION RMAXPT(50),NUMCON(50)
      DIMENSION AIRCOMB(50),TTINCO(50),PTDSCOMB(50)
      DIMENSION PRATIO(50),GROSST(50),RMOMDRAG(50),RNETT(0:50)
      DIMENSION FUELFL(50)
      DIMENSION ISTN(50,33),FAR(50,33),RMASSFL(50,33),PSTAT(50,33)
      DIMENSION PTOTAL(50,33)
      DIMENSION TSTATIC(50,33),TTOTAL(50,33),VELOS(50,33),AREA(50,33)
```

```
      DIMENSION INDRNDR(15), INDROVR(15), IOVRNDR(15), IOVROVR(15)
      CHARACTER DDUMP*6

      OPEN(UNIT=4,FILE='TMPSTORE.DAT')
      ICOUNT=0
      II=0
      IJ=0
      JI=0
      JJ=0
      I11=0
      I12=0
      I21=0
      I22=0
      I31=0
      I32=0
      I41=0
      I42=0
      RNETT(0)=0.0
      DO 60 N=1,15
      INDRNDR(N)=0
      INDROVR(N)=0
      IOVRNDR(N)=0
      IOVROVR(N)=0
   60 CONTINUE

      DO 10 K=1,50
      READ(4,101)DDUMP
      IF(DDUMP.EQ.'STOPIT')GOTO 11
      ICOUNT=ICOUNT+1
      READ(4,110)NUMCON(K),ALTI(K),RMZERO(K),TET(K),AIRIN(K),BYPASS(K),R
     1MAXPT(K),PRATIO(K)
      READ(4,112)NUMCON(K),GROSST(K),RMOMDRAG(K),RNETT(K),FUELFL(K)
      READ(4,115)NUMCON(K),AIRCOMB(K),TTINCO(K),PTDSCOMB(K)

      DO 5 L=1,33
      READ(4,111)NUMCON(K),ISTN(K,L),FAR(K,L),RMASSFL(K,L),PSTAT(K,L),PT
     1OTAL(K,L),TSTATIC(K,L),TTOTAL(K,L),VELOS(K,L),AREA(K,L)
    5 CONTINUE
      IF(ABS(RMZERO(K)-RMLIMUN).LT.0.00001.AND.ABS(ALTI(K)-RALIMUN).LT.0
     1.01)THEN
      II=II+1
      INDRNDR(II)=K
      ENDIF
      IF(ABS(RMZERO(K)-RMLIMUN).LT.0.00001.AND.ABS(ALTI(K)-RALIMOV).LT.0
     1.01)THEN
      IJ=IJ+1
      INDROVR(IJ)=K
      ENDIF
      IF(ABS(RMZERO(K)-RMLIMOV).LT.0.00001.AND.ABS(ALTI(K)-RALIMUN).LT.0
     1.01)THEN
      JI=JI+1
      IOVRNDR(JI)=K
      ENDIF
      IF(ABS(RMZERO(K)-RMLIMOV).LT.0.00001.AND.ABS(ALTI(K)-RALIMOV).LT.0
     1.01)THEN
      JJ=JJ+1
      IOVROVR(JJ)=K
      ENDIF
   10 CONTINUE
   11 CONTINUE
      CLOSE (4)
```

```
C 1: under/under
C
      DTNEG=-200000.0
      DTPOS=200000.0
      DO 20 M=1,II
      DELTRST=RNETT(INDRNDR(M))-RUNTHRST
      IF(DELTRST.LT.0.00000)THEN
C  meens that RNETT<RUNTEST
C
        IF(DELTRST.GT.DTNEG)THEN
          DTNEG= DELTRST
          I11=INDRNDR(M)
        ENDIF
      ELSE
        IF(DELTRST.LT.DTPOS)THEN
          DTPOS= DELTRST
          I12=INDRNDR(M)
        ENDIF
      ENDIF
   20 CONTINUE
C 2: under/over
C
      DTNEG=-200000.0
      DTPOS=200000.0
      DO 30 M=1,IJ
      DELTRST=RNETT(INDROVR(M))-RUNTHRST
      IF(DELTRST.LT.0.00000)THEN
C  meens that RNETT<RUNTEST
C
        IF(DELTRST.GT.DTNEG)THEN
          DTNEG= DELTRST
          I21=INDROVR(M)
        ENDIF
      ELSE
        IF(DELTRST.LT.DTPOS)THEN
          DTPOS= DELTRST
          I22=INDROVR(M)
        ENDIF
      ENDIF
   30 CONTINUE
C 3: over/under
C
      DTNEG=-200000.0
      DTPOS=200000.0
      DO 40 M=1,JI
      DELTRST=RNETT(IOVRNDR(M))-RUNTHRST
      IF(DELTRST.LT.0.00000)THEN
C  meens that RNETT<RUNTEST
C
        IF(DELTRST.GT.DTNEG)THEN
          DTNEG= DELTRST
          I31=IOVRNDR(M)
        ENDIF
      ELSE
        IF(DELTRST.LT.DTPOS)THEN
          DTPOS= DELTRST
          I32=IOVRNDR(M)
        ENDIF
      ENDIF
   40 CONTINUE
C 4: over/over
```

```
C
      DTNEG=-200000.0
      DTPOS=200000.0
      DO 50 M=1,JJ
      DELTRST=RNETT(IOVROVR(M))-RUNTHRST
      IF(DELTRST.LT.0.00000)THEN
C  meens that RNETT<RUNTEST
C
        IF(DELTRST.GT.DTNEG)THEN
          DTNEG= DELTRST
          I41=IOVROVR(M)
        ENDIF
      ELSE
        IF(DELTRST.LT.DTPOS)THEN
          DTPOS= DELTRST
          I42=IOVROVR(M)
        ENDIF
      ENDIF
   50 CONTINUE

C  Conditions printed in sorted order to file
C
      OPEN(UNIT=5,FILE='MODTEMP.DAT')

      DO 200 I=1,8
      IF(I.EQ.1)THEN
       K=I11
      ELSEIF(I.EQ.2)THEN
       K=I12
      ELSEIF(I.EQ.3)THEN
       K=I21
      ELSEIF(I.EQ.4)THEN
       K=I22
      ELSEIF(I.EQ.5)THEN
       K=I31
      ELSEIF(I.EQ.6)THEN
       K=I32
      ELSEIF(I.EQ.7)THEN
       K=I41
      ELSEIF(I.EQ.8)THEN
       K=I42
      ENDIF
      A=I
      A=A/2
      J=A
      IF(A-J.GT.0.1) THEN
       WRITE(6,175)J+1,RNETT(K)
  175 FORMAT(I4,'  Thrust, lower:          ',F10.1)

      ELSE
       WRITE(6,176)RNETT(K)
  176 FORMAT('                    Thrust, upper :      ',F10.1)
       ENDIF
      WRITE(5,102)I
      WRITE(5,110)I,ALTI(K),RMZERO(K),TET(K),AIRIN(K),BYPASS(K), RMAXPT(
     1K),PRATIO(K)
      WRITE(5,112)I,GROSST(K),RMOMDRAG(K),RNETT(K),FUELFL(K)
      WRITE(5,115)I,AIRCOMB(K),TTINCO(K),PTDSCOMB(K)
      DO 201 L=1,33
      WRITE(5,111)     I,ISTN(K,L),FAR(K,L),RMASSFL(K,L),PSTAT(K,L),PTOTA
     1L(K,L),TSTATIC(K,L),TTOTAL(K,L),VELOS(K,L),AREA(K,L)
```

```
  201 CONTINUE
  200 CONTINUE
      DDUMP='STOPIT'
      WRITE (5,101)DDUMP

      CLOSE(5)
  101 FORMAT(A)
  102 FORMAT(I4)
  110 FORMAT(I4,F12.2,F8.5,2F8.1,3F8.3)
  111 FORMAT(I4,I3,8F12.6)
  112 FORMAT(I4,3F16.2,F16.5)
  115 FORMAT(I4,2F8.2,F8.1)
      RETURN
      END


      SUBROUTINE INTERPOL(RUNMACH,RUNALT,RUNTHRST,PAR,ANSWER)
      DIMENSION ALTI(8),RMZERO(8),TET(8),AIRIN(8),BYPASS(8)
      DIMENSION AIRCOMB(8),TTINCO(8),PTDSCOMB(8)
      DIMENSION RMAXPT(8),NUMCON(8),PARTMP(6),PAR(8)
      DIMENSION PRATIO(8),GROSST(8),RMOMDRAG(8),RNETT(8),FUELFL(8)
      DIMENSION ISTN(8,33),FAR(8,33),RMASSFL(8,33),PSTAT(8,33)
      DIMENSION PTOTAL(8,33)
      DIMENSION TSTATIC(8,33),TTOTAL(8,33),VELOS(8,33),AREA(8,33)
C     DIMENSION INDRNDR(15), INDROVR(15), IOVRNDR(15), IOVROVR(15)
      CHARACTER DDUMP*6
      REAL RUNMACH,RUNALT,RUNTHRST,ANSWER
      OPEN(UNIT=5,FILE='MODTEMP.DAT')
      DO 300 J=1,8
      READ(5,102)I
      READ (5,110)I,ALTI(I),RMZERO(I),TET(I),AIRIN(I),BYPASS(I), RMAXPT(
     1I),PRATIO(I)

      READ (5,112)I,GROSST(I),RMOMDRAG(I),RNETT(I),FUELFL(I)
      READ(5,115)I,AIRCOMB(I),TTINCO(I),PTDSCOMB(I)

      DO 301 L=1,33
      READ (5,111)    I,ISTN(I,L),FAR(I,L),RMASSFL(I,L),PSTAT(I,L),PTOTA
     1L(I,L),TSTATIC(I,L),TTOTAL(I,L),VELOS(I,L),AREA(I,L)
  301 CONTINUE
  300 CONTINUE
      CLOSE(5)

      PARTMP(1)=PAR(1)+((PAR(2)-PAR(1))/(RNETT(2)-RNETT(1)))*(RUNTHRST-R
     1NETT(1))
      PARTMP(2)=PAR(3)+((PAR(4)-PAR(3))/(RNETT(4)-RNETT(3)))*(RUNTHRST-R
     1NETT(3))
      PARTMP(3)=PAR(5)+((PAR(6)-PAR(5))/(RNETT(6)-RNETT(5)))*(RUNTHRST-R
     1NETT(5))
      PARTMP(4)=PAR(7)+((PAR(8)-PAR(7))/(RNETT(8)-RNETT(7)))*(RUNTHRST-R
     1NETT(7))

      PARTMP(5)=PARTMP(1)+((PARTMP(2)-PARTMP(1))/(ALTI(3)-ALTI(1)))*(RUN
     1ALT-ALTI(1))
      PARTMP(6)=PARTMP(3)+((PARTMP(4)-PARTMP(3))/(ALTI(7)-ALTI(5)))*(RUN
     1ALT-ALTI(5))

      ANSWER=PARTMP(5)+((PARTMP(6)-PARTMP(5))/(RMZERO(5)-RMZERO(1)))*(RU
     1NMACH-RMZERO(1))
C      WRITE(1,113)PARTMP(1),PARTMP(2),PARTMP(3),PARTMP(4)
C      WRITE(1,114)PARTMP(5),PARTMP(6)
```

```
C      WRITE(1,103)

  101 FORMAT(A)
  102 FORMAT(I4)
  103 FORMAT('  ')
  110 FORMAT(I4,F12.2,F8.5,2F8.1,3F8.3)
  111 FORMAT(I4,I3,8F12.6)
  112 FORMAT(I4,3F16.2,F16.5)
  113 FORMAT(' Interm. param.:',4F12.4)
  114 FORMAT('            and.:     ',2F12.4)
  115 FORMAT(I4,2F8.2,F8.1)
      RETURN
      END

      SUBROUTINE DRAGCOEF(RCL,RMACH,RCD)
      DIMENSION CL(54),CD(54),DELCD(54)
      OPEN(UNIT=2,FILE='CDDATA')
      DO 10 J=1,54
      READ(2,100)CL(J),CD(J),DELCD(J)
   10 CONTINUE
      CLOSE(2)
  100 FORMAT(F4.2,2F8.5)
      IF(RCL.LT.CL(1).OR.RCL.GT.CL(54))THEN
       PRINT*,' CL out of range!'
       GOTO 500
      ENDIF
      DO 20 I=1,53
      IF(CL(I).LE.RCL.AND.CL(I+1).GE.RCL)THEN
        NUNDER=I
        NOVER=I+1
        GOTO 21
      ENDIF
   20 CONTINUE
   21 CONTINUE
      RCD=CD(NUNDER)+((CD(NOVER)-CD(NUNDER))/(CL(NOVER)-CL(NUNDER)))* (R
     1CL-CL(NUNDER))
      IF(RMACH.GT.0.70)THEN
        RCD=RCD+((DELCD(NUNDER)+ DELCD(NOVER))/2.0)*((RMACH-0.7)/0.06)
      ENDIF
  500 CONTINUE
      RETURN
      END
```